Polymerization in Liquid Ammonia: Acrylate Esters and Vinyl Thiolacetate

F. LEONARD, G. A. HANKS, and R. K. KULKARNI, *U. S. Army Medical Biomechanical Research Laboratory, Walter Reed Army Medical Center, Washington, D. C.*
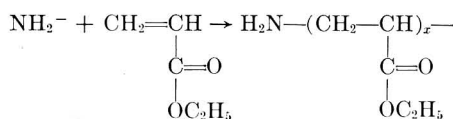
Synopsis

Methyl ethyl and *n*-propyl acrylates when polymerized by sodium in liquid ammonia, contain an average of one amino group per polymer chain, which is indicative of amide anion initiation and chain transfer to the solvent ammonia. Isopropyl acrylate and the higher homologs contain considerably less nitrogen than required by one amino group per chain indicative of another initiating and terminating mechanism. Three alternate mechanisms are discussed. Of these, alkoxide initiation seems to be the most plausible. Vinyl thiolacetate polymers prepared under the same conditions also contain less nitrogen than required by one amino group per chain. The polymer structure is predominantly poly(vinyl thiol) with intramolecular or intermolecular disulfide bridges. The acetate part of the molecule is concomitantly split off to form acetamide.

INTRODUCTION

The polymerization of vinyl or acrylic monomers in liquid ammonia can be initiated by either alkali metal amides, hydroxides, or alkali metals themselves.[1] Higginson and Wooding[2] showed that potassium initiates polymerization of styrene in liquid ammonia, through the amide ions formed in the reaction. This mechanism is supported by the work of Overberger et al.[4] in the case of methacrylonitrile in liquid ammonia.

It had been previously reported[5] that in the polymerization of ethyl acrylate in liquid ammonia with sodium, the initiation occurred by the amide anion, and the polymer contained on an average one amino group per chain, viz.,

$$NH_2{}^- + CH_2{=}CH \rightarrow H_2N{-}(CH_2{-}CH)_x{-}$$

$$\underset{\underset{OC_2H_5}{|}}{\underset{|}{C{=}O}} \qquad \underset{\underset{OC_2H_5}{|}}{\underset{|}{C{=}O}}$$

The generality of this reaction in the homologous series of the acrylic acid esters as well as the possible applicability of the reaction towards the preparation of amino poly(vinyl thiols) through the use of the monomer, vinyl thiolacetate, are presented in this paper.

EXPERIMENTAL

Materials

The acrylic acid esters, obtained as commercial products from Rohm and Haas, were purified by drying and distillation. The refractive indices were measured and used as criteria of purity of the monomers.

Vinyl thiolacetate was prepared in the laboratory by pyrolysis of β-acetoxyethyl thiolacetate (Borden Chemical Co.) at 520°C. in accordance with the technique of Richards.[6] The pyrolysis product was distilled, and the fraction boiling below 140°C. was separated. This fraction was thoroughly washed with water to remove acetic acid, with 10% aqueous lead acetate to remove mercaptans, and finally with water. The washed product was dried over anhydrous sodium sulfate, filtered, and subjected to fractional distillation. The fraction obtained at 119–121°C. had a refractive index n_D^{25} of 1.4892 which was in agreement with the literature values.[6-8] The overall yield from the original β-acetoxyethyl thiolacetate was on the average 10–15% of the theoretical. The yield was small, due to the side reactions taking place in the pyrolysis column, giving rise to other low boiling mercaptans. The large quantity of unconverted β-acetoxy compound could, however, be recovered in the distillation and recycled to increase the overall yield of the vinyl thiolacetate.

Polymerization in Liquid Ammonia

The polymerization in liquid ammonia was carried out in an equipment similar to that of Higginson and Wooding,[1] with the use of condensers containing a Dry Ice–acetone mixture as a coolant and two distillation systems in series for distilling ammonia twice before admitting it into the reaction flask fitted with a mechanical stirrer.

First, the requisite quantity of sodium was stirred in ammonia to obtain a dark blue solution. The required quantity of monomer, previously cooled to about 10°C., was then added rapidly to the solution, with vigorous stirring. The addition of a small quantity of the monomer was sufficient to discharge the blue color, but further addition caused an exothermic reaction, as evidenced by vigorously refluxing ammonia. After the addition of the monomer had been completed, the reaction mixture was agitated further for a period of $1/2$ hr., and then an excess ammonium chloride was added to neutralize the initiator. The bulk of ammonia was allowed to evaporate overnight, leaving the polymer and unreacted monomer, along with sodium and ammonium chloride. Special care was taken, by the use of soda lime drying tubes, to avoid exposure of the product to moisture.

Purification of Polymers

After evaporation of ammonia, the reaction mixture was agitated with water to remove inorganic impurities; the nonaqueous portion was dissolved in ether and extracted with water until the water washings showed no qualitative evidence of chloride ions. The polymer solution in ether

was dried over Drierite overnight, and the ether was removed by evaporation first in a desiccator with an aspirator and later in a vacuum oven at 50°C. at 2 mm. Hg until the sample reached constant weight. The color of liquid polymers obtained ranged from pale yellow to amber.

Cryoscopic Estimations

Number-average molecular weights of the liquid polymer were determined cryoscopically from the freezing point depression in benzene in the usual manner.

Analysis of Samples

The polymer samples were analyzed for C, H, and N by the National Bureau of Standards and also for nitrogen by this laboratory. The poly-(vinyl thiol) samples were analyzed for sulfur, acetate, and sulfhydryl groups by the National Bureau of Standards and Department of Radio-biology, Walter Reed Army Medical Center.

Amide and Amine Groups

To determine whether the nitrogen obtained by elemental analysis was due to amide or amino groups, the following technique was used.

(a) A weighed quantity of the polymer sample was heated in a Kjeldahl ammonia distillation apparatus, with 40% KOH and the distillate titrated with standard acid. The nitrogen content calculated by this method was negligible compared to the total nitrogen content of the polymer sample.

(b) A weighed quantity of the polymer sample was refluxed overnight with 20% HCl, 20% acetic acid, and 60% water. The solution was made alkaline with KOH and heated to boiling. The distillate was collected and titrated for ammonia with standard HCl. A negligible amount of ammonia had formed. When a sample of the same run was subjected to Kjeldahl digestion with concentrated H_2SO_4, approximately the same quantity of nitrogen was found as in the original sample.

The above experiments show that the nitrogen bound to the polymer molecules is not hydrolyzable with dilute alkali or acid under the conditions used, indicating that the nitrogen is not due to an amide but probably to an amino group attached to the end of the polymer molecule.

RESULTS AND DISCUSSION

The data are summarized in Table I. It may be observed that for the polymers from methyl, ethyl, and propyl acrylates, the number-average molecular weights determined by the cryoscopic method agreed with those calculated from the nitrogen contents, assuming one amino group attached to each polymer molecule. However, the polymers made in the same way from the isopropyl, butyl, isobutyl, and 2-ethylhexyl acrylates, had considerably smaller quantities of nitrogen, and the cryoscopic molecular weights were approximately one-third to one-fourth of the molecular weight calculated on the basis of 1 nitrogen atom per chain.

TABLE I

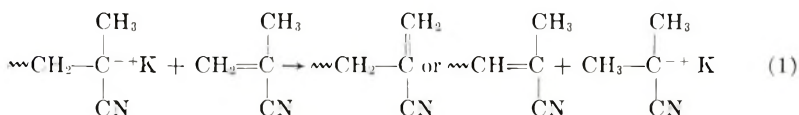Polymerization of Alkyl Acrylates in Sodium–Liquid Ammonia System

Sample no.	Monomer Used	Monomer concn., mole/l.	Sodium concn., g. atom/l.	Found			Calcd.			M_n	
				C, %	H, %	N, %	C, %	H, %	N, %	Cryoscopic in benzene	Calculated from N content
H-166-64	Methyl acrylate	1.58	0.40	56.20	7.10	2.60	54.18	7.29	2.41	580	538
H-166-58	Ethyl acrylate	1.60	0.40	60.20	8.23	0.94	59.32	8.11	0.94	1495	1496
H-205-133	Ethyl acrylate	1.60	0.35	—	—	1.81	—	—	1.89	740	774
H-166-68	n-Propyl acrylate	1.60	0.174	62.80	8.50	1.26	62.29	8.90	1.14	1223	1111
H-166-73	Isopropyl acrylate	1.60	0.200	62.60	8.90	0.30	62.20	8.91	1.25	1117	4667
H-166-51	n-Butyl acrylate	1.56	0.174	65.29	9.34	0.18	65.26	9.42	0.45	3088	7865
H-166-74	Isobutyl acrylate	1.60	0.174	64.00	9.70	1.03	63.08	9.69	3.17	442	1359
H-166-59	2-Ethylhexyl acrylate	1.60	0.17	71.50	11.00	0.31	70.74	10.96	1.11	1267	4516

The consistently low nitrogen contents of the polymers of isopropyl, butyl, isobutyl, and 2-ethylhexyl acrylates indicate that an alternate mechanism not involving nitrogen may be operating side by side with the amide ion initiation and subsequent termination by chain transfer to solvent ammonia.

The following alternate mechanisms, not involving amide anion initiation may be considered: (1) formation of anion radicals, their free-radical bimolecular termination, followed by anionic initiation of polymerization; (2) extensive chain transfer to the monomers through disproportionation; (3) initiation through the sodium alkoxides produced by the action of sodium on the alkyl acrylates.
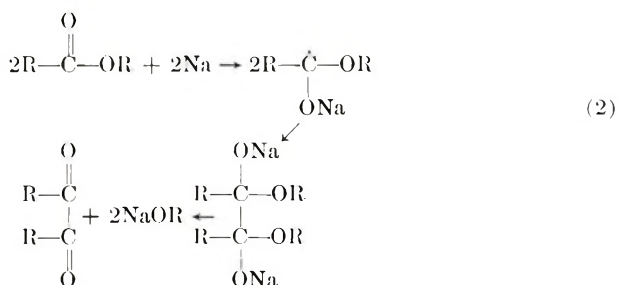
The first mechanism was postulated by Overberger and co-workers[4] in the system lithium–liquid ammonia–methacrylonitrile. If this mechanism is assumed to be partially operative in higher esters, it may explain the lower nitrogen contents, but it is not readily understandable, why the mechanism is not operative in the lower esters.

The second mechanism of chain transfer to the monomer by disproportionation, also proposed by Overberger and co-workers,[4] for methacrylonitrile is as shown in eq. (1):

$$\text{\textasciitilde}CH_2{-}\underset{\underset{CN}{|}}{\overset{\overset{CH_3}{|}}{C}}{-}{}^+K + CH_2{=}\underset{\underset{CN}{|}}{\overset{\overset{CH_3}{|}}{C}} \rightarrow \text{\textasciitilde}CH_2{-}\underset{\underset{CN}{|}}{\overset{\overset{CH_2}{||}}{C}} \text{ or } \text{\textasciitilde}CH{=}\underset{\underset{CN}{|}}{\overset{\overset{CH_3}{|}}{C}} + CH_3{-}\underset{\underset{CN}{|}}{\overset{\overset{CH_3}{|}}{C}}{-}{}^+K \quad (1)$$

This mechanism, if operative in the case of the higher acrylic acid ester homologs would also account for the lowering of nitrogen content of the polymer. Here too it is difficult to understand why the mechanism is not applicable to the lower esters as well.

The third mechanism considered is in accordance with eq. (2), as reported by Kharasch and co-workers[10,11] in the reaction of esters with sodium in liquid ammonia:

$$2R{-}\overset{\overset{O}{||}}{C}{-}OR + 2Na \rightarrow 2R{-}\underset{\underset{ONa}{|}}{\overset{\cdot}{C}}{-}OR \quad (2)$$

$$\underset{R{-}\overset{||}{C}}{\overset{R{-}\overset{O}{||}{C}}{|}}{+} 2NaOR \leftarrow \underset{R{-}\underset{ONa}{\overset{|}{C}}{-}OR}{\overset{R{-}\underset{|}{\overset{ONa}{|}}{C}{-}OR}{|}}$$

The sodium alkoxides formed through this reaction may or may not initiate the polymerization according to the strength of the corresponding alkoxide nucleophile. Although the alkoxides may form from all esters in the sodium–liquid ammonia system, the ones from the higher esters or isopropyl acrylate have a higher electron density on the alkyl oxygen and

therefore may be effective in partially initiating polymerization of the acrylic esters in addition to the normal amide ions.

It appears that the last mechanism may be of importance in the initiation of polymerization of the isopropyl and higher acrylic esters, whereas in the case of lower esters, amide anions are almost entirely effective in initiating polymerization.

Polymerization of Vinyl Thiolacetate

In the process of polymerization with sodium in liquid ammonia, under the same conditions, as with the acrylic acid esters, vinyl thiol acetate yielded a liquid polymer having disulfide and sulfhydryl groups but no acetate groups, as evidenced by the infrared spectra (Fig. 1) and elementary analysis. Also a large quantity of acetamide could be recovered
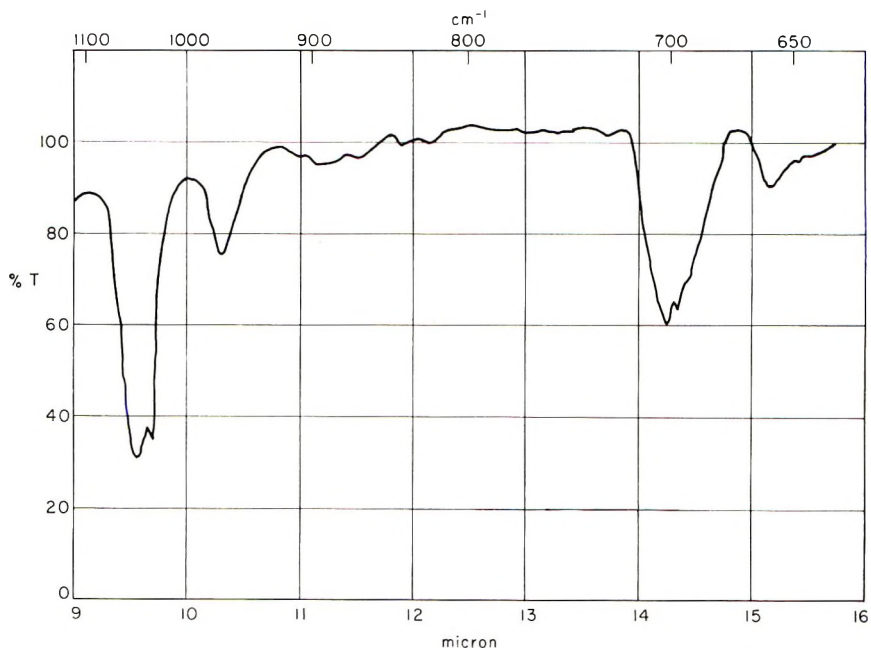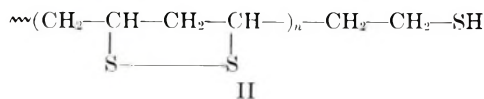

Fig. 1. Infrared spectrum for poly(vinyl thiolacetate).

from the runs as a by-product. This tends to suggest that amidification of the acetate groups, formation of the sulfhydryl groups, and partial oxidation of the sulfhydryl groups to disulfides were taking place, side by side with the anionic polymerization. The favored head-to-tail arrangement of the monomer units in the ionic reaction involved can initially give the structure I in the polymer chain:

$$\text{ww}(CH_2-CH-CH_2-CH-)_n-CH_2-CH_2$$
$$\qquad\quad |\qquad\qquad |\qquad\qquad\quad |$$
$$\qquad\quad SH\qquad\quad SH\qquad\qquad SH$$

I
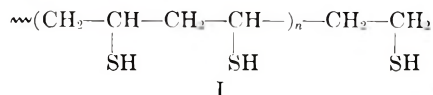
I undergoes further transformation to II:

$$\sim\sim(CH_2\text{—}CH\text{—}CH_2\text{—}CH\text{—})_n\text{—}CH_2\text{—}CH_2\text{—}SH$$

S————S

II

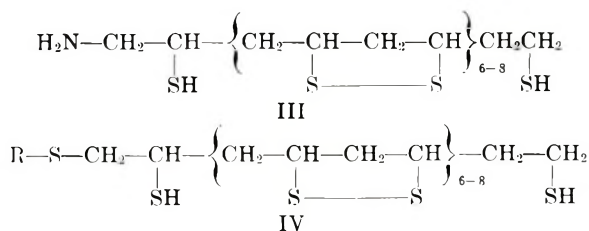and also intermolecular structures with disulfide bridges.

Similar oxidative transformations leading to five-membered disulfides have been reported by Barltrop et al.[12] in the case of 1,3-dimercaptopropane derivatives.

Considering the infrared spectra of the polymers (Fig. 1), the C-S linkage in the polymer has a stretching frequency of 699 cm.$^{-1}$ with a weak band at 659 cm.$^{-1}$. This compares favorably with the frequencies reported by Schotte[13] for the C-S linkages in cyclic disulfides. The elementary analyses of four different samples of the polymer, together with the cryoscopic molecular weight and sulfhydryl group contents, presented in Table II indicate that the structure of the polymers prepared in the present investigation may be a mixture of III (20–30%) and IV (70–80%).

TABLE II
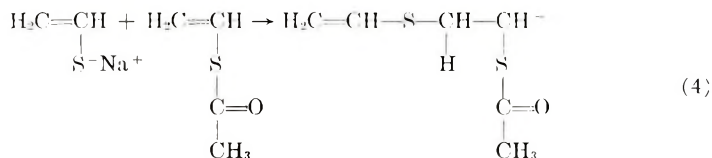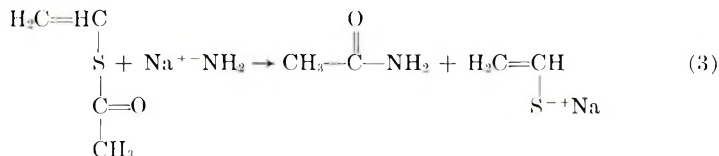Polymerization of Vinyl Thiolacetate with Sodium in Liquid Ammonia[a]

Expt. no.	Yield of polymer, %	$\overline{M}_n$ (cryoscopic)	Analysis (found)				Sulfhydryl groups, %	$\overline{M}_n$ (based on nitrogen content)
			C, %	H, %	N, %	S, %		
PVTA 3	46	934	39.86	6.75	0.20	51.85	8.14, 9.31	7000
PVTA 4	35		38.80	6.74	0.14	—	—	10,000
PVTA 5	43	956	39.0	6.50	1.46	52.60	—	9589
PVTA 6	44	1147	40.4	6.76	0.46	51.71	7.94, 8.71	3448

[a] The monomer and sodium metal concentrations were 1 mole/l. and 0.173 eq./l., respectively. The polymerization and polymer isolation procedures were similar to those in acrylic esters.

$$H_2N\text{—}CH_2\text{—}CH\text{—}\{CH_2\text{—}CH\text{—}CH_2\text{—}CH\}_{6-8}CH_2CH_2$$

SH   S————S   SH

III

$$R\text{—}S\text{—}CH_2\text{—}CH\text{—}\{CH_2\text{—}CH\text{—}CH_2\text{—}CH\}_{6-8}\text{—}CH_2\text{—}CH_2$$

SH   S————S   SH

IV

As far as the inclusion of amino group in the polymer chain, as a result of amide ion initiation is concerned, this monomer behaves the same way as the higher acrylic acid esters do, the nitrogen contents being less than one-third of that predicted by the cryoscopic molecular weights. This situa-

tion, combined with the fact that large amounts of acetamide are produced in the reaction, indicate the mechanism of eqs. (3) and (4) to occur in addition to the regular amide ion initiation.

$$
\begin{array}{l}
\text{H}_2\text{C}{=}\text{HC} \\
\quad | \\
\quad \text{S} + \text{Na}^+{}^-\text{NH}_2 \rightarrow \text{CH}_3{-}\overset{\text{O}}{\overset{\|}{\text{C}}}{-}\text{NH}_2 + \text{H}_2\text{C}{=}\text{CH} \\
\quad | \qquad\qquad\qquad\qquad\qquad\qquad\qquad\quad | \\
\quad \text{C}{=}\text{O} \qquad\qquad\qquad\qquad\qquad\qquad\quad \text{S}^{-+}\text{Na} \\
\quad | \\
\quad \text{CH}_3
\end{array}
\tag{3}
$$

$$
\begin{array}{l}
\text{H}_2\text{C}{=}\text{CH} + \text{H}_2\text{C}{=}\text{CH} \rightarrow \text{H}_2\text{C}{=}\text{CH}{-}\text{S}{-}\text{CH}{-}\text{CH}^- \\
\quad | \qquad\qquad\quad | \qquad\qquad\qquad\qquad\qquad\quad | \qquad | \\
\quad \text{S}^-\text{Na}^+ \qquad \text{S} \qquad\qquad\qquad\qquad\qquad \text{H} \quad \text{S} \\
\qquad\qquad\qquad | \qquad\qquad\qquad\qquad\qquad\qquad\qquad | \\
\qquad\qquad\qquad \text{C}{=}\text{O} \qquad\qquad\qquad\qquad\qquad\qquad \text{C}{=}\text{O} \\
\qquad\qquad\qquad | \qquad\qquad\qquad\qquad\qquad\qquad\qquad | \\
\qquad\qquad\qquad \text{CH}_3 \qquad\qquad\qquad\qquad\qquad\qquad \text{CH}_3
\end{array}
\tag{4}
$$

The sulfide ions can take part in the propagation step, precluding the inclusion of the amino groups in the polymer molecules. However, there is a good possibility of the chain transfer to the monomer and the formation of the sodium alkyl sulfides by the Kharasch[10,11] mechanism mentioned above, which may initiate polymerization.

CONCLUSION

The polymerization of the homologous series of acrylic esters with sodium in liquid ammonia is shown to proceed exclusively through amide ion initiation and chain transfer to solvent ammonia until the alkyl chain length of three carbon atoms is reached. However, when the alkoxy carbon atom is more hindered, as in case of isopropyl acrylate, and when the chain length is increased to more than three carbons, this mechanism does not seem to be wholly operative. Perhaps chain transfer to the monomer and/-or sodium alkoxide-initiated polymerization may be of importance.

It is postulated that polymerization of vinyl thiolacetate under the same conditions may take place partially through amide ions, as well as through the alkyl sulfide anion. The elementary analysis and infrared data show that the structure of the polymers from vinyl thiolacetate contains disulfide and sulfhydryl groups.

References

1. Higginson, W. C. E., and N. S. Wooding, *J. Chem. Soc.*, **1952**, 760.
2. Wooding, N. S., and W. C. E. Higginson, *J. Chem. Soc.*, **1952**, 1178.
3. Beaman, R. G., *J. Am. Chem. Soc.*, **70**, 3115 (1948).
4. Overberger, C. G., H. Yuki, and N. Urakawa, *J. Polymer Sci.*, **45**, 127 (1960).
5. Leonard, F., A. J. Szlachtun, and I. Cort, *J. Polymer Sci.*, **9**, 339 (1953).
6. Richards, L. M. (duPont), U. S. Pat. 2,418,426 (April 1947).
7. Brubaker, M. M. (duPont), U. S. Pat. 2,378,535 (June 1945).

8. Overberger, C. G., H. Biltech, and R. G. Nickerson, *J. Polymer Sci.*, **27**, 381 (1958).

9. Findlay, A., *Practical Physical Chemistry*, J. A. Kitchener, Ed., 8th ed., Longmans, Green, New York, 1958, pp. 107–112.

10. Kharasch, M. S., E. Sternfeld, and F. R. Mayo, *J. Am. Chem. Soc.*, **61**, 215 (1939).

11. Kharasch, M. S., E. Sternfeld, and F. R. Mayo, *J. Org. Chem.*, **5**, 362 (1940).

12. Barltrop, J. A., P. M. Hayes, and M. Calvin, *J. Am. Chem. Soc.*, **76**, 4348 (1954).

13. Schotte, L., *Arkiv. Kemi*, **56**, 579 (1955).

Résumé

Les acrylates de méthyle, d'éthyle, et de n-propyle, après polymérisation par le sodium dans l'ammoniac liquide, contiennent en moyenne une fonction amine par chaîne polymérique, ce qui indique une initiation par l'anion amidure et un transfert de chaîne sur le solvant ammoniac. L'acrylate d'isopropyle et les homologues plus élevés contiennent beaucoup moins d'azote qu'une fonction amine par chaîne, ce qui indique un autre mécanisme d'initiation et de terminaison. Trois mécanismes différents sont discutés. Il semble que l'initiation par l'alcoyl-oxyde est le mécanisme le plus plausible. Des polymères de thioacétate de vinyle, préparés dans les mêmes conditions, contiennent aussi moins d'azote que nécessaire pour une fonction amine par chaîne. La structure prédominante du polymère est du polyvinylthiol, avec des ponts disulfures intra- ou intermoléculaires. La partie acétate de la molécule réagit en même temps pour former l'acétamide.

Zusammenfassung

Mit Natrium in flüssigem Ammoniak polymerisierte Methyl-, Äthyl- und n-Propylacrylate enthalten im Mittel eine Aminogruppe pro Polymerkette, was für einen Start durch das Amidanion und Kettenübertragung zum Lösingsmittel Ammoniak spricht. Isopropylacrylat und die höheren Homologen enthalten beträchtlich weniger Stickstoff, als einer Aminogruppe pro Kette entspricht, was einen anderen Start- und Abbruchmechanismus erkennen lässt. Drei Alternativmechanismen werden diskutiert. Davon scheint ein Alkoxydstart am plausibelsten zu sein. Unter den gleichen Bedingungen hergestellte Vinylthiolactapolymere enthalten ebenfalls weniger Stickstoff, als einer Aminogruppe pro Kette entspricht. Die Polymerstruktur ist vorwiegend die eines Polyvinylthiols mit intra- oder intermolekularen Disulfidbrücken. Der Acetatteil des Moleküls wird gleichzeitig unter Acetamidbildung abgespalten.

Kinetics of Heterogeneous Cellulose Reactions.
I.   Cyanoethylation of Cotton Cellulose*

PRONOY K. CHATTERJEE† and CARL M. CONRAD, *Plant Fibers Pioneering Research Laboratory, Southern Utilization Research and Development Division, Agricultural Research Service, U. S. Department of Agriculture, New Orleans, Louisiana*

Synopsis

Sakurada's equation and fundamental kinetic laws were applied to the heterogeneous cyanoethylation of cellulose, performed by reacting fiber with liquid acrylonitrile, with sodium hydroxide as the catalyst. The data fit Sakurada's equation better at higher temperatures; deviation occurs at the initial stage, and the rate of reaction falls abruptly at a later stage. The degree of substitution at which the abrupt rate change occurred decreased as the temperature increased from 31 to 60°C. and also as the crystallinity of the fiber decreased. Diluting the reagent with different solvents decreased the rate of reaction and changed its transition points, but did not change the essential nature of the reaction, each segment of which fits Sakurada's equation very well. A uniform distribution of the catalyst (sodium hydroxide) throughout the fiber was attempted, and then the reaction was studied at 50°C. Diffractograms of the samples provided further evidence that the position of the rate change is associated with the change of cellulose (I) crystalline structure. Approximate energy of activation has been calculated, from the specific rate constants, between 31 and 40°C. as 10.6 kcal. and between 45 and 50°C. as 16.7 kcal. At other temperatures the determination was handicapped, due to temperature dependence of the order of reaction. An empirical relation between the constants of Sakurada's equation and the reaction temperature has been sought and correlated with the Arrhenius equation. Energies of activation, determined from this relationship, have been found to be very close to the above values. The change of order of reaction with temperature suggests that the reaction is affected by diffusion and the mechanism is interpreted as a diffusion-controlled reaction where hydrogen bonds play a significant role in diffusion.

INTRODUCTION

In the past different workers have presented many divergent theories of heterogeneous cellulose reactions, none of which are wholly acceptable. Earlier workers generally assumed that cellulose reactions are either quasi-homogeneous[1,2] or entirely macroheterogeneous.[3,4] Bernoulli and co-workers[5] tried to explain the peculiarities of their experiments on acetylation on the basis of the reaction of the different hydroxyl groups. Hess and Trogus[6] suggested that cellulose reactions are micellar-heterogeneous.

---

* Paper presented at the 149th National Meeting of the American Chemical Society, Detroit, Michigan, April 4–9, 1965.

† Postdoctoral Resident Research Associate, 1963–65.

Sakurada[7] then attempted to draw a general mechanism of all heterogeneous cellulose reactions, based on the idea of Hess and Trogus, by assuming that diffusion is the rate-controlling factor.   His equation is:

$$x = kt^m \tag{1}$$

where x is the degree of substitution, t is the time of reaction, and k and m are constants.   Bernoulli and co-workers[8] concluded from their benzoylation investigation that the reaction satisfies Hess and Trogus' concept of a micellar-heterogeneous reaction but not Sakurada's equation.   They claimed that Sakurada's equation should be modified by taking different constants for the accessible and inaccessible regions of the cellulose.   Miles and co-workers[9-11] also differed with Hess and Trogus, postulating that from the beginning the reagent penetrates between the chains of the cellulose in the crystallites and dilates them to such an extent that they react homogeneously.   During their study of acetylation, Kido and Kitojima[12] found that the reaction follows the Sakurada's equation, but Asada[13] proposed a bimolecular reaction.   Recently Frith[14] showed that an acid-catalyzed reaction proceeds essentially according to a first-order reaction, whereas Conrad et al.[15] found that Sakurada's equation is applicable to acetylation catalyzed by perchloric acid.   However, they noted that the rate of reaction changes abruptly when the degree of substitution (DS) is about 2.0.   Although some of the figures published by Sakurada's group[16,17] also showed two intersecting straight lines, these authors considered the slope of the second straight line to be zero, i.e., that the reaction was terminated.

Since a preliminary study of the cyanoethylation reaction of cellulose showed it to be similar to the acetylation reaction, it was further investigated with respect to Sakurada's idea of a diffusion-controlled reaction and also with respect to the fundamental theory of chemical kinetics.

EXPERIMENTAL METHODS

Samples

The cellulosic material used in the present study was in the form of cheesecloth supplied by the Kendall Company, Grinsville, Massachusetts. Unless otherwise noted, it was used without further treatment.

A sample having reduced crystallinity, hereafter referred to as "decrystallized," was prepared by treating some of the cheesecloth with ethylenediamine, extracting the product with acetone, and drying it in a nitrogen atmosphere.[18]   Application of the method of Wakelin[19] showed that the crystallinity was decreased about 25%.

Reaction Technique

For each experiment, about 1 g. of the cheesecloth was treated for 30 min. at room temperature with 6% sodium hydroxide solution containing

0.1% Alkamerse wetting agent. The samples were then passed through a pair or tight rollers under constant pressure to reduce the water content to about 70%. Each sample was then reacted with an excess of liquid acrylonitrile in a reaction tube fitted with an air condenser and placed in a water bath at a constant preselected temperature. At successive intervals, samples were taken out and the reaction stopped immediately by addition of 5% acetic acid solution. The samples were washed with flowing water and eventually with alcohol and finally dried at 50°C.

Test Methods

The degree of substitution of the reactant samples was computed from the nitrogen content determined by the Kjeldahl method.

X-ray diffractograms were recorded with a Philips Electronics, Inc., high precision diffractometer by the technique described by Conrad and co-workers.[20]

RESULTS

Effect of Temperature

The degree of substitution of the cellulose with cyanoethyl groups as a function of time at temperatures ranging from 31 to 60°C. are plotted in the logarithmic form of Sakurada's equation in Figure 1. For the early stage of the reaction, least-square lines are drawn, only points above DS = 0.2 being included. The general trend of the points in the initial reaction is indicated by the dashed lines. It is apparent from the curves that Sakurada's equation at temperatures above about 50°C. is well obeyed, except that the rate decreases abruptly when about two-thirds of
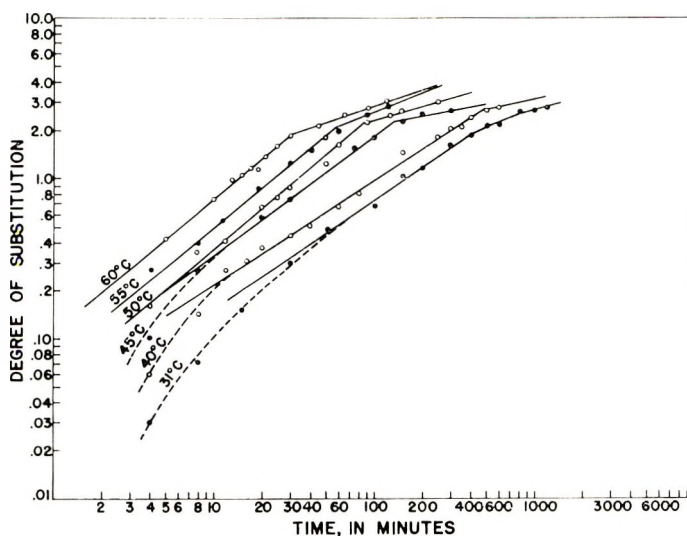
Fig. 1. Degree of cyanoethylation of cellulose as a function of time and temperature.

the cellulose hydroxyls have been reacted. The location of the point of intersection shifts towards slightly higher degrees of substitution at lower temperatures. At 31°C. no sharp change in rate occurs at the break, but the degree of substitution gradually approaches the theoretical maximum of 3. At lower reaction temperatures a deviation from linearity occurs below about DS = 0.4. While the acrylonitrile initially diffuses into the sodium hydroxide solution a condition of equilibrium sets up and then both acrylonitrile and sodium hydroxide diffuse simultaneously into the fiber. This possibly results in a rapid initial reaction followed by the Sakurada's diffusion-controlled type.

Dilution Studies

Acrylonitrile was diluted to 80% and 60% by volume with toluene and reacted at 60°C. Dilution of the reactant decreases the rate of reaction, but does not change the essential nature of the reaction which, except for the break, obeys Sakurada's equation very well (Fig. 2). In a comparable way the acrylonitrile was diluted to 80% by volume with xylene, carbon tetrachloride, and benzene, respectively, and reacted at 60°C. for different intervals of time. The results are plotted in Figure 3, the reaction with toluene being included for comparison. Pyridine was also used, but its curve was not plotted because the reaction rate was considerably faster than that for any other solvent; also, the nitrogen content was erratic, probably because the solubility of the cellulosic product in the pyridine and the degradation of the soluble ether caused further com-
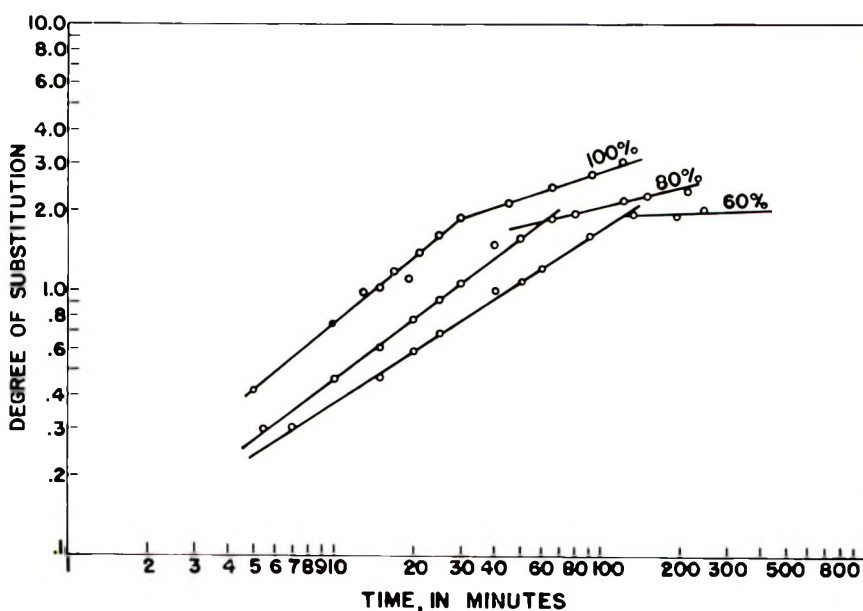
Fig. 2. Effect of dilution of acrylonitrile with toluene on the rate of cyanoethylation at 60°C.
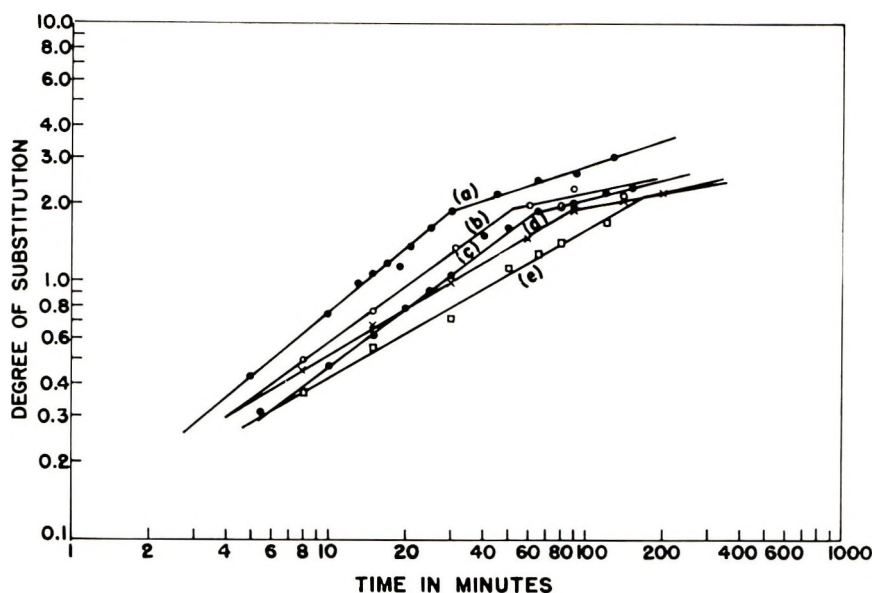
Fig. 3. Sakurada plots of the cyanoethylation of cellulose with pure acrylonitrile and with acrylonitrile diluted with 20% of different inert media: (a) pure acrylonitrile; (b) xylene added; (c) toluene added; (d) carbon tetrachloride added; (e) benzene added.

plicated reactions. Each curve in Figure 3 shows the same behavior as that of pure acrylonitrile. The time required to reach the degree of substitution at which the rate of reaction suddenly decreases, diminished in the order: benzene, carbon tetrachloride, toluene, xylene, and pyridine.

Behavior of Catalyst (Sodium Hydroxide) in the Reaction

A 6% sodium hydroxide solution was chosen as catalyst for the reaction because it gives highest efficiency with a minimum amount of by-products.[21] Also, the present results were correlated with earlier work on cyanoethylation.[20] According to Sisson and Saner,[22] the sodium hydroxide solution at that concentration does not penetrate beyond the amorphous region of the fiber, and thus the catalyst remains nonuniformly distributed in the fiber.

In order to distribute the catalyst more uniformly throughout the fiber, keeping the concentration of the catalyst about the same, the following attempt was made. The fibers were first mercerized by treating them with 17.5% sodium hydroxide, squeezing out the excess sodium hydroxide solution, and then treating them further with 6% sodium hydroxide solution for 24 hr. with continuous shaking. The solution was changed two or three times to lower the concentration of the sodium hydroxide absorbed by the fibers to about 6%. This process was expected to distribute the catalyst more homogeneously throughout the fiber. The treated sample was then reacted with acrylonitrile at 50°C. In Figure 4 are shown the resulting data which do not obey Sakurada's equation closely below DS = 1.3. When
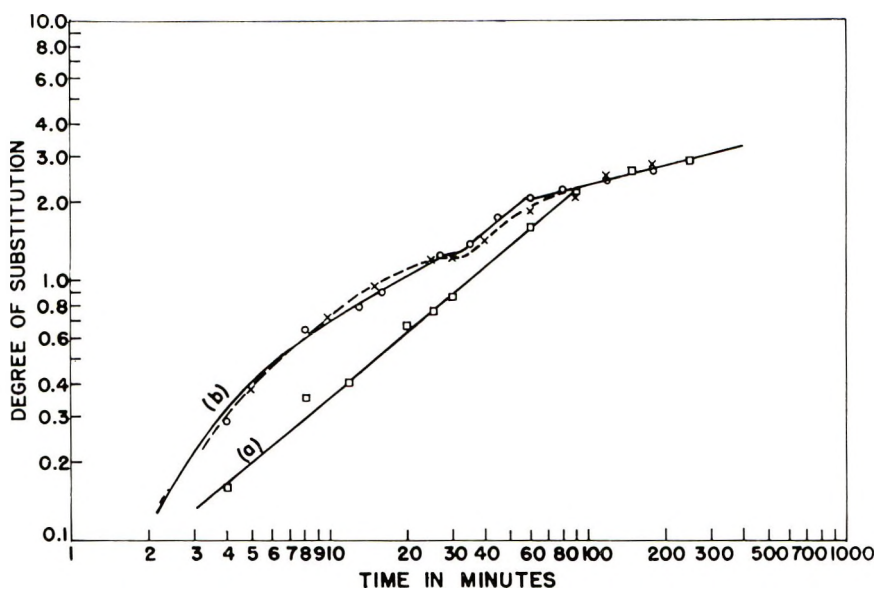
Fig. 4. Sakurada plot of degree of cyanoethylation of cellulose with acrylonitrile in 6% sodium hydroxide: (a) before and (b) after mercerization.

this experiment was repeated, an exact point-to-point reproduction of the curve was not achieved, as shown by the dotted line in Figure 4, but the course of the curve remained the same.

However, above DS = 2.0, the plot coincides with the straight line obtained for unmercerized fibers. It was thought that acceleration of the reaction during the first stage could have been due to the fact that the concentration of the sodium hydroxide had not dropped to exactly 6%, as had been intended.

Plots in Figure 4 for the mercerized fibers above DS = 1.3 could possibly be fitted to two straight lines intersecting at or in the vicinity of DS = 2.0. The deviation from Sakurada's equation which appears below DS = 1.3 for mercerized fibers presumably corresponds to that below DS = 0.4 for unmercerized fibers at the lower reaction temperatures (Fig. 1). In the latter case the deviation is assumed to be due to the predominancy of the reaction in the amorphous regions. Acrylonitrile diffuses into these regions already saturated with sodium hydroxide and thereby accelerates the reaction. The observation with mercerized fibers shows that since the catalyst is already distributed in regions that were previously crystalline, a reaction similar to that in the amorphous regions becomes significant and extends to a greater portion of the fiber. At this point one should also consider that a certain amount of the swollen crystalline region would collapse and recrystallize when the concentration of sodium hydroxide was lowered, or when the temperature increased at the time of reaction.[23] A certain amount of crystallinity might also be expected due to the formation of sodium cellulosate under the above conditions.

The behavior of the catalyst was further studied by treating the sample with 6% and 20% solutions of sodium hydroxide and reacting the wet or dry samples with acrylonitrile at 50°C. The results confirmed the expectation that the reaction in the presence of the undried catalyst is normal but is practically nil in samples that have been dried before reaction or in which the catalyst is absent.

Effect of Reducing the Crystallinity of the Fiber

When a decrystallized sample was reacted with acrylonitrile at 50°C. under the same conditions used for those not decrystallized, the reaction was accelerated, particularly during the first part of the reaction. However, no change in the nature of the reaction course was observed (Fig. 5). The fibers of reduced crystallinity follow the same course of reaction as was found with the nondecrystallized samples, except that the point of transition of rate has been lowered by 0.2 DS, a result assumed to be associated with the decreased amount of crystallinity in this sample.
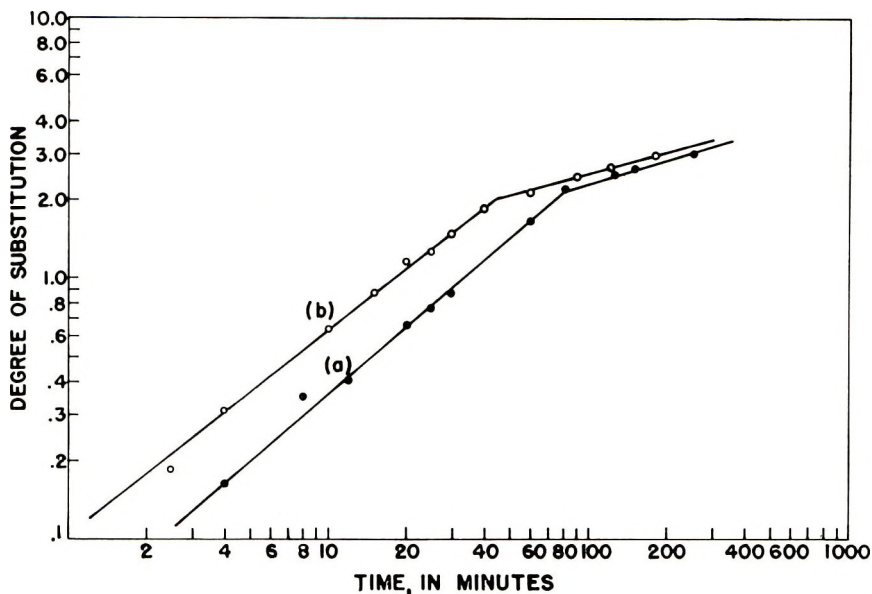
Fig. 5. Sakurada curves for cyanoethylation of cellulose: (*a*) normal fiber; (*b*) decrystallized fiber.

X-Ray Diffraction Study

The diffractograms of the decrystallized samples treated with ethylenediamine to reduce the crystallinity and then reacted at 50°C. showed a decrease of the 002 interference at $2\theta = 22.6°$, with increasing substitution (Fig. 6). The sample having a DS = 1.85 still shows some cellulose crystallinity, whereas the diffractogram of the sample substituted to DS = 2.1 resembles that of the amorphous cellulose. A comparison of the diffracto-
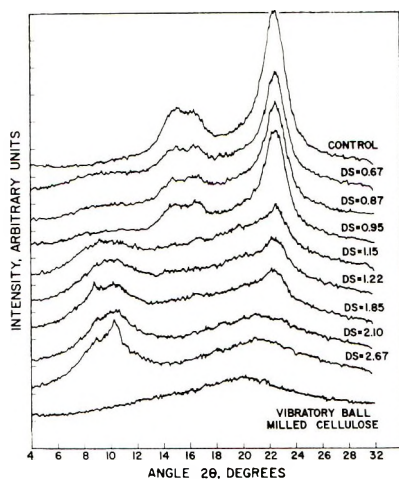
Fig. 6. X-ray diffractograms of cyanoethylated cellulose prepared from decrystallized cotton and reacted at 50°C. to different degrees of substitution.
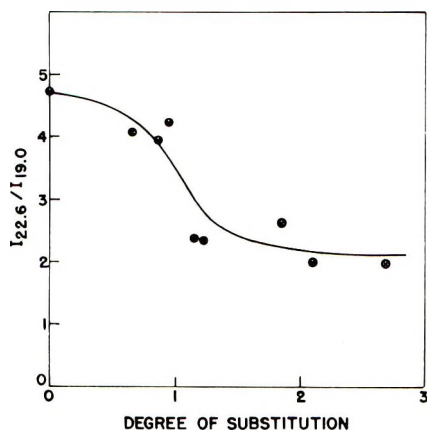

Fig. 7. Relation of relative intensity of the 002 interference of the decrystallized sample to degree of substitution.

grams with the curves of Figure 5 reveals that the rate of substitution changes abruptly when the cellulose crystalline structure is lost. The reduction of the peak height is evident at DS = 0.67, also. Of course, the dilution caused by the substituted groups may have some effect on the diffractograms. Therefore, the ratio of the height of the diffractograms at 22.6° to that at 19.0°, corrected for dilution caused by substituted groups, as suggested by Conrad and co-workers,[24] has been plotted against the degree of substitution in Figure 7. A nonuniform decrease of the crystallinity has been observed but it could be inferred that the crystalline portion reacts from the very beginning. In the present case a reduction of initial crystallinity by the diamine treatment may have induced some structural instability, which could cause a nonuniform reaction.

The rapid fall of intensity of the 002 interference band observed at about DS = 1.15, is similar to that observed in undecrystallized fibers by Conrad et al.,[20] but their observation that up to DS = 1.0 only amorphous cellulose reacts does not seem to be confirmed in the present case. However, their finding that a new peak developed at $2\theta = 10.4°$ was corroborated by the present research.

The diffractograms of samples obtained by reacting purified, but not decrystallized, cellulose with acrylonitrile at 40°C. showed similarity to the diffractograms in Figure 6, except that the complete loss of cellulose crystallinity occurred at about DS = 2.41. This result is further evidence that the abrupt fall in the substitution rate which occurs at DS = 2.45 at this temperature (Fig. 1) is associated in some way with the change of crystal structure and not with the particular degree of substitution value. The development of the peak at $2\theta = 10.4°$ was evident in this case also.

Kinetic Treatment of the Cyanoethylation of Cellulose

It has been observed that the plots of the degree of cyanoethylation of cellulose against the time of reaction are not linear at any temperature. Evidently the reaction always behaves as a higher than pseudo zero-order reaction. A first-order treatment of the reaction based on number of unreacted hydroxyl groups is plotted in Figure 8. Initially all reactions are fast, showing some concavity toward the time axis. As the temperature is raised from 31 to 60°C., the order of reaction changes from less than one
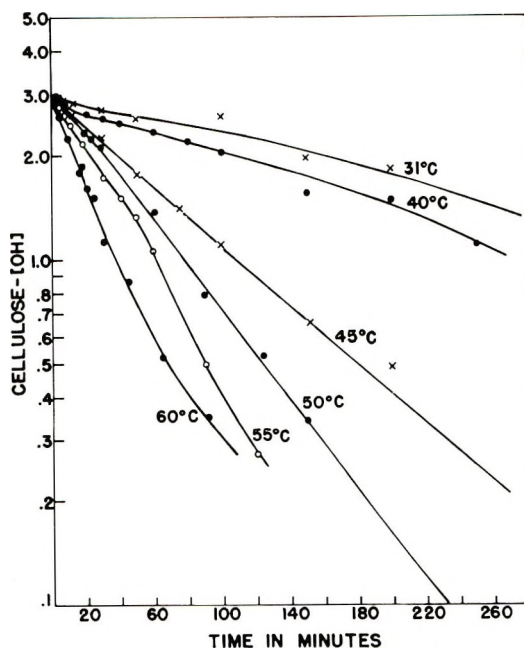

Fig. 8. Degree of substitution of cellulose as functions of time and temperature treated as a first-order reaction with respect of cellulose hydroxyls.
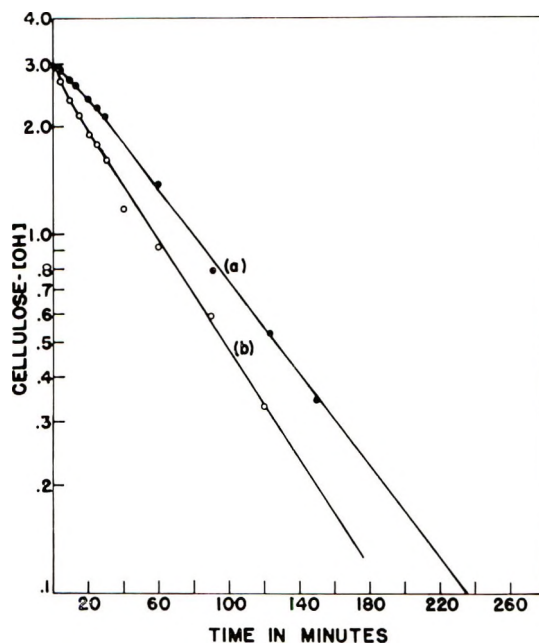
Fig. 9. Reaction of cellulose hydroxyl groups at 50°C. treated as a first-order reaction for: (a) normal fibers; (b) decrystallized fibers.
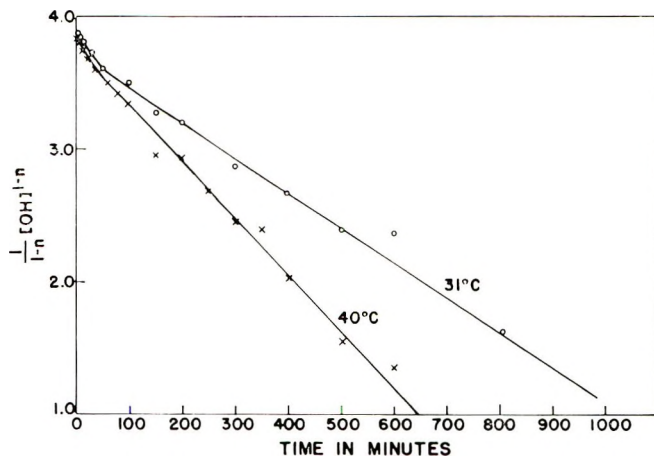

Fig 10. Cyanoethylation of cellulose at 31 and 40°C. treated as a 0.6-order reaction.

to greater than one. The transition region is 45–50°C., for which the curves indicate almost pseudo first-order reactions. Although the decrystallized sample made by the ethylenediamine treatment reacts faster, its kinetics at 50°C. is similar to that of the reaction with the untreated fiber (Fig. 9).

To determine the exact order between 31 and 40°C., a series of kinetic plots assuming various fractional orders in the general kinetic equation

between 0 and 1 were examined and found to fit with a 0.6 order. The order was then confirmed by measuring the rate of reaction of the hydroxyl groups at 40°C. at several points on the curve. A logarithmic plot of the rate versus corresponding hydroxyl concentration gave a straight line. The order of reaction determined from the slope of the straight line was found to be 0.59. This result is approximately the same as that obtained by the trial-and-error method. A 0.6th-order kinetic plot is shown in Figure 10. The orders of reaction at 55 and 60°C. were found to be 1.1 and 1.5, respectively. The dependence of order of reaction on the temperature indicates that the chemical reaction is affected by another factor, presumably diffusion. Table I shows the specific reaction rate depending on the order of reaction. Energy of activation has also been calculated for two different temperatures at which the orders were found to be the same.

TABLE I
Reaction Constants

Temp., °C.	Order of reaction n	Rate of reaction	Energy of activation, kcal./mole
31	0.6	$k[OH]^{0.6} = 2.59 \times 10^{-3}$	10.6
40	0.6	$k[OH]^{0.6} = 4.27 \times 10^{-3}$	
45	1.0	$k[OH]^{1.0} = 1.85 \times 10^{-3}$	16.7
50	1.0	$k[OH]^{1.0} = 2.82 \times 10^{-3}$	
55	1.1	$k[OH]^{1.1} = 17.23 \times 10^{-3}$	
60	1.5	$k[OH]^{1.5} = 25.0 \times 10^{-3}$	

Relation Between the Energy of Activation and Sakurada's Constants

The relationship between m, k, and T was investigated between the temperatures 31 and 60°C. The m and k values were determined from the first part of the straight line in the Sakurada plot (Table II and Fig. 1). Differentiation of Sakurada's equation gives:

$$dx/dt = m\, k^{1/m} x^{1-1/m} \qquad (2)$$

TABLE II
Effect of Temperature on Constants of Sakurada's Equation

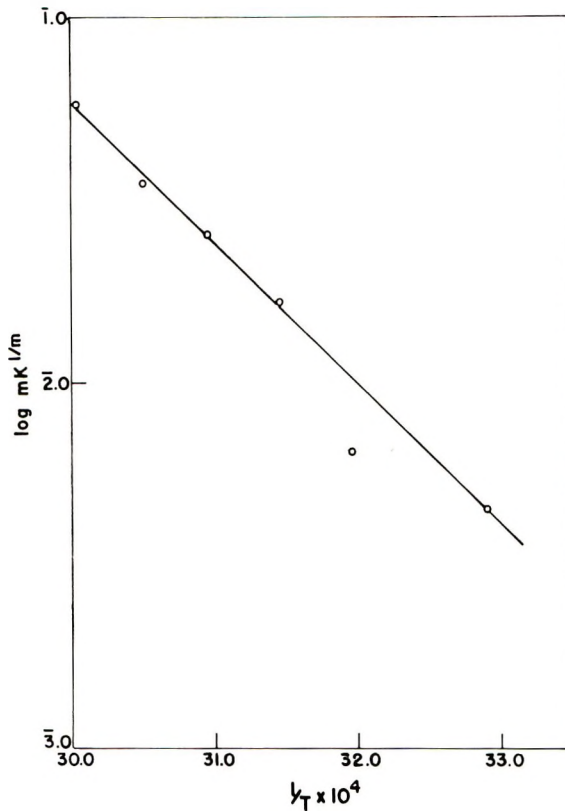| Temp., °C.	m	k	Position of rate change	Approximate calculation of rate constants $mk^{1/m}$	Energy of activation, kcal./ mole
31	0.67	0.035	No sharp change	0.0045	
40	0.66	0.047	DS = 2.60, time = 450 min.	0.0064	8.6
45	0.75	0.057	DS = 2.30, time = 135 min.	0.165	
50	0.83	0.056	DS = 2.2, time = 80 min.	0.0258	17.6
55	0.82	0.076	DS = 2.05, time = 56 min.	0.0354	
60	0.83	0.110	DS = 1.90, time = 30 min.	0.0581	

Fig. 11. Correlation between Sakurada's equation and temperature.

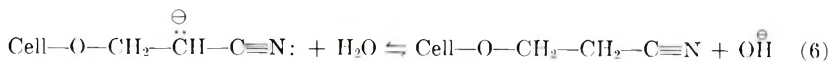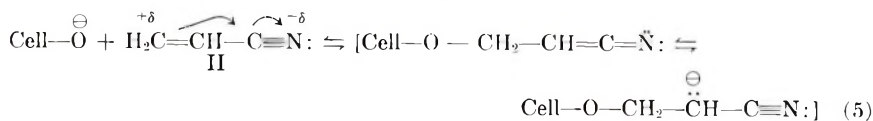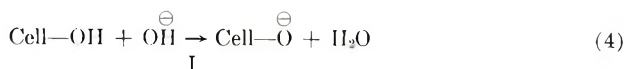If Arrhenius' equation is also applicable in this case, the equation takes the form:

$$mk^{1/m} = Ae^{-E/RT} \tag{3}$$

Thus, a plot of log $mk^{1/m}$ against $1/T$ should be a straight line if these assumptions are correct.

Figure 11 shows the relationship between Sakurada's equation and temperature. The slope of the straight line, obtained in Figure 11 gives the value of the energy of the activation as 17.6 kcal./mole, which is close to the value obtained by the individual kinetic plots. Although the plots are linear, a deviation appears at 40°C. The energy of activation calculated between 30 and 40°C., from the slope of the straight line joining these two points gives a value of 8.6 kcal./mole, which is comparable to that obtained by the previous method.

Mechanism of the Cyanoethylation Reaction

The reaction between cellulose and acrylonitrile is assumed to take place according to the mechanism shown in eqs. (4)–(6).[25]

$$Cell\text{—}OH + \overset{\ominus}{O}H \rightarrow Cell\text{—}\overset{\ominus}{O} + H_2O \qquad (4)$$
$$I$$

$$Cell\text{—}\overset{\ominus}{O} + \overset{+\delta}{H_2}C\text{=}CH\text{—}\overset{-\delta}{C}\text{≡}N: \rightleftharpoons [Cell\text{—}O\text{—}CH_2\text{—}CH\text{=}C\text{=}\ddot{N}: \rightleftharpoons$$
$$II$$
$$Cell\text{—}O\text{—}CH_2\text{—}\overset{\ominus}{C}H\text{—}C\text{≡}N:] \quad (5)$$

$$Cell\text{—}O\text{—}CH_2\text{—}\overset{\ominus}{\ddot{C}}H\text{—}C\text{≡}N: + H_2O \rightleftharpoons Cell\text{—}O\text{—}CH_2\text{—}CH_2\text{—}C\text{≡}N + \overset{\ominus}{O}H \quad (6)$$

Therefore, during cyanoethylation of the cellulose fiber the following processes may occur: (1) capillary action, i.e., diffusion of reagent to the fine capillaries, whose walls are built of anhydroglucose chains and which are formed by rupturing the hydrogen bonds during the reaction; (2) reaction according to eq. (4); (3) reaction of the product (I) with (II). Since this step is very rapid, the reaction is governed by (1) or (2) or by both, depending upon the reaction conditions.

The intermolecular spacings in the crystalline regions are not only smaller than those of the amorphous regions but also more highly hydrogen-bonded. Therefore, initially, the catalyst remains localized in the amorphous regions and the reaction is predominantly there. But at the same time, various points on the surface of the crystalline region are also attacked by the reagent, which, by rupturing hydrogen bonds, opens the crystalline portion. As capillaries are produced here, both reagent and catalyst can penetrate and diffuse further into the crystalline region. Since acrylonitrile is only partially soluble in sodium hydroxide solution, the two liquid phases diffuse simultaneously. Sodium hydroxide thus progessively spreads throughout the fiber.

As the reaction proceeds inward, the crystalline portion of the cellulose I decreases; when the reagent completely diffuses through it, cellulose I completely disappears. At this stage, equilibrium swelling occurs: at 60°C., this condition is reached at a DS = 1.9, at 45°C. at a DS = 2.45. Thus it cannot be assumed that the whole path becomes immediately saturated with the substituted product as the reagent travels through the part. Only at 31°C., both an equilibrium stage of diffusion and saturation of the path with the substituted product possibly takes place at the same time.

As soon as the diffusion of liquid reaches swelling equilibrium, the sodium hydroxide also tends toward an equilibrium concentration throughout the reaction system by diffusing from the fiber to the bulk of the reagent in the reaction vessel. Thus, the total concentration of catalyst in the fiber is decreased. Since cyanoethylation is dependent on the catalyst, this fall in its concentration must be responsible for the abrupt decrease in the reaction rate. Further, it could be observed in Figure 1 that the points do not fit the straight line at lower temperatures as closely as at temperatures above 50°C. Such a deviation can be accounted for by considering the hypothesis on which Sakurada's equation is based.

For an instantaneous reaction in gels containing simple capillaries, the rate equation is:

$$dl/dt = k/l \tag{7}$$

where l is the length of the capillary. If the structure of the fiber is considered to be similar to that of a gel—except for the nature of capillaries, which are considered here to be strongly hydrogen-bonded in the fiber—the rate of diffusion in the fiber can be written as:

$$dl/dt = kl/l^n \tag{8}$$

where n is associated with the rupture of hydrogen bonds, as has been discussed.

Sakurada then derived eq. (1) by assuming that the path traversed by the reagent was equivalent to the degree of substitution. This assumption can be made only if the reaction is instantaneous, which could only happen at a sufficiently high temperature. As the temperature is lowered, the rate of the chemical reaction falls more rapidly than does the rate of diffusion. The chemical reaction probably falls twice as fast as does diffusion, since the temperature coefficient of diffusion of many solvent–polymer systems is 1,[26] whereas the temperature coefficient of most chemical reactions is 2. Thus, at optimum temperature, both rates would become essentially equal, but below that temperature level diffusion would no longer act as the slowest or rate-governing step. But at lower temperatures also diffusion cannot proceed faster than the chemical reaction in the present system because the reagent cannot penetrate unless hydrogen bonds break, and the breaking of hydrogen bonds, in turn, depends upon chemical substitution. It is, therefore, to be expected that the resulting complex reaction mechanism would deviate from Sakurada's equation at low temperatures.

References

1. Meyer, K. H., and H. Mark, Z. Physik. Chem., **B2**, 695 (1929).

2. Mark, H., J. Soc. Dyers Colourists, **49**, 54 (1932).

3. Herzog, R. O., and G. Londberg, Ber., **57**, 329 (1924); J. Phys. Chem., **30**, 457 (1926).

4. Atsuki, K., and N. Ishii, J. Soc. Chem. Ind. Suppl. Japan, **34**, 331B (1931); ibid., **35**, 79B (1932).

5. Bernoulli, A. L., M. Schenk, and W. Hagenbuch, Helv. Chim. Acta, **13**, 534 (1930).

6. Hess, K., and C. Trogus, Z. Physik. Chem., **B15**, 157 (1931); ibid., **B12**, 268 (1931).

7. Sakurada, I., Cellulose Chem., **15**, 3 (1934).

8. Bernoulli, A. L., M. Schenk, and F. Rohner, Helv. Chim. Acta, **17**, 897 (1934).

9. Miles. F. D., Trans. Faraday Soc., **29**, 7, 110 (1933).

10. Miles, F. D., and J. Craik, *Nature*, **123**, 82 (1929).

11. Miles, F. D., and M. Milbourn, *J. Phys. Chem.*, **34**, 2598, 2607 (1930).

12. Kido, I., and H. Kitojima, *J. Soc. Textile Cellulose Ind., Japan*, **8**, 228 (1952).

13. Asada, K., *J. Soc. Textile Cellulose Ind., Japan*, **8**, 134 (1952).

14. Frith, W. C., *Tappi*, **46**, 739 (1963).

15. Conrad, C. M., P. Harbrink, and A. L. Murphy, *Textile Res. J.*, **33**, 784 (1963).

16. Nakashima, T., H. Nakahara, and I. Sakurada, *J. Soc. Chem. Ind. Japan*, **39B**, 51 (1936).

17. Sakurada, I. E., and Y. Tokuno, *J. Soc. Chem. Ind. Japan, Suppl.*, **40**, 77B (1937).

18. Loeb, L., and L. Segal, *J. Polymer Sci.*, **15**, 343 (1955).

19. Wakelin, J. H., H. S. Virgin, and E. Crystal, *J. Appl. Phys.*, **30**, 1654 (1959).

20. Conrad, C. M., D. J. Stanonis, P. Harbrink, and J. J. Creely, *Textile Res. J.*, **30**, 339 (1960).

21. Weaver, J. W., E. Klein, B. G. Webre, and E. F. DuPre, *Textile Res. J.*, **24**, 518 (1954).

22. Sisson, W. A., and W. R. Saner, *J. Phys. Chem.*, **45**, 717 (1941).

23. Ott, E., H. M. Spurlin, and M. W. Grafflin, *Cellulose and Cellulose Derivatives*, Part I, Interscience, New York, 1963, p. 284.

24. Conrad, C. M., and J. J. Creely, *J. Polymer Sci.*, **58**, 781 (1962).

25. Grant, J. N., L. H. Greathouse, J. D. Reid, and J. W. Weaver, *Textile Res. J.*, **25**, 76 (1955).

26. Freundlich, H., *Colloid and Capillary Chemistry*, English Ed., Methuen, London, 1926, p. 696.

Résumé

On a appliqué l'equation de Sakurada et les lois cinétiques fondamentales à la cyano-éthylation hétérogène de la cellulose effectuée par réaction de la fibre avec l'acrylo-nitrile liquide, l'hydroxyde de sodium servant de catalyseur. Les résultats obtenus aux températures plus élevées sont en meilleur accord avec l'équation de Sakurada; des écarts se produisent au début de la réaction et la vitesse diminue brusquement dans une phase ultérieure. Le degré de substitution, pour lequel cette variation brusque se produit, diminue quand la température passe de 31 à 60°C et quand la cristallinité de la fibre décroît. La dilution du réactif par différents solvants abaisse la vitesse de réaction et fait varier le point de transition mais n'altère pas la nature essentielle de la réaction dont chaque étape répond fort bien à l'équation de Sakurada. On s'est efforcé de distribuer uniformément le catalyseur au sein de la fibre et on a étudié la réaction à 50°C. Des diagrammes de diffraction des échantillons apportent une preuve supplémentaire du fait que la variation de vitesse est liée à un changement dans la structure cristalline de la cellulose. À partir des constantes de vitesse spécifiques, on a calculé approximativement l'énergie d'activation qui est de 10,6 Kcal entre 31 et 40°C et de 16,7 Kcal entre 45 et 50°C. Aux autres températures, on n'a pas pu la déterminer par suite d'une dépendance de l'ordre de réaction vis à vis de la température. On a cherché une relation empirique entre les constantes de l'équation de Sakurada et la température de réaction et on l'a reliée à l'équation d'Arrhénius. Les énergies d'activation déterminées de cette façon sont très proches des valeurs signalées plus haut. La variation de l'ordre de la réaction avec la température fait supposer que la réaction est influencée par la diffusion et on suggère un mécanisme de réaction contrôlé par la diffusion où les liens "hydrogènes" jouent un rôle important.

Zusammenfassung

Die Gleichung von Sakurada sowie die fundamentalen kinetischen Gesetze wurden auf die heterogene, durch Reaktion der Faser mit flüssigem Acrylnitril mit Natriumhydroxyd als Katalysator durchgeführte Cyanoäthylierung der Zellulose angewendet. Bei hoher Temperatur entsprachen die Ergebnisse der Gleichung von Sakurada besser. Abwei-

chungen traten im Anfangstadium auf, und in einem späteren Stadium fällt die Reaktions-
geschwindigkeit plötzlich ab. Der Substitutionsgrad, bei welchem die plötzliche Ge-
schwindigkeitsänderung auftrat, nahm mit Ansteigen der Temperatur von 31 auf 60°C
und auch mit abnehmender Kristallinität der Faser ab. Eine Verdünnung des Reagens
mit verschiedenen Lösungsmitteln setzte die Reaktionsgeschwindigkeit herab und än-
derte ihren Übergangspunkt; es trat jedoch keine Änderung des wesentlichen Charakters
der Reaktion auf, da jeder Abschnitt sehr gut der Gleichung von Sakurada entsprach.
Eine gleichförmige Verteilung des Katalysators (Natriumhydroxyd) in der Faser wurde
angestrebt und dann die Reaktion bei 50°C untersucht. Streudiagramme der Proben
lieferten weitere Belege dafür, dass die Lage der Geschwindigkeitsänderung mit der Än-
derung der Zellulose-(I)-kristallstruktur verknüpft ist. Ein angenäherter Wert der
Aktivierungsenergie wurde aus den spezifischen Geschwindigkeitkonstanten zwischen
31 und 40°C zu 10,6 und zwischen 45 und 50°C zu 16,7 kcal berechnet. Bei anderen
Temperaturen wurde die Bestimmung durch die Temperaturabhängigkeit der Reakti-
onsordnung verhindert. Eine empirische Beziehung zwischen den Konstanten der
Sakurada-Gleichung und der Reaktionstemperatur wurde aufgestellt und in Korrelation
zur Arrheniusgleichung gesetzt. Die aus dieser Beziehung bestimmten Aktivierungsen-
ergien lagen sehr nahe bei den oben angegebenen Werten. Die Änderung der Reaktion-
sordnung mit der Temperatur spricht dafür, dass die Reaktion durch eine Diffusion be-
einflusst wird, und ihr Mechanismus wird als der einer diffusionskontrollierten Reaktion
mit einer signifikanten Rolle der Wasserstoffbindungen bei der Diffusion interpretiert.

Precise Molecular Weight Distributions of High Polymers by Semiautomatic Solvent Extraction

RODNEY E. HARRINGTON* and P. GARTH PECORARO, *Department of Chemistry, University of Arizona, Tucson, Arizona*

Synopsis

It has been found practical to fractionate relatively monodisperse polystyrenes of molecular weights up to 4×10^6 by using a semiautomatic solvent extraction procedure. The fractionators consist of flow-through mixing chambers provided with settling regions for the removal of finely suspended solid material. Provision is made for accurate control of both temperature and solvent–nonsolvent ratio. Two such apparatus, operated in tandem, were used in the present work; in principle, several more stages could be employed if desired for most polymer systems. Results on polystyrenes prepared in well defined ways appear to be in good agreement with predicted distributions. Applicability to other polymer systems is discussed.

Fractional solution methods[1] of high polymer fractionation have the important advantage that the low molecular weight "tail effect" is almost always substantially reduced or eliminated altogether. Nevertheless, they have not been widely used because of a number of serious practical difficulties, of which one of the most important is the excessive time required in most cases for equilibration to occur.

Several modifications of fractional solution methods have been widely used. Among these are the direct extraction of a polymer in equilibrium with a large volume of solvent–nonsolvent mixture of appropriate concentrations, the extraction from a packed column,[2,3] and a variant of this, the direct extraction from a film,[4] and coacervation.[5] Of these, the last is of more limited utility, in that not all polymers form coacervates. Film extraction and extraction from a packed column substantially reduce equilibration time, and packed columns lend themselves well to automatic or semiautomatic operation,[6] but these columns are difficult to use, particularly for higher molecular weight systems, and are not always entirely free of surface adsorption effects.[3] Direct extraction methods have the important advantage that, provided equilibrium is attained, no effects other than solubility enter, and no preliminary treatment of any kind need be given the polymer. However, attainment of equilibrium is extremely slow for high polymers, and large volumes of solvent–nonsolvent mixtures are

* Present address: University of California, Davis, California, 95616. Inquiries and correspondence should be directed to this address.

required for sharp fractions, thereby limiting the amount of material that can be conveniently handled at one time. These factors, and the problem of accurate temperature control, have severely limited the usefulness of direct extraction in the past. They can be easily overcome, however, by automating the method and by making explicit provision for close control of the important thermodynamic variables.

We describe here the use of a device which successfully automates the key aspects of the fractional solution method. We have been able to obtain quite precise fractionations of polystyrene up to several million in molecular weight without appreciable tail effect and without having to subject the polymer to any prior treatment except precipitation from solution. The fractionator is furthermore capable of handling relatively large samples of polymer. We have used as much as 1.4 g. of the high molecular weight, relatively monodisperse polystyrene described below and could have conveniently used larger amounts of lower molecular weight material. This permits the fractionators to be used both for preparative and analytical purposes; in the case of the latter, the method permits more fractions to be obtained on a given polymer sample (reduction of fraction size) without sacrifice of analytical accuracy.

Although polystyrene was chosen for the present study because of the ease of preparation of this polymer in relatively monodisperse form with a characteristic distribution of molecular weights, the method would appear to be entirely applicable to most polymers for which convenient solvents and precipitants exist. We are currently using the method for the solvent extraction fractionation of high molecular weight DNA; the results of these studies will appear in a forthcoming publication.

EXPERIMENTAL

Apparatus

A schematic of the entire automatic fractionator assembly is given in Figure 1. Essential details of the fractionator units themselves have been described previously;[7] the slightly modified versions used in the present work are shown in Figure 2. These units consist basically of a lower mixing chamber where the fractionation actually occurs and an upper settling chamber for small particles of solid polymer carried by the fluid flow into this region. The chambers are separated by a constriction to minimize agitation of the fluid in the upper region. In our apparatus, this constriction was given an hourglass shape as shown to avoid entrapment of air at this point. (Many polymers, including polystyrene, become gummy as they approach their solution points, and after having settled from the upper chamber, tend to cling to the upper surface of this constriction. In extreme cases, this results in a blockage or near blockage of the constriction. We have found it sufficient periodically to push such polymer back into the mixing chamber with a length of glass rod inserted through the thermistor probe joint.)
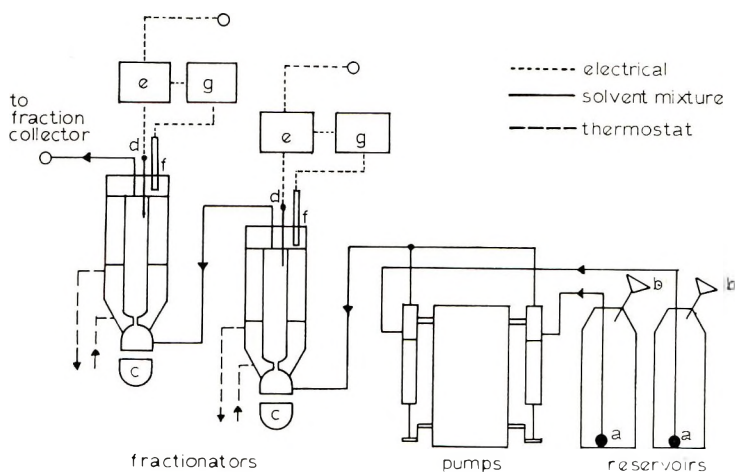
Fig. 1. Schematic of solvent extraction fractionation apparatus: (a) sintered glass prefilters (fine grade, 10 mm. diameter); (b) sintered glass reservoir funnels (coarse grade, 60 mm.); (c) magnetic stirrers; (d) thermistor probes; (e) thermistor bridge control units; (f) soldering pencil heaters; (g) 100-w. variable transformers.

The thermal gradient, established across the vacuum-jacketed portion of the settling chamber to oppose the tendency of solid polymer particles to be carried upward by the movement of the fluid, is obtained by heating the heat transfer reservoir with a small soldering tool, and is stabilized by means of a thermistor bridge control, with the probe located in the upper mixing chamber in contact with the solvent mixture near the top. The Thermistemp, Model 63RA, manufactured by Yellow Springs Instrument Co., Yellow Springs, Ohio, capable of regulating to within 0.1°C. was satisfactory here. Temperature control of the mixing chamber is considerably more critical, however, and is regulated in our apparatus to 0.01°C.

The magnitude of the thermal gradient across the mixing chamber is not critical and is determined empirically. With total flow rates on the order of 60–80 cc./hr., a 10°C. differential is found to be satisfactory in our apparatus. The magnitude of the temperature differential between the mixing chambers of the two fractionator units is much more crucial and depends upon the average molecular weight and dispersity of the polymer sample. We find that a rough solubility curve of the polymer sample, determined by titration, is nevertheless sufficient to permit an adequate assessment of this parameter. For the polymers reported here, the second stage is operated at temperatures from 2 to 8°C. below the first.

A double pump powered by a variable speed, thyratron-controlled motor (the portable vial filler, Model DAB, manufactured by National Instrument Co., Baltimore, Maryland, equipped with double stainless steel valves and 1 cc. glass syringes has proved satisfactory) simultaneously pumps benzene and methanol, mixing the two just before the first fraction-
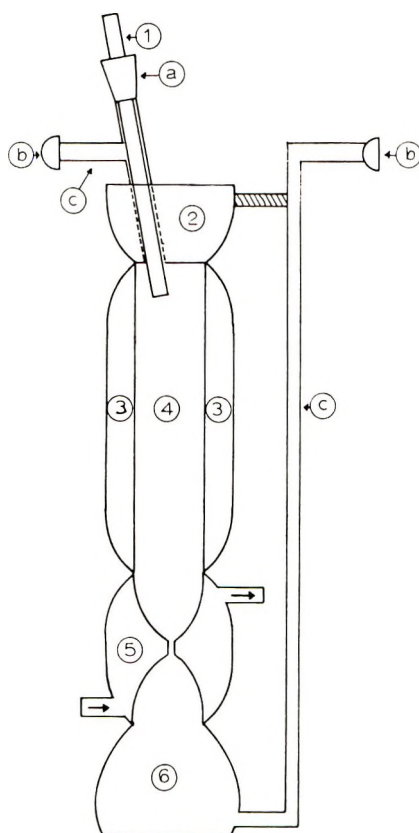
Fig. 2. Solvent extraction fractionator unit: (1) thermistor probe; (2) heat transfer medium (ethylene glycol); (3) vacuum jacket; (4) settling chamber; (5) thermostat; (6) mixing chamber; (a) 10/30 standard taper ground joint; (b) 12/1 standard taper ball-socket joint; (c) 1 mm. capillary tubing.

ator unit. In the pump used, the strokes of both syringes are separately adjustable with a locking micrometer screw, enabling the solvent–nonsolvent ratio to be set and maintained with considerable precision. The overall flow rate is set by varying the motor speed. This is independent of the ratio, unless the overall flow rate becomes so high that the constrictions to fluid flow, which are appreciably different for the two fluids, become important. Effects of this type, which arise in the prefilters and small diameter tubing and capillary used throughout the line to minimize entrapment of air bubbles, occur only at total flow rates in excess of 150 cc./hr.

Materials

The two native polystyrene samples used in these studies were prepared by living radical polymerization in the emulsion by the methods described by Bianchi et al.[8] The first (sample C) was prepared under continuous

ultraviolet irradiation at 0°C., and the viscosity-average molecular weight was 3.3×10^5. The second (sample I) was prepared by using intermittent ultraviolet light, cycled 30 sec. on followed by 6 min. off. The resulting polymer was relatively monodisperse and of quite high molecular weight (viscosity-average 3.0×10^6.)

The styrene monomer was laboratory grade, obtained from the Matheson, Coleman and Bell Division of Matheson Chemical Co., Norwood, Ohio. It was distilled at moderate temperature under vacuum immediately prior to use. Polymer sample C was prepared as follows. A 30-g. portion of styrene, 1.5 g. Dupanol (sodium lauryl sulfate), 0.3 g. $K_2S_2O_8$, and 150 g. water were placed in the polymerization flask. Water-pumped nitrogen, from which all oxygen had been removed by passage through a bed of finely divided copper heated to 600°C.[9] was bubbled through the emulsion for $1/2$ hr., after which the vessel was sealed under 3 lb./in.[2] nitrogen pressure to prevent subsequent entry of oxygen. Sample I was prepared in the same way, except that all quantities were increased by a factor of 1.3. The degraded samples were obtained by shearing the above polystyrenes in dilute toluene solution by use of a Virtis 45 macro rotary homogenizer. The double stainless-steel blade assembly and 250 ml. sample flask were used for all samples, and the motor was operated at its maximum speed of 45,000 rpm, monitored by a photoelectric tachometer. Additional details of shear degradation of polymers in high speed rotary homogenizers have been described.[10]

Procedure

The polystyrene sample is dissolved in benzene and carefully precipitated in the mixing chamber of the first fractionator. This procedure is generally found preferable to allowing the solid sample to swell in the solvent mixture, because the times required for initial equilibration of the solid material are frequently excessive. The benzene–methanol ratio is set by means of the pump stroke adjustment to an initial value slightly less than that required to elute the lowest molecular weight fractions. This ratio is estimated by careful titration at the temperature of the first mixing chamber; with a little practice, we find it possible to estimate this ratio closely enough to avoid wasting a great deal of time and solvents in getting the system to the elution point. A bypass stopcock between the pump and first fractionator permits the benzene–methanol mixture to be sampled and analyzed spectrophotometrically as required.

Block elution is used in the fractionations; the apparatus is simply allowed to run at a given benzene–methanol ratio until no more polymer is present in the eluent. Then, the ratio is increased slightly for the next fraction. Determination of the block increment, i.e., the increase in the benzene–methanol ratio between fractions, and the establishment of the various flow parameters, including total flow rate, to maintain virtual equilibrium conditions, requires considerable judgment and skill. This is particularly true for the high molecular weight, relatively monodisperse

systems studied; the lower molecular weight systems provide far less difficulty in this respect. The time required for a complete fractionation run, based on our experience, and making liberal allowances to keep the polymer always at equilibrium with the solution, ranges from a few hours for a low molecular weight material to well over a week for the high molecular weight sample I reported here.

Fractions are precipitated and redissolved in toluene, and molecular weights are determined from intrinsic viscosity by using accepted values of the Staudinger constants.[11] Polymer concentrations are in all cases determined gravimetrically. Number-average molecular weights of the polymer samples are taken as $1/2$ the viscosity-average molecular weights.

RESULTS AND DISCUSSION

The theory of polymer fractionation by solubility has been extensively discussed by Flory,[11] and essential results are briefly summarized below.

The partition factor for the distribution between two phases is obtained from the Flory-Huggins thermodynamic treatment as

$$v_x'/v_x = e^{\sigma x} \tag{1}$$

where v_x is the volume fraction of species of degree of polymerization x, σ is an algebraic function of the volume fraction of the entire polymer, the number-average degree of polymerization, and the Flory-Huggins interaction parameter, and the v'_x denotes v_x for the more concentrated phase. If V is the phase volume, the number fraction of species x in the dilute phase at equilibrium is

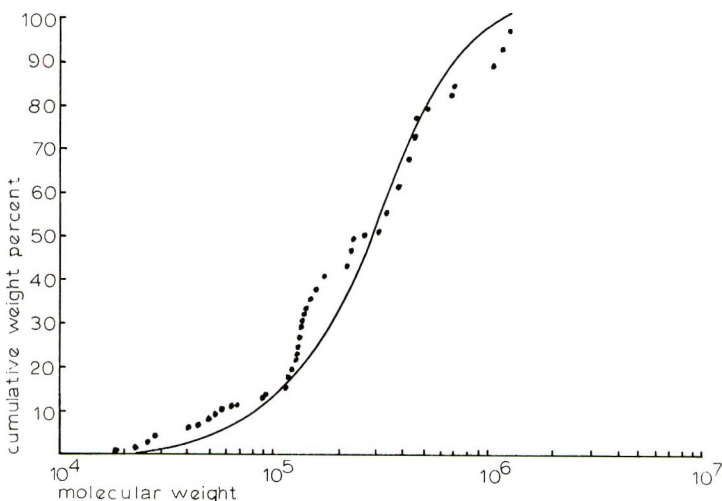$$f_x = 1/[1 + (V'/V)e^{\sigma x}] \tag{2}$$

Fig. 3. Integral molecular weight distribution curve for polystyrene sample C prepared by emulsion polymerization with continuous ultraviolet irradiation. (———)theoretical curve (see text), $<M_v> = 3.3 \times 10^5$.
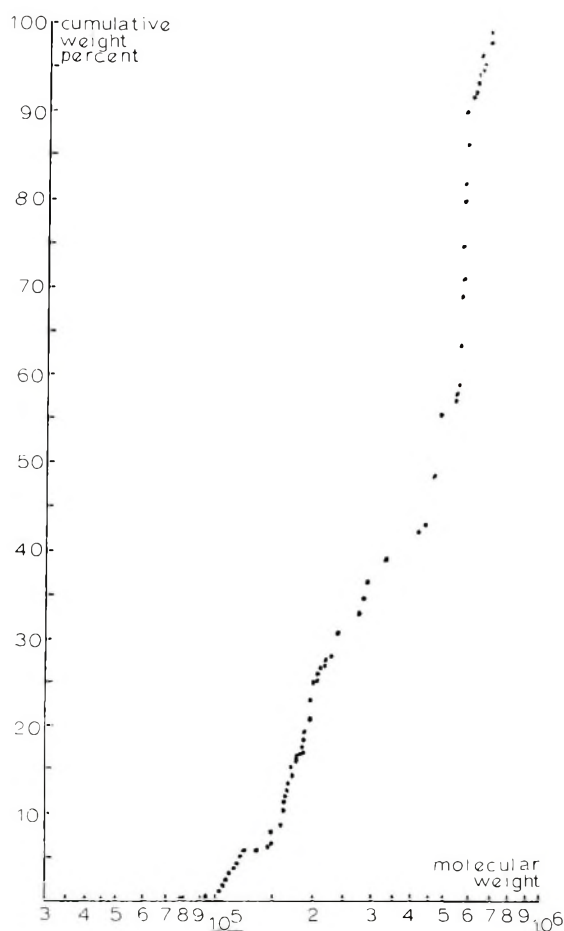
Fig. 4. Integral molecular weight distribution curve for polystyrene Sample C degraded for 5 min. in a Virtis homogenizer.

The exponential dependence of the partition factor upon molecular size operates selectively to transfer larger molecules to the concentrated phase, but if the volume of the dilute phase is very large, there will still be a favorable partitioning of lower molecular weight species in the dilute phase.

The limiting values of eq. (2) are

$$\lim_{x \to 0} f_x = V/(V + V') \tag{3}$$

$$\lim_{x \to \infty} f_x = 0 \tag{4}$$

which indicates that the number fraction of small molecules in the more dilute phase approaches unity as the dilution ratio increases. This is the so-called "tail effect" and operates to reduce the efficiency of partitioning of low molecular weight species, but is otherwise not important in solvent extraction fractionation, since low molecular weight species come off first.
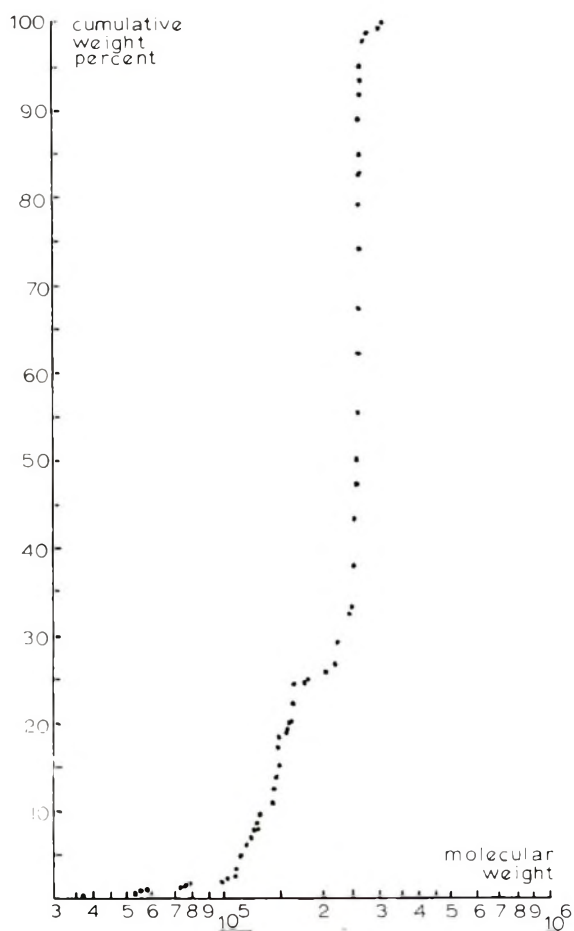
Fig. 5. Integral molecular weight distribution curve for polystyrene, sample C degraded for 360 min. in a Virtis homogenizer.

It has been established that a high dilution ratio in general favors the sharpness of the fractions.[12]   Thus, a compromise must be reached between this and the reduction of efficiency due to eq. (3) in an extraction procedure; the limiting behavior of eq. (3) also depends upon the thermodynamic parameter σ, which can be optimized by a proper choice of solvent, precipitant, and operating temperature.   For the polymer systems reported here, all of which are preponderantly of molecular weight greater than 10,[4] it is advantageous to use high dilution ratios; the ratios V'/V are typically on the order of 10^{-3}–10^{-4}, and there is no evidence of serious tailing.

Experimental results in the form of integral distributions are given in Figures 3–8.   Since the fractions are in general quite closely spaced, the midpoints of the vertical steps are plotted from the relation

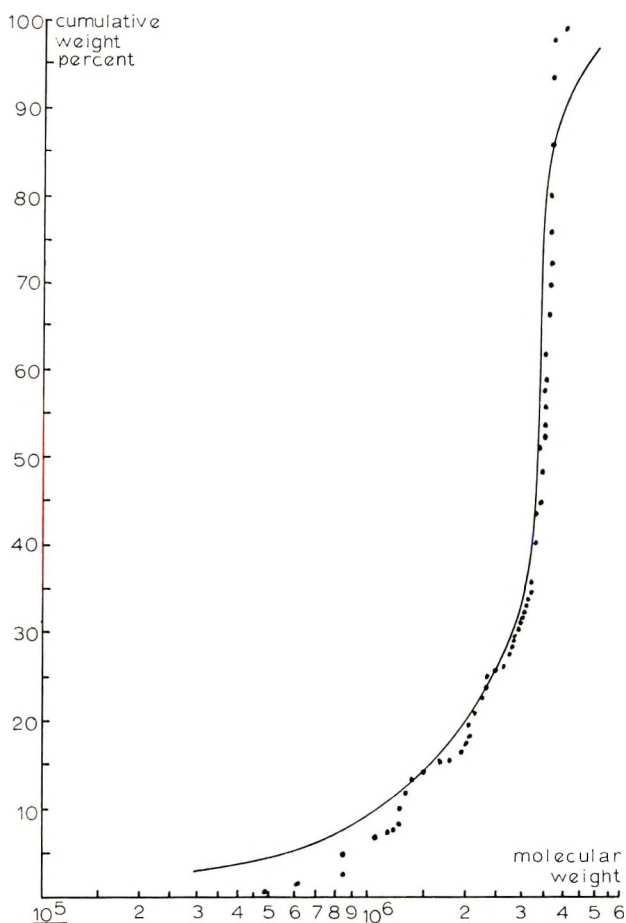$$f_i = (w_i/2) + \sum_{j=1}^{j=i-1} w_j \tag{5}$$

Fig. 6. Integral molecular weight distribution curve for polystyrene sample I, prepared by emulsion polymerization with intermittent ultraviolet irradiation: ——theoretical curve (see test); $\langle M_v \rangle = 3.0 \times 10^6$.

where w^i is the weight percentage of the ith fraction, and the summation extends over all lower molecular weight fractions. No attempt is made to draw a smooth curve through the points, however.

Theoretical distribution curves are calculated for the native polymers, and are shown as solid, smooth curves in Figures 3 and 6. Agreement between calculated and experimental distributions is satisfactory. The expected distribution for sample C in Figure 3 is the well-known "most probable" distribution[8,11]

$$dw = (M/\langle M_n \rangle^2_{av}) \exp\{-M/\langle M_n \rangle_{av}\}dM \tag{6}$$

The expected distribution of sample I (Fig. 6) is calculated according to the paper of Bianchi et al.[8]

No attempt is made to evaluate the expected molecular weight distributions of Figures 4, 5, 7, and 8. As has been pointed out in a previous
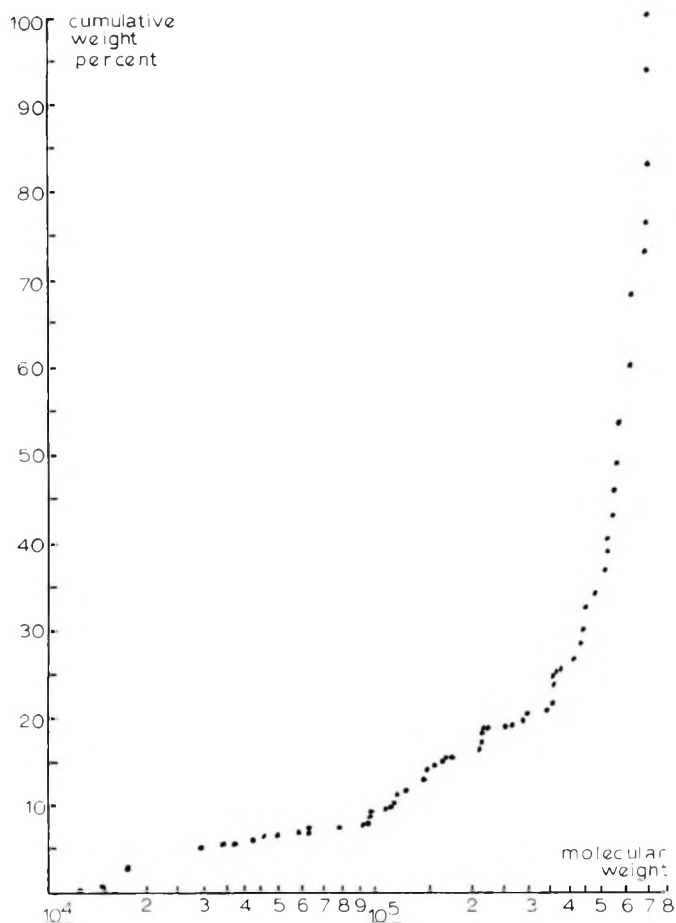
Fig. 7. Integral molecular weight distribution curve for polystyrene sample I degraded
for 30 min. in a Virtis homogenizer.

publication,[10] it is extremely difficult to interpret in a quantitative way the
degradation of polymers in rotary homogenizers, although these devices pro-
vide a practical method of degrading large quantities of material. Never-
theless, the kinetics of polystyrene degradation in rotary homogenizers
are roughly first-order in the number of bonds broken, with a time constant
on the order of several minutes, depending upon blade speed, solvent
viscosity, etc. An important degradation mechanism must therefore be
chain scission as a result of hydrodynamic forces, and if these forces are
large compared to the critical stress for bond rupture (likely to be the case
here), degradation will occur with nearly uniform *a priori* probability over
a considerable central region of the molecule.[13] This would approach the
conditions for applicability of the Montroll-Simha distribution calcula-
tions,[14] which apply strictly to an initially monodisperse polymer system
with equal *a priori* probabilities for chain scission over the length of the

molecule. These calculations predict an initial broadening of the distribution for small amounts of degradation, with the distribution sharpening up again as the degradation approaches completion.

Figures 4 and 5 are qualitatively in agreement with these ideas; the relatively broad "most probable" distribution of Figure 3 is somewhat sharpened after 5 min. of high speed shearing (Fig. 4; most of the degrada-
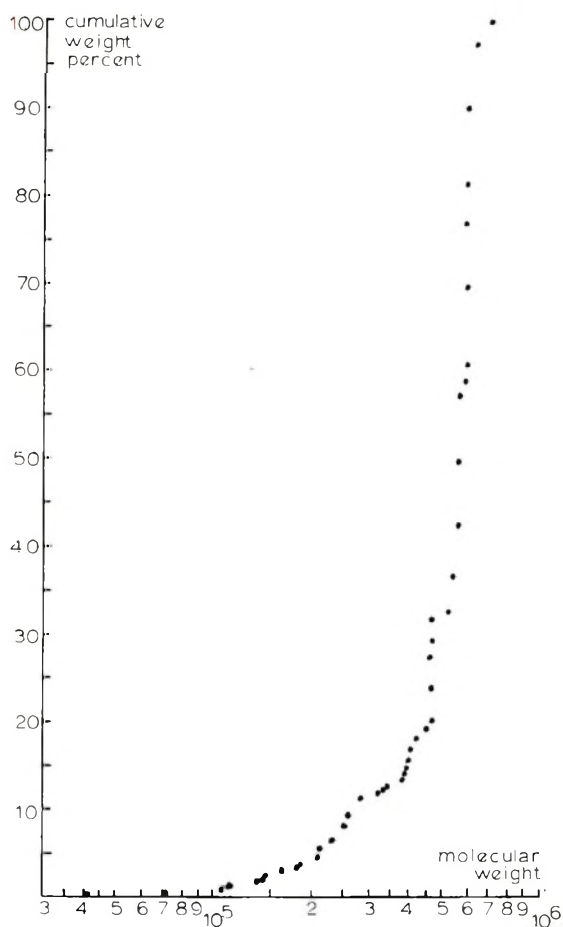

Fig. 8. Integral molecular weight distribution curve for polystyrene sample I degraded for 240 min. in a Virtis homogenizer.

tion has occurred in the high molecular weight "tail"), and the dispersion has been considerably reduced after 360 min. (Fig. 5). The same qualitative conclusions may be drawn for the initially more monodisperse sample I (Fig. 6). After 30 min. of shearing there is a considerable pile-up of lower molecular weight material (Fig. 7), but after 240 min., the low molecular weight tail has been reduced in relative size, and the monodisperse region is larger and at a lower molecular weight (Fig. 8).
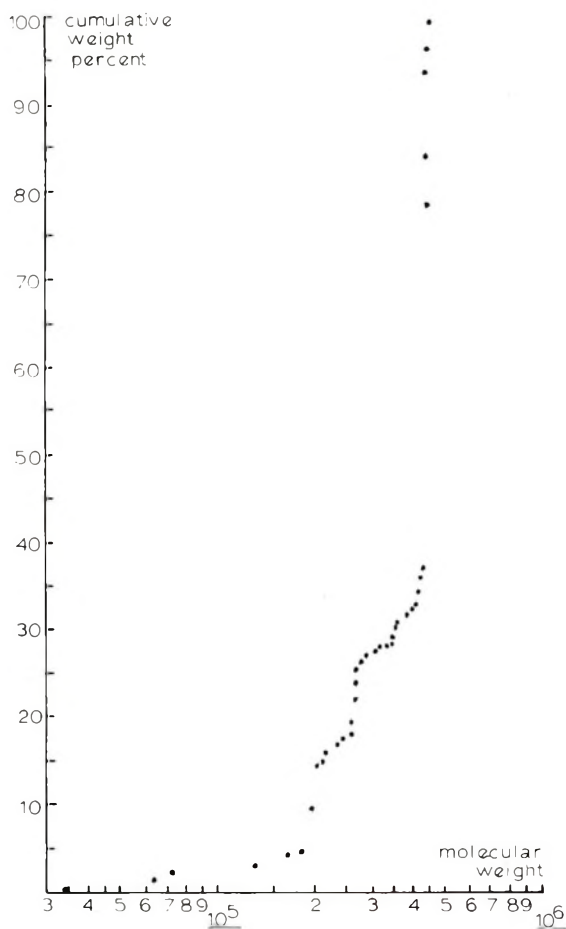
Fig. 9. Integral molecular weight distribution curve for refractionation of a fraction taken at molecular weight 5×10^5 on Fig. 4.

An attempt was made to refractionate several fractions taken near molecular weight 5×10^5 of Figure 4. Since these fractions were so closely spaced, the total amount of material available in each was small, and it was impossible to characterize the distributions within these fractions with an accuracy comparable to that of the total distribution. The results of one of these refractionations are given in Figure 9 and are certainly in good qualitative agreement with the conclusions of Schulz[15] on the dispersity of a higher molecular weight fraction of a distribution. Because of the uncertainty in both the data and the exact form of the distribution of Figure 4, we make no attempt to place this argument on a more quantitative basis.

We have made no attempt to conduct fractionation by means of temperature reduction at constant solvent composition. This would have been more difficult to do with our double fractionators, as it would have required

the simultaneous programming of four separate temperature control devices. However, for a single fractionation stage, thermal fractionation might in some circumstances be preferable and provide a greater degree of control over the thermodynamic variables of the system than the method described here. Similarly, it is possible to operate the fractionators with a single-stage pump and a single reservoir. The solvent mixture must be prepared in the reservoir. The advantage of the double-pump system is that, in event of an accidental "overshoot" of mixure ratio on the part of the operator, correction can be made easily and accurately from a knowledge of the volumes of the fractionators, the total flow rate, and the mixture ratios. This is generally worth the added cost and complication of the double-pump apparatus.

CONCLUSIONS

We have demonstrated that the advantages inherent in solvent extraction fractionation may be realized by largely automating the method to avoid the onerousness of long equilibration times and by careful control of the relevant thermodynamic variables such as solvent composition and temperature. Under these conditions, relatively precise characterization of a molecular weight distribution is obtained, and the degree of preciseness appears to be limited mainly by the care and exercise of the individuals operating the apparatus.

The method described is applicable to reasonably large quantities of polymer and could certainly be scaled up somewhat with no essential changes in design. The method is also applicable to fractionation of relatively high molecular weight, monodisperse material, even though a considerable lower molecular weight tail may exist.

References

1. Guzman, G. M., in *Progress in High Polymers*, Vol. 1, Heywood, London, 1961.
2. Baker, C. A., and R. J. P. Williams, *J. Chem. Soc.*, **1956**, 2532.
3. Krigbaum, W. R., and J. E. Kurz, *J. Polymer Sci.*, **41**, 275 (1959).
4. Fuchs, O., *Makromol. Chem.*, **7**, 259 (1952).
5. Bamford, C. H., and Tompa, H., *Trans. Faraday Soc.*, **46**, 310 (1950).
6. Desreux, V., and M. C. Spiegels, *Bull. Soc. Chim. Belg.*, **59**, 476 (1950).
7. Zimm, B. H., and F. P. Price, in preparation.
8. Bianchi, J. P., F. P. Price, and B. H. Zimm, *J. Polymer Sci.*, **25**, 27 (1957).
9. Gibbs, D. S., H. J. Svec, and R. E. Harrington, *Ind. Eng. Chem.*, **48**, 289 (1956).
10. Harrington, R. E., and B. H. Zimm, *J. Phys. Chem.*, **69**, 161 (1965).

11. Flory, P. J., *Principles of Polymer Chemistry*, Cornell Univ. Press, Ithaca, N. Y., 1953.

12. Schulz, G. V., *Z. Physik. Chem. B*, **46**, 137, 155 (1940).

13. Jellinek, H. H. G., *Degradation of Vinyl Polymers*, Academic Press, New York, 1955.

14. Montroll, E. W., and R. Simha, *J. Chem. Phys.*, **8**, 721 (1940).

15. Schulz, G. V., *Die Physik der Hochpolymeren*, Vol. 2. H. Stuart, Ed., Springer, Berlin, 1953.

Résumé

On a mis au point une méthode pratique permettant de fractionner des polystyrènes relativement monodispersés dont le poids moléculaire s'élève à 4×10^6, qui consiste un processus semi-automatique d'extraction par le solvant. Les appareils de fractionnement sont constitués de chambres de mélange traversées d'un courant liquide et pourvus d'une région de dépot où s'élimine la substance solide en fine suspension. Des précautions sont prises pour contrôler avec précision à la fois la température et le rapport solvant–non-solvant. Deux appareils de ce genre opérant en série ont été utilisés dans le présent travail. En principe on pourrait en utiliser plusieurs en série pour la plupart des systèmes de polymère. Les résultats obtenus sur du polystyrène préparé de façon bien définie correspondent à la distribution prévue. On discute les possibilités d'application à d'autres polymères.

Zusammenfassung

Verhältnismässig monodisperses Polystyrol mit Molekulargewichten bis zu 4.10^6 konnte mit einem halbautomatischen Lösungsmittelextraktionsverfahren fraktioniert werden. Die Fraktioniereinrichtung besteht aus Durchflussmischungskammern mit einem Absetzbereich zur Entfernung von fein verteilten suspendierten festen Stoffen. Eine genaue Kontrolle der Temperatur und des Lösungsmittel–Fällungsmittelverhältnisses wird durchgeführt. Zwei solche gekoppelte Apparate wurden in der vorliegenden Arbeit verwendet; im Prinzip könnten, falls erforderlich, für die meisten Polymersysteme noch mehr Stufen verwendet werden. Ergebnisse an unter gut definierten Bedingungen dargestelltem Polystyrol scheinen mit den berechneten Verteilungen in guter übereinstimmung zu sein. Die Anwendbarkeit auf andere Polymersysteme wird diskutiert.

Degradation of Polymers in High Speed Rotary Homogenizers: A Hydrodynamic Interpretation

RODNEY E. HARRINGTON,* *Department of Chemistry, University of Arizona, Tucson, Arizona*

Synopsis

Dilute solutions of DNA in neutral phosphate buffer and of polystyrene in toluene are degraded to limiting molecular weights by high speed stirring in a Virtis homogenizer equipped with special thin, highly sharpened blades. Results are interpreted and justified in terms of the hydrodynamic theory of laminar boundary layers. Estimates of critical stress values for chain scission are obtained at various limiting molecular weights for the two polymer systems, and the treatment is used to rationalize the dependence of degradation upon homogenizer speed. The agreement between the hydrodynamic theory and experimental data implies that limiting molecular degradation occurs entirely in the boundary layer region extending a distance equal to approximately the molecular contour length from the leading edge of the blade tip and that laminar flow conditions prevail in this region. It therefore seems likely that polymer molecules subjected to a critical shearing stress are essentially completely extended in the streamlines of flow. The hydrodynamic theory is finally used to explain the peculiar kinetics of molecular degradation in high speed rotary homogenizers.

It has been known for several years that solutions of high polymers can be irreversibly reduced in viscosity by high speed stirring. Alexander and Fox[1] first reported this phenomenon and attributed it to molecular weight degradation, although the possibility of complications such as molecular entanglements and aggregation existed in their experiments. More recently, Johnson and Price[2] have degraded dilute solutions of polyisobutylene and polystyrene in a high speed rotary homogenizer. Harrington and Zimm[3] have used several types of rotary homogenizers to degrade dilute solutions of DNA and polystyrene in solvents of widely different viscosities, and have presented molecular weight fall-off curves for these systems. A number of other workers have used rotary homogenizers as a preparative device to reduce the viscosity of various macromolecular systems.

In spite of the relative abundance of previous work on the subject, only the reason for the viscosity decrease has been unambiguously demonstrated. Johnson and Price,[2] in their studies on dilute solutions of polymers, have shown by correlating molecular weight data with the number of radicals formed, the latter measured by means of iodine uptake, that

---

* Present address: Department of Chemistry, University of California, Davis, California.

chain scission accounts for the viscosity decrease associated with prolonged stirring. Several additional corroborating studies are reported by these workers. The mechanism by which chain scission is accomplished, however, has not been so clearly established.

The experiments of Alexander and Fox[1] on polymer degradation were necessarily rather limited in scope. However, on the basis of parallel experiments with ultrasonic irradiation, in which it was determined that degradation could not occur in the absence of cavitation, these authors attributed the degradation mechanism of high speed stirring to cavitation associated with the rapidly moving propeller. The contention that ultrasonic degradation cannot occur in the absence of cavitation is supported by the work of Weissler[4] but is disputed by a number of other authors[5-9] except in the case of very high molecular weight polymers; it appears likely that even during ultrasonic irradiation, cavitation is not necessary for degradation to occur, although it may appreciably increase the rate, and possibly the extent of degradation.

No attempt was made in the previous work[3] to interpret the mechanism of chain scission due to high speed stirring. Nevertheless, two facts were apparent: (a) the extent of degradation was very nearly independent of the magnitude of the solvent viscosity (although solvent power appeared to be a significant factor) and (b) the overall kinetics of degradation in rotary homogenizers were observed to be strikingly inefficient, implying that molecular degradation occurred over only a small region of the homogenizer blade surface. These facts, which are corroborated by the results and considerations of the present study, appear to refute the general importance of cavitation in polymer degradation by stirring.

This apparent unimportance of cavitation as a degradation mechanism cannot be understood in the absence of more information on the physical processes associated with cavity formation and collapse. Fluid in the region of a cavity undoubtedly is in a highly turbulent state, and high velocity gradients may exist, although these are not likely to be significant compared to those developed in a laminar flow region near the surface of a moving blade. Other factors which might lead to chain scission under certain conditions are liquid impact forces and intense local adiabatic heating in the immediate vicinity of a collapsing cavity. An estimation of the importance of impact forces is difficult because of the present unsatisfactory state of the theory of cavitation.[10] The relative unimportance of thermal degradation is reasonable, however, since adiabatic heating of fluid immediately surrounding a collapsing cavity is generally not large,[11] and if cavity collapse occurs in a time short compared to the thermal lifetimes of the molecules under the experimental conditions of stirring, adiabatic heating, even if it occurs appreciably, cannot lead to appreciable degradation by a thermal mechanism. Mostafa[9] has observed a marked falloff of the ultrasonic degradation of polystyrene in benzene above frequencies of 1 Mcycle/sec. although these results are complicated by the dependence of cavitation intensity on sonic field frequency.

We assume that principal molecular degradation in a high speed stirring experiment occurs in a region of high shear rate near the leading edge of the propeller. For a sharp leading edge, hydrodynamic theory can be used to calculate velocity gradients at all points on the blade surface in this region (except in the immediate vicinity of the leading edge), and the tensile stresses on the molecules can be estimated. For polymers degraded to their limiting molecular weights, ignoring the effects of polydispersity, the tensile stress so calculated is the critical stress for chain scission.

We have previously estimated critical stress values for polystyrene in toluene and for T2 bacteriophage DNA in neutral phosphate–EDTA buffer using other methods.[3] These values are compared to the results of the present study in which these polymer systems are degraded in a rotary homogenizer with a thin, well-sharpened propeller blade which is free of nicks or other obvious defects. Agreement of critical stress values and the dependence of blade speed upon limiting molecular weight is satisfactory for both polymer systems within the stated limitations of the theory.

Other propeller shapes were tried, and were generally found to enhance the kinetic efficiency of the degradation process, although results obtained with them were not reproducible. We attribute the erratic nature of these data to variables beyond experimental control such as cavitation, turbulence and atomization of the fluid. Thus, data obtained with blade shapes other than those used here cannot be interpreted in terms of the present treatment.

THEORY

The hydrodynamic model used is the passage of fluid over a thin blade with perfectly sharp leading edge. The effect of viscous shear must always extend an infinite distance into the fluid, but since the fluid velocity along the surface of the blade is an approximately parabolic function of distance normal to the blade, the region of appreciable velocity gradient is confined to a relatively thin layer near the blade surface; this is the boundary layer, first defined in this way by Prandtl.[12] Its thickness may be determined in any of several relatively arbitrary ways.[13] We assume that all degradation occurs inside the boundary layer, and that fluid flow in the boundary layer is laminar in the region of significant shear degradation. Justification of this assumption and an analysis of the effect of turbulence in the bounadry layer will be presented later.

The fluid dynamics of the boundary layer, assuming laminar flow, can be calculated from the equations of Navier-Stokes. For a thin boundary layer, assuming no pressure distribution outside the boundary layer, these are given[14] by the conservation of energy, the conservation of mass (i.e., the equations of continuity: the divergence of the velocity is zero for a fluid of constant density, an assumption which must be made here, and which is satisfactory in the case of dilute polymer solutions), and the relation

$$v_x(\partial v_x/\partial x) + v_z(\partial v_z/\partial z) = -(1/\rho)(\partial P/\partial x) + \nu(\partial^2 v_x/\partial z^2) \qquad (1)$$

where the blade is in the xy plane with the streamlines of flow directed along the x axis. In eq. (1), v_x and v_z are the velocity components in the respective directions, ρ is the fluid density, P is the pressure, and ν is the kinematic viscosity. These equations apply strictly to both rotational and irrotational flow, provided the radius of curvature of the boundary layer is large compared to the boundary layer thickness; this will be true under the conditions of applicability of these equations to the present work.

The boundary layer equations were first solved analytically by Blasius[15] for the velocity distribution, and hence the shear rate in a given region of the boundary layer, from the following boundary conditions

$$v_x = v_z = 0 \qquad\qquad \text{At } z = 0 \qquad (2a)$$

$$\left.\begin{aligned} v_x &= V \\ v_z &= 0 \end{aligned}\right\} \qquad\qquad \text{At } z = \delta \qquad (2b)$$

where V is the velocity of the fluid relative to the blade and δ is the boundary layer thickness.

The boundary layer thickness is rigorously equal to infinity, but since it is necessary to assign it a finite magnitude here, we can define δ as that value of z at which the velocity ratio v_x/V has reached some arbitrary value very near unity. The precise definition of δ is not critical, since almost all the velocity gradient occurs within a short distance of the blade surface. Using a parabolic velocity gradient in the boundary layer, Blasius defined

$$\delta = 5.47 \sqrt{\nu x/V} = ax^{1/2} \qquad (3)$$

and obtained for the shear rate at the blade surface

$$\dot{G}_0 = 2V/\delta = 0.365 \sqrt{V^3/\nu x} \qquad (4)$$

Other definitions of boundary layer thickness result only in relatively small changes in the numerical factors of eqs. (3) and (4).

The above relations predict a direct dependence of δ and an inverse dependence of $\dot{G}_0$ upon the square root of the distance from the leading edge. Thus, the hydrodynamic theory must fail at a distance close enough to the leading edge of the blade that x and δ become of comparable magnitude. This is a consequence of the boundary condition eq. (2a). Nevertheless, at values of x larger than δ, eqs. (3) and (4) should be valid, provided x is not so large that the boundary layer itself becomes turbulent.

In the immediate region of the leading edge, the boundary layer increases rapidly from zero while the tensile stress rises from zero at the leading edge to some indeterminate large value, and then begins to fall off at that value of x corresponding to the initial region of applicability of eq. (4). This will occur at a point very near the leading edge. If the blade is moving through the fluid, a tensile stress will be developed on a molecule in the boundary layer which will tend to stretch it along the streamlines of flow, and if the tensile stress is greater than the critical stress for chain scission over a sufficiently large range of x which we may call x_c, the mole-

cule will eventually be broken. Molecular degradation may therefore occur in any region of the boundary layer where these requirements are met.

We may now describe boundary layer degradation as follows. A molecule of molecular weight m and of mean extension z normal to the streamlines of flow enters the boundary layer and is subject to shearing forces. The molecular extension in the x direction will increase to a value X_c, corresponding to the onset of irreversible degradation, provided greater-than-critical tensile stress on the molecule is maintained from x_0, where significant tensile stress is first developed, to x_c. If we assume that the z extension remains roughly constant, which is not a serious assumption,[3] we can calculate the time required for extension to X_c from the relation

$$X_c = z \int_0^t \dot{G}(t)dt \tag{5a}$$

where $\dot{G}(t)$ is the mean velocity gradient over the extension z as a function of time.

All values of $\dot{G}(t)$ giving rise to tensile stresses greater than or equal to the critical stress for chain scission over the range of integration are relevant in eq. (5a), and degradation in general occurs over a considerable region of the laminar boundary layer. There results, therefore, a spectrum of degradation times, depending upon the distance of the molecule from the blade surface in the boundary layer and from the center of rotation of the blade.

A considerable simplification results if the experimental parameters are such that chain scission can just occur. Under these conditions, the maximum tensile stress on a molecule is only infinitesimally greater than the critical value, and additional degradation will occur only in that highly restricted region of the boundary layer in which the shear rate is maximum. This condition will obtain in the fluid layer immediately adjacent to the blade surface, at the point of highest blade velocity, and is given by eq. (4) with V taken as the blade tip velocity. A molecule subject to breakage therefore must enter the boundary layer at the blade surface, and is stretched to its critical value, X_c, with one end fixed at the leading edge and the other end moving with the fluid. If $v(x)$ is the velocity of the moving end of the molecule, we have

$$X_c = z \int_{x_0}^{x_c} \dot{G}_0(x) \frac{1}{v(x)} \, dx \tag{5b}$$

where x_0 is the condition $z = \delta$.

We may now use eq. (5b) to relate x_c and X_c in terms of an analytical expression for the boundary layer velocity. If we assume that the fluid moves with respect to the blade for convenience, we may take a parabolic velocity distribution in the boundary layer near the blade surface as characteristic of laminar flow. The vertex of the parabola is located a distance δ along the z-axis from the boundary, and we have[16a]

$$v(x)/V = \left\{ 1 - [1 - (z/\delta)]^2 \right\} = 2(z/\delta) - (z^2/\delta^2) \tag{6}$$

This form of the velocity distribution has been shown to be approximately correct.[17,18]

If the mean extension of the molecule along the velocity gradient, z, is small, eq. (4) can be taken as the mean velocity gradient across this distance, and eq. (5b) becomes

$$X_c = 2 \int_{x_0}^{x_c} \frac{dx}{[2 - (z/\delta)]} = 2 \int_{p}^{x_c} \frac{x^{1/2} dx}{(2x^{1/2} - p)} \tag{5c}$$

where $p = z/a$. The integral is evaluated as

$$X_c = x_c + 2px_c^{1/2} - 2p^2 + (p^2/2) \ln[(2x_c^{1/2} - p)/p] \tag{5d}$$

We now assume that the critical molecular extension along the streamlines of flow can be suitably approximated by the contour length of the molecule. Since x_c is of the same order of magnitude, it is evident that the mean extension, z, is considerably smaller than the boundary layer thickness at x_c. Thus

$$x/\delta = p/x_c^{1/2} < 1 \tag{6}$$

and the last two terms in eq. (5d) approximately cancel. Furthermore, if the ratio in eq. (6) is sufficiently small,

$$2px_c^{1/2} < x_c \tag{7}$$

and we finally have as a good approximation

$$X_c = x_c \tag{5e}$$

In a previous publication,[3] a semiempirical expression was given for the average tensile stress upon a polymer molecule

$$\langle f \rangle_{\mathrm{av}} = \mathring{G}(\eta - \eta_0)/nz \tag{8}$$

where $\eta - \eta_0$ is the viscosity increment of the solution due to polymer molecules of concentration n and mean extension normal to the streamlines of flow z, under conditions that hydrodynamic interactions may be neglected (dilute solutions).

A possible difficulty in the use of eq. (8) in the present work arises from the fact that it was developed with the assumption that the shear rate is independent of x over the distance x_c. Substitution of eq. (4), giving the shear rate as a rapidly decreasing monotonic function of x_c into eq. (8) is therefore subject to some question. The tensile force given by eq. (8) certainly represents an average over the stress distribution on the molecule. The stress distributions on polystyrene and DNA in similar velocity gradients under critical shear conditions are as uncertain as their high shear configurations, but the maximum stress on the molecule in each case cannot be seriously different from that calculated by using eq. (8). Thus, it seems reasonable to compute the stress leading to chain scission from the mean value of eq. (4) over the interval x_0 to x_c, even though the stress distribution on a molecule in this region of the boundary layer is undoubtedly

different from that on a molecule in a velocity gradient independent of x. From eqs. (4) and (8), we therefore have

$$\langle f \rangle_c = \frac{\langle \dot{G}_0 \rangle_{\mathrm{av}}(\eta - \eta_0)}{nz} = \frac{0.365 \, \eta_{sp}\eta_0 \, M}{cNzx_c}\left(\frac{V^3}{\nu}\right)^{1/2} \int_0^{x_c} x^{-1/2} \, dx \qquad (9)$$

$$\langle f \rangle_c = \frac{0.730 \, \eta_{sp}\eta_0 \, M}{cNz}\left(\frac{V^3}{\nu x_c}\right)^{1/2}$$

in which η_{sp} is the specific viscosity and c the concentration of the solution of polymer degraded to limiting molecular weight M, η_0 is the solvent viscosity, and N is Avogadro's number.

It has been shown in a previous publication[3] that a Gaussian distribution of end-to-end distances is no longer applicable in molecules under shear stress sufficient to cause chain scission, and the molecules are therefore highly extended along the streamlines of flow. This view receives qualitative support from the model experiments of Mason and co-workers involving liquid droplets[19] and fibers[20] in velocity gradients. Although it is impossible to know the details of molecular motion during degradation, these model experiments provide some insight here, and indicate that molecular motion in high velocity gradients is largely rotatory, with a tensile stress developed at a small angle with respect to the streamlines of flow. It is this force which leads to distortion of the zero-shear molecular configuration at high shear rates and which leads to chain scission as it reaches its critical value. It is also this force (or properly, the component along the streamlines of flow; at high shear rates the difference is inconsequential) which is calculated by eqs. (8) and (9).

It seems reasonable, therefore, to estimate the molecular extension along the streamlines of flow under conditions of critical stress as the contour length of the molecule, bM. Even if the molecule maintains some coiled structure at these high rates of shear, X_c will nevertheless be roughly proportional to molecular weight. Equations (5e) and (9) may now be combined with the above relationship to obtain the critical force from experimental parameters

$$\langle f \rangle_c = (0.730 \, \eta_{sp}\eta_0/cNz)(MV^3/\nu b)^{1/2} \qquad (10)$$

EXPERIMENTAL

Materials

High molecular weight, relatively monodisperse polystyrene of viscosity-average molecular weight 3×10^6 was prepared by using the intermittent ultraviolet photoinitiation method of Bianchi et al.[21] The initial molecular weight distribution will be described elsewhere.[22] Toluene used as solvent in the degradation studies was A.R. grade with no further purification, and no attempt was made to exclude air from the reaction vessel. Addition of various concentrations of 2,2-diphenyl-1-picrylhydrazyl, obtained from

Distillation Products Industries of Eastman Kodak Co., as a free-radical scavenger produced no detectable change in either overall kinetics or limiting molecular weight under otherwise identical experimental conditions.

DNA was obtained from T2 bacteriophage grown on *E. coli B* in Difco nutrient broth and was purified and obtained by differential centrifugation and phenol extraction as described by Mandell and Hershey.[23] The native material, prior to degradation, was assumed to be molecular weight monodisperse[24] at a value of 1.3×10^8,[25,26] and was dissolved in a sodium chloride–phosphate–EDTA buffer of pH 6.8, and $0.1M$ in sodium.

Apparatus

Degradation was conducted in a Virtis 45 Macrohomogenizer. The double stainless steel shaft and blade assembly was used. The leading edges of the blades were carefully sharpened, and particular care was given to the blade tips to ensure that there were no nicks or rough spots. The same 250-cc. Pyrex degradation vessel was used for all runs. Temperature was maintained at 25.0°C. by surrounding the degradation vessel with a thermostatted water jacket.

Molecular weights were in all cases determined from intrinsic viscosity. For the degraded polystyrene samples a single-bulb, long-capillary viscometer was used having a maximum shear rate less than 200 sec.$^{-1}$. Staudinger constants for polystyrene in toluene were taken as $k = 1.7 \times 10^{-4}$ and $a = 0.69$.[27] Concentrations were obtained gravimetrically. Intrinsic viscosities of degraded DNA were measured with a four-bulb dilution viscometer (Cannon-Ubbelohde, CUSD-11, type 50, manufactured by Cannon Instrument Co.). Concentrations were determined spectrophotometrically by using an extinction coefficient of 0.0181 cm.^{2}/μg. DNA at 260 mμ.[25] Molecular weights were obtained from the intrinsic viscosities by using the data of Eigner.[28] Thermal denaturation curves were run on degraded DNA samples to determine if denaturation occurred to an appreciable extent during high speed stirring. No evidence for loss of helical structure was found.

Procedure

In order to ensure that a limiting molecular weight was reached in all runs, a 100-ml. portion of polymer solution was placed initially in the degradation flask, and 5–10 ml. samples were withdrawn periodically for molecular weight determination. When the degradation rate was substantially zero, the limiting molecular weight was assumed to have been reached. This precaution was found to be desirable, because the overall degradation kinetics, after an initial rapid molecular weight fall-off, were extremely slow. The final limiting molecular weight was in all cases reproducible using the flat, sharpened homogenizer blades. Total run time varied between 4 hr. at the highest homogenizer speeds to over 40 hr. at the lowest speeds.

Homogenizer motor speed was monitored with a Virtis photoelectric tachometer which had been recalibrated against a General Radio Co. Type 1531-A Strobotac. Adequate motor speed control over the time intervals of the runs was maintained by first thoroughly warming the homogenizer motor, and then by operating the apparatus from a voltage-regulated power source. Motor speed regulation is estimated at $\pm 1\%$ over the speed range of interest here, becoming somewhat worse at lower motor speeds.

Temperature regulation was obtained by using a Lauda U-3 circulating thermostat supplying water to a jacket surrounding the degradation vessel. Temperature regulation in the jacket was $\pm 0.05°C$.; the temperature rise in the stirred solution was not measured, but was assumed small for the relatively low viscosity solutions used.

RESULTS AND DISCUSSION

Blade Speed Dependence of Limiting Molecular Weight

Equation (10) can be used to estimate limiting molecular weight as a function of blade speed if it is assumed that the intrinsic viscosity and molecular z extension at the high rates of shear necessary to cause chain scission are essentially their zero-shear values. Although this assumption is poor, becoming worse at the larger limiting molecular weights of both polystyrene and DNA, it is the ratio of these quantities which determine $\langle f \rangle_c$ in eq. (10), and part of the shear dependence therefore cancels in this expression. For the dilute solution studied here, the ratio η_{sp}/c is taken as numerically equal to the intrinsic viscosity. Rearrangement of eq. (10) gives the following for the blade tip velocity

$$V = \left\{ \left(\frac{0.533 \; b\nu N^2 \langle f \rangle_c}{\eta_0{}^2} \right) \left(\frac{z^2}{M [\eta]^2} \right) \right\}^{1/3} \tag{11a}$$

For polystyrene in toluene, we assume the following values for the parameters in eq. (11a): $b = 2.6 \times 10^{-8}$ cm./monomer; $\eta_0 = 5.90 \times 10^{-3}$ poise; and the density of the solution is taken as the density of pure solvent so that $\rho = 0.866$. The molecular weight dependence of the molecular z extension has been obtained from light-scattering measurements as $z = 0.56 \langle M_w \rangle_{av}$ (in angstroms).[27] This relationship is used here without correction; the difference between weight-average and viscosity-average molecular weights is not large in highly degraded polymers in which the high molecular weight tail is essentially eliminated, and is certainly inconsequential in comparison to the zero-shear approximations. The constants for the Staudinger equation were the same as those used in the molecular weight determinations. Substitution of the foregoing into eq. (11a) gives for polystyrene in toluene

$$V(\text{rpm}) = 10^{0.083} \langle f \rangle_c{}^{2/3} M^{-0.42} \tag{11b}$$

where V is the homogenizer speed, related to the blade tip velocity by V (rpm) $= 5.291V$(cm./sec.). The critical tensile stress for polystyrene in toluene has been estimated by different but related methods[3] as $\langle f \rangle_c = 3.5 \times 10^{-6}$ dynes. The theoretical line in Figure 1 is calculated by using this value in eq. (11b).

For DNA in $0.1M$ saline buffer, $b = 3.4 \times 10^{-8}$ cm./base pair[29] or 5.23×10^{-11} cm./unit molecular weight, $\eta_0 = 8.937 \times 10^{-3}$ poise, and as previously, the density of the solution is taken as that of the pure solvent. The Staudinger equation constants are calculated from the data of Eigner[28] extrapolated to molecular weights below 3×10^6 and are taken as
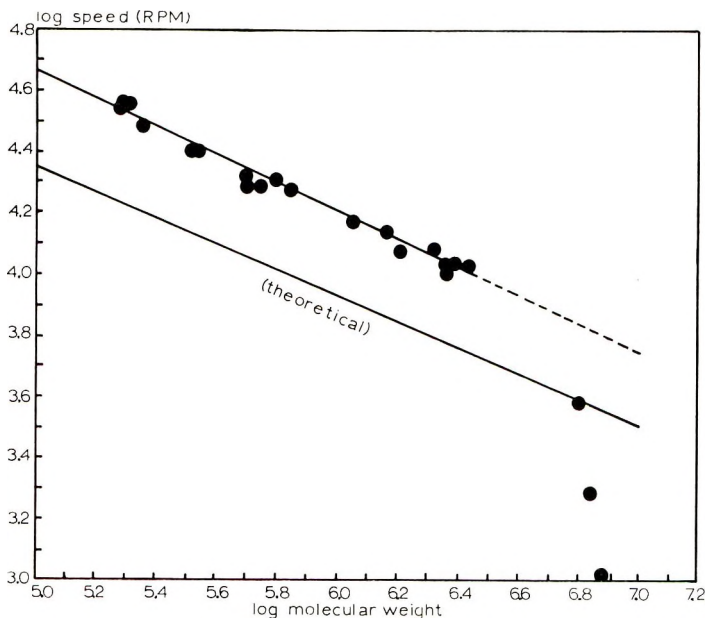

Fig. 1. Experimental and calculated homogenizer speed dependence of degradation to limiting molecular weight of polystyrene in toluene. Molecular weight values are viscosity average, and the initial polymer molecular weight was $\langle M \rangle_v = 10^7$.

$k = 1.08 \times 10^{-6}$ and $a = 1.14$. In the absence of consistent radius of gyration measurements from light scattering in the molecular weight region of interest here, the Flory-Fox equation[30] is used to estimate the molecular weight dependence of the molecular z extension. Unfortunately, this theory applies strictly to nonfree draining coils, while DNA at the molecular weights considered here must be nearly rodlike, or in any event, highly extended. Nevertheless, use of the Flory-Fox theory appears justified in the present calculations. We use the following relationship.[31]

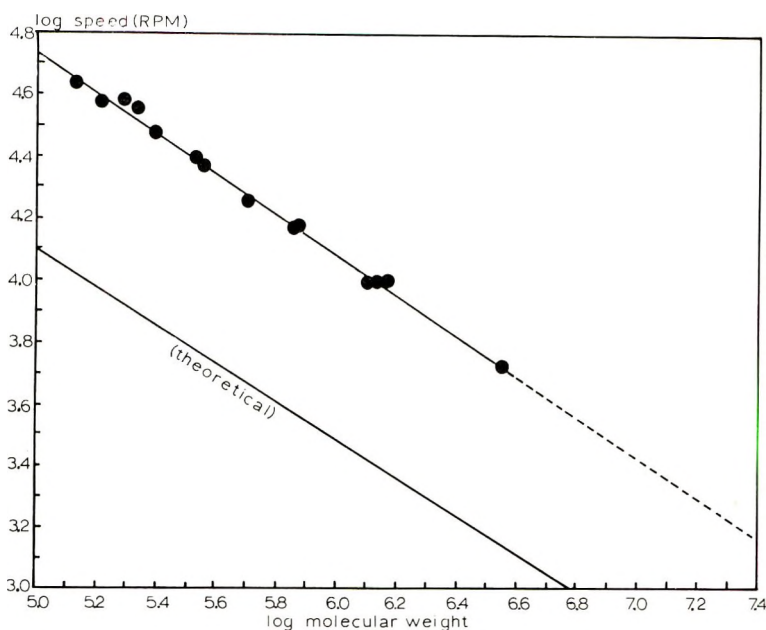$$[\eta] = 3.24 \times 10^{22} \, \rho^3_{rms}/M \tag{12}$$

Fig. 2. Experimental and calculated homogenizer speed dependence of degradation to limiting molecular weight of T2 bacteriophage DNA in phosphate, EDTA buffer (BPES), 0.1 M in sodium. Molecular weight values are viscosity averages (see text), and the initial polymer molecular weight was 1.3×10^8.

Substitution of the preceding quantities into eq. (11a) gives for DNA in neutral buffer

$$V(\text{rpm}) = 10^{10.241} \langle f \rangle_c^{2/3} \langle M \rangle_v^{-0.619}$$

$$V(\text{rpm}) = 10^{7.00} \langle f \rangle_c^{2/3} [\eta]^{-0.541} \tag{11c}$$

An independent estimate of $\langle f \rangle_c$ for DNA in neutral EDTA buffer is 3.0×10^{-5} dynes;[3] this value is used in eq. (11c) to obtain the theoretical line of Figure 2.

Experimental degradation data for polystyrene in toluene and for DNA in neutral 0.1M EDTA are shown in Figures 1 and 2 respectively, together with theoretical lines obtained from eqs. (11) Date for both systems fall reasonably well upon straight line plots.

In Figure 1, polystyrene data obtained at homogenizer speeds below approximately 10,000 rpm are not reproducible; the reason for this is not completely understood, but can probably be attributed to polydispersity of the sample. The effect of the molecular weight distribution would certainly be significant for the moderate degradation experienced by these low speed samples (i.e., reduction of the viscosity-average molecular weight by a factor of 5 or less). This is clearly seen from an extrapolation of the experimental line of Figure 1 to the initial molecular weight of the polymer. Such an extrapolation indicates that degradation cannot occur at homogenizer speeds below roughly 5600 rpm. The fact that some decrease in
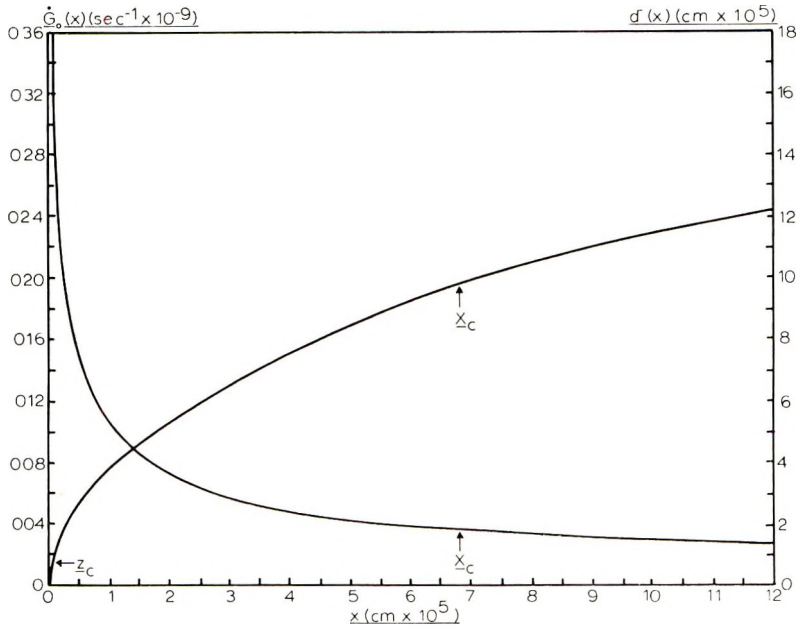
Fig. 3. Calculated shear rate and boundary layer thickness over the critical x extension, X_c, for polystyrene in toluene at a homogenizer speed 40,000 rpm. z_c is the limiting molecular weight z extension taken in the theory.
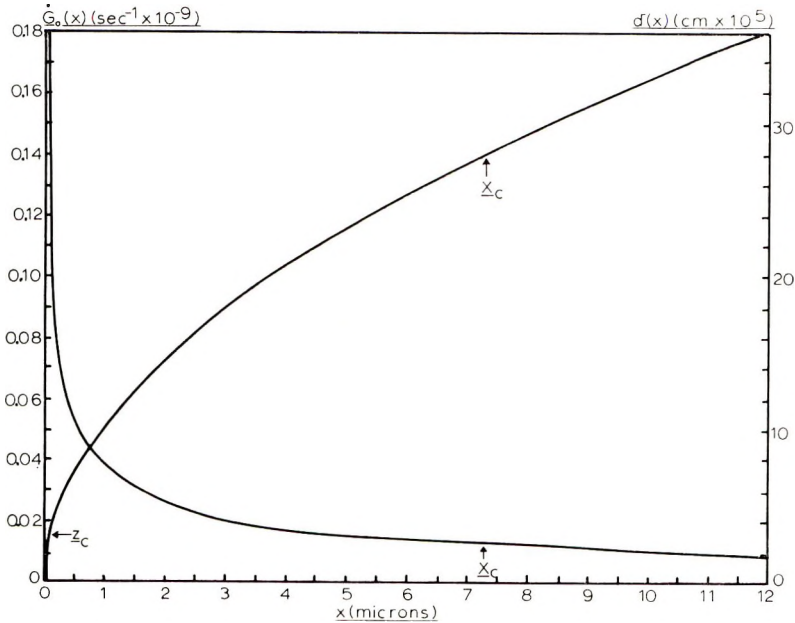

Fig. 4. Calculated shear rate and boundary layer thickness over the critical x extension, X_c, for T_2 bacteriophage DNA in phosphate, EDTA buffer (BPES), 0.1 M in sodium. Homogenizer speed, 40,000 rpm. z_c is the limiting molecular weight z extension taken in the theory.
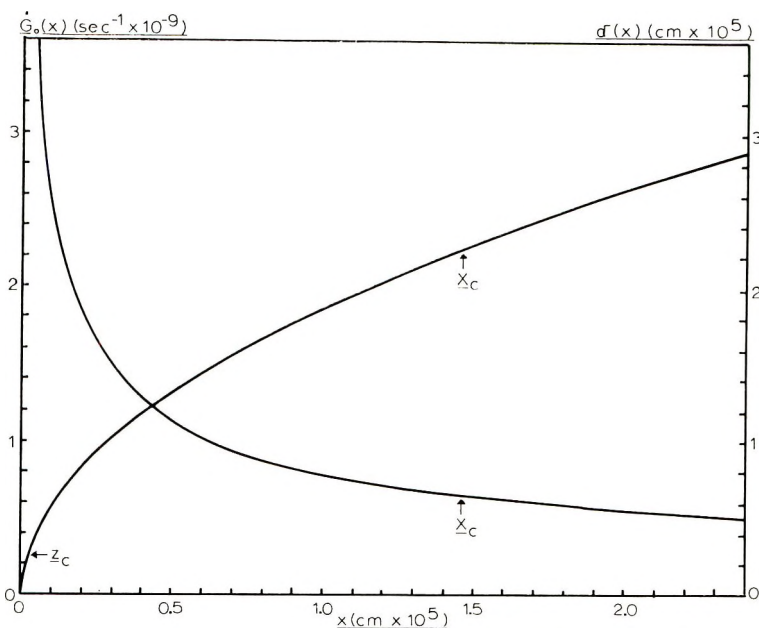
Fig. 5. Calculated shear rate and boundary layer thickness over the critical x extension, X_c for polystyrene in toluene at a homogenizer speed 10,000 rpm. z_c is the limiting molecular weight z extension taken in the theory.

molecular weight is observed at homogenizer speeds as low as 1000 rpm is evidence for the existence of a high molecular weight tail in the original sample, the loss of which accounts for much of the viscosity average fall-off at low blade speeds.

The experimental data of Figure 1 fall on a line of slope -0.46 and intercept 6.9, and the critical force obtained from this intercept is 1.6×10^{-5} dyne. The slope of the theoretical line is -0.42 and the intercept is 6.5, calculated assuming a critical force of 3.5×10^{-6} dyne as discussed previously.

The experimental data of Figure 2 fall on a line of slope -0.67 and intercept 8.0, leading to an experimental critical force value for DNA of 4.3×10^{-4} dyne. No fall-off at low blade speeds is observed with DNA as expected, since this effect is probably an artifact arising from sample polydispersity, and the undegraded polymer is monodisperse with a molecular weight at least two orders of magnitude greater than the highest limiting value. The theoretical line of Figure 2, based upon a critical force for DNA of 3.0×10^{-5} dyne,[3] has a slope of -0.62 and an intercept of 7.2. For an equivalent plot against intrinsic viscosity, the slope would have been -0.54 with an intercept of 4.0.

The speed dependence of limiting DNA degradation is somewhat less than that observed by Crothers,[32] who obtained a linear plot of $[\eta]$ versus V^{-1}. The data reported here were obtained with well sharpened blades,

whereas Crothers' degradation studies employed ordinary Virtis homogenizer blades, one side of which is quite blunt. In any case, the difference is not large in terms of possible experimental error, and both sets of data provide at least qualitative justification of the laminar boundary layer theory.

It is of interest to examine the functions $\overset{*}{G}_0(x)$ and $\delta(x)$ over the range x_c. These quantities are shown plotted against x at 40,000 rpm for polystyrene and DNA in Figures 3 and 4, respectively, and at 10,000 rpm for these polymers in Figures 5 and 6. Values of X_c and z_c (evaluated at the limiting molecular weights) are also shown. In all cases, boundary layer
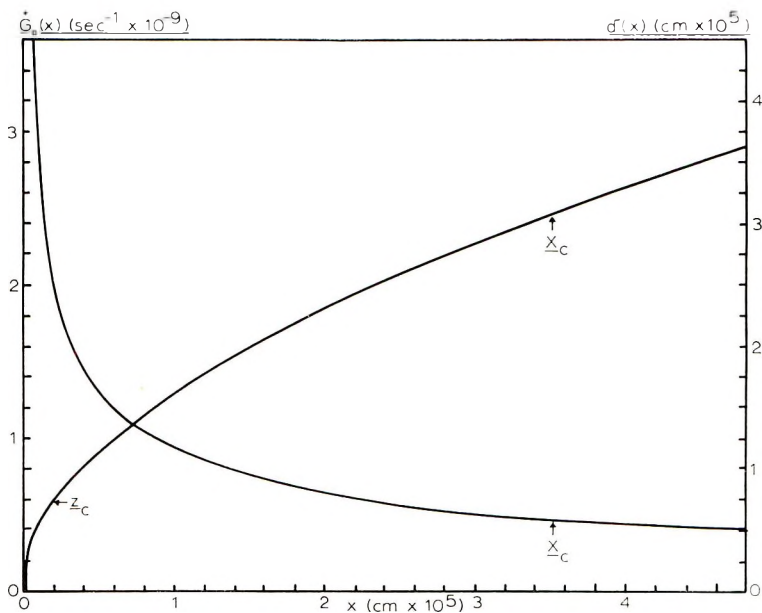

Fig. 6. Calculated shear rate and boundary layer thickness over the critical x extension, X_c, for T2 bacteriophage DNA in phosphate, EDTA buffer (BPES), $0.1M$ in sodium. Homogenizer speed, 10,000 rpm. z_c is the limiting molecular weight z extension taken in the theory.

thickness increases rapidly from the leading edge, and reaches a value equal to z_c relatively near the leading edge.

The ratio of limiting boundary layer thickness to molecular z-extension, required by eq. (6) to be considerably larger than unity, is seen from the figures and from Table I to range from a factor of 4 at the highest speed to approximately 7 at the lowest for polystyrene, and its values are twice this for DNA. Thus, eq. (5e) appears to be justified for these polymer systems, and the theoretical simplifications resulting from the use of eqs. (6) and (7) are utilized in the present calculations.

Figures 3–6 and Table I also indicate the relative extensions of the molecules in the shear gradient; the ratio X_c/z_c ranges from approximately 5

TABLE I

Data for Degradation to Limiting Molecular Weights M using a Virtis Homogenizer Equipped with Specially Sharpened Blades[a]

V, rpm	c, μg./ml.	$M \times 10^{-5}$	X_c, cm. $\times 10^5$	z_c, cm. $\times 10^5$	δ_c, cm. $\times 10^5$	δ_c/z_c	X_c/z_c
			Polystyrene in toluene				
36,000	318	2.06	3.56	0.946	4.01	4.24	5.67
36,000	410	2.03	5.28	0.938	3.98	4.24	5.63
36,000	523	1.91	4.97	0.906	3.86	4.26	5.49
31,000	786	2.28	5.93	1.00	4.52	4.52	5.93
25,600	731	3.42	8.89	1.26	6.15	4.88	7.06
25,400	744	3.32	8.63	1.24	6.06	4.89	6.96
21,000	753	4.92	12.8	1.54	8.14	5.29	8.31
21,000	752	6.20	16.1	1.75	9.13	5.22	9.20
19,000	757	5.61	14.6	1.66	9.13	5.50	8.80
19,000	760	5.00	13.0	1.56	5.59	5.51	8.33
19,000	761	7.17	18.6	1.90	10.3	5.42	9.79
15,000	706	11.3	29.4	2.45	14.6	5.96	12.0
14,000	673	14.4	37.4	2.81	17.0	6.05	13.3
12,500	1155	20.9	54.3	3.46	21.7	6.27	15.7
12,000	753	16.0	41.6	2.98	19.3	6.48	14.0
11,000	621	23.5	61.1	3.70	24.5	6.62	16.5
11,000	655	24.6	64.0	3.79	25.1	6.62	16.9
11,000	921	27.0	70.2	4.00	26.3	6.58	17.6
10,200	591	23.5	61.1	3.70	25.4	6.86	16.5
			DNA in neutral BPES				
44,000	41.2	1.35	0.706	0.149	1.47	9.87	4.74
39,000	40.7	1.95	1.02	0.194	1.92	9.90	5.26
38,000	72.8	1.63	0.852	0.171	1.78	10.4	4.98
36,000	43.0	2.15	1.12	0.208	2.10	10.1	5.38
30,000	92.1	2.48	1.30	0.231	2.47	10.7	5.62
15,000	42.6	3.36	1.76	0.287	3.15	11.0	6.13
24,000	88.5	3.59	1.88	0.301	3.33	11.1	6.25
18,000	42.3	5.01	2.62	0.382	4.54	11.9	6.86
15,000	93.8	7.17	3.75	0.493	5.95	12.1	7.61
15,000	51.8	7.45	3.90	0.506	6.10	12.1	7.71
10,000	39.6	12.6	6.59	0.737	9.93	13.5	8.94
10,000	39.4	13.3	6.96	0.766	9.93	13.0	9.09
10,000	85.5	14.8	7.74	0.828	10.5	12.7	9.35
5,000	41.2	35.6	18.6	1.55	23.0	14.8	12.0

[a] All parameters apply to limiting or critical chain length, and are defined in the text.

at 40,000 rpm to 18 at 10,000 rpm for polystyrene, and from approximately 5 to 12 over the same speed range for DNA.

Polydispersity Effects

Since the undegraded polymers had very narrow molecular weight distributions, the polydispersity after limiting degradation is determined largely by the stress distributions on the molecules leading to chain scission. In this respect, the T2 bacteriophage DNA is nearly an ideal system, since

the initial material is perfectly monodisperse (apart from any inconse-
quential shear breakage during preparation and handling of its dilute solu-
tions) and its molecular weight is large in comparison to the limiting values
observed.

When the shear rate is uniform and equal to its value at the wall, not
only along the x extension of each molecule but along the z extension as
well, the resulting stress distribution is roughly parabolic, with maximum
stress developed at the molecular center.[33]   This would be nearly the situa-
tion, for example, in a couette device or in the laminar flow region near the
wall of a capillary, beyond the region of end effects.   If the stress maxi-
mum occurs exactly at the molecular center, a system resulting from com-
plete limiting degradation of an initially monodisperse polymer is itself
monodisperse.   Owing to the finite size of the molecule, the stress distribu-
tion is never quite symmetric about the center of the molecule, but is
peaked somewhat toward the end of the molecule nearer the wall.[3,33,34]
For limiting degradation under these conditions, therefore, a distribution
of fragments results, some of which are slightly larger than the limiting
molecular weight, and some of which are slightly smaller; the final mo-
lecular weight distribution spans a range from approximately $M/2$ to M.

Figures 3–6 show that the molecular stress distributions in the boundary
layer near the leading edge of a homogenizer blade are likely to be con-
siderably different from those pictured above.   The shear rates vary
markedly over the x extension of the molecules, and the points of maximum
stress must be shifted well toward the leading edge ends.   The final mo-
lecular weight distributions are therefore expected to be broadened into the
low molecular weight region beyond the $M/2$ range, and this degree of ex-
cess polydispersity is related to the positions of the maxima in the molecular
stress distributions.   In principle, considerable information on the shape
of the stress distribution functions near the extrema could also be obtained
from sufficiently detailed and precise molecular weight distributions at
various stages of degradation for initially monodisperse, high molecular
weight polymers.   Although we have not yet been able to obtain experi-
mental molecular weight distributions of sufficient accuracy for this type
of analysis, available distributions of polystyrene sheared to limiting mo-
lecular weights as in the present study[22] do indicate polydispersity in excess
of $M/2$, and therefore qualitatively justify the skewed stress distributions
predicted by Figures 3–6.

In the absence of detailed molecular weight distributions, particularly
for DNA, it is difficult to correct the experimental data for polydispersity
effects.   The broadening of the final distributions are always in the low
molecular weight direction, so the viscosity-average molecular weight is
not an unrealistic measure of molecular weight.   However, it is likely that
polydispersity effects are small compared to other necessary approxima-
tions in the calculations given here, and therefore no attempt is made to
take them formally into consideration.

There is considerable evidence that the initial fragments of T2 bacterio-

phage DNA broken by rotary homogenization are nearly half and quarter molecules.[35] Chromatographic characterization of these fragments has been made[25,34] and similarly treated fragments of λdg DNA have been characterized chemically and genetically.[36] These experiments are not sufficiently exact to permit a precise determination of the point of breakage, and shifts away from the molecular center of the maxima in the stress distributions due to boundary layer shear at the low homogenizer speeds used may not be large. However, the results are suggestive that boundary layer shear may not be the primary degradation mechanism in the initial scission of very large DNA molecules in homogenizers with conventional blades. This is in accord with our finding that reproducible speed-limiting molecular weight relationships generally cannot be obtained with the use of homogenizer blades with dull or flat leading edges.

Turbulence in the Boundary Layer

The theory leading to eq. (10) has been developed assuming that laminar flow in the boundary layer persists at least as far from the leading edge as x_c. This assumption is justified in terms of a Reynolds number

$$R_x = Vx/\nu \tag{13}$$

defined in the usual way as the ratio of inertial to viscous forces. In the most unfavorable case (polystyrene degraded at 10,000 rpm) the value of R_x at x_c is roughly 200. Experimental evidence indicates that the transition to turbulence generally occurs at values of R_x on the order of 10^5–10^6 for sharp blades, assuming the approaching fluid to be relatively undisturbed.[16b] Although the fluid in the homogenizer vessel is moving rapidly as it contacts the blades, its velocity is extremely low relative to that of the blade tips, so it seems unlikely that the lower critical Reynolds number is reduced in this way to a value as low as 200 during an appreciable fraction of the run time.

Prandtl[37] and von Kármán[38] have developed an expression for the shear rate at the blade surface for a turbulent boundary layer. Their result, which may be compared to eq. (4), is

$$\hat{G}_0(x) = 2.28 \times 10^{-2} \left(\nu^{1/5} V^{9/5}/x^{1/5} \right) \tag{14}$$

The shear rate falls off more rapidly with x in the turbulent boundary layer than in the laminar boundary layer, although due to the greater velocity dependence of eq. (14), it may approach the laminar layer value at very small x and large V. In addition, eq. (14) is derived for statistically complete turbulence; since turbulence is cumulative with x and the range X_c so small, eq. (14) must be regarded as an upper limit to possible turbulent behavior. In the turbulent boundary layer, shear rates in the vicinity of x_c are several orders of magnitude less than the corresponding laminar flow values, and are so small over the range X_c that the experimental data of Figures 1 and 2 cannot possibly be explained in this way. We therefore conclude that negligible degradation of polymer frag-

ments near their limiting molecular weight values occurs in the boundary layer if it becomes turbulent due to fluctuations in fluid flow in the homogenizer vessel.

Overall Kinetics of Degradation

The overall kinetics of degradation in high speed homogenizers is controlled by such factors as motor speed, sample vessel shape (as it influences the efficiency with which the fluid is directed onto the blades), blade shape and design, and sample concentration. Because of the complex nature of homogenizer geometry effects, no attempt is made to compute degradation kinetics. A possible additional factor complicating the kinetics may be turbulence in the boundary layer during a fraction of the homogenizer run time, occasioned by large fluctuations in the fluid velocity directed against the rapidly rotating blades. Under these conditions, limiting degradation occurs only during periods of laminar flow, as mentioned, and the rate of bulk degradation is reduced. This is probably one of the reasons that generally irreproducible kinetics and limiting molecular weight values were obtained with other than thin, well sharpened blades.

The fact that the kinetics of polymer degradation by high speed stirring in dilute solutions are relatively slow compared to the homogenization of macroscopic particles in suspension implies a difference in mechanism for these two processes. In homogenization, we suspect that disruption of solid material occurs by the cutting action of the blades and also by the extreme turbulence developed in the suspension by the rapidly rotating blades leading to the development of moderately high local velocity gradients over distances comparable to the particle size. In this case, disruption may occur not only over a considerable portion of the leading edge of the blade, but also throughout much of the surrounding fluid. Boundary layer shear is generally unimportant, since the particle dimensions are typically large compared to the boundary layer thickness. In molecular degradation, chain scission may occur initially over a considerable portion of the blade surface (and perhaps also in the fluid due to turbulence, cavitation and atomization), but limiting degradation is confined to an extremely small boundary layer region near the leading edge of the blade tip where the shearing stresses are highly maximized. The number of molecules passing through this region per unit time is therefore very small. This accounts for the relatively rapid initial fall-off of molecular weight with time, followed by a very slow approach to M, observed in earlier studies[2,3] and in the present work.

CONCLUSIONS

In the degradation experiments reported here, a thin, well sharpened blade is passed rapidly through a dilute polymer solution. Intense velocity gradients exist in the boundary layer near the leading edges of the blades. These lead to the development of tensile forces on the molecules which,

operating through intramolecular displacements, provide a mechanical activation energy for chain scission. The magnitude of this activation energy is not known, but considerations described elsewhere[3] indicate that it probably depends strongly upon solvent environment and hence is considerably less than the dissociation energy of the breaking bond.

We have demonstrated that the hydrodynamic theory of the laminar boundary layer is evidently applicable to the limiting degradation of macromolecules in dilute solution at the surfaces of rapidly moving blades. When maximum shearing stresses developed in the system are large compared to the critical value, the degradation process is in general very complicated, and mechanisms other than boundary layer shear, such as cavitation and atomization, may be of importance. These complicating factors are not generally subject to quantitative interpretation. For degradation at the limiting molecular weight, however, the parameter of interest is the maximum tensile stress, and this is developed in a region of the laminar flow boundary layer between the leading edge of the blade tip and the x extension of the molecule of limiting molecular weight. This maximum shearing stress is evidently much larger than any other stresses developed in the system, and is unique in causing limiting chain scission.

The critical force values given here are larger than those obtained from capillary shear experiments by approximately a factor of 4 in the case of polystyrene and 10 in the case of DNA. These discrepancies may arise in part from the use of zero-shear parameters in the theory and the non-linear distribution of shear rate along the molecular extension. The larger discrepancy in the case of DNA is in the direction of a reduced solvent effect upon the critical force, and since the time required for critical stressing is several orders of magnitude less in boundary layer homogenizer shear than in capillary shear, it may therefore reflect significantly reduced solvent mobility in the region of the breaking bond. If this interpretation is correct, it may be in qualitative support of Crothers' hydrodynamic evidence for an icelike sheath around the DNA molecule in neutral solution.[39] However, a direct comparison of solvent effect factors between polystyrene and DNA is complicated by the fact that chain scission in DNA occurs primarily by C—O bond rupture, with only about 10% P—O bond rupture and no C—C bond rupture,[40] whereas C—C bond rupture must be the primary mechanism in polystyrene. Furthermore, alternative explanations of these phenomena, based upon high shear configurations of the polymers, may be available.[41] Agreement between predicted and experimental speed dependence of limiting molecular weight is excellent for polystyrene in toluene and somewhat less, but still satisfactory, for DNA.

In the case of DNA, agreement between eq. (11a) and experiment can be improved by allowing the Staudinger constant a to approach the theoretical value of 2 for rigid rods. This might have some justification at the lowest limiting molecular weights, since the molecular x extensions here are comparable in magnitude to a Kuhn statistical segment size of roughly 1500 A., estimated from light-scattering data on DNA in the 10^6 molecular

weight region,[31] but is more doubtful at higher molecular weights. Streaming birefringence studies on degraded and fractionated DNA are currently in progress to determine the range of fragment molecular weights over which the rigid rod hydrodynamic model is applicable.

The degree of concurrence between the simple theory and experiment is evidence that polymer chains breaking in a hydrodynamic shear field are virtually completely extended along the streamlines of flow. This is in qualitative agreement with the studies of Forgacs and Mason at high shear rates[20] and supports our previous conclusion that the molecules must be extended in the x direction far out of the range of applicability of Gaussian statistics.[3] The data appear further to indicate a high level of rigidity in low molecular weight DNA fragments which persists into the region of very high shear rates.

The boundary layer shear theory is capable of explaining the peculiar kinetics of molecular degradation in homogenizers. The overall kinetics are complicated by a number of factors, and our assessment of these has necessarily been speculative in nature. Nevertheless, the degradation mechanism proposed explains many important characteristics of the kinetics, and in particular, the extremely long times required to approach a limiting molecular weight in high speed stirring experiments.

References

1. Alexander, P., and M. Fox, *J. Polymer Sci.*, **12**, 533 (1954).

2. Johnson, W. R., and C. C. Price, *J. Polymer Sci.*, **45**, 217 (1960).

3. Harrington, R. E., and B. H. Zimm, *J. Phys. Chem.*, **69**, 161 (1965).

4. Weissler, A., *J. Appl. Phys.*, **21**, 171 (1950); *J. Acoust. Soc. Am.*, **23**, 370 (1951).

5. Schmid, G., and O. Rommel, *Z. Physik Chem.*, **185A**, 98 (1940).

6. Mark, H., *J. Acoust. Soc. Am.*, **16**, 183 (1945).

7. Melville, H. W., and A. J. R. Murray, *Trans. Faraday Soc.*, **46**, 996 (1950).

8. Brett, H. W. W., and H. H. G. Jellinek, *J. Polymer Sci.*, **21**, 535 (1956).

9. Mostafa, M. A. K., *J. Polymer Sci.*, **33**, 311 (1958).

10. Noltingk, B. E., and E. A. Neppiras, *Proc. Phys. Soc. (London)*, **64B**, 1032 (1951).

11. Jellinek, H. H. G., and G. White, *J. Polymer Sci.*, **7**, 21 (1951).

12. Prandtl, L., *Verhandlungen des III Intern. Mathematiker-Kongresses*, Heidelberg, 1904.

13. Tietjens, O. G., and L. Prandtl, *Applied Hydro- and Aeromechanics*, Dover, New York, 1964, p. 64.

14. Dryden, H. L., and F. D. Murnaghan, and H. Bateman, *Hydrodynamics*, Dover, New York, 1956, p. 252.

15. Blasius, H., *Z. Math. Physik*, **56**, 1 (1908).

16. Rouse, H., *Fluid Mechanics for Hydraulic Engineers*, Dover, New York, 1961 (a) p. 197; (b) p. 201.

17. Burgers, J. M., *Proc. 1st Intern. Congr. Appl. Mech., Delft*, 113 (1924).

18. Hansen, N., *Z. Angew. Math. Mech.*, **8**, No. 3, 185 (1928).

19. Bartok, W., and S. G. Mason, *J. Colloid Sci.*, **14**, 13 (1959).

20. Forgacs, O. L., and S. G. Mason, *J. Colloid Sci.*, **14**, 457, 473 (1959).

21. Bianchi, J. P., F. P. Price, and B. H. Zimm, *J. Polymer Sci.*, **25**, 27 (1957).

22. Harrington, R. E., and P. G. Pecoraro, *J. Polymer Sci.* A-1, **4**, 475 (1965).

23. Mandell, J. D., and A. D. Hershey, *Anal. Biochem.*, **1**, 66 (1960).

24. Hershey, A. D., and E. Burgi, *J. Mol. Biol.*, **3**, 674 (1961).

25. Rubenstein, I., C. A. Thomas, Jr., and A. D. Hershey, *Proc. Natl. Acad. Sci. U.S.*, **47**, 1113 (1961).

26. Davison, P. F., D. Freifelder, R. Hede, and C. Levinthal, *Proc. Natl. Acad. Sci., U. S.*, **47**, 1123 (1961).

27. Outer, P., C. I. Carr, and B. H. Zimm, *J. Chem. Phys.*, **18**, 830 (1950).

28. Eigner, J., Thesis, Harvard University, 1960.

29. Cummings, D. J., and Kozloff, L. M., *Biochim. Biophys. Acta*, **44**, 445 (1960).

30. Fox, T. G, and P. J. Flory, *J. Am. Chem. Soc.*, **73**, 1909, 1915 (1951).

31. Geiduschek, E. P., and A. Holzer, *Adv. Biol. Med. Physics*, **6**, 490 (1958).

32. Crothers, D. M., Ph.D. Thesis, University of California, San Diego, 1963.

33. Frenkel, J., *Acta Physicochim. U.S.S.R.*, **14**, 51 (944).

34. Levinthal, D., and P. F. Davison, *J. Mol. Biol.*, **3**, 674 (1961).

35. Burgi, E., and A. D. Hershey, *J. Mol. Biol.*, **3**, 458 (1961).

36. Hogness, D. S., and J. R. Simmons, *J. Mol. Biol.*, **9**, 411 (1964).

37. Prandtl, L., *Gottinger Ergebnisse*, **3**, 1 (1927); *Z. Angew. Math. Mech.*, **5**, 136 (1925).

38. von Kàrmàn, T., *Z. Angew. Math. Mech.*, **1**, 233 (1921).

39. Crothers, D. M., *J. Mol. Biol.*, **9**, 712 (1964).

40. Richards, O. C., and P. D. Boyer, *J. Mol. Biol.*, **11**, 327 (1965).

41. Zimm, B. H., personal communication.

Résumé

Des solutions diluées de DNA dans un tampon phosphate neutre et de polystyrène dans le toluène sont dégradées jusqu'à des poids moléculaires limités par une agitation à grande vitesse dans un homogénéisateur Virtis équipé de lames très tranchantes et spécialement fines. On interprète et justifie les résultats en termes d'une théorie hydrodynamique de couches laminaires. On obtient des estimations des valeurs de tension critiques pour la scission des chaînes jusqu'à des poids moléculaires variés pour les deux systèmes polymériques; le traitement est utilisé pour rationaliser la dépendance de la dégradation en fonction de la vitesse de l'homogénéiseur. L'accord entre la théorie hydrodynamique et les données experimentales suppose que la dégradation moléculaire limite se passe entièrement dans la région des couches frontières qui comporte une distance égale approximativement à la longueur du contour moléculaire à partir du bout coin tranchant de la lame, et que des conditions d'écoulement laminaire prévalent dans cette région. Il semble par conséquent probable que les molécules polymériques sujettes à une tension de cisaillement critique sont complétement étendues dans les lignes de courant du flux. La théorie hydrodynamique est finalement utilisée pour expliquer la cinétique particulière de la dégradation moléculaire dans un homogénéiseur à grande vitesse de rotation.

Zusammenfassung

Verdünnte Lösungen von DNA in neutralem Phosphatpuffer und Polystyrol in Toluol wurden durch Rühren mit hoher Geschwindigkeit in einem Virtis-Homogenisator mit dünnen, extrem scharfen Spezialkingen zu einem Grenzmolekulargewicht abgebaut. Die Ergebnisse werden mittels der hydrodynamischen Theorie der laminaren Grenzschichten interpretiert und erklärt. Kritische Spannungswerte für die Kettenspaltung werden bei verschiedenem Grenzmolekulargewicht für die beiden Polymersysteme erhalten, und die Abhängigkeit des Abbaus von der Homogenisatorgeschwindigkeit wird einer rationellen

Behandlung zugeführt.   Die Übereinstimmung zwischen der hydrodynamischen Theorie und den Versuchsergebnissen zeigt, dass der Abbau zur Molekülgrenze vollständig im Grenzschichtenbereich verläuft, der sich von der Kante der Klingenspitze über eine etwa der molekularen Konturlänge gleiche Distanz erstreckt und dass in diesem Bereich laminare Fliessbedingungen vorherrschen.   Es ist daher wahrscheinlich, dass die einer kritischen Schubspannung unterworfenen Polymermoleküle im wesentlichen völlig in der Stromlinienrichtung des Fliessens ausgestreckt sind.   Schliesslich wird die hydrodynamische Theorie zur Frklärung der kinetischen Besonderheiten des Molekülabbaus in Hochgeschwindigkeitsrotationshomogenisatoren herangezogen.

Interfacial Anodic Polymers from Benzene in Hydrogen Fluoride*

A. F. SHEPARD and B. F. DANNELS, *Hooker Research Center, Hooker Chemical Corporation, Niagara Falls, New York*

Synopsis

Benzene–HF mixtures containing two liquid phases exhibit unusual electrical conductivity characteristics on the addition of small amounts of H_2O or KF. Maximum conductivity is obtained with the anode contacting the interface between the phases and the cathode either contacting the interface or situated in the HF layer. On electrolysis, with the anode contacting the interface, polymer forms as a flat horizontal plate extending out from the anode at interface level; hydrogen is evolved at the cathode. The polymer is swollen by the cell liquid, and this composite appears to conduct electricity by a nonionic mechanism, and shows directional variation of conductivity. After removal of cell liquid from the polymer deposit, the remaining polymer is infusible, insoluble, and possesses excellent heat and chemical and electrical resistance. Elementary analyses of dry polymers from water bearing systems show loss of more than 2H per C_6H_6 molecule and introduction of variable amounts of F and O. Organic anionic complexes appear to be involved in the polymerization.

INTRODUCTION

Benzene and HF are but slightly soluble[1a,2] in each other and the resulting solutions of C_6H_6 in HF, or of HF in C_6H_6, are poor electrical conductors. When minor amounts of H_2O or KF are added (~5% by weight of additive on the HF), the mutual solubilities of the C_6H_6-rich and HF-rich phases are not greatly changed and the electrical conductivities of the separate phases remain low.

RESULTS AND DISCUSSION

It is surprising, therefore, to find that these two-phase systems can be, with certain positioning of electrodes, excellent conductors of electricity. Typical conductivity data are given in Table I.

It will be noted that maximum conductivity is obtained with the anode in contact with the liquid–liquid interface and with the cathode in contact with the interface or the HF layer. With this positioning of the electrodes, current passes readily on application of 1.5 v. or more, yielding H_2 at the cathode and a dark polymer deposit on the anode. The H_2 is evolved

TABLE I

Conductivity of a Mixture of Benzene, Water, and Hydrogen Fluoride[a]

Location of		Current,
Anode	Cathode	amp.
C_6H_6 layer	C_6H_6 layer	0.0
HF layer	C_6H_6 layer	0.0
C_6H_6 layer	HF layer	0.0
C_6H_6 layer	Through interface	0.0
Through interface	C_6H_6 layer	0.0
HF layer	HF layer	0.1
HF layer	Through interface	0.1
Through interface	Through interface	1.9
Through interface	Just touching interface	1.0
Through interface	HF layer	2.0
Just touching interface	Through interface	1.9

[a] Components: C_6H_6, 135 g.; HF, 230 g.; H_2O, 50 g. Electrodes: sheet Pt rectangles 3.7 cm. $\times$ 5 cm.; situated with long dimension horizontal and with main surfaces parallel, vertical and 6 cm. apart. Cell: polyethylene cylinder 10 cm. $\times$ 8 cm. diam. Approximately half of electrode surface was in each phase in the "through interface" location. Applied potential 3 v.; current was recorded 5 min. after application.

quite uniformly over the surface of the cathode exposed to the HF layer, while the polymer deposit forms mainly as a thin horizontal layer extending out from the anode at interfacial level. A coating of polymer deposit, relatively small in amount, also develops on the entire surface of anode exposed to the HF phase. The thin horizontal layer can be grown out for a distance of 5 cm. or more from the anode and undergoes no substantial increase in thickness during the horizontal growth. The mode of formation of the polymer deposit on the anode, together with the observations of Table I, indicate that electrons reach the anode mainly through a process involving oxidative polymerization of benzene or a benzene complex at the growing edge of the polymer layer.

The cathode process is not similarly constricted, as witnessed by the fact that H_2 is evolved over all parts of cathode surface exposed to the HF layer, and also by the fact that the cathode need only contact the HF layer to establish good conductivity.

The interfacial anodic polymerization observed here appears to be characteristic of systems containing HF and small amounts of water or other substance, such as KF, capable of yielding F^- ions in HF.[1b] Thus, no similar conductivity phenomena are noted for two-phase mixtures of C_6H_6 with H_3PO_4 or HCN containing minor amounts of water. Likewise, mixtures of C_6H_6 with HF which has been very carefully dried fail to show either deposit of a horizontal polymer layer at the C_6H_6–HF interface, or high conductivity with the anode located in the interface. (See polymer F, Table II and related footnotes.)

The polymer deposit, as formed in the cell, is swollen with cell liquor. This composite of polymer and cell liquor possesses the property of con-

TABLE II

Effect of Electrolysis Conditions on Polymer Composition

Polymer	Approx. bath composition			Electrolysis		Empirical formula[a]			
	Benzene, g.	HF, g.	H_2O, g.	Voltage, v.	Current amp. avg.	C	H	F	O
A	50	215	75	4.5	1	6.00	3.4	1.0	0.4
B	50	215	75	1.5	0.04	6.00	3.9	0.7	0.5
C	50	215	43	3.0	2	6.00	3.3	0.4	0.3
D	50	215	15	4.5	5	6.00	3.3	0.5	0.3
E	50	215	15	1.5	0.1	6.00	3.6	0.1	0.1
F[b]	50	156	—	20	0.2				
Acetone-soluble sublimate from F[c]						6.00	4.1	0.04	0.0
Acetone-insoluble sublimate from F						6.00	4.2	0.03	0.0
Sublimation residue from F[d]						6.00	4.1	0.03	0.0

[a] Average values based on analyses of polymers A–E for C, H, and F, with O by difference, performed by both Galbraith Laboratories, Knoxville, Tenn. and Huffman Microanalytical Laboratories, Wheatridge, Col. Values for polymer F are based only on analyses by the former.

[b] Polymer F did not build up as an interfacial layer; it was largely obtained as a residue on evaporating the cell liquor, with a minor portion being obtained by scraping the anode surface which had been in contact with HF. It was separated into the indicated fractions by vacuum sublimation and acetone extraction of the sublimate.

[c] Colorless; molecular weight 400 by vapor pressure osmometry in tetrahydrofuran; represents $^1/_4$ total polymer; its infrared spectrum indicates presence of an o-disubstituted benzene.

[d] Fusible; represents about $^1/_2$ total polymer; its infrared spectrum indicates presence of a p-disubstituted benzene.

ducting electricity by what appears to be a nonionic process. The non-ionic nature of the conductance by the deposit is evident from the fact that the polymer layer may grow outward horizontally several inches from the anode, with little increase in thickness or evolution of gases at the
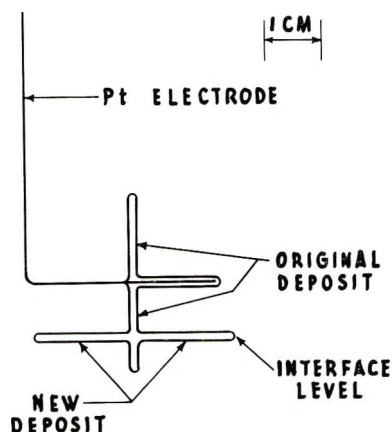

Fig. 1. Pattern of deposition of polymer upon previously formed polymer layer.

metal anode. As further evidence of nonionic conductivity, the anode and adhering deposit may be relocated in the cell in such a way that the metal anode is in the C_6H_6 phase and does not contact the interface, while the deposit extends through the C_6H_6–HF interface. With this arrangement good conductivity is obtained and, on electrolysis, a new polymer deposit forms on the side of the original deposit and grows horizontally along the C_6H_6–HF interface. Practically no growth occurs at the former growing edge of the original polymer deposit. Figure 1 shows the general pattern of polymer deposition under these conditions.

The swollen composite of polymer and cell liquor also exhibits directional variation of conductivity. Thus, a deposit may be formed on a Pt anode and then removed from the cell and its conductivity measured by touching Pt probes to it while applying a direct current potential of about 1.5 volts. The conductivity is greatest with the positive and negative probes situated in the same relative positions as the positive and negative electrodes during electrolysis, and is considerably reduced when the positions of the positive and negative probes are reversed.

Nature of Polymers

After washing the polymer composites with water and drying, they become excellent insulators. These dry acid-free products, hereafter simply called polymers, vary slightly in composition according to experimental conditions, as shown in Table II.

Thus, polymer obtained at low voltage and with little water present (polymer E) approaches the empirical formula $(C_6H_4)_x$ of a polyphenyl. At higher voltages, the F contents of the polymers increase, while the presence of larger proportions of water makes for a higher content of F and O.

The polymers of Table II are grey to brownish black in color. Polymers A–E are infusible and insoluble, and some of their physical and spectral properties are similar to the properties of polyphenyls prepared by Kovacic,[3-7] Marvel,[8-10] and others.[11-13] However, they all contain fluorine and thus differ in composition from previously known polymers. Their sulfonation products also appear to be different. For example, a sulfonation product of polymer C containing 14.5% S merely swells in water, but does not dissolve, whereas a similar sulfonation product obtained by Marvel from his polymer is water-soluble.[10]

None of the polymers A–E is moldable in the ordinary sense, although all may be compacted into disks at 200–220°C. and 1400–2800 kg./cm.[2] pressure. They have excellent heat and electrical resistance. Polymer C, for example, (disk 0.16 × 1.27 cm.) undergoes a weight loss of only 11% in 24 hr. at 540°C. in N_2, while remaining a good insulator; its arc resistance[14] is high (120 sec. versus 5 sec. for typical phenolic resins).

Neither the polymer deposit nor the cell liquor from the preparation of a typical polymer contains substantial amounts of C_6H_5F or low polymers such as diphenyl.

Possible Mechanisms for Polymer Formation

The observed phenomena with respect to interfacial anodic polymerization in the C_6H_6-HF-H_2O system may be explained by assuming the anions involved are complexes comprising benzene and F^-. This is in keeping with polymer deposition at as low as 1.5 v., which is in contrast with the 3 v. normally thought to be required to set free F[15], and which suggests the presence of a fluoride-benzene complex in which the electron affinity of F has been reduced. It is also in keeping with the localized deposition of polymer composite at the interface level, with the lack of products which might form by attack of F on C_6H_6, such as diphenyl or C_6H_5F, and with the failure of diphenyl to yield the same type of polymer or to show similar conductance.

As an illustration of how organic anionic complexes may form with interfacial anionic polymerization resulting, a process of the following sort is visualized. At the interface the benzene molecules distribute themselves in a more or less ordered arrangement, thus forming an ordered surface array of benzenoid hydrogen atoms. Fluoride ions, or their solvates with HF, are attracted to these hydrogen atoms of the interfacial surface. This further restricts the movement of the benzene molecules, and gives rise to a horizontal layer of anionic complex.

When electrolysis is carried out at less than the 3 v. reported necessary for the evolution of elemental F, it appears reasonable to assume that it is these complexes which lose their electrons to the anode. After loss of the electrons, elimination of F as HF and coupling of the benzene residues are likely.

Where complexed fluoride ions are plentiful, an average of more than two intermolecular linkages per ring should develop. Polymer E of Table II may represent such a situation. On the other hand, where complexed fluoride ions are less plentiful, as in the making of polymer F (Table II), a more soluble, less crosslinked polymer should, and does, result.

In systems of high water content, occasional formation of oxygen-bearing anions is to be expected. Their discharge at the anode and interaction with the growing polymer could account for the oxygen content of some polymers, while the presence of combined F in polymers could be ascribed to incomplete aromatization of the postulated F-bearing intermediates, or possibly in some cases, to the use of voltages high enough to set free elemental F.

The cations in the system are not similarly restricted to the interface by the complex formation requirement and are only restricted to the HF-H_2O layer. Consequently, on electrolysis, H_2 is liberated over all the surface of the cathode in contact with the HF-H_2O phase.

The mechanics of polymer growth require either the discharge of anions at the growing edge of the polymer (the apparent site of chemical reaction), or their discharge at the anode proper, followed by the migration of the discharged species to the growing edge of the polymer. The latter possibility seems unlikely, since the discharged anionic material would have to

survive as much as several inches travel from the anode proper and, more-
over, no driving force for such a migration is apparent.   It is therefore
considered that current flow involves electron release at the growing edge
of the polymer, followed by nonionic conductance of the electrons through
the swollen polymer composite to the metal of the anode.   In this connec-
tion, it is noteworthy that bringing the growing edge of the polymer into
direct contact with the cathode results in little increase in conductance.

EXPERIMENTAL

All equipment was constructed of polyethylene except where noted.
Polymers A–F were prepared in a cylindrical container 12 cm. in diameter.
It was provided with a tight fitting lid which carried a reflux condenser
and a gas inlet tube.   Electrical lead wires passed through the lid.   They
were insulated with polyethylene sleeves as desired, and were sealed in place
with paraffin wax.   Cell contents were kept at about 10°C. by external
cooling.

Reagent grade C_6H_6 and Matheson Co. anhydrous HF (99.9% min.)
were used throughout.   In most cases, HF was distilled from the supply
cylinder into the cell just before use.   Prior to electrolyses dry N_2 was
passed through the cell to remove air.

As noted under Table I, conductivity experiments were conducted with
Pt electrodes.   Conductivity of a two-phase mixture of 250 g. 85% H_3PO_4
and 50 g. C_6H_6 measured at 3 v. in the same equipment, with electrodes in
the through interface position, was 0.1 amp., while a two-phase mixture of
100 g. HCN, 10 g. H_2O, and 100 g. C_6H_6 was even less conductive (< 0.01
amp. at 6 v.).

The polymers A–E of Table II were prepared by using square Ni elec-
trodes (9 × 9 × 0.08 cm.), which were situated 5.5 cm. apart with their
square faces vertical and parallel to each other.   Similar Pt electrodes were
used for preparation of polymer F.   Small polyethylene spacers were used
to hold the electrodes in position.   Prior to use, the electrodes were heated
to a dull red heat in a gas flame.   Little corrosion occurred with Pt or Ni
anodes up to 4.5 v.

Polymer deposits were detached from the electrodes, washed with water
till acid-free, and dried to constant weight in vacuum at 100°C.

For sulfonation, a 3-g. portion of polymer C was heated with 100 g. 20%
oleum for 16 hr. at 140°C. and 4 hr. at 170–180°C.   The polymer swelled
but did not dissolve.   The sulfonated product was recovered by filtering
off the swollen solid, washing it thoroughly with water, and drying at
100°C. under vacuum.   The dried product contained 14.5% S; it was
quite hygroscopic and became gelatinous but did not dissolve when soaked
in water.

Evolved gases were collected during an electrolysis conducted at a steady
current of 1 amp. and 3–3.2 v. with Pt electrodes in a bath of composition
similar to that used in making polymer C.   A sample collected midway

during a 370-min. run was freed of HF and then contained 96.3% H_2 as shown by combustion with O_2. The average rate of gas evolution was 3.06×10^{-4} mole/min. (calc. from current, 3.11×10^{-4} mole H_2/min.). Polymer (5.4 g.) of composition $C_6H_{3.09}F_{0.35}O_{0.20}$ was obtained from the anode.

In examining for the formation of diphenyl and fluorobenzene the liquid organic phase remaining after a similar electrolysis was recovered and examined by gas chromatography and infrared spectroscopic methods. No diphenyl or fluorobenzene was found; the gas chromatographic procedure was sensitive to less than 0.05% of these materials.

References

1. Simons, J. H., *Fluorine Chemistry*, Academic Press, New York, 1950, Vol. I (a), p. 239; (b) p. 241.

2. Kilpatrick, M., and F. E. Luborsky, *J. Am. Chem. Soc.*, **75**, 577 (1955).

3. Kovacic, P., and R. M. Lange, *J. Org. Chem.*, **28**, 968 (1963).

4. Kovacic, P., and F. W. Koch, *J. Org. Chem.*, **28**, 1864 (1963).

5. Kovacic, P., and C. Wu, *J. Polymer Sci.*, **47**, 45 (1960).

6. Kovacic, P., and A. Kyriakis, *Tetrahedron Letters*, **No. 11**, 467 (1962); *J. Am. Chem. Soc.*, **85**, 454 (1963).

7. Kovacic, P., and J. Oziomek, *J. Org. Chem.*, **29**, 100 (1964).

8. Marvel, C. S., and G. E. Hartzell, *J. Am. Chem. Soc.*, **81**, 448 (1959).

9. Marvel, C. S., J. J. Bloomfield, D. A. Frey, and P. E. Kiener, Air Force Systems Command, Wright Patterson Air Force Base, Ohio, ASD-TDR-62-200 (Jan. 1962); C. S. Marvel, W. DeWinter, A. Abdul-Karim, S. C. Ray, P. E. Kiener, and W. R. Cavaness, *ibid.*, Part II (Feb. 1963).

10. Marvel, C. S., T. Moeller, and J. T. Bailar, Jr., WADD Technical Report 61-12, Wright Air Development Division, Wright Patterson Air Force Base, Ohio, April, 1961, pp. 37, 42.

11. Edwards, G. A., and G. Goldfinger, *J. Polymer Sci.*, **16**, 589 (1955).

12. Zielinski, A. Z., T. Komornicka, and R. Wyrzykowski, *Chem. Stosowana*, **3**, 487 (1959), *Chem. Abstr.*, **54**, 17299 (1964).

13. Thomas, C. A., *Anhydrous AlCl₃ in Organic Chemistry*, Reinhold, New York, 1941, p. 716.

14. *ASTM Standards 1964*, American Society for Testing and Materials, Philadelphia, Pa., D495-61.

15. Simons, J. H., U. S. Pat. 2,519,983 (August 22, 1950).

Résumé

Des mélanges de benzène–HF contenant deux phases liquides, possèdent des caractéristiques de conductivité électrique inhabituelles lors de l'adjonction de petites quantités d'H_2O ou de KF. Une conductivité maximale est obtenue ou bien quand l'anode est en contact avec l'interface entre les phases, ou bien lorsque la cathode se trouve en contact avec l'interface ou plonge dans la phase HF. Lors de l'électrolyse où l'anode est en contact avec l'interface, les polymères forment une plaque horizontale plane s'étendant

depuis l'anode au niveau de l'interface; de l'hydrogène se dégage à la cathode. Le polymère est gonflé par le liquide de la cellule, et dans cet état il conduit le courant électrique par un mécanisme non ionique, et laisse apparaître une variation dirigée de conductivité. Après extraction du liquide de la cellule hors du polymère, celui-ci est infusible, insoluble et possède une excellente résistance thermique, chimique et électrique. Des analyses élémentaires de polymères secs, provenant de systèmes contenant de l'eau, indiquent une perte de plus de 2H par molécule de C_6H_6 et l'introduction de quantités variables de F et O. Il semble que des complexes organiques anioniques interviennent dans la polymérisation.

Zusammenfassung

Benzol–HF-Mischungen mit zwei flüssigen Phasen zeigen bei Zusatz kleiner Mengen von H_2O oder KF eine ungewöhnliche elektrische Leitfähigkeitscharakteristik. Maximale Leitfähigkeit wird erhalten, wenn die Anode die Grenzfläche zwischen den Phasen berührt und die Kathode entweder die Grenzfläche berührt oder sich in der HF-Schicht befindet. Bei Elektrolyse mit der die Grenzfläche berührenden Anode bildet sich Polymeres als eine flache horizontale Platte, die sich von der Anode aus im Grenzflächenbereich erstreckt; an der Kathode wird Wasserstoff entwickelt. Das Polymere quillt in der Zellflüssigkeit, und diese Masse scheint die Elektrizität durch einen nichtionischen Mechanismus zu leiten und zeigt eine Richtungsabhängigkeit der Leitfähigkeit. Nach Entferen der Zellflüssigkeit aus dem polymeren Niederschlag ist das zurückbleibende Polymere unschmelzbar, unlöslich und besitzt eine ausgezeichnete Hitze-, chemisch- und elektrische Beständigkeit. Die Elementaranalyse trockener Polymerer aus wasserhältigen Systemen zeigt einen Verlust von mehr als 2H pro C_6H_6-Molekül und eine Einführung wechselnder Mengen an F und O. An der Polymerisation scheinen organische anionische Komplexe beteiligt zu sein.

Polymers from the Iterated Addition of Hydrogen Sulfide to Diolefins

JOHN G. ERICKSON, *Central Research Laboratories, Minnesota Mining and Manufacturing Company, Saint Paul, Minnesota*
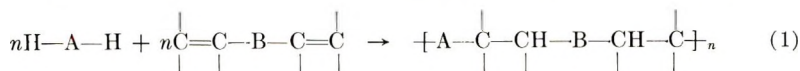
Synopsis

This paper describes polyesters and polyamides obtained by the base-catalyzed additions of hydrogen sulfide to α,β-unsaturated diesters and diamides. The compounds employed were ethylene diacrylate, the diacrylate of *trans*-1,4-bis(hydroxymethyl)cyclohexane, *p*-xylylene diacrylate, hydroquinone diacrylate, the diacrylate of 1,4-butanedithiol, tetraethylene glycol dimethacrylate, 1,4-butylene dicrotonate, 1,4-butylene dicinnamate, methylene bisacrylamide, and *m*-xylylene bisacrylamide. The polymers possess the general formula, $-\!\!\left(CHR^1CHR^2\!-\!CXR^3XCCHR^2CHR^1S\right)\!\!\!\overset{O\ \ \ \ \ O}{\underset{\|\ \ \ \ \ \ \|}{}}\!\!-_n$, wherein R^1 is hydrogen, methyl, or phenyl, R^2 is hydrogen or methyl, R^3 is an alkylene, aralkylene, or oxyalkylene group, and X is oxygen, sulfur, or the imino group. Polymers with as many as several hundred repeating units were obtained. Depending upon the structure, the products are liquids, rubbers, or solids, the polymers are obtained with vinyl or sulfhydryl termination and the efficiency of this termination is very high, as was shown by chain extension of a sulfhydryl-terminated polymer through oxidation to a polydisulfide, $-\!\!\left(RSS\right)\!\!-_n$, having a molecular weight 30 times as great as that of the parent dimercaptan. The syntheses of several new monomers are described.

INTRODUCTION

Several workers have prepared polymers by reactions of compounds containing two or more active hydrogen atoms with compounds possessing two or more double bonds. These reactions are of two types, one being nucleophilic additions, usually base-catalyzed, to double bonds activated by adjacent groups, and the other being free-radical additions to double bonds which are, as a rule, not so activated. The present discussion is devoted only to the nucleophilic additions.

In the absence of side reactions and apart from considerations of end-groups, the additions of pairs of bifunctional reagents involve equimolar amounts of these compounds and produce unbranched polymers with, of course, alternating units derived from each of the reagents involved. With functionality higher than two, branching and crosslinking result. The fundamental reaction for difunctional reagents is illustrated in eq. (1).

$$n\text{H}-\text{A}-\text{H} + n\overset{|}{\text{C}}=\overset{|}{\text{C}}-\text{B}-\overset{|}{\text{C}}=\overset{|}{\text{C}} \rightarrow -\!\!\left(\text{A}-\overset{|}{\text{C}}-\overset{|}{\text{CH}}-\text{B}-\overset{|}{\text{CH}}-\overset{|}{\text{C}}\right)\!\!-_n \quad (1)$$

The nature of A, B, and the substituents on the vinyl groups in eq. (1), as well as the functionality of the reagents, have been varied to a considerable degree. For example, Wegler and Ballauf[1] found that hydrogen sulfide and a triene, triacrylylhexahydro-s-triazine, react in alkaline solution, yielding insoluble, cross-linked polymers. Schoene[2] prepared polymers by the base-catalyzed reactions of active methylene compounds with divinyl sulfone; activating groups in these methylene compounds include carboalkoxy, carbonyl, cyano, amide, and sulfone groups. Marvel and Markhart[3] and Marvel and Wexler[4] added hexamethylene dimercaptan to dibenzalacetone in the presence of piperidine and obtained polymers thereby. Hamann,[5] with the use of base catalysis, added several bis(cyanomethyl) compounds and a bis(acetoacetyl) derivative to dicrotonates and to triacrylylhexahydro-s-triazine. Hulse[6] has also described polymers obtained by nucleophilic addition of active hydrogen compounds to activated double bonds. As active hydrogen compounds he employed ammonia, amines, dimercaptans, a diphenol, acetophenone, p-toluenesulfonamide, and dibenzyl ketone; the use of hydrogen sulfide was suggested, but not described. Hulse used strong bases as catalysts except in those cases involving the addition of ammonia or amines, where no added catalyst was needed. Faerber[7] prepared polyesters by heating dicarboxylic acids with divinyl ethers; no added catalyst was found necessary.

It is seen that hydrogen sulfide has not been employed as the active hydrogen compound in reactions with difunctional reagents. This paper describes some polyesters and polyamides obtained by its use with diesters and diamides of α,β-unsaturated monoacids with glycols and diamines.

DISCUSSION

Hurd and Gershbein have studied the addition of hydrogen sulfide[8] and of mercaptans[9] to various α,β-unsaturated aldehydes, monoacids, and derivatives of the latter with monofunctional reagents. Several β-mercapto derivatives were prepared and the effects of structure and of basic catalysis were established. The yield of methyl thiodipropionate from hydrogen sulfide and methyl acrylate was excellent (but little, if any, reaction was observed between hydrogen sulfide and methyl methacrylate in the presence of a base).

It is seen from the foregoing that the reactions of hydrogen sulfide with the esters of some unsaturated monoacids produce the diesters of thiodiacids. In the present work this reaction was applied to diesters of unsaturated monoacids and the products were polyesters of thiodiacids. Thus, ethylene diacrylate yields poly(ethylene thiodipropionate):

$$nCH_2=CHCOCH_2CH_2OCCH=CH_2 + nH_2S \rightarrow$$

$$+CH_2CH_2OCCH_2CH_2SCH_2CH_2CO+_n \quad (2)$$
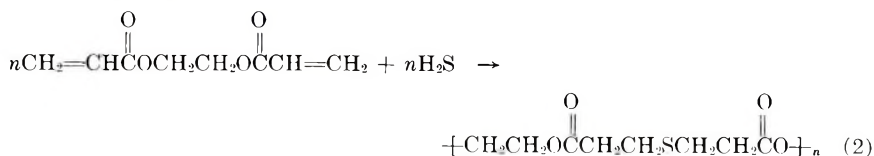
Several diacrylates were employed in this manner. Also used were di-methacrylates, a dicrotonate, a dicinnamate, and two diacrylamides. These polymerizations are readily carried out, usually at room temperature, by addition of hydrogen sulfide in small portions to a mixture of the diester or diamide, a suitable solvent (pyridine is usually very satisfactory), and a basic catalyst. Tertiary aliphatic amines, such as triethylamine, and hindered secondary amines, such as diisopropylamine, are effective catalysts. The polymerizations by this procedure are complete in from one to several days at 25°C. The reactions may also be carried out with the total amount of each reagent present from the beginning of the re-action. Table I lists the polymers obtained in this work, together with analytical values.

The molecular weights and endgroups of the polymers are determined by the relative amounts of the reagents, by the rate of addition of hydrogen sulfide, and the time allowed for reaction. In principle, given very pure reagents, freedom from side reactions, and sufficient time, an equimolar ratio of hydrogen sulfide to diacrylate should result in a polymer with a molecular weight approaching the infinite. In practice, of course, these conditions are not realized, and the result is not usually desired. Because the additions of mercaptans are faster than those of hydrogen sulfide, two stages can be recognized in the polymerization, particularly when incremental addition of hydrogen sulfide is employed. In the first stage, poly-merization occurs as hydrogen sulfide adds to double bonds, forming sulf-hydryl-terminated molecules. These mercaptans then add to other double bonds and the polymer chains grow in stepwise fashion. At any moment in this stage the mixture contains polymer molecules whose termination is sulfhydryl, vinyl, or both. If hydrogen sulfide is used in less than equi-molar amounts with the diolefin, the ultimate polymer is terminated by vinyl endgroups. In the second and later stage the polymer chains have been made uniformly terminated. If the total amount of hydrogen sul-fide used is appreciably greater than equimolar with that of the diolefin, there is a high molar ratio of free hydrogen sulfide to polymer end groups. The principal reaction occurring in this later stage is then formation of sulfhydryl endgroups. Growth of polymer chains becomes slow because the vinyl endgroups necessary for this growth have largely been converted to sulfhydryl groups. In practice it is convenient to attain the desired molecular weight in the first stage and then to add a considerable excess of hydrogen sulfide so as to ensure complete production of sulfhydryl groups.

As a rule, this polymer-forming reaction is very efficient and there is little, if any, side reaction such as cleavage of ester groups by hydrogen sulfide. Polymers were obtained with 200 or more repeating units. The efficiency of the sulfhydryl termination is also high, iodine oxidation of a polyester with molecular weight of 4100 yielding a polydisulfide with molecular weight of approximately 125,000.

In the light of the statement by Hurd and Gershbein regarding the non-addition of hydrogen sulfide to methyl methacrylate, it is interesting to

TABLE I

Polymers Obtained by Polyaddition of Hydrogen Sulfide to Diunsaturated Esters and Amides

$$\left[\begin{matrix} & & \overset{O}{\|} & & \overset{O}{\|} & & \\ CH & -CHCXR^3 & XCCH & -CH-S \\ R^1 & R^2 & & R^2 & R^1 \end{matrix}\right]_n$$

R¹	R²	X	R³	Physical state or m.p., °C	Inherent viscosity		Calculated				Found			
					⟨η⟩	Solvent	C, %	H, %	S, %	N, %	C, %	H, %	S, %	N, %
H	H	O	—CH₂CH₂—	Liquid	0.37	CHCl₃	47.0	5.9			47.4	6.1		
H	H	O	$trans$-1,4-CH₂C₆H₁₀CH₂—	Rubber	0.71	CHCl₃	58.7	7.7	11.2		57.2	7.6	13.0	
H	H	O	p-CH₂C₆H₄CH₂—	Rubber	0.84	C₅H₅N	60.0	5.8	11.4		59.6	5.7	11.2	
H	H	O	p-C₆H₄	165–170	0.15	m-C₇H₇OH	57.1	4.8	12.7		56.8	4.9	12.3	
H	H	S	—(CH₂)₄—	Liquid	0.10	CHCl₃	45.4	6.1	36.4		46.2	7.0	33.7	
H	CH₃	O	—(CH₂CH₂O)₄—	Liquid	0.73	CHCl₃	52.7	7.7	8.8		52.4	7.7	8.8	
CH₃	H	O	—(CH₂)₄—	Liquid	0.06	CHCl₃	55.4	7.7			54.9	7.6		
C₆H₅	H	O	—(CH₂)₄—	Liquid	0.13	CHCl₃	68.7	6.3	8.3		68.8	6.4	7.3	
H	H	NH	—CH₂—	>305	0.18	CF₃COOH	44.7	6.4	17.0	14.9	44.9	6.5	15.9	14.3
H	H	NH	m-CH₂C₆H₄CH₂—	170–175	0.30	m-C₇H₇OH	60.4	6.5		10.1	58.6	6.4		9.6

note (Table I) the high polymer obtained from hydrogen sulfide and the dimethacrylate of tetraethylene glycol. Other dimethacrylates, not reported in this paper, have yielded similar polymers with hydrogen sulfide.

The author is indebted to the referee for putting forth the possibility of charge-transfer reactions between hydrosulfide anions and oxygen, HS radicals being thereby produced and adding to vinyl groups. The new radicals so formed, by chain transfer with hydrogen sulfide, would generate new HS radicals and chain reactions would be underway, producing by a radical mechanism the same polymers as would the ionic mechanism intimated in this paper. For several reasons, the radical mechanism does not appear to be involved in the present study. There was no notable difference between polymerizations carried out in the presence of atmospheric oxygen and those performed in ampules sealed under vacuum with reagents and solvents frozen at $-196°$ during the process of sealing. The polymerforming additions of dimercaptans to diolefins similarly appear to be unaffected by oxygen. All polymerizations involving acrylates and methacrylates had small amounts of hydroquinone or di-*tert*-amylhydroquinone present to prevent vinyl polymerizations and these inhibitors would interfere with any other chain radical reactions. Also, it is known that oxygen can act as an inhibitor, as well as initiator, of radical reactions. Finally, should radical reactions be involved, they would be expected to produce crosslinked gel by vinyl polymerization of the diunsaturated compounds when the concentration of hydrogen sulfide (the chain transfer agent) is low; this condition would exist particularly in the early stages of the polymerizations when incremental addition of hydrogen sulfide is employed. No gel was ever observed.

A series of sulfhydryl-terminated polymers with different molecular weights was prepared by hydrogen sulfide addition to the dimethacrylate of tetraethylene glycol. From end-group titrations of these polymers molecular weight has been related to inherent viscosity (determined in chloroform) by a modified Mark-Houwink equation:

$$\bar{M} = 7.01 \times 10^4 \; (<\eta>)^{1.4}$$

This relation was seen to hold satisfactorily over as great a range as the accuracy of the endgroup titration permitted (up to a molecular weight of approximately 15,000).

Among the advantages of the present polymer-forming reaction is that it provides a route to certain high polymers not easily available by other means. Thus, MacGregor and Pugh[10] obtained polymers of only low molecular weight from thiodipropionic acid and ethylene glycol or trimethylene glycol. Koroly and Beavers[11] attempted the esterification of thiodipropionic acid with propylene glycol; some cleavage of the acid, or of its esters, occurred, and satisfactory polymer was not obtained.

A noteworthy derivative of thiodipropionic acid is its p-xylylene polyester. As shown in Table I, this was obtained as a rubber with a molecular weight of approximately 50,000. Although uncured and completely

soluble in pyridine and in dimethylformamide, this rubber possessed a tensile strength, based upon the cross section at rupture, of approximately 4000 psi, with 525% elongation. The x-ray diffraction showed the unstretched polyester to be crystalline with no preferred orientation; the x-ray pattern of the stretched material showed a fairly high degree of preferred orientation. This crystallinity takes the place of crosslinking in conferring strength upon the rubber. Similar effects, although not as pronounced, were observed with the polyester of thiodipropionic acid and trans-1,4-bis(hydroxymethyl)cyclohexane (Table I).

EXPERIMENTAL

Starting Materials

Acrylyl chloride, ethylene diacrylate, and tetramethylene diacrylate were obtained from the Monomer-Polymer Laboratories Division of the Borden Company, the dimethacrylate of tetraethylene glycol from Union Carbide Corporation, 1,4-bis(hydroxymethyl)cyclohexane from Eastman Kodak Company, p-xylylene glycol from Diamond Alkali Company, methylene bisacrylamide from American Cyanamid Company, and m-xylylenediamine from Oronite Division of Standard Oil Company of California.

Diacrylate of trans-1,4-Bis(hydroxymethyl)cyclohexane

A mixture of trans-1,4-bis(hydroxymethyl)cyclohexane (36.1 g., 0.25 mole), triethylamine (55.6 g., 0.55 mole), and benzene (500 ml.) was stirred and held at 25–30°C. while a solution of acrylyl chloride (49.8 g., 0.55 mole) in benzene (100 ml.) was added dropwise. The stirring was continued for 30 min. after the addition was complete. The mixture was then filtered and the filtrate was washed with saturated aqueous sodium sulfate solution, aqueous sodium bicarbonate solution, and water. A trace of hydroquinone was added, the benzene solution was dried over calcium sulfate hemihydrate, and the benzene was removed under reduced pressure. The residue was recrystallized from heptane to yield 4.1 g. of white flakes, m.p. 81–82°C.

ANAL. Calcd. for $C_{14}H_{20}O_4$: C, 66.6%; H, 8.0%. Found: C, 66.8%; H, 8.1%.

p-Xylylene Diacrylate

A mixture of p-xylylene glycol (14.0 g., 0.10 mole), acrylic acid (15.8 g., 0.22 mole), benzene (250 ml.), di-tert-amylhydroquinone (0.5 g.), and p-toluenesulfonic acid (1.6 g.) was refluxed for 30 hr. in an apparatus which permitted withdrawal of the azeotroped water of reaction. It was then washed with sodium bicarbonate solution and water. Distillation of the benzene from the solution left a solid residue which was recrystallized repeatedly from heptane to yield 8.6 g. of product, m.p. 67–72°C. Further

recrystallization from heptane and aqueous ethanol produced white flakes, m.p. 74–75°C.   (lit.[12] m.p. 68–71°C.).

ANAL.   Calcd. for $C_{14}H_{14}O_4$:   C, 68.3%; H, 5.7%; Found: C, 68.3%; H, 5.6%.

Hydroquinone Diacrylate

A mixture of hydroquinone (11.0 g., 0.10 mole), triethylamine (22.8 g., 0.225 mole), and benzene (100 ml.) was stirred and held at 25°C. while a solution of acrylyl chloride (20.4 g., 0.225 mole) in benzene (50 ml.) was added dropwise. The mixture was stirred an additional 2 hr. and filtered, the filter cake being washed with benzene (50 ml.). Combined filtrate and washings were evaporated to dryness *in vacuo*. Repeated recrystallization, first from heptane and finally from aqueous ethanol gave a low yield of product as white flakes, m.p. 85–86°C. (lit.[13,14] m.p. 81°C., 88°C.).

ANAL.   Calcd. for $C_{12}H_{12}O_4$:   C, 66.0%; H, 4.6%.   Found: C, 65.7%; H, 4.5%.

Diacrylate of 1,3-Butanedithiol

A solution of β-chloropropionyl chloride (27.9 g., 0.22 mole) in benzene (30 ml.) was added in portions to a mixture of 1,4-butanedithiol (12.2 g., 0.10 mole), triethylamine (22.2 g., 0.22 mole), and benzene (400 ml.) The temperature was held at 25–30°C. After 4 days the mixture was filtered and the filtrate was washed repeatedly with water and sodium bicarbonate solution and dried over calcium sulfate hemihydrate. Evaporation of the benzene *in vacuo* at 25°C. left 16.0 g. of brown liquid. This was redissolved in benzene and treated at 25°C. with tetramethylguanidine (14.0 g.). Heptane was then added and the mixture was washed with water until the washings were neutral. The organic layer was filtered, dried over calcium sulfate hemihydrate, and evaporated *in vacuo* at 25°C., leaving 1.0 g. of the diester as a light yellow oil. It was not possible to purify it further, as it polymerized very readily.

1,4-Butylene Dicrotonate

A mixture of 1,4-butanediol (27.0 g., 0.30 mole), benzene (300 ml.), and triethylamine (62.0 g., 0.61 mole) was stirred and held at 30–35°C. while crotonyl chloride (75.0 g., 0.72 mole) was added over a period of 45 min. It was stirred 45 min. longer and filtered. The filtrate was washed with water and sodium bicarbonate solution until it was neutral. Two distillations gave 48.1 g. (71%) of colorless liquid, b.p. 70–71°C./(0.025 mm.), n_D^{25} 1.4517.

ANAL.   Calcd. for $C_{12}H_{18}O_4$:   C, 63.7%: H, 8.0%.   Found: C, 63.7%; H, 8.1%.

1,4-Butylene Dicinnamate

A solution of cinnamoyl chloride (91.3 g., 0.55 mole) in benzene (50 ml.) was added dropwise to a mixture of 1,4-butanediol (22.5 g., 0.25 mole), triethylamine (55.6 g., 0.55 mole), and benzene (150 ml.) while the mixture

was stirred and held at 25–30°C. It was then filtered and the filter cake was washed with benzene. Combined filtrate and washings were washed with water and with sodium bicarbonate solution, then evaporated *in vacuo* at 60°C. The residue was recrystallized twice from heptane, yielding 59.0 g. (67%) of white product, m.p. 93–94°C.

ANAL. Calcd. for $C_{22}H_{22}O_4$: C, 75.4%; H, 6.3%. Found: C, 75.8%; H, 6.5%.

m-Xylylenebisacrylamide

A mixture of *m*-xylylenediamine (60.0 g., 0.44 mole), water (200 ml.), carbon tetrachloride (350 ml.), and sodium bicarbonate (81.5 g., 0.97 mole) was stirred and held at 25–30°C. while a solution of β-chloropropionyl chloride (123.0 g., 0.97 mole) in carbon tetrachloride (100 ml.) was added dropwise. The thick mixture was stirred for 1 hr. after the addition had been completed, allowed to stand for 18 hr., and filtered. The filter cake was slurried in very dilute hydrochloric acid, filtered, washed repeatedly with water, and dried, yielding 152.8 g. of the bis(β-chloropropionamide). Of this, 142.8 g. was dissolved in pyridine (700 ml.) which was refluxed for 18 hr.

The solid which separated from the pyridine upon cooling was the dipyridinium derivative. It was filtered off and dissolved in water (700 ml.). This solution was made strongly basic with sodium hydroxide; an oil appeared and solidified to a light yellow solid. This was filtered off, washed repeatedly with water and dried, yielding 117 g. of the crude bisacrylamide. After recrystallization from methanol its melting point was 147.5–148.5°C.

ANAL. Calcd. for $C_{14}H_{16}N_2O_2$: C, 68.8%; H, 6.6%; N, 11.5%. Found: C, 68.7%; H, 6.5%; N, 11.4%.

Polyesters and Polyamides

The following procedure was employed with some polyesters and polyamides. The final step illustrates the act of introducing complete sulfhydryl termination. A mixture of tetraethylene glycol dimethacrylate (330 g., 1.0 mole), pyridine (400 g.), and diisopropylamine (20 g.) was stirred and exposed intermittently to hydrogen sulfide at atmospheric pressure. After one day, 27.0 g. of hydrogen sulfide had been added. A stream of hydrogen sulfide was then bubbled through the mixture for 2 hr., the mixture was allowed to stand for 5 hr., and the polymer was precipitated in heptane. It was redissolved in methylene chloride, reprecipitated in heptane, washed with heptane, and dried. Yield of liquid polymer, 335 g.: $<\eta>$ (chloroform), 0.128; sulfhydryl content, 1.6%.

Vinyl-terminated polymers are prepared by this process by using less than equivalent amounts of hydrogen sulfide. Either sulfhydryl- or vinyl-terminated polymers may also be prepared in one step by adding all of the hydrogen sulfide at once under supraatmospheric pressure.

Another experiment yielded a polymer of considerably higher molecular weight. Hydrogen sulfide was added in small portions over a period of

several hours to a solution of p-xylylene diacrylate (7.38 g., 0.03 mole) and diisopropylamine (0.5 g.) in pyridine (40 g.). When hydrogen sulfide persisted, as shown by tests with paper dipped in lead acetate solution, the mixture was precipitated in heptane. The precipitated mass was swelled in methylene chloride overnight, dropped in small pieces into heptane, washed with fresh heptane, and dried *in vacuo*. This yielded 8.3 g. of tough, rubbery polymer fully soluble in pyridine and in dimethylformamide; $<\eta>$ (pyridine), 0.842; $<\eta>$ (dimethylformamide), 0.533.

Poly-N,N'-methylene-β,β'-thiodipropionamide

A somewhat different procedure was employed with this polymer because of its low solubility. Methylenebisacrylamide (15.4 g., 0.10 mole) and diisopropylamine (5.0 g.) were dissolved in m-cresol (150 g.). Hydrogen sulfide was added in portions at 25°C. After 2.4 g. had been added, much precipitate had formed. The mixture was then heated while hydrogen sulfide was passed over its surface; the mixture was almost homogeneous at 210°C. After 1 hr. the mixture was cooled and filtered. The filter cake, washed thoroughly with methanol and dried, yielded 14.5 g. of polymer, soluble in hot m-cresol, cold trifluoroacetic acid, or cold calcium thiocyanate. It was purified by precipitation from the latter solvent into water and washing with water. Analyses and properties are given in Table I.

References

1. Wegler, R., and A. Ballauf, *Chem. Ber.*, **81**, 530 (1948).
2. Schoene, D. L., U. S. Pat. 2,493,364 (Jan. 3, 1950).
3. Marvel, C. S., and A. H. Markhart, *J. Polymer Sci.*, **6**, 711 (1951).
4. Marvel, C. S., and H. Wexler, *J. Am. Chem. Soc.*, **75**, 6318 (1953).
5. Hamann, K. (to Farbenfabriken Bayer A.G.), Ger. Pat. 835,809 (1952).
6. Hulse, G. E., U. S. Pat. 2,759,913 (Aug. 21, 1956).
7. Faerber, G., U. S. Pat. 2,875,181 (Feb. 24, 1959).
8. Gershbein, L. L., and C. D. Hurd, *J. Am. Chem. Soc.*, **69**, 241 (1947).
9. Hurd, C. D., and L. L. Gershbein, *J. Am. Chem. Soc.*, **69**, 2328 (1947).
10. MacGregor, J. H., and C. Pugh, *J. Chem. Soc.*, **1950**, 736.
11. Koroly, J. E., and E. M. Beavers, *Ind. Eng. Chem.*, **45**, 1060 (1953).
12. Rohm and Haas Company, Brit. Pat. 729,028 (April 27, 1955).
13. Badische Anilin-u. Soda-Fabrik A.G., Brit. Pat. 779,277 (July 17, 1957).
14. Hayes, N. F., and R. H. Thomson, *J. Chem. Soc.*, **1956**, 1585.

Résumé

Cet article décrit les polyesters et polyamides obtenus par l'addition catalysée par les bases d'hydrogène sulfuré á des diesters et diamides insaturés en α,β. Les composés étudiés étaient le diacrylate d'éthylène, le diacrylate de *trans*-1,4-bis (hydroxy méthyl) cyclohexane, le diacrylate de p xylylène, le diacrylate d'hydroquinone, le diacrylate de 1,4-butane-dithiol, le diméthacrylate de tétraéthylène-glycol, le dicrotonate de 1,4-butylène, le dicinnamate de 1,4-butylène, le méthylène-bisacrylamide et le m-xylylène

bisacrylamide.   La formule générale des polymères est $-(CHR^1-CHR^2-CXR^3X$

$$\overset{O}{\underset{\|}{C}}-CHR^2-CHR^1-S)_n-,$$

où R^1 est de l'hydrogène, un groupe méthyle ou phényle, R^2 hydrogène ou méthyle, R^3 un groupe alkylène, aralkylène, ou oxyalkylène et X de l'oxygène, du soufre ou un groupe imine.   On a obtenu des polymères contenant plusieurs centaines d'unités.   Les produits sont liquides, caoutchouteux ou solides, selon leur structure. Les polymères sont obtenus avec terminaison vinylique ou sulfhydrique et l'efficacité de cette terminaison est très élevée comme le démontre l'allongement de chaîne d'un polymère à terminaison sulfhydrique par oxydation en polydisulfure $+\text{RSS}+_n$ possédant un poids moléculaire trente fois plus élevé que le dimercaptan correspondant.   On décrit la synthèse de plusieurs nouveaux monomères.

Zusammenfassung

In der vorliegenden Arbeit werden durch basenkatalysierte Addition von Schwefelwasserstoff an α,β-ungesättigte Diester und Diamide erhaltene Polyester und Polyamide beschrieben.   Folgende Verbindungen wurden verwendet: Äthylendiacrylat, das Diacrylat von *trans*-1,4-Bis(hydroxymethyl)cyclohexan, *p*-Xylylendiacrylat, Hydrochinondiacrylat, das Diacrylat von 1,4-Butandithiol, Tetraäthylenglycoldimethacrylat, 1,4-Butylendicrotanat, 1,4-Butylendicinnamat, Methylenbisacrylamid und *m*-Xylylen-

bisacrylamid.   Die Polymeren besitzen die allgemeine Formel $+CHR^1CHR^2-CXR^3$-

$$\overset{O}{\underset{\|}{X}}CCHR^2CHR^1S+_n,$$

wo R^1 Wasserstoff, Methyl oder Phenyl, R^2 Wasserstoff oder Methyl, R^3 eine Alkylen, Aralkylen- oder Oxyalkylengruppe und X Sauerstoff, Schwefel oder die Iminogruppe ist.   Es wurden Polymere mit bis zu mehreren hundert Kettengliedern erhalten.   Je nach der Struktur sind die Produkte Flüssigkeiten, Kautschuke oder Festkörper.   Die Polymeren werden mit Vinyl- oder Sulfhydrylendgruppen erhalten, und Anteil dieser Endgruppen ist, wie durch Kettenverlängerung eines Polymeren mit Sulfhydridengruppen durch Oxydation zu einem Polydisulfid, $+\text{RSS}+_n$, mit einem Molekulargewicht 30 mal so gross wie das Ausgangsdimercaptan, gezeigt wurde, sehr hoch. Die Synthese einiger neurer Monomerer wird beschrieben.

# New High Temperature Polymers.   I. Wholly Aromatic Ordered Copolyamides

J. PRESTON, *Chemstrand Research Center, Inc., Durham, North Carolina*

Synopsis

Wholly aromatic ordered copolyamides of unusually high thermal stability were prepared by the condensation of aromatic diacid chlorides with symmetrical diamines containing preformed aromatic amide units in an ordered arrangement. The preservation of order in the condensation step was assured by using interfacial or solution polymerization techniques at temperatures below 50°C. Each polymer contains units derived from aminobenzoic acids, arylene diamines, and arylene diacids. By use of *para*- and *meta*-phenylene units, eight different polymers are possible; all were prepared. Differential thermal analyses and thermogravimetric analyses showed these polymers to have melting points or decomposition temperatures in a range from 410°C. for the all-*meta* polymer to 555°C. for the all-*para* one. Substitution of the internal N-hydrogens of the diamines with methyl groups or phenyl groups leads to additional ordered copolymers. Several were prepared, but their melting points were much lower than those of the parent polymers limiting their usefulness in high temperature applications. Tough pliable films were prepared from all eight unsubstituted polymers, and crystalline fibers with tenacities of ca. 6 g./den. were prepared from three of the polymers. The properties of the fibers were retained to a high degree even when determined at temperatures up to 400°C. Fibers aged at 300°C. for extended periods of time showed remarkable retention of fiber properties.

INTRODUCTION

It has long been recognized that aromatic polyamides, because of intermolecular bonding and chain stiffness, possess high thermal stability. In general, two types of wholly aromatic polyamides have been reported: those prepared by the polycondensation of aminobenzoic acid derivatives[1–4] and those prepared by the polycondensation of arylene diamines with arylene diacid chlorides.[5–7] Examples are found in the polyamide of *m*-aminobenzoic acid and poly(*m*-phenylene isophthalamide).[5]


I

II
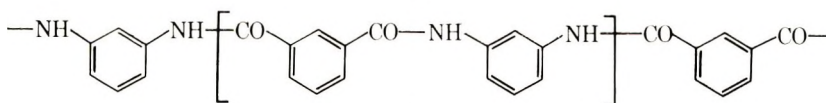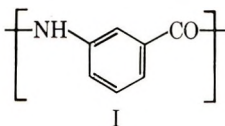
This paper describes the preparation and properties of high molecular weight film-forming and fiber-forming aromatic polyamides[8] of unusually high thermal stability which contain units derived from aminobenzoic acids, arylene diamines, and arylene diacids which are present in a regular ordered sequence. Order is achieved in these polymers by the use of a symmetrical diamine in which the sequence is predetermined, such as diamine A. These diamines contain preformed amide linkages. Interfacial or solution polymerization of these diamines with diacid chlorides yields polymers of the alternating arrangement since no redistribution of groups takes place because of the low polymerization temperature.[9] A typical alternating ordered copolyamide was prepared as shown in eq. (1).
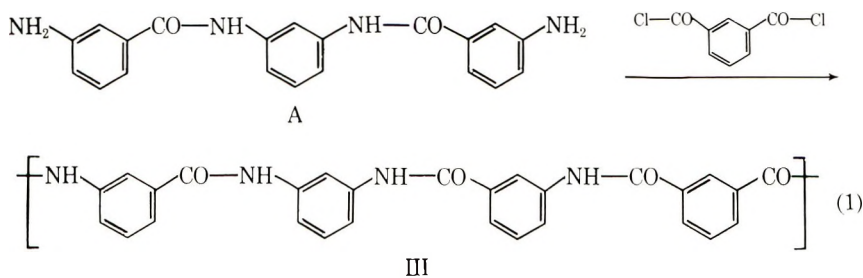
It can be seen that while polymers I and II contain distinctly different structural units, and polymer III contains the units of both I and II, the empirical formula, C_7H_5NO, is the same for all three. By using all possible combinations of m- and p-phenylene units in both the symmetrical primary diamines and the diacid, chlorides eight distinctly different polymers of formula C_7H_5NO are possible; all have been prepared. A more general picture of I, II, and III is seen by considering I to be an +AB+ type polyamide and II to be an +AA-BB+ type polymer; the repeat unit of III is then seen to be +AB-BB-AB-AA+.

Stephens[10] has prepared aromatic polyamides of empirical formula C_7H_5NO from primary diamines such as B in which the preformed amide linkages are the reverse of those in diamine A.
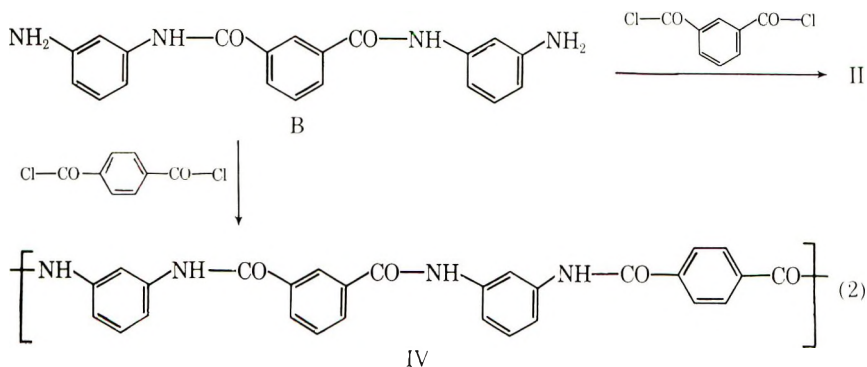
Since no benzamide structural units were incorporated by Stephens, only two ordered copolyamides (e.g., IV) containing four phenylene rings in the shortest repeat unit can be obtained from the eight possible combinations. Four of the combinations yield homopolymers which are made more conventionally from simple diamines and diacid chlorides, e.g., structure II from m-phenylenediamine with isophthaloyl chloride.[4] None of the benzamide-containing polyamides reported here correspond to any of Stephens' polyamides.

In addition to the polyamides prepared from primary diamines, several ordered polyamides were prepared from N,N'-dimethyldiamines and N,N'-diphenyldiamines.

EXPERIMENTAL

Polymer melt temperatures (PMT) were obtained by differential thermal analysis (DTA), and the temperature at which the rapid onset of loss of weight (decomposition point) began was obtained by continuous thermogravimetric analysis (TGA). Inherent viscosities (η_{inh}) were obtained at 30°C. on a solution of 0.5 g. of polymer dissolved in 100 ml. solvent. Diacid chlorides were prepared by conventional means. The preparation of the aromatic diamines containing amide linkages is given below.

N,N'-Phenylenebis(aminobenzamides)

The aromatic diamines containing preformed amide linkages were prepared from simple phenylene diamines and nitroaroyl chlorides, with subsequent reduction of the dinitro intermediate (Table I).

Nearly quantitative yields of pure materials were obtained in the preparation of the dinitro intermediates and the corresponding diamines (Table II). In a typical preparation, a solution of 0.2 mole of a nitrobenzoyl chloride in 40 ml. tetrahydrofuran (THF) was poured all at once into a Waring Blendor jar containing 0.1 mole of a phenylenediamine and 0.2

TABLE I
N,N'-Phenylenebis(nitrobenzamides)

No.	Compound	Melting point, °C. (uncor.)
1	N,N'-m-Phenylenebis(m-nitrobenzamide)	269–271
2	N,N'-m-Phenylenebis(p-nitrobenzamide)	279–281
3	N,N'-p-Phenylenebis(m-nitrobenzamide)	333–335
4	N,N'-p-Phenylenebis(p-nitrobenzamide)	378–380
5	N,N'-Dimethyl-N,N'-p-phenylenebis-(m-nitrobenzamide)	191–193
6	N,N'-Dimethyl-N,N'-p-phenylenebis-(p-nitrobenzamide)	248–250
7	N,N'-Diphenyl-N,N'-p-phenylenebis-(m-nitrobenzamide)	283–285

mole sodium hydroxide in 200 ml. ice-cold water. Diamines of high purity were obtained by reduction with stannous chloride or by catalytic hydrogenation in dimethylacetamide (DMAc) when the dry, crude dinitro intermediates were recrystallized from DMAc prior to reduction. Certain diamines [11](1,2) of Table II have been reported, but no properties were given; a diamine containing N-methyl-substituted amide groups (6, Table II) was also reported earlier.[12] An important feature of these aromatic diamines is the fact that they are stable toward the effects of air, light, moisture, and common organic solvents.

TABLE II
N,N'-Phenylenebis(aminobenzamides)

No.	Compound	Melting point, °C. (uncor.)	Analysis, % N	
			Calcd.	Found
1	N,N'-m-Phenylenebis(m-aminobenz-amide)[a]	213–214	16.14	16.13, 16.08
2	N,N'-m-Phenylenebis(p-aminobenz-amide)[a]	227–228	16.14	15.93, 15.89
3	N,N'-p-Phenylenebis(m-aminobenz-amide)	289–291	16.14	16.17, 16.20
4	N,N'-p-Phenylenebis(p-aminobenz-amide)	346–348	16.14	16.17, 16.07
5	N,N'-Dimethyl-N,N'-p-phenylenebis-(m-aminobenzamide)	231–233	14.97	15.07, 15.13
6	N,N'-Dimethyl-N,N'-p-phenylenebis-(p-aminobenzamide)	256–258[b]	14.97	14.50, 14.71
7	N,N'-Diphenyl-N,N'-p-phenylenebis-(m-aminobenzamide)	240–243	11.99	10.8, 11.0

[a] Reported[11] but no physical properties given.
[b] Reported[12] m.p. 255°C.

Interfacial Polymerization

Selected polymers were prepared by the interfacial polycondensation method;[13,14] The inherent viscosities obtained were only 0.7–1.4. Thus, when diamine 1 (Table II) dispersed in water was reacted in a Blendor jar with isophthaloyl chloride dissolved in THF the η_{inh} of the resulting polymer was only 0.7. A higher η_{inh} was obtained by using a more finely divided diamine prior to polymerization; this was done by placing ice and sodium carbonate in a hot solution of diamine dihydrochloride in a Blendor jar. Isophthaloyl chloride in THF was added immediately to the rapidly stirred mixture; by this method diamine 1 gave a polymer of $\eta_{inh} = 1.4$ but diamine 2 with isophthaloyl chloride gave a polymer of $\eta_{inh} = 0.7$.

Low Temperature Solution Polymerization

By low temperature solution polymerization[15] more consistent results and higher inherent viscosities were obtained than by the interfacial poly-

TABLE III
Wholly Aromatic Ordered Copolyamides

	Prepared from		η_{inh} (DMAc, 5% LiCl)	PMT, °C.[a]	Comments
	Diamine (Table II)	Dicarbonyl chloride			
III	1	Isophthaloyl	1.48	410	Tough films and excellent crystalline fibers (Table IV)
V	1	Terephthaloyl	1.92	450	Tough films and excellent crystalline fibers (Table IV)
VI	2	Isophthaloyl	1.27	475	Tough films and excellent crystalline fibers (Table IV)
VII	2	Terephthaloyl	1.42	490	Tough films
VIII	3	Isophthaloyl	1.30	460	Tough films
IX	3	Terephthaloyl	1.31	467	Tough films
X	4	Isophthaloyl	0.99	480	Tough films
XI	4	Terephthaloyl	1.98[b]	555	Tough films
XII	5	Isophthaloyl	0.42	265[c]	Tough films
XIII	5	Terephthaloyl	0.65	300[c]	Tough films
XIV	6	Isophthaloyl	0.78		Film somewhat brittle
XV	6	Terephthaloyl			Brittle film
XVI	7	Isophthaloyl			Brittle film
XVII	7	Terephthaloyl			Brittle film

[a] Polymer melting temperature observed by differential thermal analysis (DTA).

[b] Determined on a 0.5% solution in concentrated sulfuric acid at 25°C.

[c] Approximate melting points obtained by observing flow points upon heating film, not PMT observed by DTA.

merization described above. Polymers (Table III) of very high inherent viscosities were obtained by reacting a diacid chloride with a diamine (Table II) dissolved or dispersed in a liquid medium which functioned both as acid acceptor and solvent. Such solvents include DMAc containing 5% dissolved lithium chloride, and N-methyl-pyrrolidone. The reaction temperature was usually −20°C. upon addition of the acid chloride, and the temperature was permitted to rise to 15–25°C. after 30 min. The solutions were usually neutralized with lithium hydroxide prior to casting films or spinning fibers.

Random Copolymer

A polymer of the same overall molar composition as III was prepared which did not have the ordered sequences of III. This random copolymer was prepared by the interfacial polymerization of the monomers used to make I and II. Thus, into a Blendor jar were charged 1.08 g. (0.01 mole) m-phenylenediamine, 6.5 g. sodium carbonate, 0.2 g. Dupanol ME, 75 ml. water, and 25 ml. THF. A slurry of 3.84 g. (0.02 mole) m-aminobenzoyl chloride hydrochloride[1,2] in a solution of 2.03 g. (0.01 mole) isophthaloyl

chloride in 17 ml. of aniline-free benzonitrile (the use of benzonitrile was reported[2] to be necessary for obtaining high molecular weight I) and 9 ml. THF was poured all at once into the rapidly stirred contents of the Blendor jar.   After 15 min. the polymer was collected, washed with hot water, then washed with acetone and dried.   The yield of polymer, η_{inh} 0.7, was 92% of theory.   The random copolymer, unlike I, II, or III, softened at 300°C. and was a clear melt at 350°C.

RESULTS AND DISCUSSION

Thermal Properties of Polymers

The eight polymers made from the four primary diamines (diamines 1–4, Table II) had melting points or decomposition temperatures ranging from 410°C. for the all-*meta* polymer to 555°C. for the all-*para* one.   That the high melting points were dependent on the regular order of the various units along the chain was shown by comparison of the thermal stabilities of an order copolyamide with that of a random copolymer made up of the same building blocks.   Thus, a copolymer of the same overall composition as the ordered copolymer III was prepared interfacially by polymerizing the monomers used to make I and II in the same ratio as found in III.   The high molecular weight copolymer produced, which was judged to be either a completely random or block copolymer, had a softening point of only 300°C., which was considerably lower than that (> 350°C.) of the regularly alternating copolymer, III, and the random copolymer was a clear melt at 350°C., whereas the ordered copolymer had a DTA melting point of 410°C.*

In general, the thermal stability of aromatic ordered copolyamides increases as the *p*-phenylene content increases.   In Figure 1 DTA curves (in nitrogen) are shown which clearly point out the rise in polymer melting temperature (with decomposition) as the number of *p*-phenylene units per polymer repeat unit is increased from one to four.   This trend is also seen in the tabulation of the DTA melting points for the various polymers in Table III.   That the thermal stability is increased with the increase of *p*-phenylene content was also shown by TGA.   In Figure 2 are contrasted the retention of weight curves (TGA) at elevated temperatures in nitrogen for a wholly aromatic ordered copolyamide containing only *m*-phenylene units and another containing three *m*-phenylene units and a *p*-phenylene unit per polymer repeat unit.

A number of polymers were made from secondary diamines (polymers XII–XVII, Table III) to determine the effect of *N*-substitution on the thermal properties of the polymers.   In these polymers the number of *N*-hydrogens is reduced to one-half those in the polymers made from the primary diamines, and consequently, the number of possible hydrogen

---

* The polymers do not melt in the conventional sense.   An endothermic transition by DTA is observed in nitrogen; this transition is attributed to an incipient melting phenomenon prior to decomposition.

bonds is reduced accordingly. As expected, the melting points of the polymers were greatly reduced (Table III). However, it is surprising that a polyamide, such as XII (Table III), which contains rigid phenylene units and has only one-half of its amide groups N-substituted, melts at only
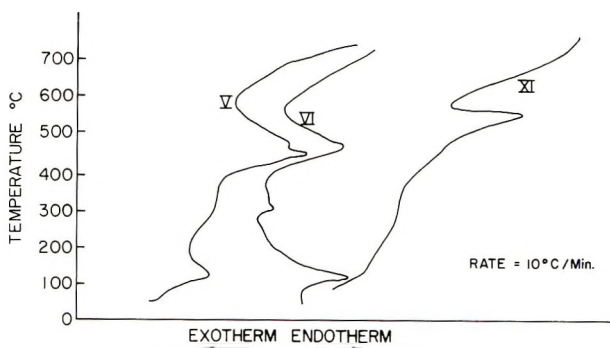

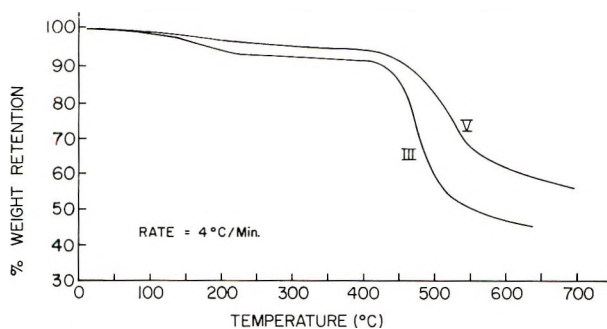Fig. 1. Programmed DTA (in nitrogen) of wholly aromatic ordered copolyamides.

Fig. 2. Programmed TGA (in nitrogen) of wholly aromatic ordered copolyamides.

265°C., while a polyamide which has a highly flexible alkylene chain and is wholly N-substituted, such as the polyamide from terephthalic acid and N,N'-dimethylhexamethylenediamine,[16] melts at 260°C.

Fabrication of Polymers

The ordered copolyamides have been prepared with high inherent viscosities, up to 2.0 (Table III). Almost all of these polymers could be cast to tough, flexible films, and several of these polymers were spun to excellent crystalline fibers. Although these wholly aromatic ordered copolyamides are generally very insoluble in the common organic solvents, DMAc containing dissolved lithium chloride is a solvent for all of them. DMAc alone is a solvent for those polymers containing N-methyl groups but not for the rest unless HCl or an inorganic salt is dissolved in it. Strong acids, such as sulfuric acid, readily dissolved nearly all of the compositions, and the polymers could be recovered with no apparent degradation.

Fig. 3. X-Ray diagram of a wholly aromatic ordered copolyamide fiber (III, Table IV).

The usual aliphatic polyamide solvents, such as formic acid, are without effect on these polymers.

The solubility of the ordered copolyamides was found to decrease with increase in *p*-phenylene content. It was nevertheless possible to polymerize even the polymers with high *p*-phenylene content by solution polymerization and to keep all of them in solution. However, once isolated as dry polymers some of these polymers could not be redissolved.

Film Properties. All of the films of the ordered copolyamides, except XI, could be drawn at temperatures from 200–400°C.; XI did not appear to draw even at 400–500°C. Several of the films became opaque upon drawing. Films of III and VI were studied by means of the penetrometer and found to have softening points above 425°C.; glass transition temperatures T_g were found to be 290 and 335°C., respectively. DTA indicated T_g's of 305 and 295°C., for VIII and IX, respectively.

All films studied were essentially colorless. Even when contacted with base, only the polymer containing all *p*-phenylene units (XI, Table III) developed a yellow color; the yellow color could be removed by the addition of acid. This phenomenon for aromatic polyamides is similar to that observed by Frazer and Wallenberger,[17] who proposed that the yellow

TABLE IV
Fiber Properties of Wholly Aromatic Ordered Copolyamides

Properties[a]	Polymer (Table III)		
	III	V	VI
Tenacity, g./den.	5.1	6.0	5.8
Elongation, %	37	23	9
Initial modulus, g./den.	89	101	101
Moisture regain[b]	—	5.2	—
Density, g./cc.	1.35	1.36	1.36

[a] Fiber properties are for unboiled-off samples.
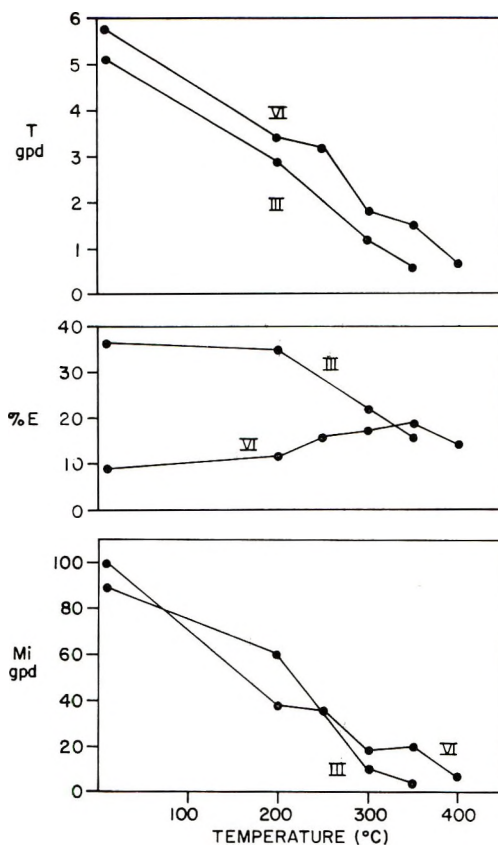[b] Equilibrium moisture at 70°F. and 65% R.H.

Fig. 4. Fiber properties of III and VI tested at elevated temperatures (T = tenacity, E = elongation, M_i = initial modulus).

color of aromatic polyhydrazides exposed to strong base was due to the hydrazide groups partaking in extended conjugation.

Fiber Properties. In Table IV are summarized the properties of the fibers obtained from three of the wholly aromatic ordered copolyamides listed in Table III. The excellent tenacities for the fibers listed in Table IV are probably due to the high degree of orientation and crystallinity developed in these fibers. The high initial moduli of these fibers are apparently due to chain stiffness in the polymers and the presence of strong intermolecular forces, including hydrogen bonding. Figure 3 shows a typical x-ray diagram for one of the fibers listed in Table IV.

In Figure 4 are plotted the fiber properties of polymers III and VI at various testing temperatures.

VI
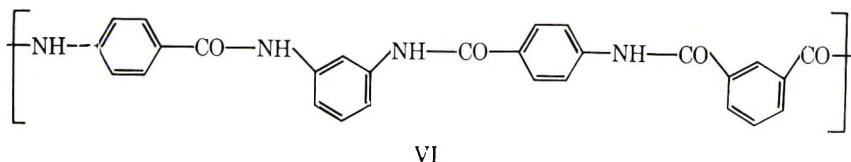
The retention of useful fiber properties to higher temperatures in the case of VI reflects greater chain stiffness due to the presence of p-phenylene units and may reflect better hydrogen bonding and chain packing.

Air aging of fibers for long periods of time at 300°C. showed that physical properties were retained to a remarkable degree (Table V).

TABLE V
Effect on Physical Properties of Wholly Aromatic Ordered
Copolyamides after Prolonged Exposure in Air at 300°C.[a]

	Fiber III[b]				Fiber V[b,c]			
Time, hr.	Tenacity, g./den.	Elonga-tion, %	Initial modulus, g./den.	Work to break, g.-cm./den.-cm.	Tenacity, g./den.	Elonga-tion, %	Initial modulus, g./den.	Work to break, g.-cm./den.-cm.
0	5.1	37	89	1.25	6.0	23	101	0.94
17	3.5	28	81	0.46	4.2	16	82	0.47
24	3.3	25	94	0.66	3.5	9	74	—
120	2.7	16	88	0.33	2.5	4	84	—
168	2.6	13	89	0.25	2.0	3	75	—

[a] Free shrinkage allowed.

[b] Fibers of Table IV.

[c] Data supplied by H. S. Morgan of the Chemstrand Research Center, Inc.

References

1. Stephens, C. W., Brit. Pat. 901,159 (1962).

2. Huffman, W. A. H., R. W. Smith, and W. T. Dye, Jr., Belg. Pat. 620,511 (1962).

3. Preston, J., and R. W. Smith, Belg. Pat. 637,260 (1964).

4. Colonge, J., and E. Fichet, *Bull. Soc. Chim. France*, **1955**, 412.

5. Katz, M., Belg. Pat. 569,760 (1958).

6. Mark, H. F., S. M. Atlas, and N. Ogata, *J. Polymer Sci.*, **61**, 849 (1962).

7. Dine-Hart, R. A., B. J. C. Moore, and W. W. Wright, *J. Polymer Sci. B*, **2**, 369 (1964).

8. Preston, J., and F. Dobinson, *J. Polymer Sci. B*, **2**, 1171 (1964).

9. Lyman, D. J., and S. L. Jung, *J. Polymer Sci.*, **40**, 407 (1959).

10. Stephens, C. W., U. S. Pat. 3,049,518 (1962).

11. Bower, G. M., and L. W. Frost, *J. Polymer Sci. A*, **1**, 3135 (1963).

12. Allen, C. F. H., J. V. Crawford, G. F. Frame, J. E. Jones, E. R. Webster, and C. V. Wilson, *J. Org. Chem.*, **13**, 666 (1948).

13. Wittbecker, E. L., and P. W. Morgan, *J. Polymer Sci.*, **40**, 289 (1959).

14. Morgan, P. W., and S. L. Kwolek, *J. Polymer Sci.*, **40**, 299 (1959).

15. Morgan, P. W., *J. Polymer Sci.*, C**4**, 1075 (1963).

16. Shashoua, V. E., and W. M. Eareckson, *J. Polymer Sci.*, **40**, 343 (1959).

17. Frazer, A. H., and F. T. Wallenberger, *J. Polymer Sci. A*, **2**, 1147 (1964).

Résumé

On a préparé des copolyamides ordonnés entièrement aromatiques de stabilite thermique inhabituellement elevée, par condensation de chlorures de diacides avec des diamines symetriques, contenant en un arrangement ordonné des unités amides aromatiques préformées. On a assuré la préservation de l'ordre au moment de la condensation en utilisant des techniques de polymérisation interfaciale ou en solution à des températures inférieures à 50°C. Chaque polymère contient des unités dérivées des acides aminobenzoiques, des arylenes-diamines et des arylene-diacides. En utilisant des unités *para*- et *méta*-phénylène, huit polymères différents sont possibles; on les a tous préparés. Les analyses thermiques différentielles et les analyses thermogravimétriques montrent que ces polymères ont des points de fusion et des températures de décomposition situés aux environs de 410°C pour les polymères entièrement méta et 555°C pour ceux entièrement para. La substitution des hydrogènes N internes des diamines par des groupes méthyles ou des groupes phényles conduit á des copolymères supplémentaires ordonnés. On en a préparé plusieurs, mais leurs points de fusion étaient beaucoup plus bas que ceux des polymères mères limitant leur utilité dans les applications à haute température. On a préparé des films pliables résistants au départ des huit polymères non-substitués, et des fibres cristallines avec des tenacités d'environ 6 gpd à partir de trois des polymères. Les propriétés des fibres étaient conservées jusqu'à un haut degré même quand elles étaient déterminées à des températures atteignant 400°C. Des fibres vieillies à 300°C pendant des périodes prolongées montrent une conservation remarquable des propriétés fibreuses.

Zusammenfassung

Vollaromatische geordnete Copolyamide mit ungewöhnlich hoher thermischer Stabilität wurden durch Kondensation aromatischer Diacidchloride mit symmetrischen Diaminen, welches vorgebildete aromatische Amideinheiten in einer geordneten Struktur enthielten, dargestellt. Die Aufrechterhaltung der Ordnung beim Kondensationsschritt wurde durch Heranziehung des Grenzflächen- oder Lösungspolymerisationsverfahrens bei Temperaturen unterhalb 50°C erreicht. Jedes Polymere enthält von Aminobenzoesaüren, Arylendiaminen und Arylendiaciden abgeleitete Bausteine. Bei Verwendung von *para*- und *meta*-Phenylenbausteinen sind acht verschiedene Polymere möglich; alle diese wurden dargestellt. Differentialthermoanalyse und thermogravimetrische Analyse zeigten, dass diese Polymeren Schmelzpunkte oder Zersetzungstemperaturen im Bereich von 410°C für die All-*meta*- Polymeren bis 555°C für die All-*para*-Polymeren besassen. Substitution des inneren N-Wasserstoffs der Diamine durch Methyl- oder Phenylgruppen führt zusätzlich zu geordneten Copolymeren. Es wurden einige dargestellt, ihre Schmelzpunkte waren jedoch viel niedriger als diejenigen der Ausgangspolymeren, was ihre Brauchbarkeit für Hochtemperaturverwendungszwecke begrenzte. Zähe, faltbare Filme wurden aus allen acht unsubstituierten Polymeren dargestellt, und kristalline Fasern mit einer Festigkeit von ca. 6 gpd wurden aus drei der Polymeren dargestellt. Die Eigenschaften dieser Fasern wurden zu einem hohen Grade sogar bei Temperaturen bis zu 400°C beibehalten. Bei Langzeitalterung bei 300°C zeigten die Fasern eine bemerkenswerte Retention ihrer Eigenschaften.

Increased Rates of Initiation of Polymerization by 4-4'-Dicyano-4-4'-azopentanoic Acid in the Presence of Ferric Salts

E. A. S. CAVELL and I. T. GILSON, *Department of Chemistry, The University, Southampton, England*

Synopsis

The initiation of the polymerization of acrylamide by 4-4'-dicyano-4-4'-azopentanoic acid in aqueous solution has been studied kinetically at 25°C. Ferric chloride and ferric sulfate were used to terminate polymerization so that rates of initiation could be calculated from the rates of production of ferrous iron. Velocity coefficients at 25°C. for the initiation reaction were found to be $(25.7 \pm 2.8) \times 10^{-7}$ sec.$^{-1}$ for the ferric chloride terminated reaction and $(73.6 \pm 0.6) \times 10^{-7}$ sec.$^{-1}$ for the ferric sulfate-terminated polymerization. The value reported for the initiation reaction when acrylamide is polymerized in the absence of metal salts is 1.29×10^{-7} sec.$^{-1}$. Velocity coefficients for the termination reaction have been calculated from the overall rates of polymerization obtained with ferric salts present. In the case of the ferric chloride-terminated reaction, it has been shown that the rate of polymerization is reduced by increasing the total concentration of chloride ions. Termination velocity coefficients at 25°C. for the inner sphere complexes $FeCl^{2+} \cdot 5H_2O$ and $FeSO_4^{+} \cdot 4H_2O$ have been calculated to be 18.9×10^4 and 7.98×10^4 l./mole-sec., respectively. The dependence on the concentration of ferric chloride of the molecular weights of the polymers produced has also been considered.

INTRODUCTION

The use of ferric salts as oxidative chain terminators provides, in principle, a valuable method for determining the rates of initiation of radical polymerization reactions. If experimental conditions are such that chains are exclusively terminated by a reaction which is first-order with respect to both the ferric salt and the polymer radicals, then the rate of production of ferrous ions may be equated to the rate of chain termination and hence, in the steady state, to the rate of initiation of chains. The method has been employed successfully to measure rates of initiation of a number of polymerization reactions,[1] although in the case of the polymerization of acrylamide in aqueous solution initiated by 4-4'-dicyano-4-4'-azopentanoic acid (ACV), complications arise which limit the usefulness and applicability of the kinetic data obtained for the initiation reaction from the measured rates of reduction of the ferric salt.

Reference has been made in a previous paper[2] to the increased rates of initiation observed with ACV, when ferric perchlorate is present in the solution. The present investigation is principally concerned with the

effects of ferric chloride and, to a lesser extent, ferric sulfate on the kinetics of the initiation and termination reactions involved. Ferric chloride is itself able to initiate the polymerization of acrylamide,[3] presumably by an electron transfer mechanism, and this is an additional factor to be considered in the interpretation of the appropriate rate data.

EXPERIMENTAL

Materials

The initiator, 4-4'-dicyano-4-4'-azopentanoic acid was prepared and purified as described in an earlier paper.[4] The monomer, acrylamide, was purified by successive crystallization from chloroform and benzene followed by vacuum drying, m.p. 84.5 ± 0.5°C. Water used as solvent was purified by distillation followed by percolation through Amberlite monobed resin MB-1. Microanalytical grade hydrochloric and sulfuric acids were used without further purification. Stock solutions of ferric salts were prepared by dissolving the freshly precipitated hydroxide in the appropriate diluted acid. These solutions were analyzed both gravimetrically and volumetrically for iron and volumetrically for hydrogen ions. Solutions of ferric salts, after being diluted to the concentration required for kinetic studies, were allowed to stand for several days before use to ensure complete ionic equilibration.

Measurements

Rates of polymerization were determined either by precipitating and weighing the polymer produced in a suitable interval of time or by measuring the rate of contraction which occurs during polymerization. A more detailed account of both procedures has been given in an earlier paper.[4] Dioxane was found to be the most satisfactory precipitant for polyacrylamide and a shrinkage factor of 0.050 mmoles of acrylamide polymerized for a contraction of 1 mm. in a capillary of 1 mm. diameter was used to calculate rates of polymerization from rates of contraction.[5]

The procedure adopted for measuring the change in concentration of ferrous ions during the course of polymerization was as follows. Solutions of monomer and initiator, the latter containing the ferric salt were placed in separate flasks connected by an inverted U-tube, which itself was fused to one arm of a T-piece. One of the remaining limbs of the T-piece was connected to a vacuum line, the other to a small flask with a side arm closed by means of a self-sealing rubber serum cap capable of withstanding a vacuum of 10^{-5}–10^{-6} mm. Hg. The reactant solutions were degassed in the usual way and then the whole apparatus was filled with oxygen-free nitrogen. In order to ensure the complete absence of oxygen, the nitrogen used was first passed through a solution containing sodium dithionite and sodium anthraquinone-β-sulfonate and then dried over barium perchlorate and phosphoric oxide.

With a small positive pressure of nitrogen being maintained within it, the apparatus containing the reactants was removed from the vacuum line and transferred to a thermostat operating at $25.00 \pm 0.02°C$. When the reactants had attained this temperature, they were thoroughly mixed and the apparatus replaced in the thermostat. After a suitable interval of time, some of the polymerizing solution was transferred to the small flask attached and from this about 5 ml. of solution was removed by piercing the serum cap with a fine hypodermic needle attached to a surgical syringe. The small internal positive pressure of nitrogen was intended to eliminate as far as possible the ingress of oxygen at this stage. Samples removed in this way by means of the syringe were then analyzed spectrophotometrically for ferrous ions. o-Phenanthroline was used as complexing agent and absorption measurements were made at 504 mμ. The spectrophotometer had been previously calibrated at this wavelength by means of solutions of known composition.
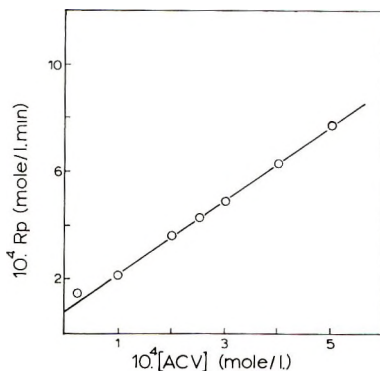
Fig. 1. Variation of rate of polymerization R_p with initiator concentration [ACV]: $[FeCl_3] = 2.58 \times 10^{-5}M$, $[M_1] = 1.00M$, $[HCl] = 0.122M$, temp. $= 25°C$.

A calibrated Ostwald viscometer was used to measure the viscosities of suitably diluted solutions of polymer prepared under conditions identical with those employed for kinetic measurements. Limiting viscosity numbers were obtained by graphical extrapolation.

RESULTS AND DISCUSSION

Overall Rates of Polymerization

Plots showing the effect of the rate of polymerization R_p of varying the concentrations of the initiator (ACV) and ferric chloride are given in Figures 1 and 2. Since the rate is directly proportional to the initiator concentration and inversely proportional to that of the ferric salt, linear termination of chains must presumably predominate. It is apparent, however, that in both plots, the best straight line through the experimental points does not pass through the origin, but gives a positive intercept on
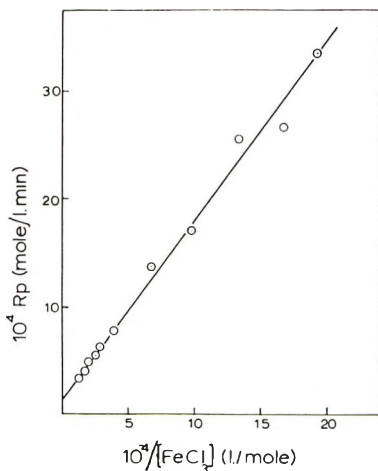
Fig. 2. Variation of rate of polymerization R_p with the reciprocal of the ferric chloride concentration; [ACV] $= 5.00 \times 10^{-4}M$, [M_1] $= 1.00M$, [HCl] $= 0.122M$, temp. $= 25°C$.

the rate axis. The values of these intercepts are approximately the same for both series of experiments. These observations suggest that ferric chloride is itself able to initiate polymerization of acrylamide in aqueous solution.

Rates of polymerization R_p^0 obtained with no initiator other than ferric chloride present were found to be independent both of the ferric chloride concentration and of the total concentration of chloride ions.[3] The mean value of R_p^0 obtained from these experiments was $(0.96 \pm 0.12) \times 10^{-4}$ mole/l.-min. at $25°C$. For R_p^0 to be independent of the concentration of ferric chloride, the rates of both initiation and termination must be directly proportional to the ferric chloride concentration.

In the presence of ferric chloride, therefore, the overall rate of polymerization (R_p) observed when the initiator ACV is also present will be given by eq. (1), in which k_1 is the specific rate constant for initiation by ferric chloride, k_4 is the rate constant for linear termination by a ferric salt and the other symbols have their usual significance.

$$R_p = k_p[M_1](k_1[FeCl_3] + f_i k_i[ACV])/k_4[FeCl_3]$$

$$= R_p^0 + k_p[M_1](f_i k_i[ACV]/k_4[FeCl_3]) \tag{1}$$

Plots of R_p against [ACV] and [$FeCl_3$]$^{-1}$ should therefore be linear and both should give a positive intercept on the rate axis equal to R_p^0. Values of 1.0×10^{-4} and 1.2×10^{-4} mole/l.-min., estimated for these intercepts from the plots shown in Figures 1 and 2, are in close agreement with the mean value of R_p^0 obtained from direct measurements with no initiator other than ferric chloride present.

The average value of the ratio $k_p[M_1]f_i k_i/k_4$ estimated from the slopes of the linear plots shown in Figures 1 and 2 is 3.43×10^{-5} mole/l.-min.

From this result and from those obtained for the corresponding intercepts, a mean value of 3.21 has been calculated for $k_1/f_i k_i$.

Rates of Formation of Ferrous Ions

The rates of production of ferrous ions summarized in Table I for different concentrations of initiator (ACV) and ferric salt (chloride and sulfate) are average values of a number of replicate experiments. When polymerization is terminated by ferric sulfate, $d[\mathrm{Fe(II)}]/dt$ is independent of the concentration of ferric salt. This indicates that the sulfate, in contrast to the chloride, does not by itself initiate the polymerization of acrylamide, and this has been confirmed experimentally. Under stationary-state conditions, therefore, the rate of reduction of ferric sulfate may be equated to the rate of initiation of polymerization by ACV as indicated in eq. (2):

$$d[\mathrm{Fe(II)}]/dt = f_i k_i [\mathrm{ACV}]$$

$$= k_4[\mathrm{Fe(III)}] R_p/k_p [\mathrm{M_1}] \qquad (2)$$

The mean value of the ratio $R_p[\mathrm{Fe(III)}]/[\mathrm{M_1}][\mathrm{ACV}]$ for the ferric sulfate-terminated reaction is $(10.3 \pm 1.0) \times 10^{-5}$ min.$^{-1}$ at 25°C. Both $f_i k_i$ and k_4 can therefore be calculated from the measured rates of formation of ferrous ions by means of eq. (2) since k_p is known to be 1.80×10^4 l./mole-sec. at 25°C.[5] The numerical values obtained are summarized in Table I.

TABLE I

Rates of Production of Ferrous Ions at 25°C. from Ferric Sulfate with $0.05M$ H_2SO_4 and Ferric Chloride with $0.122M$ HCl at a Monomer Concentration of $1.00M$

$[\mathrm{Fe(III)}] \times 10^4$, mole/l.	$[\mathrm{ACV}] \times 10^4$, mole/l.	$d[\mathrm{Fe(II)}]/dt \times 10^8$ mole/l.-min.	$f_i k_i \times 10^6$, sec.$^{-1}$	$k_4 \times 10^{-4}$, l./mole-sec.
Ferric sulfate, $H_2SO_4 = 0.050M$				
1.00	2.00	8.75	7.30	7.65
10.0	2.00	8.90	7.42	7.78
Ferric chloride, HCl $= 0.122M$				
0.258	5.00	12.0	3.00	9.45
0.258	9.66	18.3	2.69	8.47
5.15	9.66	53.2	2.08	6.55
10.0	2.00	99.	2.49	7.84

One consequence of the ability of ferric chloride to initiate the polymerization of acrylamide is that $d[\mathrm{Fe(II)}]/dt$ now depends on the concentration of the ferric salt employed, as illustrated by the experimental data summarized in Table I. Initiation by ferric chloride presumably involves electron transfer and therefore contributes to the observed growth in

concentration of ferrous ions. Consequently, under stationary-state conditions, the rate of formation of ferrous iron will be given by eq. (3).

$$d[\text{Fe(II)}]/dt = k_1[\text{FeCl}_3] + k_4[\text{FeCl}_3]R_p/k_p[\text{M}_1]$$

$$= 2k_1[\text{FeCl}_3] + f_i k_i[\text{ACV}] \qquad (3)$$

Now the mean values of $k_1/f_i k_i$ and $k_p[\text{M}_1]f_i k_i/k_4$ have been found to be 3.21 and 3.43 $\times$ 10^{-5} mole/l.-min., respectively. Numerical values of $f_i k_i$ and k_4 for the ferric chloride-terminated polymerization can therefore be found by making the appropriate substitutions in eq. (3). These are shown in Table I.

Molecular Weights of Polymers

Average molecular weights for the polymers produced in the ferric chloride-terminated reaction were calculated from the corresponding limiting viscosity numbers by means of Scholtan's relation.[6] Since linear termination of polymerization predominated under the experimental conditions employed, it has been assumed that viscosity-average degrees of polymerization ($\bar{r}_v$) obtained are approximately twice the number-average values. Accordingly, $2/\bar{r}_v$ has been plotted against the concentration of ferric chloride as shown in Figure 3. The best straight line through the experimental points has a slope of 4.26, and this may be equated with $k_4/k_p[\text{M}_1]$. The monomer concentration was $1M$ throughout. The value of k_4 calculated from molecular weight determinations is, therefore, 7.67 $\times$ 10^4 l./mole-sec. at 25°C compared with a mean value of 8.08 $\times$ 10^4 l./mole-sec. obtained from kinetic measurements (Table I).

With a fixed concentration of ferric chloride, average molecular weights were found to be independent of the concentration of initiator (ACV)
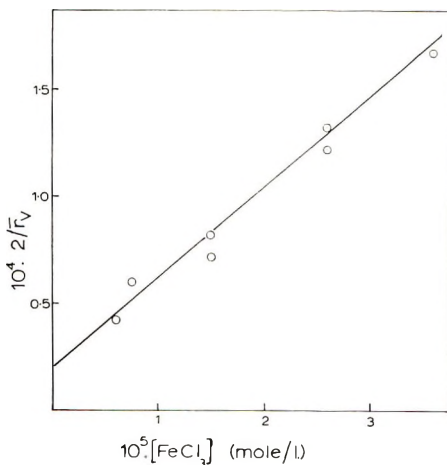

Fig. 3. Effect of ferric chloride concentration on viscosity-average degrees of polymerization $\bar{r}_v$; polymers prepared with $[\text{M}_1]$ = $1.00M$, $[\text{ACV}]$ = $5.00 \times 10^{-4}M$, $[\text{HCl}]$ = $0.122M$, temp. = 25.0°C.

employed. The positive intercept on the ordinate axis of Figure 3 has therefore been taken to indicate nondegradative chain transfer to monomer. The value of 2×10^{-5} for the intercept is in reasonable agreement with values of 1.6×10^{-5} and 1.2×10^{-5} reported by previous workers[4,5] for the ratio k_{fm}/k_p at $25°C.$, where k_{fm} is the rate constant for chain transfer to monomer.

Effect on Kinetics of Added Potassium Chloride

A recent study[7] of the spectroscopic and other properties of ferric chloride in aqueous solutions of hydrochloric acid has shown that, in such solutions, association between ferric and chloride ions is limited principally to the formation of the inner sphere complex $FeCl^{2+} \cdot 5H_2O$. The fraction β of the total ferric chloride in the form of the inner sphere complex will, of course, depend on the concentration of chloride ions present. Under our experimental conditions, however, the value of β does not depend significantly on the concentration of ferric chloride, owing to the relatively high total chloride ion concentrations employed.

In the presence of ferric chloride, the rate of polymerization of acrylamide is reduced by increasing the total concentration of chloride ions in the solution. This change in overall rate is due to the composite character of the chain termination reaction involved. For a large, fixed concentration of chloride ions, the rate of polymerization remains inversely proportional to the concentration of the ferric chloride, as illustrated in Figure 4 for two different total chloride ion concentrations. The slopes of the straight lines obtained by plotting R_p against $[FeCl_3]^{-1}$, decline with increasing chloride ion concentration. Composite velocity coefficients k_4
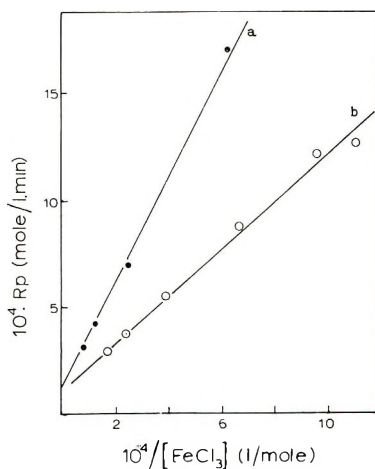

Fig. 4. Effect of total chloride ion concentration on the variation of rate of polymerization R_p with the reciprocal of the ferric chloride concentration; $[M_1] = 1.00M$; temp. $= 25.0°C.$; (a) $[HCl] = 0.052M$, $[HClO_4] = 0.070M$, $[ACV] = 4.00 \times 10^{-4}M$; (b) $[HCl] = 0.122M$, $[KCl] = 0.244M$, $[ACV] = 5.00 \times 10^{-4}M$.

TABLE II

Effect of Total Chloride Ion Concentration on Composite Velocity Coefficients of the Ferric Chloride Termination Reaction at 25.0°C., $[M_1] = 1.00M$; $[H_3O^+] = 0.122M$

[HCl], mole/l.	[KCl], mole/l.	$k_4 \times 10^{-4}$, l./mole-sec.	$Q = [FeCl^{2+}]/$ $[Fe^{3+}][Cl^-]$, l./mole
0.052[a]	0	4.54	6.59
0.122	0	8.08	6.59
0.122	0.024	8.90	5.97
0.122	0.122	9.34	4.51
0.122	0.244	12.54	3.69

[a] $HClO_4 = 0.07M$.

have been evaluated for the termination reaction from the slopes of the plots concerned for each concentration of chloride ions examined and are summarized in Table II.

The composite termination coefficient k_4 may be represented by the relation

$$k_4 = k_{40} (1 + \beta) + k_{42}\beta \qquad (4)$$

in which k_{40} and k_{42} are the termination velocity constants for $Fe^{3+} \cdot 6H_2O$ and $FeCl^{2+} \cdot 5H_2O$ respectively. However, an alternative formulation in terms of the total chloride ion concentration and the equilibrium quotient $Q(= [FeCl^{2+}]/[Fe^{3+}][Cl^-])$ of the ion association reaction, as shown in eq. (5)

$$k_4 (1 + Q [Cl^-]) = k_{40} + k_{42} Q[Cl^-] \qquad (5)$$

is more suitable for the graphical evaluation of the appropriate rate constants. Equilibrium quotients for the ionic strengths concerned were calculated from the data reported by Woods et al.,[7] and a linear plot of the left-hand side of eq. (5) against $Q[Cl^-]$ is shown in Figure 5. The inter-
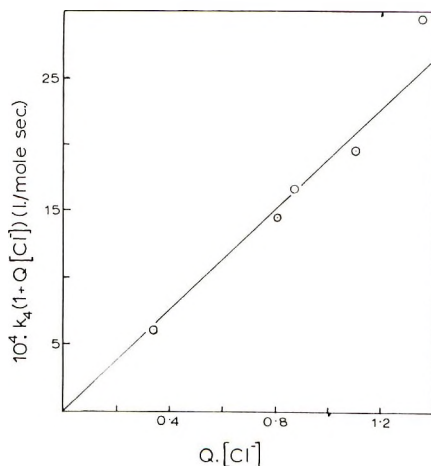

Fig. 5. Plot of left-hand side of eq. (5) against $Q. [Cl^-]$ for data given in Table II.

cept is too small for an accurate, graphical evaluation of k_{40} to be made, but from the slope, k_{42} has been estimated to be $(18.9 \pm 0.8) \times 10^4$ l./mole-sec. for $25°C$.

Comparison of Initiation and Termination Rate Coefficients

From a study of the association of ferric and sulfate ions in perchloric acid solutions, Willix[8] has concluded that the principal ion pair formed in these solutions is the inner sphere complex, $FeSO_4^+ \cdot 4H_2O$. After making due allowance for the effect of the sulfate–bisulfate equilibrium, we have estimated that for the ionic strengths employed in our measurements, about 96.7% of the ferric sulfate was present as this inner sphere complex. The remainder was presumably in the form of aquated ferric ions, the termination velocity constant for which is known to be 2.8×10^3 l./mole-sec. at $25°C$.[9] The termination velocity constant for $FeSO_4^+ \cdot 4H_2O$ computed from the composite coefficients quoted in Table I is therefore 79.8×10^3 l./mole-sec. compared with a value of 189×10^3 l./mole-sec. obtained for the corresponding chloride inner sphere complex, $FeCl^{2+} \cdot 5H_2O$. This is the reverse of the order of reactivity usually found in anion-catalyzed electron transfer reactions.[8,10] Among factors responsible for this difference in reactivity may be the larger size of the sulfate ion and the smaller ionic charge of the corresponding inner sphere complex.

Values of the rate coefficients for the initiation reaction obtained in the presence of various ferric salts are compared in Table III with a value of $f_i k_1$ calculated from kinetic measurements made with no metal salt present.

TABLE III

Effect of Ferric Salts on the Value of the Velocity Coefficient $(f_i k_i)$ for Initiation of Polymerization by ACV at $25°C$.

Ferric salt	Fraction as inner sphere complex	$f_i k_i \times 10^7$, sec.$^{-1}$	Reference
None	—	1.29	4
Perchlorate	Small	4.62	2
Chloride	0.446	25.7	Present work
Sulfate	0.967	73.6	

The effect of the addition of a ferric salt is to increase markedly the initiation rate coefficient, presumably by facilitating the decomposition of the initiator (ACV). It is known that in dimethylformamide solution, ACV is readily decarboxylated by ferric chloride at $60°C$.,[11] a reaction which may be connected with the increased initiation velocity coefficients observed here. The capacity of a ferric salt to facilitate initiation of polymerization seems to be paralleled by its tendency to form inner sphere complexes, and the two properties may be related.

References

1. Bamford, C. H., A. D. Jenkins, and R. Johnston, *Proc. Roy. Soc. (London)*, **A239**, 214 (1957); *J. Polymer Sci.*, **29**, 355 (1958).

2. Cavell, E. A. S., I. T. Gilson, and A. C. Meeks, *Makromol. Chem.*, **73**, 145 (1964).

3. Cavell, E. A. S., and I. T. Gilson, *Nature*, **202**, 1005 (1964).

4. Cavell, E. A. S., *Makromol. Chem.*, **54**, 70 (1962).

5. Dainton, F. S., and M. Tordoff, *Trans. Faraday Soc.*, **53**, 499 (1957).

6. Scholtan, W., *Makromol. Chem.*, **14**, 169 (1954).

7. Woods, M. J. M., P. K. Gallagher, and E. L. King, *Inorg. Chem.*, **1**, 55 (1962).

8. Willix, R. L. S., *Trans. Faraday Soc.*, **59**, 1315 (1963).

9. Collinson, E., F. S. Dainton, B. Mile, S. Tazuke, and D. R. Smith, *Nature*, **198**, 26 (1963).

10. Silverman, J., and R. W. Dodson, *J. Phys. Chem.*, **56**, 846 (1952).

11. Entwistle, E. R., *Trans. Faraday Soc.*, **56**, 284 (1960).

Résumé

On a étudié la cinétique d'initiation de la polymérisation de l'acrylamide, par l'acide 4-4'-dicyano-4-4'-azopentanoique, en solution aqueuse à 25°C. Le chlorure ferrique et le sulfate ferrique ont été employés pour terminer la polymérisation et pour ainsi calculer les vitesses d'initiation à partir des vitesses de production de fer ferreux. On a trouvé que les coefficients de vitesse à 25°C sont de $(25{,}7 \pm 2{,}8) \times 10^{-7}$ sec^{-1} et de $(73{,}6 \pm 0{,}6) \times 10^{-7}$ sec^{-1} suivant que la polymérisation est terminée par le chlorure ou le sulfate ferrique. La valeur trouvée pour la réaction d'initiation lorsque l'acrylamide est polymérisée en l'absence totale de sels, est de $1{,}29 \times 10^{-7}$ sec^{-1}. Les coefficients de vitesse de la réaction de terminaison ont été calculés à partir de toutes les vitesses de polymérisation obtenues en présence de sels ferriques. Lorsque la réaction est terminée par le chlorure ferrique, on a montré que la vitesse de polymérisation diminue lorsque la concentration totale en ions chlorures augmente. Les coefficients de vitesse de la terminaison à 25°C pour des complexes produits par coordination sphérique interne, $FeCl^{2+} \cdot 5H_2O$ et $FeSO_4^+ \cdot 4H_2O$ sont respectivement de $18{,}9 \times 10^4$ et $7{,}98 \times 10^4$ l. mole^{-1} sec^{-1}. On a également considéré la dépendance vis-à-vis de la concentration en chlorure ferrique des poids moléculaires des polymères obtenus.

Zusammenfassung

Der Start der Polymerisation von Acrylamid durch 4-4'-Dicyan-4-4'-azopentansäure in wässriger Lösung wurde bei 25°C kinetisch untersucht. Zum Polymerisationsabbruch wurden Ferrichlorid und Ferrisulfat verwendet, sodass die Startgeschwindigkeit aus der Bildungsgeschwindigkeit der Ferroionen berechnet werden konnte. Die Geschwindigkeitskoeffizienten der Startreaktion bei 25°C waren bei Abbruch durch Ferrichlorid $(25{,}7 \pm 2{,}8) . 10^{-7}$ sec^{-1} und bei Abbruch mit Ferrisulfat $(73{,}6 \pm 0{,}6) \times 10^{-7}$ sec^{-1}. Bei Abwesenheit von Metallsalzen wird für die Startreaktion der Polymerisation von Acrylamid ein Wert von $1{,}29 . 10^{-7}$ sec^{-1} angegeben. Die Geschwindigkeitskoeffizienten für die Abbruchsreaktion wurden aus der bei Gegenwart von Ferrisalzen erhaltenen Bruttopolymerisationsgeschwindigkeit berechnet. Im Fall des Reaktionsabbruchs durch Ferrichlorid wurde gezeigt, dass die Polymerisationsgeschwindigkeit durch Erhöhung der Gesamtkonzentration an Chloridionen herabgesetzt wird. Die Abbruchsgeschwindigkeitskoeffizienten wurden bei 25°C für die inneren Komplexe $FeCl^{2+} \cdot 5H_2O$ und $FeSO_4^+ \cdot 4H_2O$ zu $18{,}9 \times 10^4$ bzw. $7{,}98 . 10^4$ l.Mol^{-1}sec^{-1} berechnet. Schliesslich wurde auch die Abhängigkeit des Molekulargewichts des gebildeten Polymeren von der Konzentration des Ferrichlorids bestimmt.

Polyquinoxalines.   III

J. K. STILLE and F. E. ARNOLD, *Department of Chemistry, University of Iowa, Iowa City, Iowa*

Synopsis

Six thermally stable polyquinoxalines have been prepared by the reactions of combinations of three tetraamines, 3,3′,4,4′-tetraaminodiphenyl sulfone (II), and 3,3′,4,4′-tetraaminodiphenyl ether (V), with two bisglyoxals, 4,4′-diglyoxalyldiphenyl sulfide dihydrate (III) and 4,4′-diglyoxalyldiphenyl sulfone dihydrate (IV). The polymers were prepared from polymerization in two stages. The first stage, a solution polymerization, produces an initially low or moderate molecular weight material, which is advanced to a high molecular weight ($\eta_{inh} > 1.0$) by heating at 375°C. under reduced pressure. All the polyquinoxalines have excellent thermal stability both in nitrogen and in air and improved solubility.

Introduction

In earlier publications[1-3] it was shown that polymers containing the quinoxaline nuclei could be prepared by melt and solution polymerizations of suitable aromatic bisglyoxals and aromatic tetraamines. The polyquinoxalines exhibit excellent thermal stability both in air and in nitrogen atmospheres. The quinoxaline polymers described are insoluble in common organic solvents and are very difficultly soluble in such solvents as hexamethylphosphoramide, dimethylformamide, and dimethyl sulfoxide.
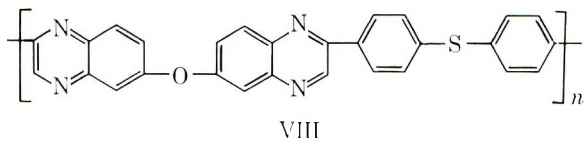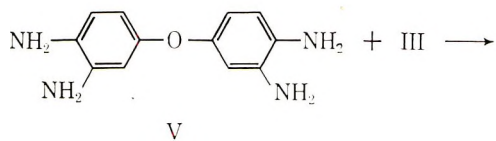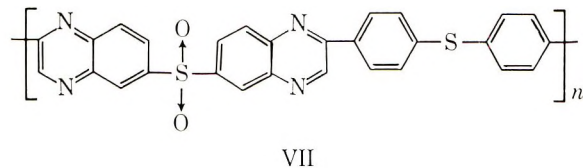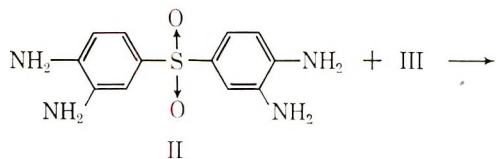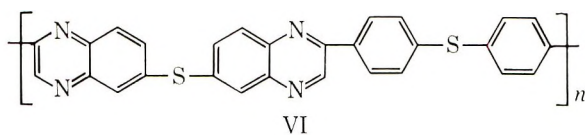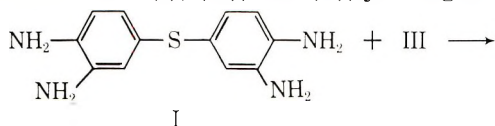
With the introduction of a flexible oxygen group between the aromatic and quinoxaline segments, we have shown[3] that solubility was increased over that of polymers containing no such group. Flexibility improved the solubility of the polymer but no sacrifice in thermal stability was made. In continuing this series, several new polyquinoxalines have been prepared containing other flexible groups (sulfide and sulfone) between the aromatic and quinoxaline segments. It was hoped that the incorporation of these flexible groups would produce polyquinoxalines which would be more amenable to fabrication.

DISCUSSION

Four new polyquinoxaline monomers, 3,3′,4,4′-tetraaminodiphenyl sulfide (I), 3,3′,4,4′-tetraaminodiphenyl sulfone (II), 4,4′-diglyoxalyldiphenyl sulfide dihydrate (III), and 4,4′-diglyoxalyldiphenyl sulfone dihydrate (IV) were synthesized for this study. The monomer 3,3′,4,4′-tetraaminodiphenyl ether was also employed as a comonomer.

I   II

III

IV   V
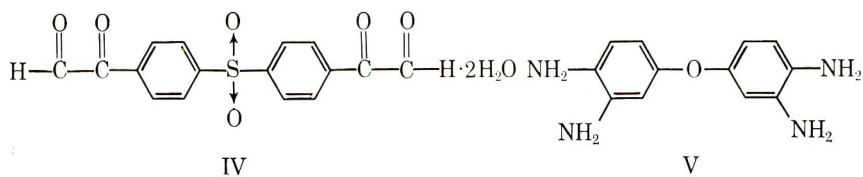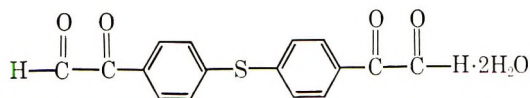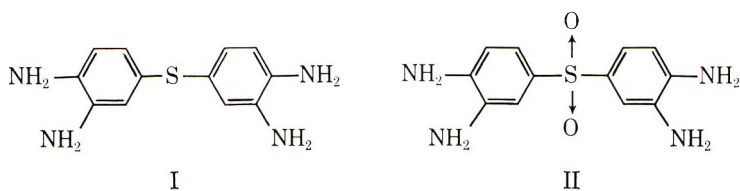
The bisglyoxals 4,4'-diglyoxalyldiphenyl sulfide dihydrate (III), and 4,4'-diglyoxalyldiphenyl sulfone dihydrate (IV) were polymerized each with the tetraamines (I), (II), and (V), yielding the polymers VI–XI.

I

VI

II

VII

V

VIII

NH$_2$—⟨ ⟩—S—⟨ ⟩—NH$_2$ + IV ⟶

NH$_2$ NH$_2$

I

IX

NH$_2$—⟨ ⟩—S—⟨ ⟩—NH$_2$ + IV ⟶

NH$_2$ NH$_2$

II

X

NH$_2$—⟨ ⟩—O—⟨ ⟩—NH$_2$ + IV ⟶

NH$_2$ NH$_2$

V

XI
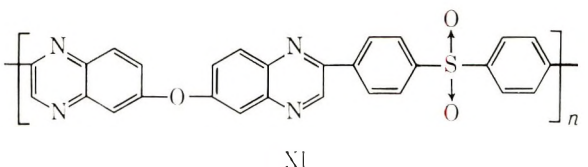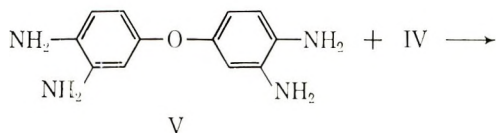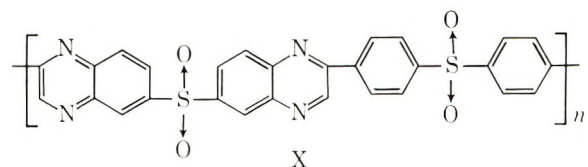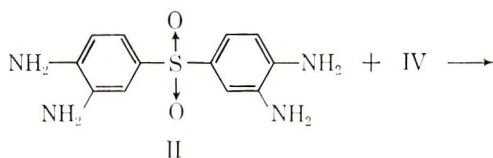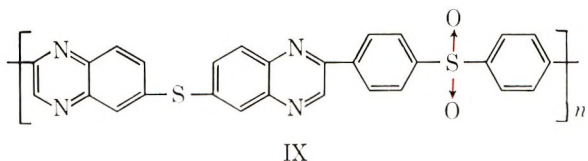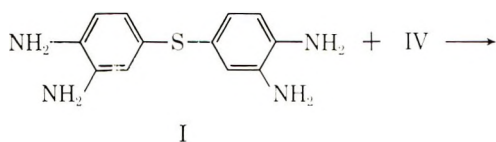
The polymerizations were carried out in two stages. In the first stage, a solution polymerization in hexamethylphosphoramide afforded a prepolymer with an intermediate molecular weight. The second stage consisted of heating the prepolymer, in the solid phase under reduced pressure, to 375°C. The material from the high temperature heating cycle always showed an increased inherent viscosity (Table I). The technique employed for these polymerizations has been previously described.[2]

The structures of the polymers (VI–XI) have been so written that the aromatic phenylene units which are incorporated from the respective bisglyoxals are attached to the 2- and 2'-positions on the quinoxaline nuclei. It has been shown from previous work[2] that aromatic tetraamines react with phenylglyoxal to give only the 2,2' positional isomer rather than the 3,3' or mixtures of both.

The thermal stabilities (Table I) of all the polymers (VI–XI) are very good in both air and nitrogen, as evidenced by thermal gravimetric analysis.

TABLE I
Physical Properties of Polyquinoxalines.

Polymer[a]		Color	Soluble, %[b]		$[\eta]^c$	TGA (air), °C.
			HMP	H_2SO_4		
VI	1	Brown	100	100	0.35	
	2	Black	70	100	2.40	500
VII	1	Yellow	75	100	0.45	
	2	Brown	55	90	0.80	440
VIII	1	Yellow	100	100	0.35	
	2	Black	19	70	1.07	460
IX	1	Brown	100	100	0.41	
	2	Black	50	80	1.12	460
X	1	Tan	100	100	0.33	
	2	Brown	21	80	1.22	420
XI	1	Yellow	100	100	0.26	
	2	Black	14	60	1.11	420

[a] Polymers obtained from the first-stage (1) solution polymerization at 180°C. and the subsequent second-stage (2) solid-phase polymerization at 375°C.

[b] Numbers refer to the per cent of the polymer which was soluble in the indicated solvents; HMP = hexamethylphosphoramide.

[c] Inherent viscosities were obtained in HMP at a concentration of 0.25 g./100 ml.

The thermal gravimetric analysis (Fig. 1) of poly[2,2'-(4,4'-thiodiphenylene)-6,6'-thiodiquinoxaline] shows initial weight loss in air occurring at 500°C. and is typical of the stabilities of the polymers in this series.

The solubilities (Table I) of the polyquinoxalines were increased with the introduction of the flexible sulfide and sulfone groups into the polymer chain. However, these polymers are still difficultly soluble in common organic solvents and appreciably soluble only in such solvents as hexamethylphosphoramide and concentrated sulfuric acid. The polymers
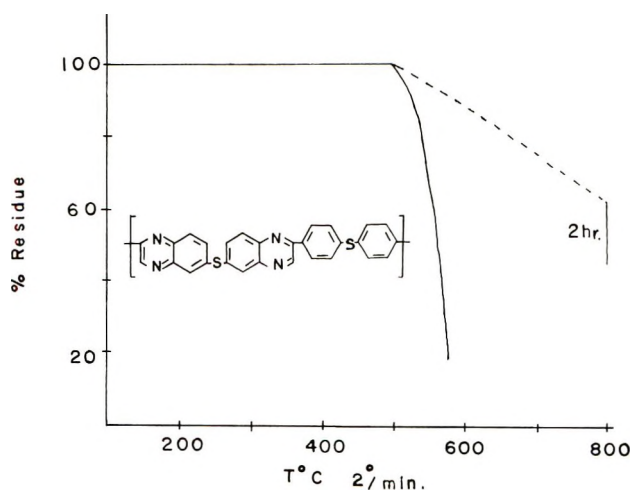

Fig. 1. TGA of poly[2,2'-(4,4'-thiodiphenylene)-6,6'-thiodiquinoxaline].

formed from the solution polymerizations are completely soluble in hexamethylphosphoramide, with one exception. Their solubilities decrease only after the second solid-phase polymerization. The decrease in solubility during the high temperature heating cycle may be the result of a certain amount of crosslinking occurring in the second stage of the polymerization; however, there are no convenient crosslinking sites along the polymer chain.

EXPERIMENTAL

Monomers

3,3′,4,4′-Tetraaminodiphenyl Ether (V). This monomer was prepared as previously described.[3] Acetylation of *p*-oxydianiline followed by nitration, deacetylation, reduction, and treatment with base led to a 50% overall yield of the tetraamine. The product obtained from the base treatment was purified by sublimation at 159–175°C./0.1 mm., m.p. 150–151°C. (lit.:[4] 150–151°C.).

3,3′,4,4′-Tetraaminodiphenyl Sulfone (II). To 140 g. (0.816 mole) of 4,4′-diaminodiphenyl sulfide suspended in 300 ml. of glacial acetic acid was added 120 ml. of acetic anhydride, dropwise with stirring. The mixture was heated to the reflux temperature of 2 hr. and then poured into 3 l. of an ice–water mixture. A white solid precipitated which was collected by fitration, washed with water until free of acid, and dried under reduced pressure. The 4,4′-diacetamidodiphenyl sulfide was recrystallized from a 1:1 water–ethyl alcohol mixture to yield 195.6 g. (90%), m.p. 223–224°C., (lit.:[3] 223–224°C.).

To 750 ml. of glacial acetic acid was added 80 g. (0.266 mole) of 4,4′-diacetamidodiphenyl sulfide, and the solution was heated until homogeneous. After the solution cooled to room temperature 44 g. of 30% hydrogen peroxide was added and the mixture was stirred at room temperature for 4 hr. The solution was heated to 50°C. and held at that temperature for an additional 2 hr. The white solid, 4,4′-diacetamidodiphenyl sulfone, which formed on cooling to room temperature was recrystallized from acetic acid to yield 70 g. (81.3%), m.p. 275–278°C.).

To 300 ml. of fuming nitric acid cooled to 0°C. was added 70 g. (0.0310 mole) of 4,4′-diacetamidodiphenyl sulfone with stirring. The diacetamido sulfone was not readily soluble; however, allowing the solution to warm up to room temperature produced a clear pale yellow solution. The reaction mixture was poured onto an ice–water mixture and a yellow solid precipitated. The 3,3′-dinitro-4,4′-diacetamidodiphenyl sulfone was purified by recrystallization from acetone to yield 88 g. (66.6%) m.p. 247–248°C.

To a warm solution containing 44 g. (0.0104 mole) of 3,3′-dinitro-4,4′-diacetamidodiphenyl sulfone in 250 ml. of absolute ethyl alcohol was added dropwise with stirring 150 ml. of hydrochloric acid. The mixture was heated to the reflux temperature for 4 hr. and cooled to room temperature.

The solution was dropped into water and an orange-brown solid precipitated. The solid was washed with cold water and dried under reduced pressure. The 3,3'-dinitro-4,4'-diaminodiphenyl sulfone hydrochloride was purified by recrystallization from acetone to yield 25 g. (56%), m.p. 307–308°C. (lit.[7] 309°C.).

To 250 ml. of concentrated hydrochloric acid containing 150 g. of stannous chloride dihydrate was added 24.2 g. (0.059 mole) of 3,3'-dinitro-4,4'-diaminodiphenyl sulfone hydrochloride. The reaction mixture was heated to the reflux temperature under a nitrogen atmosphere for 2 hr., and the solution became homogeneous. After cooling to room temperature, the hydrochloric acid was removed by a flash evaporator. The oily yellow residue was dissolved in deoxygenated water and added dropwise, under nitrogen atmosphere, to 500 ml. of a 50% sodium hydroxide solution. The gray solid that resulted consisted of free amine, insoluble sodium chloride, and occluded stannous hydroxide. After the solid was dried under reduced pressure it was extracted in a continuous liquid-solid extractor, peroxide-free anhydrous ether being used as the liquid. Upon the removal of the ether, a white crystalline solid remained which was recrystallized from absolute ethyl alcohol. The yield of 3,3',4,4'-tetraaminodiphenyl sulfone which melted at 174–174.5°C. (lit.[8] 173–174°C.) was 6 g. (37%).

ANAL. Calcd. for $C_{12}H_{14}N_4O_2S$: C, 51.80%; H, 5.04%; N, 19.40%. Found: C, 51.82%; H, 5.17%; N, 19.69%.

3,3',4,4'-Tetraaminodiphenyl Sulfide (I).

To 250 ml. of yellow fuming nitric acid at $-10°C$. was added 30 g. (0.100 mole) of 4,4'-diacetamidodiphenyl sulfide. The material was added at such a rate as to keep the temperature below 0°C. After the addition was complete, the reaction mixture was stirred for 2 hr. and then poured into 1 liter of an ice–water mixture which precipitated a light yellow solid. The yellow solid was filtered and washed several times with water until the solid was acid-free. The 3,3'-dinitro-4,4'-diacetamidodiphenyl sulfide was recrystallized from acetone, yielding 28 g. (72%), m.p. 187–188°C.

To a solution containing 150 ml. of concentrated hydrochloric acid and 150 ml. of 95% ethyl alcohol was added 20 g. (0.051 mole) of 3,3'-dinitro-4,4'-diacetamidodiphenyl sulfide. The mixture was heated to reflux temperature for 2 hr. and upon cooling, a dark red precipitate formed. The red solid was washed with small amounts of cold water and dried under reduced pressure. The yield of 3,3'-dinitro-4,4'-diaminodiphenyl sulfide hydrochloride was 15 g. (75%), m.p. 168–170°C. The material was not purified but used in its isolated form for the next step in synthesis.

To a vigorously stirred solution of 158 g. of stannous chloride dihydrate in 350 ml. of concentrated hydrochloric acid was added 37.9 g. (0.100 mole) of 3,3'-dinitro-4,4'-diaminodiphenyl sulfide hydrochloride. The addition was carried out under a nitrogen atmosphere at such a rate as to maintain the temperature at 40–50°C. After the addition was com-

pleted, a light tan precipitate formed. The mixture was heated to 80°C. for 4 hr., whereupon it became homogeneous. The reaction mixture was cooled to room temperature and the hydrochloric acid was removed by means of a flash evaporator. The oily material which remained was slowly dropped under a nitrogen atmosphere into 500 ml. of a 50% sodium hydroxide solution. The white solid, which consisted of the free amine, insoluble sodium chloride, and occluded stannous hydroxide, was then filtered through a sintered glass filter and dried under reduced pressure. The solid mixture was placed in a continuous liquid–solid extractor and extracted with peroxide free anhydrous diethyl ether. A light tan oil remained on the removal of the diethyl ether, which formed a white crystalline solid on the addition of absolute ethyl alcohol. The solid was recrystallized from absolute ethyl alcohol to yield 8 g. (34%) of 3,3',-4,4'-tetraaminodiphenyl sulfide, m.p. 102.5–103°C.

ANAL. Calcd. for $C_{12}N_{14}N_4S$: C, 58.50%; H, 5.69%; N, 22.79%. Found: C, 58.66%; H, 5.79%; N, 22.51%.

4,4'-Diglyoxalyldiphenyl Sulfide Dihydrate (III).

The monomer precursor, 4,4'-diacetyldiphenyl sulfide, was prepared in a 75% yield by the Friedel-Crafts acetylation of diphenyl sulfide in a tetrachloroethylene solvent.[9] The pure product, recrystallized from 95% ethanol, had a m.p. 89–90°C. (lit.:[9] b.p. 215–222°C./11 mm.).

To a solution of 44.4 g. (0.400 mole) of selenium dioxide in 200 ml. of dioxane and 4 ml. of water containing three drops of hydrochloric acid was added 50 g. (0.1851 mole) of 4,4'-diacetyldiphenyl sulfide. The mixture was heated at the reflux temperature for 4 hr., during which time the selenium metal precipitated. The mixture was filtered, and the red filtrate was stirred overnight with 8 g. of charcoal to remove the red selenium metal. After gravity filtration the mixture was added to 300 ml. of water and a yellow solid precipitated, which was recrystallized from a 50/50 mixture of water–dioxane to yield 49.4 g. (80%), m.p. 100–100.5°C.

ANAL. Calcd. for $C_{16}H_{14}O_6S$: C, 57.50%; H, 4.19%; Found: C, 57.81%; H, 4.43%.

4,4'-Diglyoxalyldiphenyl Sulfone Dihydrate (IV).

The monomer precursor, 4,4'-diacetyldiphenyl sulfone, was prepared in a 92% yield by the peroxide oxidation of 4,4'-diacetyldiphenyl sulfide in acetic acid.[10] The pure product, recrystallized from glacial acetic acid, had a m.p. 208–209°C. (lit.:[10] 208–209°C.).
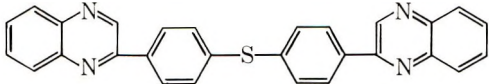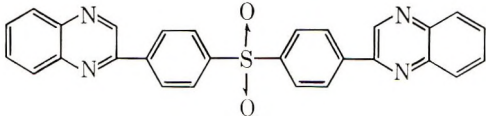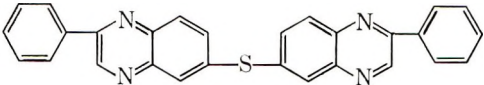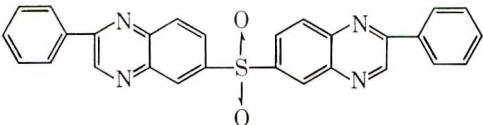
Selenium dioxide oxidation of 4,4'-diacetyldiphenyl sulfone as described for 4,4'-diglyoxalyldiphenyl sulfide dihydrate, afforded a white solid (65%), m.p. 138–139°C.

ANAL. Calcd. for $C_{16}H_{14}O_8S$: C, 52.50%; H, 3.28%; Found: C, 52.57%; H, 4.15%.

Model Compounds

Four quinoxaline model compounds have been prepared by the same general quinoxaline-forming condensation reaction described previously.[1-3] The ultraviolet spectra for these compounds appear in Table II.

TABLE II
Ultraviolet Spectra of Quinoxaline
Model Compounds in Hexamethylphosphoramide

Compound	Structure	λ, mμ	$\epsilon \times 10^{-3}$
XII		264 355	29.86 22.17
XIII		261 332	34.01 16.26
XIV		272 368	33.01 17.68
XV		260 345	18.48 12.00

4,4′-Di(2-quinoxalyl)diphenyl Sulfide (XII). To a solution containing 0.2751 g. (0.00082 mole) of 4,4′-diglyoxalyldiphenyl sulfide dihydrate dissolved in 20 ml. of a 50/50 dioxane–water mixture was added 0.1782 g. (0.0165 mole) of freshly sublimed o-phenylenediamine. The mixture was heated to the reflux temperature for 1 hr., and on cooling a light yellow solid crystallized. The solid was washed with water and recrystallized from a 50/50 water–ethanol mixture to yield 0.34 g. (94.5%), m.p. 194–195°C.

ANAL. Calcd. for $C_{28}H_{18}N_4S$: C, 76.01%; H, 4.08%; N, 12.69%. Found: C, 76.11%; H, 4.07%; N, 12.49%.

4,4′-Di(2-quinoxalyl)diphenyl Sulfone (XIII). To a boiling solution containing 0.1565 g. (0.00044 mole) of 4,4′-diglyoxalyldiphenylsulfone in 30 ml. of water was added 0.0950 g. (0.00088 mole) of sublimed o-phenylenediamine. Upon the addition of the amine, a light tan compound precipitated. The solution was heated for 1 hr. at 60°C. and cooled to room temperature. The light tan solid was recrystallized from 95% ethanol to yield 0.1960 g. (94%), m.p. 297–298°C.

ANAL. Calcd. for $C_{28}H_{18}N_4O_2S$: C, 71.00%; H, 3.80%. Found: C, 70.84%; H, 3.98%.

2,2'-Diphenyl-6,6'-thiodiquinoxaline (XIV). To a solution containing 0.2143 g. (0.00084 mole) of 3,3',4,4'-tetraaminodiphenyl sulfide dissolved in 30 ml. of *p*-dioxane was added 0.2562 g. (0.00168 mole) of phenylglyoxal hydrate. The solution was heated to 70°C. and maintained at that temperature for 1 hr. On cooling the solution, a solid precipitate formed which was collected and recrystallized from 95% ethanol to afford 0.300 g. (81%) of light yellow crystals, m.p. 306–307°C.

ANAL. Calcd. for $C_{28}H_{18}N_4S$: C, 76.01%; H, 4.42%; N, 12.60%; Found: C, 75.80%; H, 4.42%; N, 12.75%.

2,2'-Diphenyl-6,6'-sulfonyldiquinoxaline (XV). To a solution containing 0.2000 g. (0.00073 mole) of 3,3',4,4'-tetraaminodiphenyl sulfone dissolved in 20 ml. of a 50/50 dioxane–water mixture was added 0.2365 g. (0.00146 mole) of phenylglyoxal hydrate. On addition of the glyoxal a light yellow precipitate was formed. The solution was heated to 50°C. and allowed to cool to room temperature. The yellow solid was collected and recrystallized from absolute ethanol to yield 0.3079 g. (89%), m.p. 274–275°C.

ANAL. Calcd. for $C_{28}H_{18}N_4O_2S$: C, 70.22%; H, 3.79%; H, 11.81%. Found: C, 70.17%; H, 4.28%; N, 11.66%.

Polymers

The polymer synthesis was carried out in two stages. The first stage consisted of a solution polymerization under a nitrogen atmosphere in hexamethylphosphoramide to afford moderate molecular weight polymers. The hexamethylphosphoramide was freshly distilled under nitrogen before each polymerization into the reaction vessel. All polymers were treated to a second-stage heating cycle (375°C.) to produce higher molecular weight polymers. The polymers were heated under reduced pressure in a rotating flask to which had been added two 8 mm. diameter steel ball

TABLE III
Ultraviolet Spectra of Polyquinoxalines in Hexamethylphosphoramide

Polymer	λ, mμ	$\epsilon \times 10^{-3}$ [a]
VI	287	25.60
	380	21.60
VII	258	30.46
	347	14.33
VIII	262	17.40
	360	12.00
IX	288	32.99
	378	19.10
X	261	22.15
	356	11.67
XI	265	30.06
	353	19.14

[a] The molar extinction coefficients were calculated from the weight of the polymer recurring unit.

bearings to facilitate mixing. The ultraviolet spectra of the polymers in hexamethylphosphoramide are shown in Table III. The ultraviolet spectra of the polymers are consistent with the structures by comparison with the spectra of the model compounds.

Poly[2,2′-(4,4′-thiodiphenylene)-6,6′-thiodiquinoxaline] (VI). To a solution containing 0.5000 g. (0.00204 mole) of 3,3′-4,4′-tetraaminodiphenyl sulfide in 50 ml. of hexamethylphosphoramide was added, under a nitrogen atmosphere, 0.6843 g. (0.00204 mole) of 4,4′-diglyoxalyldiphenyl sulfide dihydrate. On contact of the two monomers a red color immediately formed. The solution was slowly heated to 180°C., and, as the temperature increased, the solution became darker. The temperature was maintained at 180°C. for 10 hr. under a stream of nitrogen. After cooling the solution to room temperature, it was added dropwise to 300 ml. of methanol which precipitated 1.4134 g. of a light brown solid. The solid was placed in a Soxhlet extractor and extracted overnight with benzene. The polymer was dried under reduced pressure.

In the second cycle, 0.5000 g. of the prepolymer was treated at 375°C. for 2 hr. in a rotating flask under reduced pressure (0.1 mm.). During this heating the material became dark brown and lost 0.2342 g. This indicates approximately a yield of 0.7490 g. (80%) of polymer (free of hexamethylphosphoramide) that was obtained from the solution polymerization.

ANAL. Calcd. for $(C_{28}H_{16}N_4S_2)_n$: C, 63.44%; H, 4.30%. Found: C, 62.67%; H, 4.85%.

Poly[2,2′-(4,4′-sulfonyldiphenylene)-6,6′-sulfonyldiquinoxaline] (X). The reaction of 1.000 g. (0.00359 mole) of 3,3′,4,4′-tetraaminodiphenyl sulfone dissolved in 50 ml. of hexamethylphosphoramide with 1.3139 g. (0.00359 mole) of 4,4′-diglyoxalyldiphenyl sulfone dihydrate as described above, gave 2.7282 g. of a light tan solid. The polymer was extracted with benzene overnight in a Soxhlet extractor and then dried under reduced pressure.

In the second cycle, 0.5000 g. of the prepolymer was treated at 375°C. for 2 hr. in a rotating flask under reduced pressure (0.1 mm.). As the temperature increased, the polymer gradually turned from a light tan to a dark brown and lost 0.1832 g. This indicates approximately a yield of 1.6488 g. (87%) of polymer (free of hexamethylphosphoramide) that was obtained from the solution polymerization.

ANAL. Calcd. for $(C_{28}H_{16}N_4O_4S_2)_n$: C, 62.62%; H, 2.99%. Found: C, 63.08%; H, 4.39%.

Poly[2,2′-(4,4′-thiodiphenylene)-6,6′-sulfonyldiquinoxaline] (VII). The reaction of 0.5030 g. (0.00150 mole) of 4,4′-diglyoxalyldiphenyl sulfide dihydrate dissolved in 50 ml. of hexamethylphosphoramide with 0.5000 g. (0.00150 mole) of 3,3′,4,4′-tetraaminodiphenyl sulfone as described above, gave 0.8208 g. of yellow polymer which was subsequently extracted overnight with benzine in a Soxhlet extractor.

In the second-stage polymerization cycle, 0.5000 g. of the prepolymer was treated at 375°C. for 2 hr. in a rotating flask under reduced pressure (0.1 mm.). After 1 hr. of heating at 375°C., the material turned from a light yellow to a dark brown. The weight loss in the high temperature polymerization cycle was 0.1324 g. This indicates approximately a yield of 0.6034 g. (82%) of polymer (free of hexamethylphosphoramide) that was obtained from the solution polymerization.

ANAL. Calcd. for $(C_{28}H_{16}N_4O_2S_2)_n$: C, 66.66%; H, 3.17%. Found: C, 65.96%; H, 3.80%.

Poly[2,2'-(4,4'-sulfonyldiphenylene)-6,6'-thiodiquinoxaline] [IX]. The reaction of 0.5000 g. (0.002049 mole) of 3,3',4,4'-tetraaminodiphenyl sulfide dissolved in 50 ml. of hexamethylphosphoramide with 0.7499 g. (0.002049 mole) of 4,4'-diglyoxalyldiphenyl sulfone dihydrate gave 1.2359 g. of a light brown polymer.

In the second-stage polymerization, 0.5000 g. of the prepolymer was treated at 375°C. for 2 hr. in a rotating flask under reduced pressure (0.1 mm.). After 1 hr. of heating at 375°C. the prepolymer changed in color from a light brown to a bluish black. The weight loss in the high temperature polymerization cycle was 0.1521 g. This indicates approximately a yield of 0.8602 g. (86%) of polymer (free of hexamethylphosphoramide) that was obtained from the solution polymerization.

ANAL. Calcd. for $(C_{28}H_{16}N_4O_2S_2)_n$: C, 66.66%; H, 3.17%. Found: C, 66.05%; H, 5.40%.

Poly[2,2'-(4,4'-thiodiphenylene)-6,6'-oxydiquinoxaline] (VIII). The reaction of 1.2347 g. (0.002658 mole) of 4,4'-diglyoxalyldiphenyl sulfide dihydrate dissolved in 60 ml. of hexamethylphosphoramide with 0.6114 g. (0.002658 mole) of 3,3',4,4'-tetraaminodiphenyl ether gave 1.4545 g. of a light yellow polymer.

In the second-stage polymerization cycle, 0.5000 g. of the prepolymer was treated at 375°C. for 2 hr. in a rotating flask under reduced pressure (0.1 mm.). After 1 hr. of heating at 375°C., the polymer turned to a metallic black and adhered to the walls of the flask. The loss of weight from the polymerization was 0.1358 g. This indicates approximately a yield of 1.0598 g. (95%) of polymer (free of hexamethylphosphoramide) that was obtained from the solution polymerization.

ANAL. Calcd. for $(C_{28}H_{16}N_4OS)_n$: C, 73.68%; H, 3.50%. Found: C, 74.38%; H, 4.40%.

Poly[2,2'-(4,4'-sulfonyldiphenylene)-6,6'-oxydiquinoxaline] (XI). The reaction of 1.5006 g. (0.0041 mole) of 4,4'-diglyoxalyldiphenyl sulfone dihydrate in 100 ml. of hexamethylphosphoramide with 0.9430 g. (0.0041 mole) of 3,3',4,4'-tetraaminodiphenyl ether as described above, gave 2.5184 g. of a light yellow solid. The solid was collected and extracted overnight with benzene in a Soxhlet extractor. The polymer was then dried under reduced pressure.

In the second-stage polymerization cycle, 0.5000 g. of the prepolymer was treated at 375°C. for 2 hr. in a rotating flask under reduced pressure (0.1 mm.). The material turned from a light yellow to a metallic black and lost 0.1320 g. This indicates approximately a yield of 1.8536 g. (95%) of polymer (free of hexamethylphosphoramide) that was obtained from the solution polymerization.

ANAL. Calcd. for $(C_{28}H_{16}N_4O_3S)_n$: C, 68.85%; H, 3.27%. Found: C, 68.24%; H, 3.67%.

References

1. Stille, J. K., and J. R. Williamson, *J. Polymer Sci. B*, **2**, 209 (1964).

2. Stille, J. K., and J. R. Williamson, *J. Polymer Sci. A*, **2**, 3867 (1964).

3. Stille, J. K., J. R. Williamson, and F. E. Arnold, *J. Polymer Sci. A*, **3**, 1013 (1965).

4. Foster, R., and C. S. Marvel, *J. Polymer Sci. A*, **3**, 417 (1965).

5. Raiziss, G. W., L. W. Clemence, M. Severac, and J. C. Molsch, *J. Am. Chem. Soc.*, **61**, 2763 (1959).

6. Szasz, G. J., *J. Am. Chem. Soc.*, **62**, 3521 (1940).

7. Ullman, F., and J. Korselt, *Ber.*, **40**, 647 (1907).

8. Yokugaku, Z., *J. Pharm. Soc. Japan*, **70**, 77 (1950).

9. Smith, C. M., U. S. Pat. 2,903,461 (1959).

10. Hu, P. F., *J. Chem. Soc.*, **1959**, 178.

Résumé

Six poly-quinoxalines thermiquement stables ont été préparées par les réactions de combinaisons de trois tétramines, la 3,3′,4,4′-tétraaminodiphényl-sulfone (II) et le 3,3′,4,4′-tétramino-diphényl-éther (V) avec deux bisglyoxals, le dihydrate du 4,4′-diglyoxal diphényl-sulfure (III) et le dihydrate de la 4,4′-diglyoxalyl-diphényl-sulfone (IV). Les polymères sont préparés á partir d'une polymérisation en deux étapes La première étape, une polymérisation en solution, produit un polymère initialement de poids moléculaire bas ou moyen, qui est transformé en polymère de haut poids moléculaire ($\eta_{inh} > 1,0$) par chauffage à 375°C et sous pression réduite. Toutes les polyquinoxalines ont une stabilité thermique excellente dans l'azote et dans l'air, et une solubilité ameliorde.

Zusammenfassung

Sechs thermische stabile Polychinoxaline wurden durch Reaktion der Kombination dreier Tetramine, 3,3′,4,4′-Tetraaminodiphenylsulfon (II) und 3,3′,4,4′-Tetraaminodiphenyläther (V) mit zwei Bisglyoxalen, 4,4′-Di-glyoxalyldiphenylsulfiddihydrat (III) und 4,4′-Diglyoxaldiphenylsulfondihydrat (IV) dargestellt. Die Polymerisation wurde in zweif Stufen ausgeführt. Die erste Stufe, eine Lösungspolymerisation, führt zu einem Material mit anfänglich niedrigen oder mässigem Molekulargewicht, welches durch Erhitzen auf 375°C unter vermindertem Druck in einem hochmoleuklaren ($\eta_{inh} > 1,0$) Körper übergeführt wird. Alle Polychinoxaline besitzen sowohl unter Stickstoff als auch unter Luft eine ausgezeichnete thermische Stabilität sowie eine verbesserte Löslichkeit.

Radiation-Induced *cis–trans* Isomerization of Polyisoprenes and Temperature Dependence of the Equilibria

JITSUO TSURUGI, TSUGIO FUKUMOTO, MASAYUKI YAMA-
GAMI, and HIROSHI ITATANI,* *Department of Chemistry, Radiation
Center of Osaka Prefecture, Sakai, Osaka, Japan*

Synopsis

The *cis–trans* interconversion of polyisoprenes in solutions induced by γ-radiation in the presence of a sensitizer, which is any one of organic bromides or *n*-butyl mercaptan, was studied by using hevea and gutta percha as starting substances. The percentage *cis* remaining or converted after irradiation were determined by the infrared absorption. The equilibrium constants for the interconversion at 22, 60, and 100°C. were found to be 3.00, 5.25, and 7.33, respectively. The first-order rate constants for *cis* → *trans* and *trans* → *cis* isomerizations at 22°C. were calculated to be 9.05 and 2.91, respectively. The results were interpreted by the mechanism proposed by Golub, according to which the double bonds from π complexes with radiolytic fragments from sensitizers give a radical transition state capable of interconversion. However, our results showing that heating shifts the equilibrium toward *trans* isomer are not in accord with the mechanisms of the radiation-induced isomerization of polybutadiene of Golub and those for photoisomerization of aromatic azo compounds.

INTRODUCTION

Since *cis* → *trans* isomerization of polybutadiene by means of ultraviolet irradiation was first observed by Golub,[1] several papers treating the chemically[2] or ionizing radiation-induced isomerization of unsaturated high polymers have appeared. Golub also reported the radiation-induced isomerization of polybutadiene[3,4] in the presence of a sensitizer and the unsensitized isomerization of polybutadiene by γ-rays.[5] In the sensitized γ-ray-induced isomerization of polybutadiene, the *cis/trans* ratios at equilibrium were 5/95 in the presence of allyl bromide[3] and 8/92 in the presence of diphenyl disulfide,[4] both at room temperature. Therefore, it might be experimentally difficult to follow the *trans* → *cis* isomerization by using *trans*-1,4-polybutadiene as a starting substance, because the percentage *trans* at equilibrium lies near the starting value. In the unsensitized isomerization of polybutadiene the rate is too slow to permit determination of the equilibrium state.

* Present address: Department of Chemistry and Chemical Engineering, University of Illinois, Urbana, Illinois, U. S. A.

Natural rubber was reported[6] to be isomerized partially to *trans* isomer by γ-rays in the presence of a sensitizer. However, no information was obtained about the equilibrium. Radiation-induced *trans → cis* isomerization of *trans*-1,4-polyisoprene naturally occurring in gutta percha has never been reported.

The present paper is concerned with *cis–trans* interconversion of polyisoprenes in benzene solution induced by γ-rays in the presence of a sensitizer, which may be any of the organic bromides or mercaptan. The present authors were able successfully to examine the temperature dependence of *cis–trans* interconversion equilibria by starting from both *cis*-1,4 and *trans*-1,4-polyisoprenes. Thus the present paper may provide further knowledge of radiation-induced interconversion of unsaturated high polymers.

Experimental

The pale crepe (hevea) and gutta percha used as *cis*-1,4- and *trans*-1,4-polyisoprene, respectively, in this work were purified by two precipitations with methanol and acetone from benzene solution. The pale crepe had a viscosity-average molecular weight of 250,000, and that of the gutta percha was 100,000.

Stock solutions of each polyisoprene in benzene were made up to a concentration of 10 g./l., to which were added various amounts of ethyl bromide, ethylene bromide, and *n*-butyl mercaptan as sensitizers. Portions of sensitized solutions were placed in tubes, each of which had a ground glass stopper, and irradiated at room temperature with 6300 c. from Co^{60} source. To determine the temperature dependence of the isomerization rate, the tubes were placed in an electric heater kept at $60 \pm 1°C$. or $100 \pm 1°C$. The total irradiation dose for each tube was determined by placing a tube at a given distance from the source. Including irradiation in the heater, the dose rates were determined by Fricke dosimeters at various distances from the source. Therefore, the effect of dose rate on isomerization rate was assumed in this study to be negligible. Irradiations were carried out in air, because Golub[3] showed that gelation of the polymer occurred with irradiated in nitrogen. He also reported that although irradiation in air led to rapid degradation of the polymer, the rate of isomerization was unaffected by the accompanying chain scission. After a given period of irradiation the polymers were precipitated with methanol, dried under reduced pressure, and dissolved again in benzene. Thin polymer films were cast on rock salt plates from the benzene solutions.

The polymer structures were determined on the films by infrared absorption measurements with a Perkin-Elmer Model 21 spectrophotometer. Richardson[7] pointed out that intensity at the intersection (815 cm.$^{-1}$) of the spectra of hevea and gutta percha indicates the total 1,4 concentration, and intensity at 843 cm.$^{-1}$ depends on the *cis/trans* ratio. Optical
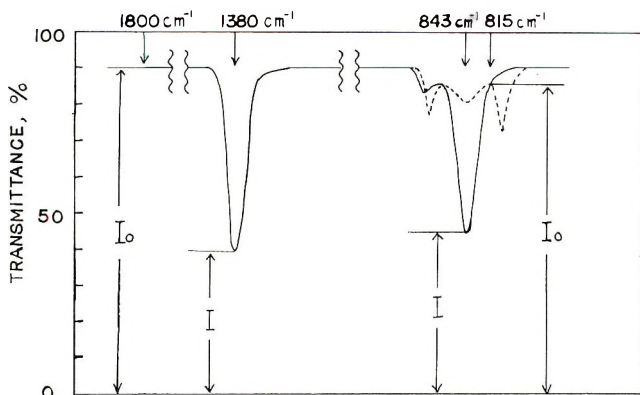
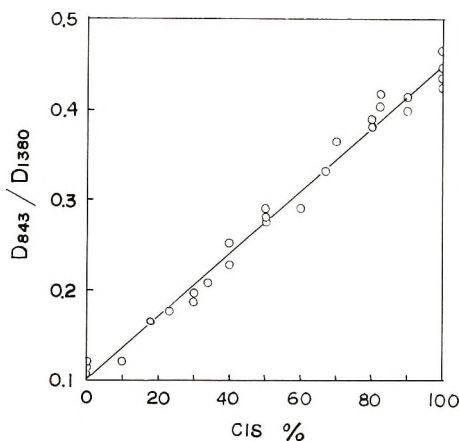Fig. 1. Base line method for infrared absorption spectra.

Fig. 2. Relation between infrared absorption measurements and the percentage of *cis* component of mixtures containing various proportions of hevea and gutta percha.

densities at 843 cm.$^{-1}$ of polymer films were written as follows, by using the base line method illustrated in Figure 1 :

$$D_{843} = \log(I_0/I)$$

where I_0 indicates intensity at 815 cm.$^{-1}$ and I that at 843 cm.$^{-1}$. To eliminate the effect of thickness of polymer films, the band at 1380 cm.$^{-1}$ originating from C-H bending vibration[7] of the CH_3 group in hevea and gutta percha was chosen as a standard band.   As in the case at 843 cm.$^{-1}$, optical densities at 1380 cm.$^{-1}$ were written as

$$D_{1380} = \log(I_0/I)$$

where I_0 indicates intensity at 1380 cm.$^{-1}$ and I that at 1800 cm.$^{-1}$ as base line.   The values of D_{843}/D_{1380} were plotted against percentage *cis* of the polymer films prepared from benzene solutions containing various propor-

tions of hevea and gutta percha, assuming both polymers to be pure *cis* and *trans*, respectively. The linear relationship which was found to hold in the range where transmittance at 1380 cm.$^{-1}$ did not exceed $40 \pm 5\%$ is shown in Figure 2; this relation was used to determine the percentage *cis* of the irradiated polymers.

Results

Plots of percentage of *cis* component remaining or converted after irradiation at room temperature of *cis*-1,4 or *trans*-1,4-polyisoprene in benzene solution, respectively, against radiation dose are shown in Figure 3.

The curves were used to obtain the equilibrium constant of *cis–trans* interconversion in the presence of sensitizers. Figure 3 clearly indicates that the two curves obtained with *n*-butyl mercaptan as a sensitizer approach asymptotically a horizontal line cutting the ordinate at 25% *cis* component. When ethylene bromide in 1 mole/l. concentration was used, the same equilibrium value was obtained.

In the case of the γ-ray-induced and sensitized *cis* → *trans* isomerization of polybutadiene the expression for a first-order reversible process

$$k' = \frac{-2.303K}{1 + K} \cdot \frac{d \ln (1 - x/x_e)}{dR} \tag{1}$$

was proposed,[3] where K is the equilibrium constant, x is per cent *cis* changed into *trans* following a radiation dose R, x_e is the per cent *cis* converted at equilibrium, and k' is a quantity which is related to the rate constant.
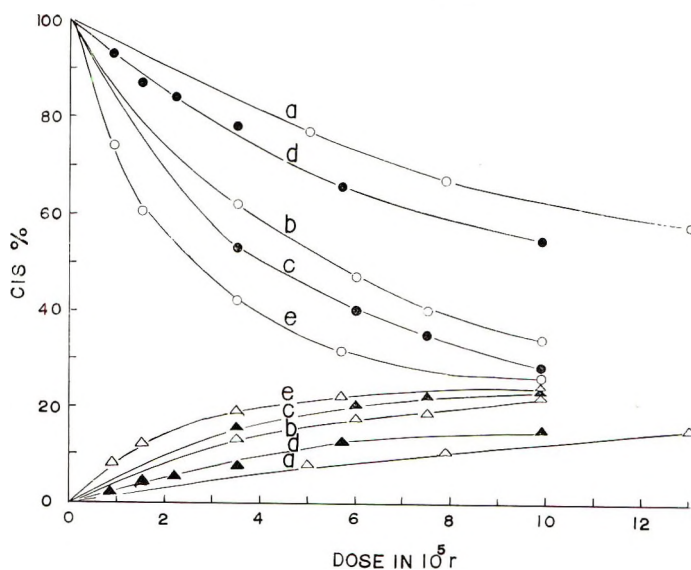

Fig. 3. Changes of isomeric compositions with radiation dose at room temperature; (O,●) *cis* → *trans* and (△,▲) *trans* → *cis* isomerizations in the presence of: (*a*) ethyl bromide, 0.173 mole/l.; (*b*) ethyl bromide, 0.5 mole/l.; (*c*) ethyl bromide, 1.0 mole/l.; (*d*) ethylene bromide, 0.1 mole/l.; (*e*) *n*-butyl mercaptan, 0.1 mole/l.

The value of k' should be the sum of the rate constants for both sensitized and unsensitized isomerizations.[3] However, the results in the present study indicate that in the unsensitized isomerization of *cis*-1,4- and *trans*-1,4-polyisoprene at room temperature, 91% *cis* remained and 4% *trans* was changed at total dose of 22×10^5 r. The unsensitized rate was found, therefore, to be negligible, and the sensitized rate should depend on the concentration of the sensitizer.[3] Then,

$$k' = k[\text{bromide}]^b \qquad (2)$$

Equations (1) and (2) can be applied also to *trans* → *cis* isomerization if the term *cis* is replaced by *trans* in the terms in these equations. The subscripts c and t will be used to represent *cis* → *trans* and *trans* → *cis* isomerization, respectively.

The curves in Figure 3 were transferred to $\log(1 - x/x_e)$ versus radiation dose scale by using $(x_e)_c = 75$ and $(x_e)_t = 25$; this is shown in Figure 4. The points for the same sensitizer at the same concentration fell on the same straight line for both *cis* → *trans* and *trans* → *cis* isomerizations. This overlapping of the points for both isomerizations has been observed for the first time by the present authors, and indicates the applicability of eq. (1) to the *cis–trans* interconversion. The average values of k' calculated by using eq. (1) are listed in Table I.

The values of k' in the presence of ethylene bromide in various concentrations were calculated; results are summarized in Table II.

A log–log plot of k'_c and k'_t against the concentration of ethylene bromide showed two parallel lines with the same slope, from which the exponent b in eq. (2) was determined to be 0.41. The value of b was reported[3] to be

TABLE I

Radiation-Induced Interconversion of Polyisoprene in the Presence of a Sensitizer

Sensitizer	Concn., mole/l.	$k'_c \times 10^7/r$	$k'_t \times 10^7/r$
C_2H_5Br	0.17	2.37	0.77
$C_2H_4Br_2$	0.10	3.54	1.16
n-BuSH	0.10	14.73	4.43

TABLE II

Radiation-Induced Interconversion of Polyisoprene in the Presence of Ethylene Bromide

[Bromide], mole/l.	$k'_c \times 10^7/r$	$k_c \times 10^7/r$ $(\text{mole/l.})^{-0.41}$	$k'_t \times 10^7/r$	$k_t \times 10^7/r$ $(\text{mole/l.})^{-0.41}$
1.0	9.01	9.01	3.01	3.01
0.5	6.88	9.14	2.18	2.89
0.2	4.56	8.83	1.45	2.81
0.1	3.54[a]	9.09	1.16[a]	2.98
0.05	2.70	9.20	0.84	2.86
		Av. 9.05		Av. 2.91

[a] From Table I.

0.45 in radiation-induced *cis* → *trans* isomerization of polybutadiene in the presence of allyl bromide, ethyl bromide, or ethylene bromide as a sensitizer. By putting $b = 0.41$ into eq. (2), the rate constants k_c and k_t were calculated and are listed Table II. The rate constant for *cis* → *trans*
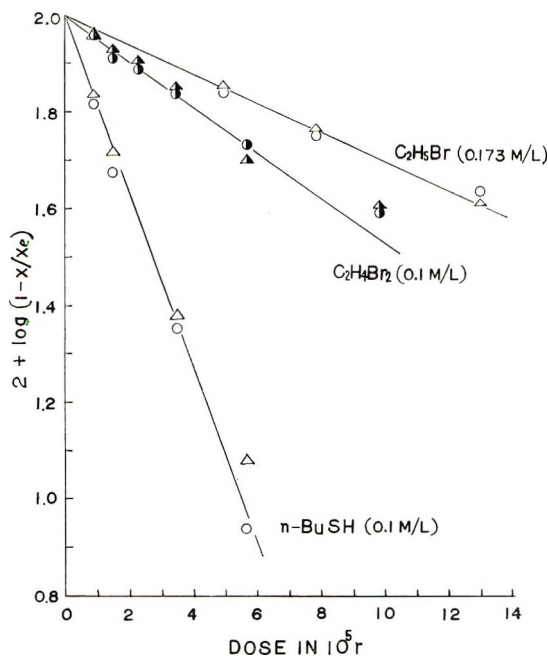

Fig. 4. Rate of isomerizations: (O,◑) *cis* → *trans* and (△,▲) *trans* → *cis*. The concentrations of sensitizers are given in parenthesis.
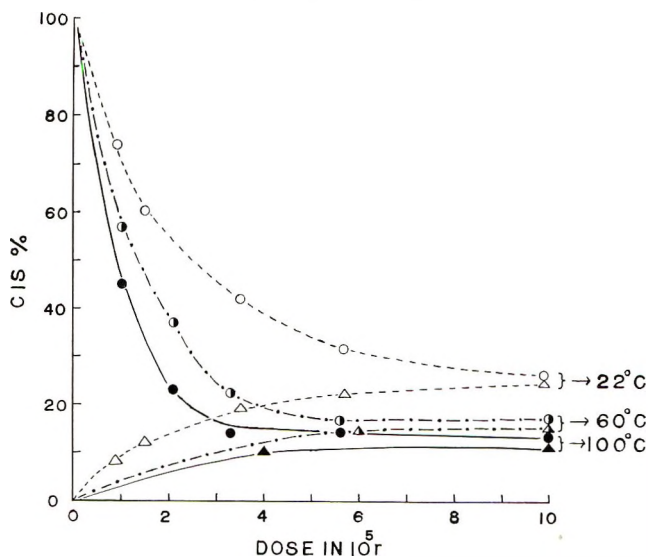

Fig. 5. Temperature dependence of the equilibrium values for isomerizations: (O,◑,●) *cis* → *trans* and (△,▲,▲) *trans* → *cis*.

isomerization of polybutadiene in the presence of ethylene bromide was also reported by Golub[3] to be 9.74×10^{-7}.

The effect of temperature on the rate for both *cis* → *trans* and *trans* → *cis* isomerizations was determined. The percentage of *cis* component remaining or converted after irradiation at various temperatures in the presence of a given concentration of *n*-butyl mercaptan is plotted against radiation dose in Figure 5, where the values of $(x_e)_c$ are indicated to be 84 at 60°C. and 88 at 100°C.; hence, K_c is 5.25 at 60°C. and 7.33 at 100°C. Irradiations carried out at room temperature might be considered to indicate data at 22°C. because temperature of irradiation room was kept at 22 ± 1°C. The values of k' for *cis* → *trans* isomerization were determined by the same procedure as described above. However, those for *trans* → *cis* isomerization at higher temperatures were calculated from the corresponding *cis* → *trans* ones by using the relation $K_c = k'_c/k'_t$, because the percentage *cis* on irradiation of *trans*-1,4 polymer was less accurately determined than the percentage *cis* of *cis*-1,4 polymer remaining. The average values of k'_c and k'_t thus obtained are listed in Table III.

TABLE III

k_c' and k_t' Values at Various Temperatures in the Presence of *n*-Butyl Mercaptan (0.1 mole/l.)

Temperature, °C.	$k'_c \times 10^6/r$	$k'_t \times 10^6/r$
22[a]	1.47	0.44
60	2.63	0.50
100	3.85	0.53

[a] From Table I.

Together with the values of k'_c and k'_t cited in Table I, these values in Table III gave the Arrhenius plots indicated in Figure 6. The overall activation energy for *cis* → *trans* isomerization was calculated to be 2.7 kcal./mole and that for *trans* → *cis* isomerization to be nearly zero.

Discussion

The γ-induced, sensitized *cis*→*trans* isomerization of polybutadiene in solution was viewed by Golub[3,4] to follow the scheme:

$$\text{Sensitizer} \longrightarrow \text{Radical } (R \cdot)$$
$$cis\text{-}P + R \cdot \; \rightleftarrows \; cis\text{-}PR \cdot$$
$$trans\text{-}P + R \cdot \; \rightleftarrows \; trans\text{-}PR \cdot$$
$$cis\text{-}PR \cdot \; \rightleftarrows \; trans\text{-}PR \cdot$$
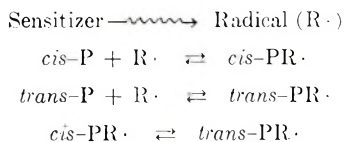
When complexed radicals (*cis* and *trans*-PR) are subsequently released and the double bond reestablished, the geometric configuration formed predominantly is that of the more stable isomeric form which may be the *trans* form.[3] However, the predominance of the *trans* form is considered not to be so considerable in isomerization of polyisoprene as with polybutadiene,

Fig. 6. Arrhenius plots for the rate of cis → trans and trans → cis isomerization.

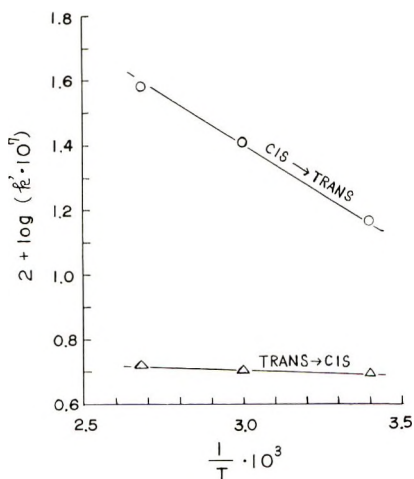because of the steric effect of polyisoprene. This conclusion is supported by the present results that the *cis/trans* ratio at equilibrium of polyisoprene is shifted toward the *cis* form as compared with that of polybutadiene reported by Golub.[3,4]

The temperature dependence of the equilibrium constants indicated in Figure 5 may seem extraordinary, because heating causes a shift of equilibrium toward the *trans* isomer, which should be the more stable form. This shift of equilibrium can be explained by the results indicated in Figure 6 that the rate for *cis* → *trans* isomerization increases to a great extent with heating, while the *trans* → *cis* rate is almost independent of temperature.

In the photoisomerization of aromatic azo compounds Fischer[8] observed that cooling causes a pronounced shift of equilibrium toward the *trans* isomer and interpreted the results by the fact that the rate for *cis* → *trans* isomerization is practically independent of temperature, while the *trans* → *cis* rate is considerably lowered on cooling. The dependence of the rates on the temperature indicates that the isomerization involves thermal steps with sufficiently high potential barrier. Such steps might include the thermal interconversion of π-complexed *cis* and *trans* double bonds as suggested by Fischer.[8] In the present study the reason why the barrier for conversion from *cis* complexed double bond to the *trans* complex is higher than another barrier is not clear at the present time. The difference between the results of this and Fischer's studies may come from the fact that the entity undergoing isomerization in this study is a segment constituting a long polymer chain. When Golub[4] examined the temperature effect of the rate of thiyl radical-sensitized isomerization of polybutadiene, he assumed that heating causes a shift in equilibrium toward the *cis* form as in the low molecular weight compounds. His assumption contradicts our results which need a clear-cut interpretation in the future.

References

1. Golub, M. A., *J. Polymer Sci.*, **25,** 373 (1957).
2. Bishop, W. A., *J. Polymer Sci.*, **55,** 827 (1961).
3. Golub, M. A., *J. Am. Chem. Soc.*, **80,** 1794 (1958).
4. Golub, M. A., *J. Am. Chem. Soc.*, **81,** 54 (1959).
5. Golub, M. A., *J. Am. Chem. Soc.*, **82,** 5093 (1960).
6. Shimozawa, R., Y. Tabata, and K. Sofue, *Ann. Rept. Japan. Assoc. Rad. Res. Polymers*, **2,** 315 (1960).
7. Richardson, W. S., and A. Sacher, *J. Polymer Sci.*, **10,** 353 (1953).
8. Fischer, E., *J. Am. Chem. Soc.*, **82,** 3249 (1960).

Résumé

L'interconversion *cis* ⇌ *trans* dans les solutions de polyisoprènes, induites par les rayons-γ en présence d'un sensibilisateur constitué d'un bromure organique ou de *n*-butyl-mercaptan, a été étudiée en employant comme produits de départ l'hévéa et le gutta-percha. Les pourcentages de *cis* maintenus ou transformés après irradiation sont déterminés par la méthode d'absorption infra-rouge. Les constantes d'équilibre pour l'interconversion à 22,60 et 100°C sont respectivement 3.00, 5.25 et 7.33. Les constantes de vitesse du premier ordre des isomérations *cis → trans* et *trans → cis* sont respectivement 9.05 et 2.91. Les résultats sont interprétés sur la base du mécanisme proposé par Golub, suivant lequel les doubles liaisons forment des complexes avec les fragments radiolytiques provenant du sensibilisateur en donnant des états de transition capables d'isomériser. Néanmoins nos résultats montrent que l'augmentation de température produit un déplacement d'équilibre vers l'isomère *trans*, ce qui est en contradiction avec les résultats de Golub pour l'isomérisation du polybutadiène, induite par irradiation at avec les résultats obtenus lors de la photoisomérisation des produits atoiques aromatiques

Zusammenfassung

Die durch γ-Strahlen in Gegenwart eines Sensibilisators, nämlich eines organischen Bromids oder von *n*-Butylmercaptan, induzierte *cis* ⇌ *trans*-Umlagerung von Polyisoprenen in Lösung wurde mit Hevea und Guttapercha als Ausgangsmaterial untersucht. Der nach der Bestrahlung zurückbleibende oder neu auftretende *cis*-Gehalt wurde durch Infrarotabsorption bestimmt. Die Gleichgewichtskonstanten für die Umlagerung bei 22, 60 und 100°C waren 3,00, 5,25 bzw. 7,33. Die Geschwindigkeitskonstanten erster Ordnung wurden für die *cis → trans* und die *trans → cis* Isomerisierung bei 22°C zu, 9,05 bzw. 2,91 berechnet. Die Ergebnisse wurden anhand des von Golub vorgeschlagenen Mechanismus interpretiert, wobei angenommen wird, dass die Doppelbindungen der π-Komplexe mit radiolytischen Sensibilisator-bruchstücken unter Bildung des zur Umlagerung befähigten Radikalüber-gangszustandes reagieren. Unsere Befunde über die Verschiebung des Gleichgewichts zum *trans*-Isomeren durch Erhitzen stehen jedoch in Widerspruch zu denjenigen über die strahlungsinduzierte Isomerisation von Polybutadien von Golub und denjenigen über die Photoisomerisierung aromatischer Azoverbindungen.

Inorganic Coordination Polymers.   VII.   Zinc(II) Dimethyl-, Methylphenyl-, and Diphenylphosphinates*

SELWYN H. ROSE and B. P. BLOCK, *Technological Center, Pennsalt Chemicals Corporation, King of Prussia, Pennsylvania*

Synopsis

Zinc dimethyl-, methylphenyl-, and diphenylphosphinate have been prepared by the reaction of $Zn(C_2H_3O_2)_2 \cdot 2H_2O$ with the appropriate acid or salt and found to exist in amorphous and crystalline forms.   Zinc methylphenylphosphinate, the most tractable, exhibits many of the physical attributes of polymeric materials, both in solution and bulk form, supporting our earlier suggestion that these compounds are double-bridged coordination polymers.   Thermogravimetric analysis indicates initial decomposition temperatures of 440, 425, and 490°C., respectively, for the three polymers, but long-term studies show initiation of decomposition at somewhat lower temperatures.

INTRODUCTION

Our study of coordination polymers[1] has led us to a detailed examination of systems in which there are double phosphinate bridges between coordination centers.   The simplest class of these polymers has the general formula $(MX_2)_x$, where X represents a bridging group with a charge of -1.   We have already made a preliminary report[2] on this class of metal–phosphinate polymers and wish now to give a more detailed presentation of our studies of some zinc phosphinates which we have used as prototypes.

EXPERIMENTAL

Apparatus

The reactions involving $(C_2H_5)_2Zn$ were carried out by standard manipulative techniques in a high vacuum apparatus.   The x-ray powder patterns were obtained with the use of a General Electric XRD-5 with vertical tube mount and standard General Electric 14.32-cm. diameter cameras.   The apparent intrinsic viscosities were determined at $33 \pm 0.1°C.$ with a Cannon-Ubbelohde dilution viscometer by standard procedures.[3]   The intrinsic viscosities under anhydrous conditions were determined in a modified Cannon-Zhukov viscometer loaded in a dry box.   The melt indexes were measured in an extrusion plastometer constructed according to ASTM D1238-62T.   Molecular weight measurements were carried out in a

---

Mechrolab vapor pressure osmometer, Model 301A, or in a modified Ray-type ebulliometer.

Starting Materials

The methods used for the preparation of the phosphinic acids have been described in the preceding paper.[1] Table I summarizes the analytical data for the samples used in this investigation. Methylphenylphosphinic acid was repeatedly recrystallized from 95% ethanol until its melting point was constant, extensively dried in a vacuum oven at 60°C., and stored in a desiccator.

TABLE I
Analytical Values for RR'P(O)OH

R	R'	Melting point, °C.	Calculated C, %	H, %	P, %	Found C, %	H, %	P, %
C_6H_5	C_6H_5	195–196	66.1	5.1	14.2	66.2	4.9	14.1
CH_3	C_6H_5	135–136	53.85	5.81	19.84	53.80	6.08	19.98
CH_3	CH_3	93.5–95	25.5	7.5	32.9	25.3	7.3	32.7

Zinc acetate 2-hydrate was used as obtained from the J. T. Baker Chemical Co. and stored in a sealed bottle.

ANAL. Calcd. for $C_4H_{10}O_6Zn$: C, 21.90%. Found: C, 22.11%.

Diethylzinc was obtained commercially and fractionally distilled on the vacuum apparatus to a purity in excess of 99.5 mole-%.[4]

$$\{Zn[OP(C_6H_5)_2O]_2\}_x$$

This material was prepared by the addition of a 100-ml. aqueous solution containing 10 mmole of $Zn(C_2H_3O_2)_2 \cdot 2H_2O$ to a solution of 20 mmole of $(C_6H_5)_2P(O)OH$ in 300 ml. of 95% ethanol, followed by addition of 19.7 mmole of aqueous NaOH. The resulting white precipitate was filtered and washed extensively with water and acetone. A yield of about 4.2 g. (85%) was obtained after drying in an oven at 110°C.

ANAL. Calcd. for $C_{24}H_{20}O_4P_2Zn$: C, 57.7%; H, 4.0%; P, 12.4%; Zn, 13.1%. Found: C, 57.4%; H, 4.2%; P, 12.7%; Zn, 13.6%.

The white powder is insoluble in water, benzene, chloroform, and other common organic solvents and is infusible to above 450°C.

A comparison of the x-ray powder patterns of $\{Zn[OP(C_6H_5)_2O]_2\}_x$ samples made by the above procedure and by various modifications [use of other acid acceptors, reaction of $(C_6H_5)_2P(O)OK$ with $Zn(C_2H_3O_2)_2 \cdot 2H_2O$, slight modifications of the interfacial polymerization procedure,[2] etc.] reveals that the samples range from almost completely amorphous to mostly crystalline. Two distinct diffraction patterns were repeatedly observed. The material obtained by the preparation reported here is designated the β modification and the other material the γ modification; the d spacings of both crystalline forms are recorded in Table II.

TABLE II
X-Ray Powder Patterns of $\{Zn[OP(R)(R')O]_2\}_x$[a]

β-$(C_6H_5)_2$		γ-$(C_6H_5)_2$		$(CH_3)_2$		β-$(CH_3)(C_6H_5)$		γ-$(CH_3)(C_6H_5)$	
d, A.	I[b]	d, A.	I[b]	d, A.	I[b]	d, A.	I[b]	d, A.	I[b]
11.2	100	16	40	7.5	100	11.7	100	12.2	30
6.45	10	11.5[c]	70	6.9	10	7.7	35	10.8	100
5.9	5	10.7	100	5.7	20	7.0	30	8.3	40
5.6	5	9.0	20	4.45	25	6.1	40	7.2	20
5.35	50	8.2	50	4.1	60	5.6	20	5.8[c]	15
4.4	10	7.0	30	3.7	50	4.7	80	5.4	10
4.2[c]	30	5.4	40	3.53	50	4.3	30	5.1	80
4.1	10	5.1	50	3.4	30	4.1	15	4.7[c]	20
3.43	20	4.45	40	3.0	10	3.9	5	4.5	30
3.18	10	4.2	40	2.82	40	3.7[c]	35	4.2	10
		4.0	30	2.73	15	3.5	5	3.8	10
		3.8	10	2.57	20	3.36	10	3.65	10
		3.68	10	2.48	15	3.10	15	3.55	10
		3.25[c]	20	2.37	20	2.98	5	3.04	30
		2.93	40	2.31	20	2.82	10	2.79	10
								2.68	5

[a] Cu $K\alpha$ radiation was used.

[b] Relative intensities estimated visually.

[c] Broad line.

$\{Zn[OP(CH_3)_2O]_2\}_x$

A white precipitate resulted upon addition of 10 mmole of finely divided $Zn(C_2H_3O_2)_2 \cdot 2H_2O$ to a solution of 20 mmole of $(CH_3)_2P(O)OH$ in 200 ml. of absolute ethanol. A yield of 2.4 g. (96%) was obtained after several ethanol washings and overnight vacuum drying at 40°C.

ANAL. Calcd. for $C_4H_{12}O_4P_2Zn$: C, 19.1%; H, 4.8%; P, 24.6%; Zn, 26.0%. Found: C, 19.3%; H, 4.8%; P, 25.0%; Zn, 25.8%.

The white powder is soluble in water but insoluble in chloroform, benzene, and other common organic solvents. The molecular weight in water, by vapor pressure osmometry, was found to be 115 (calcd. for the monomer: 251).

The partly crystalline solid (see Table II for x-ray powder pattern) melts at approximately 340°C. to a viscous fluid, which hardens at room temperature to a glass amorphous to x-rays. The glass softens at approximately 100°C. and is also soluble in water and insoluble in benzene and chloroform.

$\{Zn[OP(CH_3)(C_6H_5)O]_2\}_x$
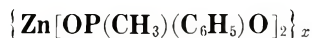
Solution Polymerization in Ethanol. A white precipitate resulted on addition of 7.718 g. (35.50 mmole based on carbon analysis) of finely divided $Zn(C_2H_3O_2)_2 \cdot 2H_2O$ to a solution of 11.088 g. (71.02 mmole) of (CH_3)-$(C_6H_5)P(O)OH$ in 600 ml. of ethanol. The mixture was stirred for 2 hr. at room temperature, then filtered and the precipitate washed twice with ethanol. The yield was 11.8 g. (95%) after drying overnight in a 60°C. vacuum oven.

ANAL. Calcd. for $C_{14}H_{16}O_4P_2Zn$: C, 44.8%; H, 4.3%; P, 16.5%; Zn, 17.4%. Found: C, 44.7%; H, 4.5%; P, 16.3%; Zn, 17.5%.

A sample of $\{Zn[OP(CH_3)(C_6H_5)O]_2\}_x$ was gradually heated to 275°C. while under vacuum and maintained at 275°C. overnight. The heated sample had a melt index of 2.0. (All melt indexes are in grams/10 min. at 190°C. with a 2100-g. piston load. See section on fluid behavior.)

Reaction Study with $(C_2H_5)_2Zn$. To a reaction tube on the vacuum apparatus containing a rigorously anhydrous mixture of 14.10 mmole of $(CH_3)(C_6H_5)P(O)OH$ and 15 ml. of toluene was added 7.10 mmole of $(C_2H_5)_2Zn$. The $(C_2H_5)_2Zn$ was measured as a liquid ($d_{20} = 1.205^5$) in a graduated tube and distilled into the reaction vessel. The mixture was stirred with an electromagnetic spiral type stirrer at −80°C., then at intermediate temperatures and finally for several hours at room temperature, resulting in a clear solution. The evolved ethane was removed periodically by fractional distillation and measured as a gas at room temperature in a calibrated volume connected to a mercury manometer. Calculated for the quantitative reaction, $(C_2H_5)_2Zn + 2(CH_3)(C_6H_5)P(O)OH \rightarrow 2C_2H_6 + 1/x[Zn(OP(CH_3)(C_6H_5)O)_2]_x$: 14.10 mmole; found: 14.14 ± 0.07 mmole.

The polymer was separated from toluene solution by precipitation with petroleum ether, washed extensively with petroleum ether, and dried in a vacuum desiccator.

ANAL. Calcd. for $C_{14}H_{16}O_4P_2Zn$: C, 44.8%; H, 4.3%; P, 16.5%; Zn, 17.4%. Found: C, 45.0%; H, 4.4%; P, 15.6%; Zn, 17.4%.

Other Preparations of $\{Zn[OP(CH_3)(C_6H_5)O]_2\}_x$ This phosphinate has also been prepared by the reaction of $(CH_3)(C_6H_5)P(O)OH$ with exact stoichiometric quantities of $Zn(C_2H_3O_2)_2 \cdot 2H_2O$ in refluxing benzene or xylene. In the latter solvent, the acetic acid produced by the reaction was distilled out of the reaction mixture. In both cases the polymer was separated from the solvent by precipitation with petroleum ether. Another interesting preparation, which is amenable to very large scale-up, is the melt polymerization reaction of a slight stoichiometric excess of $(CH_3)(C_6H_5)P(O)OH$ with $Zn(C_2H_3O_2)_2 \cdot 2H_2O$. An intimate mixture was gradually heated to 260°C. under nitrogen to form a clear viscous melt. The degree of polymerization was increased, as evidenced by increasing melt viscosities, by heating under vacuum at 275°C.

All of these preparations yield products similar to those obtained from the solution polymerization in ethanol. If minor deviations are made, such as the use of impure starting materials or nonstoichiometric amounts of starting materials, samples with reduced melt viscosities (higher melt indexes) result.

General Properties of $\{Zn[OP(CH_3)(C_6H_5)O]_2\}_x$. Typical samples of $\{Zn[OP(CH_3)(C_6H_5)O]_2\}_x$ are soluble in chloroform and benzene, slightly soluble in water, and insoluble in other common nonaromatic organic solvents. They have the appearance and physical properties normally associated with polymeric materials in that they swell with suitable solvents,

may be drawn into fibers from solution or from the melt, and cast into films. The polymer, a glassy solid at room temperature, softens at about 90°C. to form a viscous melt which retains a high melt viscosity to above 400°C.

In earlier work, particularly with ethanol or benzene as the solvent, another form of $\{Zn[OP(CH_3)(C_6H_5)O]_2\}_x$ which is insoluble in water, chloroform, and benzene was occasionally found, frequently together with the form already described. X-ray analysis indicates that the insoluble form (designated β) is crystalline and the soluble form (designated α) amorphous. The low molecular weight α samples tend to convert to a second crystalline form (designated γ) on standing, whereas the higher molecular weight samples remain amorphous. Heating to elevated temperatures converts both the β form (m.p. 209–211°C.) and the γ form (m.p. 200–205°C.) to the α form. The d spacings of the two crystalline forms are recorded in Table II.

Fluid Behavior of $\{Zn[OP(CH_3)(C_6H_5)O]_2\}_x$. The melt indexes of various samples of $\{Zn[OP(CH_3)(C_6H_5)O]_2\}_x$ have been measured at 190°C. and have been found to be directly proportional to the size of the piston load used (Newtonian behavior). Consequently, all the melt indexes regardless of piston load have been converted to grams extruded per 10 min. for a 2100-g. piston load. The values range from 1.5–2.5 for the higher molecular weight preparations to >20 (the limit of measurements obtainable at 190°C.). Occasionally the more viscous samples have given indications of viscoelastic behavior, in that the extruded rods have had diameters as large as 0.103 in. as compared with the 0.083-in. diameter of the orifice.

The melt index of $\{Zn[OP(CH_3)(C_6H_5)O]_2\}_x$ increases upon prolonged exposure to atmospheric moisture at room temperature. No decomposition occurs, however, since the melt index drops to its original value when the material is heated at elevated temperatures. Therefore, all of the measurements have been made on freshly dried samples or on samples stored in an inert atmosphere.

The melt indexes of a typical sample at varying temperatures follow: 0.626 at 166 ± 1°C., 1.19 at 177 ± 1°C., 2.41 at 190 ± 0.05°C., 5.73 at 209.5 ± 0.5°C., and 14.32 at 230 ± 0.05°C.

Stability Studies

All three phosphinates were subjected to our usual thermogravimetric analysis procedure on a modified Chevenard thermobalance[6] in a nitrogen atmosphere at a heating rate of 5°C./min. The resulting weight–temperature relationships are shown in Figure 1. In addition, $\{Zn[OP(CH_3)(C_6H_5)O]_2\}_x$ was run in air, and $\{Zn[OP(C_6H_5)_2O]_2\}_x$ in a 3:1 oxygen–water atmosphere. The results were virtually identical with those obtained under nitrogen.

The long-term thermal stability of $\{Zn[OP(CH_3)(C_6H_5)O]_2\}_x$ under nitrogen was determined by modified thermogravimetric analysis as recorded in Table III. The first sample was placed in the thermobalance at room temperature and raised to a test temperature of 399°C. at a rate of 5°C./min. Since there was substantial weight loss at this temperature, the
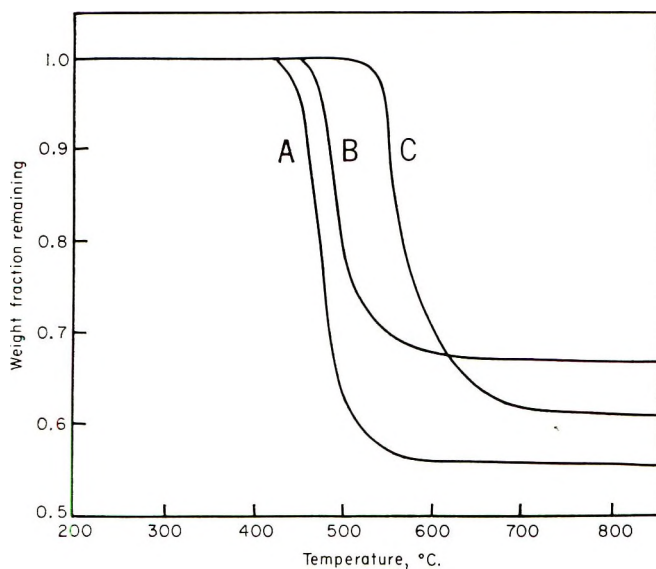
Fig. 1. TGA of (A) $\{Zn[OP(CH_3)(C_6H_5)O]_2\}_x$, (B) $\{Zn[OP(CH_3)_2O]_2\}_x$, and (C) $\{Zn-[OP(C_6H_5)_2O]_2\}_x$ in nitrogen with a heating rate of 5°C./min.

test temperature was reduced in successive runs by 28°C. increments until the sample did not appear to lose weight. The overall weight loss was determined by weighing the sample before and after the thermobalance run. The long term stability of $\{Zn[OP(CH_3)(C_6H_5)O]_2\}_x$ in air was similarly determined. In addition a $\{Zn[OP(C_6H_5)_2O]_2\}_x$ sample was run in air for a 20-hr. period at 440°C. These results are also recorded in Table III.

The thermal stability of $\{Zn[OP(CH_3)(C_6H_5)O]_2\}_x$ was studied at 316°C. under high vacuum ($\sim 10^{-3}$ mm.) by observing the melt index of a sample as a function of time. It had values of 2.03 after 7 hr., 2.07 after 31 hr., 1.92 after 101 hr., and 1.77 after 220 hr. The evaporation rate of $\{Zn[OP-(CH_3)(C_6H_5)O]_2\}_x$ under high vacuum (average $\sim 5 \times 10^{-4}$ mm.) was measured at 316°C. by pumping on a 1.22-g. sample which was removed

TABLE III
Modified Thermogravimetric Analysis of Zinc Phosphinates[a]

Temp., °C.	Atmosphere	Time, hr.	Weight loss, %
399	Nitrogen	19	39.4
371	Nitrogen	17	16.9
344	Nitrogen	200	7.1
316	Nitrogen	200	2.5
288	Air	200	3.7[b]
260	Air	200	0.8
440	Air	20	2.8[c]

[a] All data are for $\{Zn[OP(CH_3)(C_6H_5)O]_2\}_x$ except as noted.

[b] Despite the small weight loss, visual observation indicated that decomposition was taking place, as judged by the extent of darkening.

[c] For $\{Zn[OP(C_6H_5)_2O]_2\}_x$.

periodically and weighed under anhydrous conditions.   A total of 0.143 g. or 11.7% volatilized over a 267-hr. period, with an evaporation rate of approximately 0.0004 g./hr. after volatilization of the lower molecular weight species.

The effect of long-term exposure to atmospheric moisture was measured by heating a sample at 129°C. in the atmosphere and periodically measuring its melt index.   A sample with an initial melt index of 2.62 was found to have a melt index of 2.70 after 46 hr. and 3.07 after 210 hr.

Radiation resistance was determined by exposing a sample with an initial melt index of 2.58 to a Co^{60} source of 230,000 r./hr. for 240 hr. After exposure, the melt index was 2.45.

DISCUSSION

Our findings indicate that $\{Zn[OP(CH_3)(C_6H_5)O]_2\}_x$ has a polymeric structure.   Although no substantial direct evidence is presented for the polymeric nature of $\{Zn[OP(CH_3)_2O]_2\}_x$ and $\{Zn[OP(C_6H_5)_2O]_2\}_x$, it is probable that they are likewise polymers.   Additional evidence to support this thesis is presented in a companion paper.[7]

The structure (I) postulated for these polymers in our earlier communica-

I
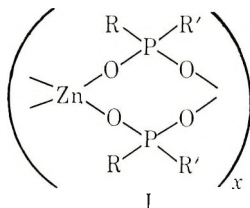
tion[2] receives further support from recent findings.   A detailed x-ray structure determination of the chromium(III) dimer,[8] $\{Cr(AcCHAc)_2[OP-(C_6H_5)_2O]\}_2$, has confirmed the existence of phosphinate double bridges, and a related double-bridged backbone has been found in the x-ray investigation of $[Mn(CH_3COOC_2H_5)_2(PCl_2O_2)_2]_x$.[9]   Other structures possible for the zinc phosphinates are a crosslinked octahedral structure in which zinc atoms share oxygen atoms and a crosslinked, single-bridged tetrahedral structure. Neither is likely because of the low-melting, soluble character of $\{Zn[OP-(CH_3)(C_6H_5)O]_2\}_x$.   Positive evidence for a tetrahedral configuration lies in the observation that the crystalline species are isomorphous with the corresponding blue cobalt species.[7]

A double-bridged structure for the zinc phosphinates is very plausible when one considers that in solution the phosphinic acids are dimeric[10] (structure II), so that polymer formation can easily result from the substitution of zinc(II) for protons.
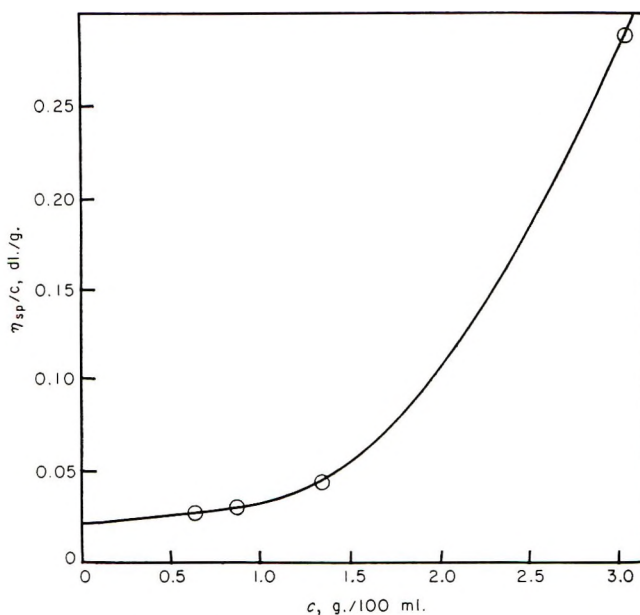

II
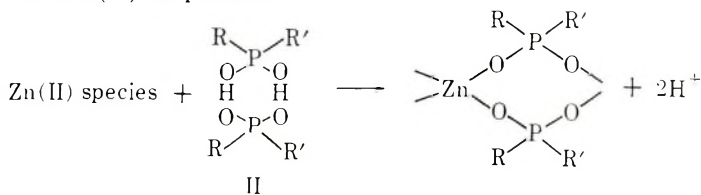
Fig. 2. Plot of η_{sp}/c vs. c for $\{Zn[OP(CH_3)(C_6H_5)O]_2\}_x$ in benzene.

The physical properties of the $\{Zn[OP(CH_3)(C_6H_5)O]_2\}_x$ polymer are in general not intermediate between those of the $[Zn(OP(C_6H_5)_2O)_2]_x$ and $\{Zn[OP(CH_3)_2O]_2\}_x$ polymers. Zinc methylphenylphosphinate softens below 100°C. and is soluble in benzene and chloroform as opposed to the high-melting, insoluble character of the latter two materials. This may be largely attributed to the reduction in crystallinity (or tendency to crystallize) in the unsymmetrical $\{Zn[OP(CH_3)(C_6H_5)O]_2\}_x$ polymer. Examination of Stuart-Briegleb models (E. Leybold's Nachfolger, manufacturer) of these polymer structures suggests that there is a great increase in structural flexibility in the backbone when the first phenyl is replaced with the less bulky methyl side group. Any further increase in flexibility due to the replacement of the second phenyl group is apparently outweighed by the crystallinity inherent in the more symmetrical form.

The molecular weights of the various $\{Zn[OP(CH_3)(C_6H_5)O]_2\}_x$ samples have been measured by a number of absolute and relative techniques. As measured by ebulliometry and vapor pressure osmometry in benzene and chloroform, the molecular weights have ranged from 2500 to greater than 10,000 (the practical limit of these techniques), with the samples prepared by our best procedures fairly consistently measuring above 10,000. These same samples have typically yielded values for the intrinsic viscosity in benzene (either reagent grade or rigorously anhydrous and thiophene-free) and chloroform on the order of 0.02 dl./g., which is below what one would expect for high polymers. However, the plot of η_{sp}/c versus c in benzene (Fig. 2) is no longer linear when c exceeds 1 g./100 ml., and at 3 g./100 ml. η_{sp}/c is 0.3 dl./g.

The reaction of $(CH_3)(C_6H_5)P(O)OH$ with $(C_2H_5)_2Zn$ in a vacuum system was undertaken in an attempt to estimate the degree of polymerization of high molecular weight $\{Zn[OP(CH_3)(C_6H_5)O]_2\}_x$. The quantity of ethane evolved is a direct measure of the extent of reaction, with a quantitative reaction presumably being indicative of high polymer formation. Since the ethane could be measured and correlated with the starting materials with an estimated overall accuracy of at least 1%, the quantitative reaction obtained would appear to indicate a degree of polymerization exceeding 100 units (molecular weight >35,000). In agreement with our other preparations the $\{Zn[OP(CH_3)(C_6H_5)O]_2\}_x$ produced had a molecular weight >10,000 by ebulliometry in chloroform and an intrinsic viscosity of 0.02 in benzene.

The melt viscosity of a polymer is proportional to its molecular weight according to the following relationship:[11] $\eta = KM^a$, where η is melt viscosity, a is 1 or 3.5, M is molecular weight, and K is a constant for a given polymer. Since the melt index of a polymer is approximately inversely proportional to its melt viscosity, a qualitative comparison of the molecular weights of $\{Zn[OP(CH_3)(C_6H_5)O]_2\}_x$ samples can be obtained by comparing their melt indexes. Samples that gave molecular weights >10,000 by colligative methods had melt indexes of approximately 2, a value comparable to the melt indexes obtained with reasonably high molecular weight organic polymers.

In summary, these measurements, together with the observed physical properties of zinc methylphenylphosphinate, lead us to conclude that it is a polymer with at least moderately high molecular weight. Similarly zinc dimethylphosphinate appears to be polymeric in bulk form, as evidenced by its formation of a viscous fluid at 350°C., despite its complete dissociation in water.

In our standard thermogravimetric analysis procedure, which involves a heating rate of 5°C./min., $\{Zn[OP(C_6H_5)_2O]_2\}_x$ starts to lose weight at approximately 490°C., $\{Zn[OP(CH_3)(C_6H_5)O]_2\}_x$ at approximately 425°C., and $\{Zn[OP(CH_3)_2O]_2\}_x$ at approximately 440°C. The results of such nonequilibrium studies are frequently misleading. Some long term studies were therefore undertaken. It was found that $\{Zn[OP(C_6H_5)_2O]_2\}_x$ underwent a very small weight loss after being heated at 440°C. for 20 hr. in air, and that $\{Zn[OP(CH_3)(C_6H_5)O]_2\}_x$ lost very little weight after 200 hr. in nitrogen at 316°C. or after 200 hr. in air at 260°C.

The use of change in weight alone as the criterion for breakdown of a polymer structure is, however, questionable. A more realistic criterion for the stability of a polymer is the deterioration of a critical physical property such as tensile strength for a plastic or fiber or melt index for a fluid. Accordingly the thermal stability of $\{Zn[OP(CH_3)(C_6H_5)O]_2\}_x$ was studied at 316°C. under high vacuum by observing the melt index as a function of time. The results clearly show that the sample was only slightly affected by prolonged heating at high vacuum for over 200 hr. The slight decrease in melt index observed is, moreover, in the direction of increased molecular

weight. No substantial crosslinking occurred, since the polymer was still readily soluble in chloroform after the prolonged heating.

References

1. Saraceno, A. J., and B. P. Block, *Inorg. Chem.*, **3**, 1699 (1964), Part VI.

2. Block, B. P., S. H. Rose, C. W. Schaumann, E. S. Roth, and J. Simkin, *J. Am. Chem. Soc.*, **84**, 3200 (1962).

3. Sorenson, W. R., and J. W. Campbell, *Preparative Methods of Polymer Chemistry*, Interscience, New York, 1961, pp. 34–42.

4. Rose, S. H., B. P. Block, and J. E. Davis, *Inorg. Chem.*, **3**, 1258 (1964).

5. Jander, G., and C. Fischer, *Z. Elektrochem.*, **62**, 965 (1958).

6. Soulen, J. R., and I. Mockrin, *Anal. Chem.*, **33**, 1909 (1961).

7. Rose, S. H., and B. P. Block, *J. Polymer Sci. A-1*, **4**, 583 (1966).

8. Wilkes, C. E., and R. A. Jacobson, *Inorg. Chem.*, **4**, 99 (1965).

9. Danielsen, J., and S. E. Rasmussen, *Acta Chem. Scand.*, **17**, 1971 (1963).

10. Kosolapoff, G. M., and J. S. Powell, *J. Chem. Soc.*, **1950**, 3535.

11. Bueche, F., *Physical Properties of Polymers*, Interscience, New York, 1961, p. 74.

Résumé

On a préparé le phosphinate de diméthyl zinc, de méthylphényle zinc et de diphényle zinc par la réaction de $Zn(C_2H_3O_2)_2 \cdot 2H_2O$ avec l'acide ou le sel approprié et on a trouvé qu'ils existaient sous les formes amorphes et cristalline. Le phosphinate de méthylphényle zinc, le plus maniable, présente plusieurs propriétés physiques de matériaux polymériques, aussi bien en solution qu'à l'état solide, ce qui confirme notre suggestion antérieure, à savoir que ces composés sont des polymères de coordination doublement pontés. Des analyses thermogravimétriques indiquent des températures initiales de décomposition de 440, 425, et 490°C respectivement pour ces trois polymères mais des études à long terme montrent une initiation de la décomposition à des températures un peu plus basses.

Zusammenfassung

Zinkdimethyl-, methylphenyl- und diphenylphosphinat wurden durch Reaktion von $Zn(C_2H_3O_2)_2 \cdot 2H_2O$ mit der geeigneten Säure oder dem Salz dargestellt; sie treten in amorphen und kristallinen Formen auf. Zinkmethylphenylphosphinat, das ammeisten untersuchte, zeigt sowohl in Lösung als auch in Substanz viele physikalische Eigenschaften polymerer Stoffe, was für unsere frühere Ansicht spricht, dass diese Verbindungen Doppelbrückenkoordinationspolymere sind. Thermogravimetrische Analyse zeigt einen Zersetzungsbeginn für die drei Polymeren bei 440, 425 bzw. 490°C, Langzeitversuche lassen jedoch einen Zersetzungsstart bei etwas niedrigeren Temperaturen erkennen.

Inorganic Coordination Polymers.   VIII.   Cobalt(II) and Zinc(II) Phosphinate Polymers and Copolymers*

SELWYN H. ROSE and B. P. BLOCK, *Technological Center, Pennsalt Chemicals Coporation, King of Prussia, Pennsylvania*

Synopsis

The preparation, properties, x-ray powder patterns, and TGA curves are given for cobalt(II) dimethyl-, methylphenyl- and diphenylphosphinate. The polymeric character of cobalt(II) methylphenylphosphinate is demonstrated by its colligative properties and melt indexes. These cobalt(II) phosphinates along with hybrid copolymers of zinc-(II) or cobalt(II) were prepared by the reaction of the metal acetate with the appropriate phosphinic acid or mixture of phosphinic acids. A consideration of the hybrid copolymers leads to the conclusion that both the zinc(II) and cobalt(II) dimethyl- and diphenylphosphinates are likewise polymeric. Thermal stability is discussed in terms of the structures suggested, and it is shown that crystallinity is related to polymer symmetry.

INTRODUCTION

In the preceding paper[1] we presented detailed studies of selected zinc(II) phosphinates. These materials represent the simplest class of metal phosphinate polymers $(MX_2)_x$, where X is a bridging phosphinate group with a charge of -1. We now wish to describe the characterization of the analogous cobalt(II) dimethyl-, methylphenyl-, and diphenylphosphinates and, as well, some cobalt(II) and zinc(II) phosphinate polymers containing two different phosphinate bridging groups. Although cobalt(II) phosphinates have been reported,[2–4] their characterization as polymers has been very incomplete. Furthermore, we have observed properties not previously noted. The zinc(II) and cobalt(II) polymers containing two different phosphinates represent, to the best of our knowledge, a new structural type of copolymer, which we propose to call hybrid copolymers for reasons presented in the discussion.

EXPERIMENTAL

Apparatus and Starting Materials

The apparatus used in this study has been described in the preceding paper.[1]

The methods used for the preparation of the phosphinic acids and typical

---

analytical data for the samples used in this investigation have been given in preceding papers.[1,5]

Zinc acetate 2-hydrate and $Co(C_2H_3O_2)_2 \cdot xH_2O$ were used as obtained from the J. T. Baker Chemical Co. The former was stored in a sealed bottle.

ANAL. Calcd. for $C_4H_{10}O_6Zn$: C, 21.90%. Found: C, 22.11%.

The quantities of cobalt acetate hydrate utilized in reactions were based on the cobalt assay.

ANAL. Found: Co, 25.9%; C, 20.8%; C: Co ratio, 3.94:1.

$$\{Co[OP(C_6H_5)_2O]_2\}_x$$

In general the polymers and the hybrid copolymers were made by the reaction between stoichiometric amounts of the acid or acids and the metal acetate in the presence of a solvent. For example, a solution of 10 mmole of $Co(C_2H_3O_2)_2 \cdot xH_2O$ in 100 ml. of ethanol reacted with a solution of 20 mmole of $(C_6H_5)_2P(O)OH$ in 250 ml. of ethanol to give 4.6 g. of a dark blue precipitate (93% yield) after work-up, i.e., filtration, extensive washing with ethanol, and drying in an oven at 110°C. The blue powder was insoluble in benzene, chloroform, and other common organic solvents, but

TABLE I
X-Ray Powder Patterns of $\{Co[OP(R)(R')O]_2\}_x$[a]

(C₆H₅)₂		(CH₃)₂		β-(CH₃)(C₆H₅)		γ-(CH₃)(C₆H₅)	
d, A.	I[b]	d. A.	I[b]	d, A.	I[b]	d, A.	I[b]
11.5	100	7.5	100	12.0	100	10.8	100
10.5	30	4.5	10	7.8	30	8.3	40
5.3	50	4.1	40	7.1	20	7.2	20
4.75	10	3.7	35	6.2	40	5.9	25
4.3	10	3.55	30	5.7	25	5.4	5
4.1[c]	20	3.38	10	4.7	60	5.1	80
3.75	10	2.82	20	4.3	20	4.8	10
3.2	10			4.0	5	4.6	50
				3.7	25	4.2	20
						3.8	20
						3.68	15
						3.58	15
						3.45[c]	10
						3.3	5
						3.2	15
						3.07	30
						2.98	5
						2.80	20
						2.69	10

[a] Cr Kα radiation was used.
[b] Relative intensities estimated visually.
[c] Broad line.

somewhat soluble in water.   The crystalline solid is infusible to over 450°C.
(Where solids are designated crystalline or amorphous, the criterion used
is x-ray examination.)   Its x-ray powder pattern is summarized in Table I.

ANAL.   Calcd. for $C_{24}H_{20}CoO_4P_2$: C, 58.4%; H, 4.1%; Co, 12.0%; P, 12.6%.
Found: C, 58.7%; H, 4.2%; Co, 12.2%; P, 12.9%.

$\{Co[OP(CH_3)_2O]_2\}_x$

In a variation of the general procedure 18 mmole of $Co(C_2H_3O_2)_2 \cdot xH_2O$
was added to a solution of 36 mmole of $(CH_3)_2P(O)OH$ in 150 ml. of ethanol,
and the resulting mixture was refluxed for 2 hr.   The blue precipitate that
resulted was filtered from the hot mixture in a steam-heated funnel,
repeatedly washed with hot ethanol, and dried at 110°C.   The yield was
4.2 g. (95%) of a crystalline blue solid soluble in water and insoluble in
common organic solvents.   (See Table I for the x-ray powder pattern.)   It
melts at 342–343°C. to a viscous fluid that cools to a hard amorphous solid.
The amorphous solid softens at approximately 85°C. and is soluble in water
but insoluble in ethanol, benzene, and chloroform.

ANAL.   Calcd. for $C_4H_{12}CoO_4P_2$: C, 19.6%; H, 4.9%; Co, 24.1%; P, 25.3%. Found:
C, 19.9%; H, 5.7%; Co, 23.6%; P, 24.2%.
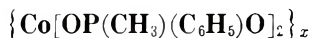
$\{Co[OP(CH_3)(C_6H_5)O]_2\}_x$

The latter procedure was also used to make $\{Co[OP(CH_3)(C_6H_5)O]_2\}_x$
from 30 mmole of $Co(C_2H_3O_2)_2 \cdot xH_2O$ and 60 mmole of $(CH_3)(C_6H_5)P(O)$-
OH in 90% yield.   The crystalline blue solid, designated β in Table I, is
soluble in water and insoluble in common organic solvents.   It melts at
210–211°C. to a viscous, dark-blue fluid that cools to a hard glassy solid.

The resultant amorphous solid softens at approximately 130°C. and
is soluble in chloroform, benzene, and water.   Molecular weights deter-
mined in benzene and chloroform by ebulliometry and vapor pressure
osmometry ranged from 3000 to >10,000, with typical samples giving
>10,000.   A typical sample had a melt index of 5.8 g./10 min. at 190°C.
with a 2100-g. piston load.   Intrinsic viscosities ranged from 0.02 to
0.05 dl./g. in chloroform and benzene.

ANAL.   Calcd. for $C_{14}H_{16}CoO_4P_2$: C, 45.5%; H, 4.4%; CO, 16.0%; P, 16.8%.
Found: C, 45.6%; H, 4.3%; Co, 16.6%; P, 17.2%.

The same reaction run in benzene, rather than ethanol, yielded a second
crystalline modification of $\{Co(OP(CH_3)(C_6H_5)O)_2\}_x$ designated γ in
Table I.   This blue solid is also soluble in water and insoluble in common
organic solvents.   It melts at 226–227°C.   The cooled melt forms amor-
phous, benzene-, and chloroform-soluble $\{Co[OP(CH_3)(C_6H_5)O]_2\}_x$ with a
molecular weight of 5300 by ebulliometry in chloroform.

Hybrid Co(II)–OP(C_6H_5)$_2$O–OP(CH$_3$)(C$_6$H$_5$)O Copolymer

The addition of 20.0 mmole of $Co(C_2H_3O_2)_2 \cdot xH_2O$ to a solution of 20.0
mmole of $(C_6H_5)_2P(O)OH$ and 20.0 mmole of $(CH_3)(C_6H_5)P(O)OH$ in

600 ml. of ethanol, followed by prolonged reflux, resulted in 5.7 g. of crude 1:1 hybrid copolymer. Evaporation of the chloroform extract of this product yielded 5.2 g. of 1:1 hybrid copolymer. The product softened at approximately 140°C. to a viscous fluid and had a molecular weight of 3,500 by ebulliometry in chlororoform.

ANAL. Calcd. for $C_{19}H_{18}CoO_4P_2$: C, 52.9%; H, 4.2%; Co, 13.7%; P, 14.4%. Found: C, 53.1%; H, 4.8%; Co, 12.6%; P, 14.1%.

Hybrid Co(II)–OP(C_6H_5)$_2$O–OP(CH_3)$_2$O Copolymer

This approximately 1:1 hybrid copolymer was prepared similarly with substitution of $(CH_3)_2P(O)OH$ for $(CH_3)(C_6H_5)P(O)OH$. There resulted 4.6 g. of blue solid (63% yield) only partially soluble in benzene and chloroform. However, in this case, instead of separating the soluble fraction from the insoluble fraction by chloroform extraction, a portion of the mixture was converted to an amorphous glass by heating it to 275°C. The amorphous hybrid copolymer had a molecular weight of 5000 by ebulliometry in chloroform.

ANAL. Calcd. for $C_{14}H_{16}CoO_4P_2$: C, 45.5%; H, 4.4%. Found: C, 49.3%; H, 4.4%.

Hybrid Zn(II)–OP(C_6H_5)$_2$O–OP(CH_3)(C_6H_5)O Copolymer

Under similar conditions a boiling solution of 10 mmole of $(C_6H_5)_2P(O)$-OH and 10 mmole of $(CH_3)(C_6H_5)P(O)OH$ in 400 ml. of ethanol reacted with 10 mmole of $Zn(C_2H_3O_2)_2 \cdot 2H_2O$ to give 3.7 g. (85% yield) of a white solid after filtration, extensive ethanol washing, and vacuum drying. The molecular weight of this 1:1 hybrid copolymer was found to be 5400 by ebulliometry in chloroform.

ANAL. Calcd. for $C_{19}H_{18}O_4P_2Zn$: C, 52.1%; H, 4.2%; P, 14.2%; Zn, 14.9%. Found: C, 51.9%; H, 4.0%; P, 14.2%; Zn, 14.6%.

In a similar reaction, 4.212 g. of $Zn(C_2H_3O_2)_2 \cdot 2H_2O$ (19.20 mmole) was added to a solution of 4.190 g. of $(C_6H_5)_2P(O)OH$ (19.20 mmole) and 3.028 g. of $(CH_3)(C_6H_5)P(O)OH$ (19.40 mmole) in 500 ml. of absolute ethanol, resulting in a white precipitate. To this mixture was added 500 ml. of xylene. The ethanol and the volatile reaction products were removed by distillation and the resulting xylene solution was refluxed for several hours. The solution was cooled to room temperature and excess petroleum ether was added to precipitate the hybrid copolymer. The xylene-swollen polymer thus isolated had definite rubbery properties. Extensive washing with petroleum ether and vacuum drying resulted in an amorphous white powder which softens at approximately 150°C. to a jelly-like fluid. The hybrid copolymer is soluble in benzene and chloroform and insoluble in water. It has a melt index of 6.0 g./10 min. at 265°C. under a 2100-g. piston load, a molecular weight >10,000 by vapor pressure osmometry in benzene, and an intrinsic viscosity of about 0.02 dl./g. in benzene.

Hybrid Zn(II)–OP(C₆H₅)₂O–OP(CH₃)₂O Copolymer

This amorphous 1:1 hybrid copolymer was similarly precipitated from ethanol by the reaction of equimolar quantities of $Zn(C_2H_3O_2)_2 \cdot 2H_2O$, $(C_6H_5)_2P(O)OH$, and $(CH_3)_2P(O)OH$. It softens at approximately 120°C., is soluble in benzene and chloroform, and has a molecular weight of 3000 by ebulliometry in benzene.

ANAL. Calcd. for $C_{14}H_{16}O_4P_2Zn$: C, 44.8%; H, 4.3%; P, 16.5%; Zn, 17.4%. Found: C, 45.9%; H, 4.9%; P, 16.2%; Zn, 17.3%.

Hybrid Zn(II)–OP(CH₃)(C₆H₅)O–OP(CH₃)₂O Copolymer

This amorphous 1:1 hybrid copolymer was also prepared in analogous fashion. It softens at about 95°C., is soluble in benzene, chloroform, and water, and has a molecular weight of 4000 by ebulliometry in benzene.

ANAL. Calcd. for $C_9H_{14}O_4P_2Zn$: C, 34.5%; H, 4.5%; P, 19.8%; Zn, 20.9%. Found: C, 35.5%; H, 5.0%; P, 18.5%; Zn, 20.9%.

Thermogravimetric Analysis

$\{Co[OP(C_6H_5)_2O]_2\}_x$, $\{Co[OP(CH_3)(C_6H_5)O]_2\}_x$, and $\{Co[OP(CH_3)_2O]_2\}_x$ were subjected to our usual thermogravimetric analysis procedure on a
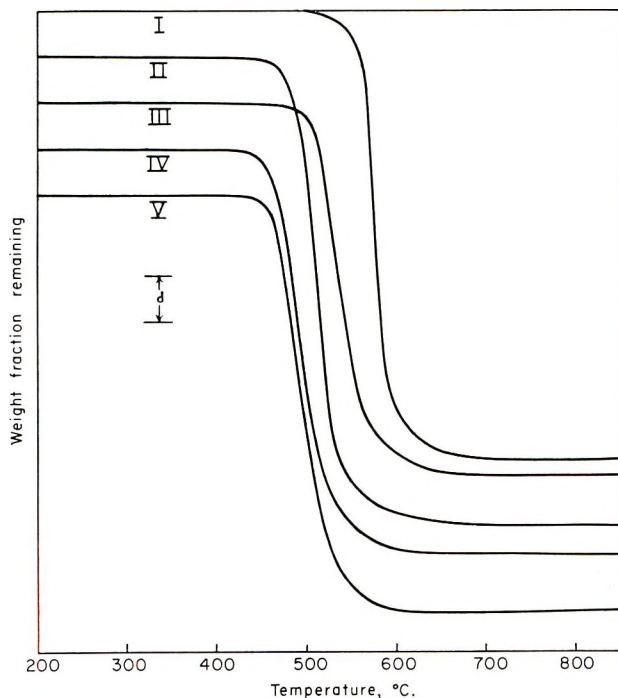
Fig. 1. TGA of (I) $\{Co[OP(C_6H_5)_2O]_2\}_x$, (II) $\{Co[OP(CH_3)(C_6H_5)O]_2\}_x$, (III) $\{Co[OP-(CH_3)_2O]_2\}_x$, (IV) 1:1 $\{Zn[OP(C_6H_5)_2O]_2\}_x-\{Zn[OP(CH_3)(C_6H_5)O]_2\}_x$, and (V) 1:1 $\{Zn[OP(C_6H_5)_2O]_2\}_x-\{Zn[OP(CH_3)_2O]_2\}_x$ in nitrogen with a heating rate of 5°C./min. All the curves start at a weight fraction remaining of 1.00 at 200°C. For each, the distance d represents a weight loss of 5%.

modified Chevenard thermobalance[6] in a nitrogen atmosphere at a heating rate of 5°C./min., as were the 1:1 hybrid copolymers of zinc(II) with diphenyl- and methylphenyl- and with diphenyl- and dimethylphosphinates. The resulting weight–temperature relationships are shown in Figure 1.

Decomposition

A sample of $\{Zn[OP(C_6H_5)_2O]_2\}_x$[1] was gradually heated to over 500°C. in a closed system and the volatile decomposition products were collected. A liquid that was identified as virtually pure C_6H_6 by its mass spectrum was the only volatile decomposition product.

DISCUSSION

The series of compounds, $[Co(OPRR'O)_2]_x$, where R and R' are C_6H_5 and/or CH_3 has been prepared. All are crystalline, high melting solids insoluble in organic solvents, in agreement with the observations of Coates and Golightly.[2] We find, however, that $\{Co[OP(CH_3)_2O]_2\}_x$ melts at 342°C. to form a polymeric fluid as do both the β (210°C.) and γ (226°C.) crystalline modifications of $\{Co[OP(CH_3)(C_6H_5)O]_2\}_x$ we isolated, whereas Coates and Golightly report their preparations to be infusible below 350°C. We have repeated their procedure for the preparation of $\{Co[OP(CH_3)-(CH_3)(C_6H_5)O]_2\}_x$ several times and have for the most part obtained a form of $\{Co[OP(CH_3)(C_6H_5)O]_2\}_x$ which appears identical to our β form. In addition, on one occasion, part of the product obtained was γ-$\{Co[OP-(C_6H_5)O]_2\}_x$. All the products obtained by their procedure melt to form the amorphous polymer, with molecular weights ranging from 3500 to >10,000 by ebulliometry in chloroform. Although we were unable to repeat their observations, it is possible, in view of the multiplicity of crystalline forms prevalent for the tetrahedral metal phosphinates, that they isolated a form of $\{Co[OP(CH_3)(C_6H_5)O]_2\}_x$ infusible below 350°C.

The properties of the amorphous form of $\{Co[OP(CH_3)(C_6H_5)O]_2\}_x$, which was obtained by cooling the melt from either crystalline form, offer the strongest support for the polymeric nature of these cobalt species. The molecular weights obtained by ebulliometry or vapor pressure osmometry, along with the magnitude of the melt indexes, offer direct evidence that this product is a polymer. The structural arguments that led us to postulate a double bridged linear structure for the zinc analog[1] are equally applicable to $\{Co[OP(CH_3)(C_6H_5)O]_2\}_x$. In this case the arguments gain additional support from the products' blue color which is characteristic of tetrahedral cobalt(II).[7]

The $[Co(OPRR'O)_2]_x$ polymers are similar to the $[Zn(OPRR'O)_2]_x$ polymers in that, as with $\{Zn[OP(CH_3)(C_6H_5)O]_2\}_x$, the thermal properties of $\{Co[OP(CH_3)(C_6H_5)O]_2\}_x$ are, unexpectedly, not intermediate between those of the diphenyl and dimethyl species. This may similarly be explained by a reduction in the tendency to crystallize on the part of the unsymmetrical $\{Co[OP(CH_3)(C_6H_5)O]_2\}_x$ and by the great increase in structural flexibility obtained by replacement of one phenyl with the less

bulky methyl sidegroup. Any further increase in flexibility due to replacement of the second phenyl group is apparently outweighed by the crystallinity inherent in the more symmetrical $\{Co[OP(CH_3)_2O]_2\}_x$. The tendency of $\{Co[OP(CH_3)(C_6H_5)O]_2\}_x$ to crystallize appears to be greater than that of the analogous zinc polymer because it is generally initially formed as a crystalline rather than as an amorphous material.

The reduction in crystallinity as a consequence of the reduction in symmetry in the polymer molecule is further demonstrated by the preparation of a chloroform soluble hybrid copolymer of cobalt(II) with diphenyl- and methylphenylphosphinate having a low softening point. More dramatic evidence of this effect is afforded by the hybrid copolymer of cobalt(II) with diphenyl- and dimethylphosphinates. This hybrid copolymer (of two high melting, highly crystalline materials insoluble in organic solvents) forms a viscous fluid at 275°C., which on cooling is completely soluble in chloroform.

Similarly, the three possible zinc hybrid copolymers containing methyl and phenyl groups, i.e., with $OP(C_6H_5)_2O^-$ and $OP(CH_3)(C_6H_5)O^-$, with $OP(C_6H_5)_2O^-$ and $OP(CH_3)_2O^-$, and with $OP(CH_3)(C_6H_5)O^-$ and $OP(CH_3)_2O^-$, were prepared. All of these amorphous materials are polymeric in benzene and chloroform solution and form very viscous fluids at moderately elevated temperatures. The use of copolymerization to reduce crystallinity in the polymer molecule, well known in the field of organic polymer chemistry, thus proves to be equally effective for these polymers.

No direct evidence has been obtained for the polymeric nature of $\{Zn[OP(C_6H_5)_2O]_2\}_x$ and $\{Co[OP(C_6H_5)_2O]_2\}_x$, and qualitative melt viscosity observations constitute the only evidence for the polymeric character of $\{Zn[OP(CH_3)_2O]_2\}_x$ and $\{Co[OP(CH_3)_2O]_2\}_x$. However, the preparation of tractable hybrid copolymers containing the $[OP(C_6H_5)_2O]^-$ and $[OP(CH_3)_2O]_2^-$ catenating groups constitutes excellent indirect evidence for the polymeric nature of all of the homopolymers involving symmetrical phosphinates.

Hybrid copolymers of zinc(II) with $OP(C_6H_5)_2O^-$ and $OP(CH_3)(C_6H_5)O^-$ were studied in greater detail than the other hybrid copolymers. Samples of the 1:1 hybrid copolymer with molecular weights in excess of 10,000 exhibited "rubbery" properties when plasticized. Hybrid copolymers may be prepared with any desired composition by altering the ratio of the phosphinic acids in the original ethanol solution. As the relative amount of diphenylphosphinate increases, the properties rapidly tend toward insolubility and higher softening points. For example, the 2:1 hybrid copolymer is insoluble in benzene and chloroform, starts to soften at approximately 300°C., and turns into a jelly-like material at about 400°C. Yet even a very small amount of $[OP(CH_3)(C_6H_5)O]^-$ imparts some tractability to the hybrid copolymer as opposed to pure $\{Zn[OP(C_6H_5)_2O]_2\}_x$; a sample of the 9:1 hybrid copolymer exhibited some softening when heated rapidly to 450°C.

In concept these hybrid copolymers differ markedly from conventional copolymers. The latter generally consist of randomly alternating monomer units, e.g., —X—Y—X—Y—X—X—Y—Y—X—. The hybrid copolymers reported here presumably consist of metal atoms joined together by randomly distributed catenating groups, as shown in structure I.

I
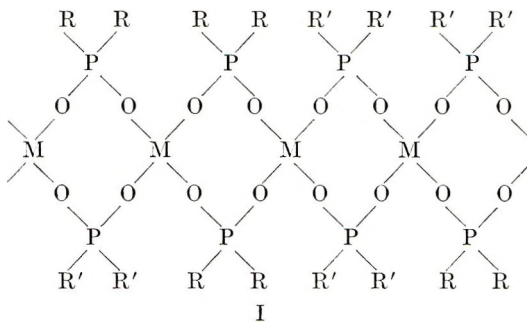
There are in this structure three kinds of monomer units instead of the two found in a conventional copolymer, i.e., units containing double bridges which consist of (1) two $OP(R)_2O^-$ groups, (2) two $OP(R')_2O^-$ groups, and (3) one $OP(R)_2O^-$ and one $OP(R')_2O^-$ group. In forming this type of copolymer, we achieve a new double bridge which is not found in either homopolymer. Furthermore, on the basis of steric considerations such units are expected to predominate in hybrid copolymers containing bulky catenating groups such as $OP(C_6H_5)_2O^-$. We propose that copolymers with this feature be referred to as hybrid copolymers.

The x-ray diffraction patterns (Table I, this paper and Table II, preceding paper[1]) indicate that $\{Co[OP(C_6H_5)_2O]_2\}_x$ is isomorphous with the β crystalline modification of $\{Zn[OP(C_6H_5)_2O]_2\}_x$, the β and γ forms of $\{Co[OP(CH_3)(C_6H_5)O]_2\}_x$ are isomorphous with the β and γ forms of the corresponding zinc polymer, and that $\{Co[OP(CH_3)_2O]_2\}_x$ and $\{Zn[OP-(CH_3)_2O]_2\}_x$ are also isomorphous. (Since relatively little work was done with $\{Co[OP(C_6H_5)_2O]_2\}_x$, $\{Co[OP(CH_3)_2O]_2\}_x$, and $\{Zn[OP(CH_3)_2O]_2\}_x$ as compared with the other polymers of interest, the isolation of only one crystalline modification of these materials is not considered significant.) This similarity of crystalline structure is quite understandable in view of the similar size of Zn(II) and Co(II) ions and the similarity in properties of the analogous polymers.

These materials, with initial TGA weight losses starting well over 400°C., are of interest as thermally stable polymers. In analogy to the zinc series the most stable thermally is $\{Co[OP(C_6H_5)_2O]_2\}_x$ with an initial weight loss at 485°C., whereas $\{Co[OP(CH_3)(C_6H_5)O]_2\}_x$ and $\{Co[OP(CH_3)_2O]_2\}_x$ both start losing weight at approximately 445°C. The two other materials tested, the 1:1 hybrid copolymers of zinc(II) with diphenyl- and methylphenylphosphinate and with diphenyl- and dimethylphosphinates, both start to lose weight at approximately 430°C.

An indication of the mode of decomposition of these polymers is provided by the identification of benzene as a decomposition product of $\{Zn[OP(C_6H_5)_2O]_2\}_x$ at $500°C$. The infrared spectrum of the decomposition residue has a peak at $12.5\ \mu$, which can be attributed to a $p\text{-}C_6H_4$ absorption.[8] This suggests the decomposition route shown in eq. (1):

$$
\begin{array}{c}
C_6H_5 \quad C_6H_5 \\
\diagdown P \diagup \\
O \quad O \\
Zn \quad Zn \\
O \quad O \\
\diagup P \diagdown \\
C_6H_6 \quad C_6H_5 \\
C_6H_5 \quad C_6H_5 \\
P \\
O \quad O \\
Zn \quad Zn \\
O \quad O \\
P \\
C_6H_5 \quad C_6H_5
\end{array}
\quad \xrightarrow{\ \Delta\ } \ C_6H_6 \ + \
\begin{array}{c}
C_6H_5 \quad C_6H_5 \\
P \\
O \quad O \\
Zn \quad Zn \\
O \quad O \\
P \\
C_6H_5 \quad C_6H_4 \quad C_6H_5 \\
P \\
O \quad O \\
Zn \quad Zn \\
O \quad O \\
P \\
C_6H_5 \quad C_6H_5
\end{array}
\tag{1}
$$
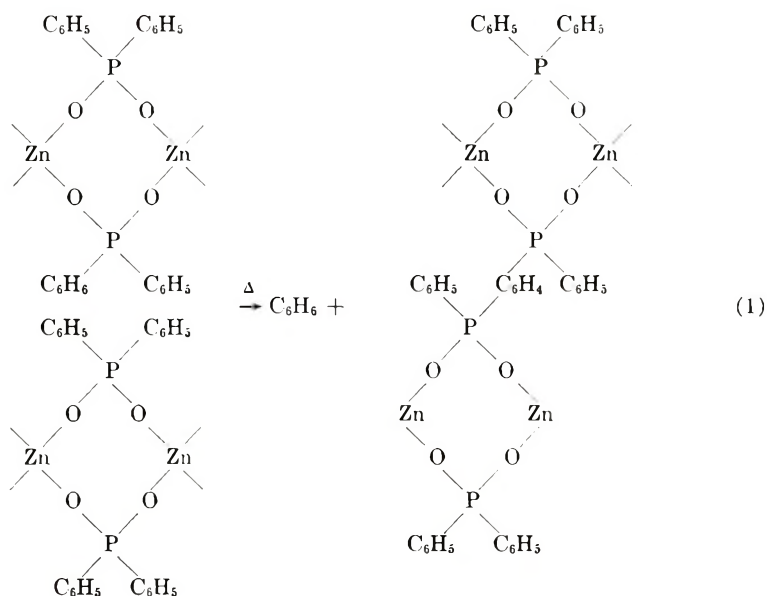
Since the initial decomposition appears to take place without rupture of the polymer backbone, the eventual promise of the metal phosphinate polymers may be somewhat understated by the thermal stability data.

A possible explanation of the substantial thermal stability of these poly-(metal phosphinates) follows. It is necessary to break two bonds of a double-bridged structure to effect rupture of the backbone. Since after the first bond has been thermally cleaved the atoms are still held in the same general vicinity, the second bond must be broken before the first bond can reform in order to decompose the material. This type of kinetic argument has provided much of the impetus for the work with double chain polymers.[9]

Alternatively, the polymer backbone can be considered to be an interlocking chelate system. The metal atoms are each involved in two eight-membered chelate rings. The extra energy imparted by this chelation then stabilizes the polymer backbone. The stabilization of polymers by means of this additional chelation energy has been the goal of various investigators.[10]

References

1. Rose, S. H., and B. P. Block, *J. Polymer Sci. A-1*, **4**, 573 (1966), Part VII.
2. Coates, G. E., and D. S. Golightly, *J. Chem. Soc.*, **1962**, 2523.
3. Block, B. P., S. H. Rose, C. W. Schaumann, E. S. Roth, and J. Simkin, *J. Am. Chem. Soc.*, **84**, 3200 (1962).
4. Crescenzi, V., V. Giancotti, and A. Ripamonti, *J. Am. Chem. Soc.*, **87**, 391 (1965).
5. Saraceno, A. J., and B. P. Block, *Inorg. Chem.*, **3**, 1699 (1964).
6. Soulen, J. R., and I. Mockrin, *Anal. Chem.*, **33**, 1909 (1961).
7. Katzin, L. I., and E. Gebert, *J. Am. Chem. Soc.*, **75**, 2831 (1953). Wells, A. F., *Structural Inorganic Chemistry*, 3rd Ed., Oxford Univ. Press, London, England, 1962, p. 266.
8. Bellamy, L. J., *The Infra-red Spectra of Complex Molecules*, Wiley, New York, 1958, pp. 65, 78.
9. Brown, J. F., Jr., *J. Polymer Sci. C*, **1**, 83 (1963).
10. Block, B. P., in *Inorganic Polymers*, F. G. A. Stone and W. A. G. Graham, Eds., Academic Press, New York, 1962, p. 498 ff.

Résumé

On donne la préparation, les propriétés, les résultats de diffraction aux rayons X par la méthode des poudres et les courbes de TGA pour les phosphinates de diméthyl-, méthylphényl- et diphényl- Co(II). Le caractère polymérique du phosphinate de méthylphényl-Co(II) est démontré par ses propriétés colligatives et par ses indices de fusion. Ces phosphinates de cobalt(II) ainsi que des copolymères hybrides de zinc(II) ou de cobalt(II) ont été préparés par la réaction de l'acétate métallique avec l'acide ou le mélange d'acides phosphiniques appropriés. Une étude des copolymères hybrides montre que les diméthyl- et diphényl-phosphinates de zinc(II) et cobalt(II) sont aussi polymériques. La stabilité thermique est discutée en fonction des structures suggérées et il apparaît que la cristallinité est reliée à la symétrie du polymère.

Zusammenfassung

Für Kobalt-(II)-dimethyl-, methylphenyl- und -diphenylphosphinat werden Darstellung, Eigenschaften, Röntgenpulverdiagramme und TGA-Kurven angegeben. Der polymere Charakter von Kobalt-(II)-methylphenylphosphinat wird durch seine kolligativen Eigenschaften und durch den Schmelzindex bewiesen. Diese Kobalt-(II)-phosphinate sowie Hybridkopolymere mit Zink(II) oder Kobalt(II) wurden durch Reaktion der Metallacetate mit der geeigneten Phosphinsäure oder mit einer Mischung von Phosphinsäuren dargestellt. Die Hybridkopolymeren führen zu dem Schluss, dass auch die Zink(II)- und Kobalt(II)dimethyl- und -diphenylphosphinate polymere Stoffe sind. Die thermische Stabilität wird in Hinblick auf die vorgeschlagene Struktur diskutiert, und es wird gezeigt, dass die Kristallinität in Beziehung zur Polymersymmetrie steht.

Permeation, Sorption, and Diffusion of Water in Ethyl Cellulose

J. D. WELLONS and V. STANNETT, *Camille Dreyfus Laboratory, Research Triangle Institute, Durham, North Carolina*

Synopsis

The permeability of ethyl cellulose to water vapor and liquid water was measured as a function of temperature. A change of slope was found in the Arrhenius plots at about 50°C., close to the glass transition. The sorption isotherms showed essentially zero heat of mixing in agreement with other workers. The diffusion constants were measured in four ways, viz., sorption, desorption, time lag, and by dividing the permeability constants by the equilibrium solubility coefficients. The time lag method gave diffusion constants which were independent of concentration, whereas the other three methods led to diffusion constants which steadily decreased with concentration. All the methods, however, extrapolated to about the same value at zero concentration. The decreasing diffusivities are believed to be due to the clustering of water molecules in the polymer. However, no clustering appeared to take place under the conditions of the time lag measurements.

In previous papers[1,2] the results of a study of the permeation, diffusion and solution of water in a number of polymers were reported. Equilibrium sorption isotherms were measured in addition to steady-state permeation rates and time lag diffusion constants. Two different patterns of behavior were found. In the case of polyethylene, polypropylene, and poly(ethylene terephthalate) the diffusion constants measured by the time lag method were in excellent agreement with the values calculated from the quotient of the permeability constants and equilibrium solubility coefficients. In all three polymers the diffusion constants were independent of concentration and Henry's solubility law was obeyed. In the case of rubber hydrochloride and ethyl cellulose, however, a different behavior was noted. The diffusivities measured by the time lag method were again found to be independent of concentration, but Henry's law was not obeyed and the sorption isotherms were of the familiar B.E.T. type II and type III shapes for ethyl cellulose and rubber hydrochloride, respectively. The diffusion constants calculated from the permeability constants and equilibrium solubility coefficients were therefore essentially decreasing with concentration. Subsequent work[3] showed that poly(ethyl methacrylate) also showed this behavior. It was decided to investigate this phenomenon in more detail, and ethyl cellulose was selected for the study since it showed the greatest deviations from ideality. This paper will describe the results of this investigation.

EXPERIMENTAL

The ethyl cellulose used was of density 1.11 g./cc., had an ethoxyl content of 48.7%, and was obtained from the Dow Chemical Company. Films were cast from acetone solution on to mercury and dried under vacuum.

The permeability constants and time lags were measured in a modified version of the high vacuum method of Barrer[4] described in detail previously.[2] The liquid water permeabilities were measured by using degassed distilled water. The sorption isotherms and rates of sorption and desorption were measured by using a conventional quartz helix microbalance enclosed in an air thermostat regulating to $\pm 0.5°C$. The balance tube containing the sample was also immersed in a water bath thermostatted to $\pm 0.01°C$. A few measurements were also made with the use of a thermostatted Cahn RG electronic microbalance.

RESULTS AND DISCUSSION

Permeability Data

The permeability constants for liquid water and for water vapor and the time lag diffusion constants for water vapor are presented in the form of Arrhenius plots in Figure 1, and the energies of activation and preexponential factors are given in Table I. It was not possible to measure time lags in the case of liquid water without substantial modification to the equipment. It can be seen that there is an inflection in the diffusivity plots and a weak inflection in the permeabilities at about 50°C. Such inflections are often found at the glass transition points; a differential scanning calorimeter study on the same sample also showed evidence of a weak transition at that temperature range. It can be seen that there is a small but definite increase in the permeability constants for liquid water compared with water vapor, the difference tending to get less at higher temperatures. At 25°C., the lowest temperature studied, the difference is only about 25% between the liquid and vapor permeabilities. At 25°C. the permeabilities were measured at a number of vapor pressures, and the results are plotted in Figure 2 in the form of transmission rate versus relative vapor pressure. The curve is linear, i.e., the permeability constant is independent of vapor pressure up to about 60% R.H. The permeability constants then gradually

TABLE I

Temperature Dependence of the Permeability and Diffusivity of Water in Ethyl Cellulose[a]

Condition		P_0, cc.(STP)/cm.^{2}/cm./sec./cm. Hg.	E_p, kcal./mole	D_0, cm.^{2}/sec.	E_d, kcal./mole
Vapor	<50°C.	1.75×10^{-5}	-1.5	0.0072	6.3
	>50°C.	2.39×10^{-8}	-2.8	1.0	9.5
Liquid	<50°C.	6.9×10^{-8}	-2.2	—	—
	>50°C.	9.2×10^{-6}	-3.5	—	—

[a] Vapor measurements at less than 50% R.H.
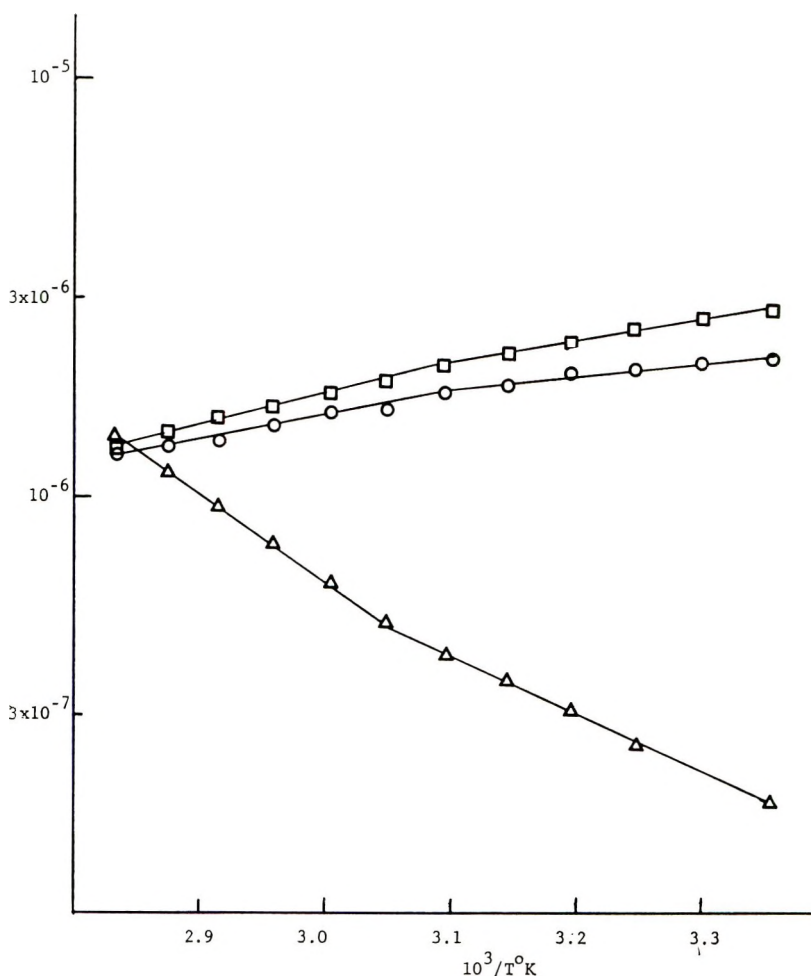
Fig. 1. Permeability and diffusivity of water in ethyl cellulose as a function of temperature: ($\square$) permeability (liquid), in cc./cm.²/sec./cm. Hg; ($\bigcirc$) permeability (vapor) at $<50\%$ R.H.; ($\triangle$) diffusivity (vapor), in cm.²/sec.

increase to the liquid water value. All the vapor data in Figure 1 were well within the linear range. In a previous paper the curves seemed linear to about 90% R.H., but this was not investigated in any detail, and no liquid point was measured. The small increases are not unexpected for a cellulosic material and are undoubtedly due to plasticization by the sorbed water. The time lag diffusivities were also measured at various vapor pressures at 25°C. and the results are included in Figure 5. It can be seen that the diffusion constants are independent of concentration, at least up to 4% of sorbed water, i.e., at 85% R.H.

Sorption-Desorption Data

The sorption isotherm for water at 25°C. in the ethyl cellulose film used in this investigation is shown in Figure 3. The results of Barrer and
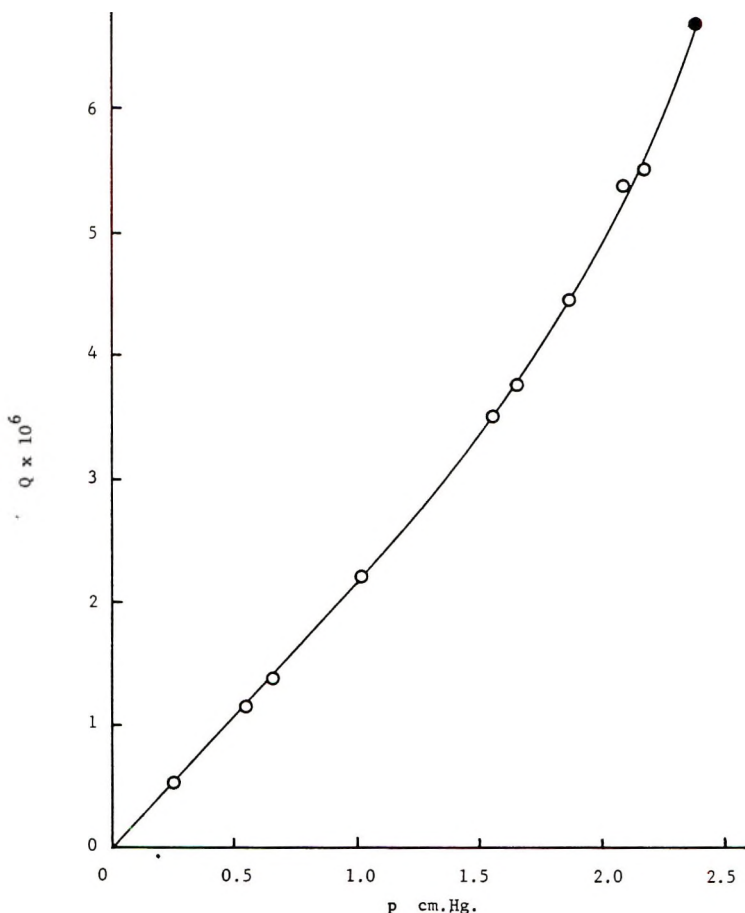
Fig. 2. Water vapor transmission in ethyl cellulose at 25°C. vs. vapor pressure.   Solid circle is liquid water point.

Barrie[5] at 50–80°C. fit well with the present data showing, in agreement with these authors, that there is essentially zero heat of mixing.   There was a small but definite hysteresis on desorbing amounting to about 10% increase in the maximum case.   The sorption isotherms reported previously[2] for a different sample of ethyl cellulose showed a small but definite specific site region at low humidities familiar with many cellulose derivatives.   The present sample, however, failed to yield this type of isotherm even when used in the original granule form but always gave an isotherm similar to that found by Barrer and Barrie.[5]   Presumably, the differences are due to changes in the distribution of the hydroxyl groups or other chemical or structural features.

The rates of sorption and desorption gave excellent linear, i.e., Fickian, plots of weight increase versus the square root of time when the quartz helix was used.   However, the more precise trace from the Cahn RG recording microbalance showed that there is a small acceleration in rate with
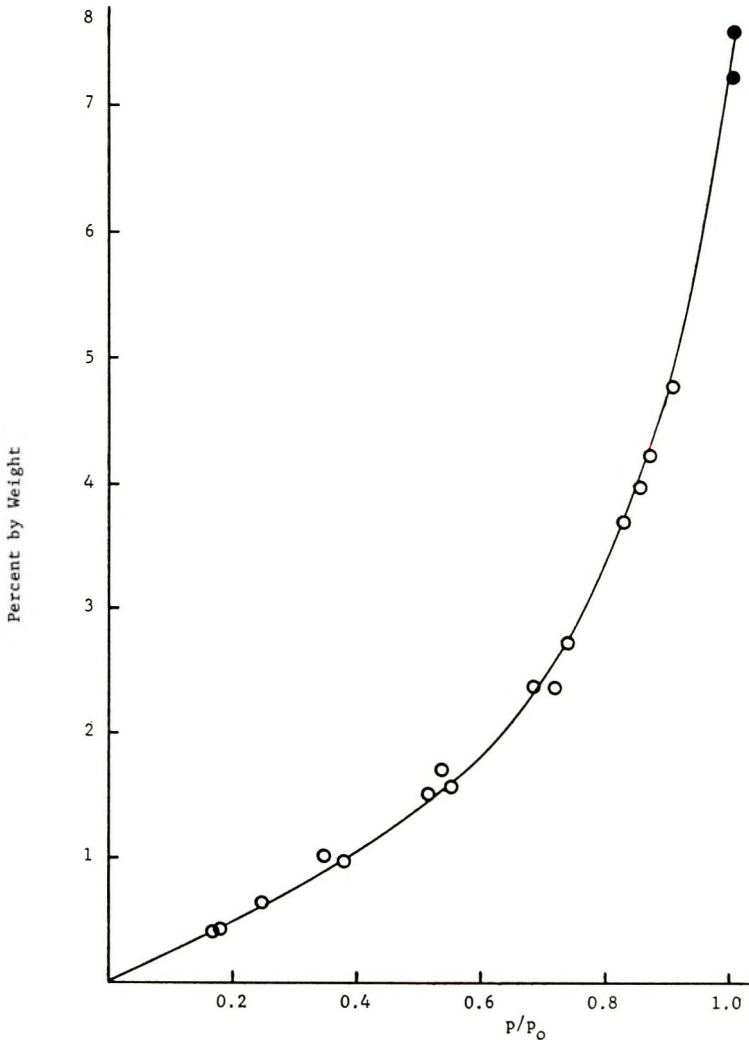
Fig. 3. Sorption isotherm for water in ethyl cellulose at 25°C. Solid circles are liquid water points.

time, as shown by the typical sorption and desorption rate curves in Figure 4. Such types of sorption curves are usually ascribed to relaxation processes accompanying the sorption of solvent or plasticizer into glassy polymers. The diffusivities calculated from the average slopes of the curves presented in Figure 4 are in good agreement with the less sensitive quartz helix values.

There are definite errors in the measurement of diffusion constants by sorption–desorption techniques due to the effect of the heat of sorption. The latter is largely the heat of condensation of water vapor in the case of ethyl cellulose. A mathematical analysis has been made of the effects of the heat of sorption on the rate of sorption and a method developed to
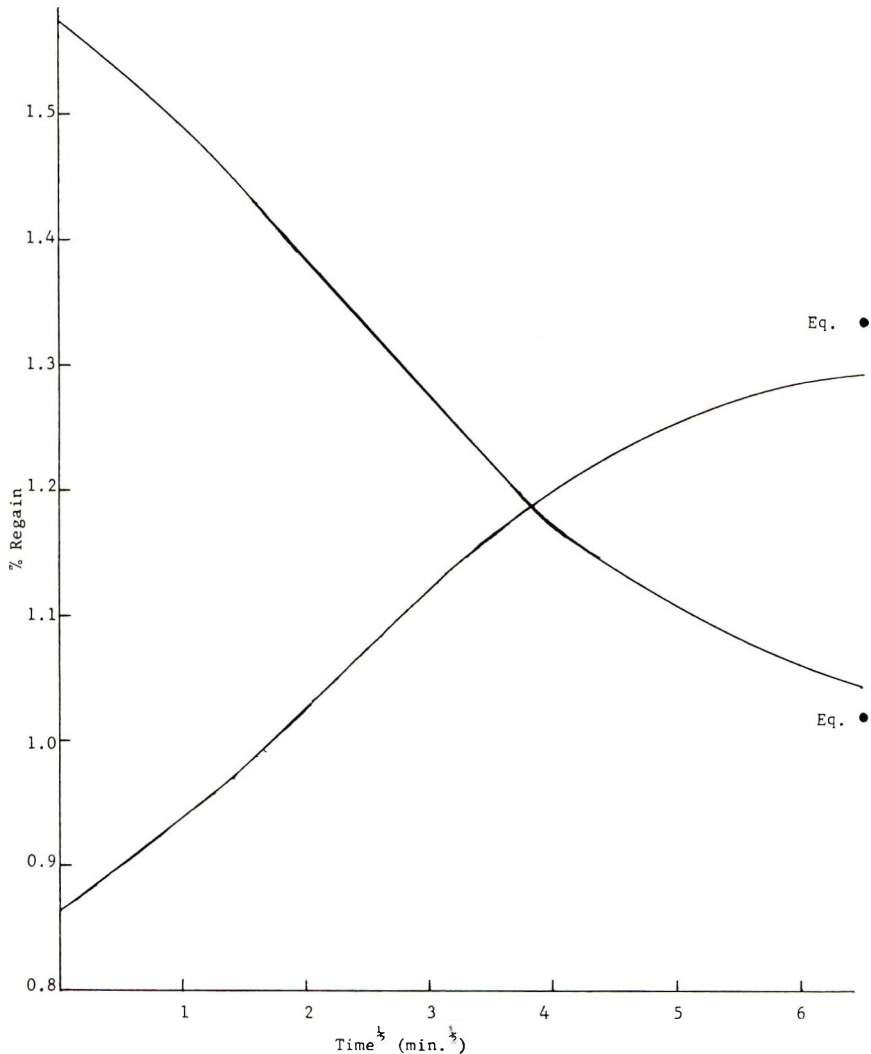
Fig. 4. Typical plots of absorption and desorption of water into ethyl cellulose at 25°C. Data obtained by use of the Cahn microbalance. Solid circles are equilibrium points.

enable the necessary corrections to be made. The changes in temperature during the sorption and desorption of water vapor in ethyl cellulose film were measured by cementing a thermocouple between two films to make up a film of the original thickness used for the sorption rate experiments. In addition, the heat transfer coefficient between the film surface and its surroundings was measured by conventional non-steady state heating experiments. Full details of these experiments and of the mathematical analysis leading to the calculation of the correct diffusion constants have been presented elsewhere.[6] If 1% increments in weight are used for the sorption or desorption experiments the corrections are small, being between
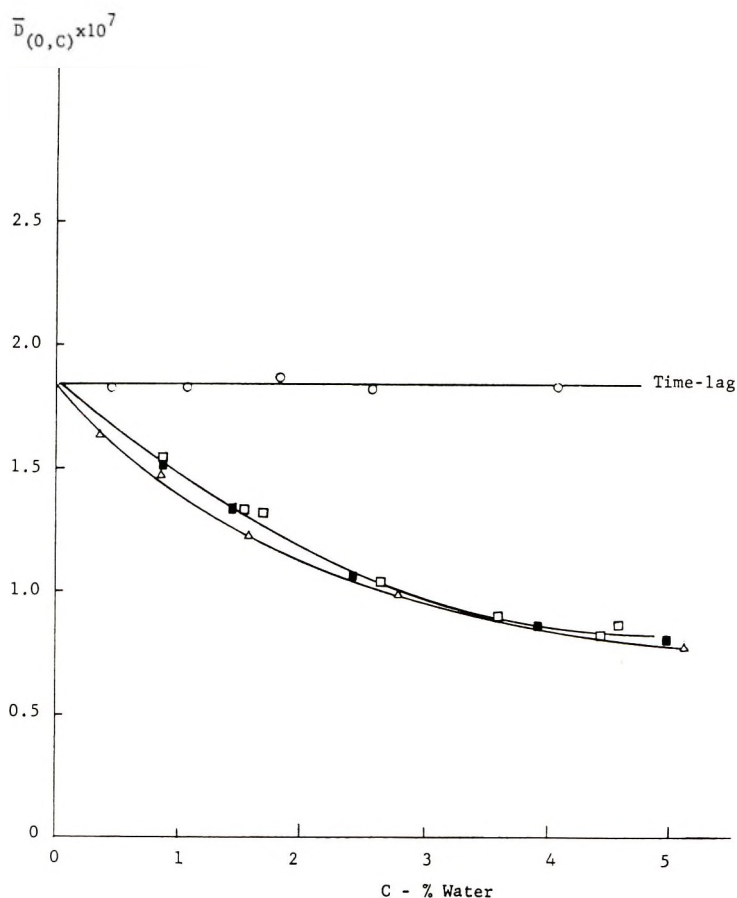
Fig. 5. Diffusion constants for water in ethyl cellulose at 25°C.: ($\square$) sorption; ($\blacksquare$) desorption; ($\triangle$) P/S_{eg}.

5-10%. The corrected integral diffusion constants at 25°C. are presented in Figure 5 plotted against the concentration of water in the film. It can be seen that, in contrast to the time lag values, the diffusivities decrease with increasing concentration but extrapolate back to the time lag values at zero water content. It can also be seen that the corrected values are similar for both sorption and desorption. This is in contrast to the results of F. Bueche,[7] who found concentration-independent values from the sorption data in the case of water in poly(methyl methacrylate). No details of the sorption values were given, however, in this report.

Combined Sorption and Permeation Data

A fourth method for estimating the integral diffusion constants is to divide the steady-state permeability constants by the equilibrium solubility coefficients obtained from the sorption isotherms. These values at 25°C. are also included in Figure 5 and show excellent agreement with the

sorption and desorption values and again extrapolate to the time lag value at zero concentration. The decreasing value of the diffusivity with concentration for water in ethyl cellulose has been reported previously by others[2,5] and has been ascribed to the clustering of the water molecules in the polymer. This suggestion was first made by Rouse[8] to account for similar results found with water in polyethylene (see Yasuda and Stannett[2] for a discussion of these experimental findings). In the case of ethyl cellulose, additional evidence was brought forward by Barrer and Barrie[5] to demonstrate the existence of clusters, including the development of opacity in the water saturated films.

It was considered[5,8] that water molecules present in the clusters would be essentially immobilized, due to the extra energy needed to break them away from a cluster, compared with isolated single molecules. However, since the chemical potential of the water must be similar if the clusters are in equilibrium with the free molecules, this does not seem to be a tenable explanation. The comparative immobility will arise, however, since the probability of an effective diffusion jump per molecule will be much less for a molecule contained in a cluster than in the case of an isolated water molecule.

The sorption, desorption, and permeability-sorption isotherm methods all involve the weight of the films as a function of time and at equilibrium at a given relative humidity. Thus, the concentration term includes also the clustered water; if only the isolated molecules contribute to the diffusion process, it is easy to see that the measured diffusivities will decrease as the relative humidity and degree of clustering increase. Consequently, following Barrer and Barrie,[5] the flux

$$Q = -D_T(\partial C_1/\partial x)$$

where D_T is the true diffusion constant and C the concentration of isolated molecules. This must be equal to $-D(\partial C/\partial x)$, where D is the measured (apparent) diffusion constant and C the total concentration of water. Hence,

$$D = D_T(\partial C_1/\partial C)$$

since this ratio decreases with increasing concentration D(measured) decreases with increasing concentration.

The case of the time lag is less clear since only the water which passes through the film is actually measured. The time lag, however, should also include the time taken for cluster formation.

Analysis of the problem of diffusion accompanied by immobilization in clusters is similar in many ways to diffusion with chemical reaction or with specific site adsorption or with partial diffusion into pores. Mathematical analyses of these problems have been made by Crank,[9,10] Michaels et al.[11] Standing et al.,[12] among others.

Considering the simplest case when the isotherms of the single molecule sorption and the clustered sorption may be approximated by linear rela-

tionships, then C_1 (single species) $= Sp$, and C_n (clustered species) $= Ap$, where S and A are the corresponding solubility coefficients. Then the total concentration of sorbed water is given by

$$C = C_1 + C_n = (1 + A/S)C_1$$

If this substitution is made into the derivation of the time lag equations of Daynes[13] and Barrer,[4] the following is obtained:

$$Q = (D_T C_1/l)[t - (1 + A/S)l^2/6D_T]$$

where Q is the flux and l the film thickness. When $Q = 0$, then $t = \tau$ the time lag and:

$$D_T = (1 + A/S)l^2/6\tau$$

whereas the measured diffusion constant is $D = l^2/6\tau$ and $D = [1/(1 + A/S)]D_T$, i.e., is smaller than the true diffusion constant. It is known from the shape of the sorption isotherms (see Fig. 3) that there is a more complex relationship than linear between the concentration and pressure and, in fact, the relationship is close to an exponential. Any more complex relationship, however, leads to nonlinear differential equations which cannot be solved analytically. It is clear, however, from the shape of the isotherms that the degree of clustering will increase with concentration over and above the linear increase already discussed. The measured diffusion constants will therefore be smaller as the concentration increases, as was found with the methods involving sorption and desorption.

In fact, however, as can be seen from the data presented in Figure 5, the time lag diffusivities are quite constant, at least up to 85% R.H. Furthermore, the values obtained by the other methods extrapolate back to the time lag value at zero concentration. One is forced to the inescapable conclusion, therefore, that, under the condition of the time lag experiments clusters are not formed. This could be due, for example, to a slow nucleation process for cluster formation leading to a pseudo-steady state. It would be gratifying to be able to demonstrate the lack of clustering under permeation condition by an independent method, but so far no suitable experiment has been devised.

References

1. Myers, A. W., J. A. Meyer, C. E. Rogers, V. Stannett, and M. Szwarc, *Tappi*, **44**, 58 (1961).
2. Yasuda, H., and V. Stannett, *J. Polymer Sci.*, **57**, 907 (1962).
3. Stannett, V., and J. L. Williams, *J. Polymer Sci.*, in press.
4. Barrer, R. M., *Trans. Faraday Soc.*, **35**, 628, 644 (1939).
5. Barrer, R. M., and J. A. Barrie, *J. Polymer Sci.*, **28**, 377 (1958).
6. Armstrong, A. A., and V. Stannett, *Makromol. Chem.*, in press.
7. Bueche, F., *J. Polymer Sci.*, **14**, 414 (1954).
8. Rouse, P. E., *J. Am. Chem. Soc.*, **69**, 1068 (1947).

9. Crank, J., *The Mathematics of Diffusion*, Oxford Univ. Press, 1956, Chap. 8.

10. Crank, J., *Trans. Faraday Soc.*, **53**, 1083 (1957).

11. Michaels, A. S., W. R. Vieth, and J. A. Barrie, *J. Appl. Phys.*, **34**, 13 (1963).

12. Standing, H. A., J. O. Warwicker, and H. F. Willis, *J. Textile Inst.*, **38**, T335 (1947).

13. Daynes, H. A., *Proc. Roy. Soc. (London)*, **A97**, 286 (1920).

Résumé

La perméabilité de l'éthyl-cellulose vis-à-vis de la vapeur d'eau et de l'eau liquide a été mesurée en fonction de la température. Il y a un changement de la pente des droites d'arrhénius à environ 50°C, à proximité de la température de transition vitreuse. Les isothermes d'absorption montraient principalement une chaleur de mélange nulle, ce qui correspond aux résultats des autres auteurs. Les constantes de diffusion ont été mesurées par quatre méthodes: l'absorption, la désorption, le retard "time lag" et par la division des constantes de perméabilité par les coefficients de solubilité à l'équilibre. La méthode au retard "time lag" donne des constantes de diffusion indépendantes de la concentration, les autres méthodes au contraire donnent des constantes de diffusion qui diminuent graduellement avec la concentration. Cependant les extrapolations de toutes les méthodes à la concentration zéro, donnent les mêmes valeurs. On croit que les diffusion décroissantes sont dues à l'agglomération des molécules d'eau dans le polymère. Cependant, il semblait qu'il n'y ait pas d'agglomération lors des mesures de retard.

Zusammenfassung

Die Permeabilität von Athylzellulose für Wasserdampf und flüssiges Wasser wurde in Abhängigkeit von der Temperatur gemessen. Bei etwa 50°C in der Nähe der Glasumwandlung wurde im Arrheniusdiagramm eine Änderung der Neigung festgestellt. Die Sorptionsisothermen zeigten in Übereinstimmung mit den Befunden anderer Autoren im wesentlichen eine Mischungswärme null. Die Diffusionskonstanten wurden nach vier verschiedenen Methoden bestimmt, nämlich aus der Sorption, der Desorption, der Derchbruchszeit und aus dem Verhältnis zwischen der Permeabilitätskonstanten und den Gleichgewichtsloslichkeitskoeffizienten. Die Durch bruchszeitmethode lieferte von der Konzentration unabhängige Diffusionskonstanten, während die anderen drei Methoden zu stetig mit der Konzentration abnehmenden Diffusionskonstanten führten. Nach allen Methoden wurde jedoch durch Extrapolation auf die Konzentration null etwa der gleiche Wert erhalten. Die abnehmende Diffusionsfähigkeit wird auf Clusterbildung der Wassermoleküle im Polymeren zurückgeführt. Unter den Bedingungen der Durchbruchszeitmessungen schien jedoch keine Clusterbildung aufzutreten.

Promotion of Base-Catalyzed Siloxane Rearrangements by Dimethyl Sulfoxide

GLENN D. COOPER, *Department of Chemistry, New Mexico State University, University Park, New Mexico,* and JOHN R. ELLIOTT, *General Electric Research Laboratory, Schenectady, New York*

Synopsis

The effect of small amounts (0.01%–1%) of dimethyl sulfoxide on base-catalyzed polymerization and equilibration of methylsiloxanes has been examined. The addition of 0.5% of the sulfoxide increases the rate of potassium hydroxide-catalyzed polymerization of octamethylcyclotetrasiloxane by factors of 100–1000 and amounts as low as 0.01% have a large effect when low (12 ppm) catalyst concentrations are used. The rate of base-catalyzed equilibration of hexamethyl disiloxane with octamethylcyclotetrasiloxane is similarly enhanced by dimethyl sulfoxide. The equilibration occurs rapidly at 80°C. with 0.01% of potassium hydroxide and 1% of dimethyl sulfoxide, but does not proceed at a measurable rate with potassium hydroxide alone. The combination of 0.01% potassium hydroxide and 1% dimethyl sulfoxide is more effective than 0.1% of tetramethylammonium hydroxide. The large accelerating effect of the sulfoxide is believed to be due to solvation of the cation, which promotes ionization of the metal silanolate, increasing the concentration of silanolate anions.

The use of dimethyl sulfoxide as a solvent for base-catalyzed organic reactions has been described in a number of papers.[1–4] The rates of many of these reactions are thereby greatly enhanced; for example, Cram[1] found that the methoxide ion-catalyzed racemization of 2-methyl-3-phenylpropionitrile is faster by a factor of approximately 10^9 in dimethyl sulfoxide than in methanol. Even simple aliphatic olefins undergo base-catalyzed isomerization under moderate conditions in dimethyl sulfoxide.[3]

In the cases previously reported the sulfoxide was used as solvent, or as a major component of a mixed solvent. The magnitude of the rate effects suggests, however, that in suitable cases dimethyl sulfoxide could be an effective promoter for base-catalyzed reactions even at low concentrations. The present study deals with the influence of small amounts (0.1–1%) of dimethyl sulfoxide on the rate of some polymerizations and rearrangements of methylsiloxanes. The abbreviations M and D are used throughout this paper to represent $(CH_3)_3SiO_{1/2}$ and $(CH_3)_2SiO$ units, respectively.[5]

POLYMERIZATION OF OCTAMETHYLCYCLOTETRASILOXANE

Many cyclic siloxanes form linear polysiloxanes under the influence of acidic or basic catalysts. The reaction which has been most thoroughly

studied is the conversion of octamethylcyclotetrasiloxane (D₄) to a high molecular weight linear dimethylsilicone polymer upon heating with alkali metal hydroxide or other basic catalysts. Because of this extensive background,[6-14] the polymerization of octamethylcyclotetrasiloxane by potassium hydroxide was the first reaction selected for testing the promoting ability of dimethyl sulfoxide. The reaction may be represented as

$$x/_4[(CH_3)_2SiO]_4 \rightarrow [(CH_3)_2SiO]_x \tag{1}$$
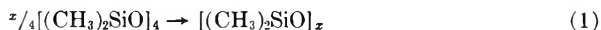
where the linear polysiloxane is terminated by silanol or silanolate end-groups. It has been reported that this reaction is accelerated by the use of polar diluents such as nitrobenzene,[9-11] tetrahydrofuran,[12,13] o-dichlorobenzene,[11,14] or acetonitrile,[15] but previous work involved the use of relatively high concentrations of the polar compounds.

Experimental

Materials. Octamethylcyclotetrasiloxane (D₄) was prepared by fractional distillation of the hydrolysis product of dimethyldichlorosilane and redistillation over calcium hydride.[6] No impurities were detected on gas chromatographic analysis. Potassium hydroxide was employed in the form of a 1% suspension in D₄. Dimethyl sulfoxide was purified by fractional distillation at reduced pressure, dried over Linde Molecular Sieve 5A, and redistilled.

Polymerization. Polymerizations were carried out in a 100-ml. round-bottomed flask equipped with a mechanical stirrer and immersed in a constant-temperature bath. A 50-ml. portion of D₄ was introduced and stirred vigorously while a slow stream (10 cc./min.) of dry nitrogen was directed over the surface of the liquid. The catalyst suspension was added under nitrogen from a hypodermic syringe, followed immediately by the dimethyl sulfoxide. Observations were made of the time at which the first visible increase in viscosity of the mixture occurred and of the time required for formation of a gum which was so stiff that the mechanical stirrer was stopped. In some cases iodine was added at this point to stop polymerization.[8] The polymer was then dissolved in benzene, stirred with silver powder, filtered through a bed of Celite, and the solvent removed under vacuum. Intrinsic viscosities were measured in toluene, and the number-average molecular weight was calculated from the Barry relationship:[16]

$$[\eta] = 2 \times 10^{-4} M_n^{0.66}$$

Results

The type of observations made permit only an approximate estimate of the magnitude of the rate enhancement, but the effect of the sulfoxide is so great that no more refined method is necessary to establish the remarkable promoting ability of small amounts of dimethyl sulfoxide on this reaction. For example, in the first experiment attempted, D₄ was heated at 131°C.,

and enough of the potassium hydroxide suspension was added to make the concentration 0.01% by weight. Dimethyl sulfoxide (1%) was then added from a pipet; before addition was complete, a matter of only a few seconds, a thick gum was produced. In the absence of the promoter no increase in viscosity was noted until after 40 min., and 110 min. was required to produce a gum comparable in viscosity to that obtained in less than 1 min. with the sulfoxide present.

Addition of dimethyl sulfoxide causes polymerization to proceed at a reasonable rate even at room temperature. A stiff gum was produced in 5 hr. when D_4 was stirred at 25°C. with 0.01% potassium hydroxide and 1% dimethyl sulfoxide. In the absence of the promoter no polymerization was detected after 5 days.

TABLE I

Effect of Dimethyl Sulfoxide on Bulk Polymerization
of Octamethylcyclotetrasiloxane at 95 ± 1 °C.

| Expt. no. | KOH, ppm | Sulfoxide, wt.-% | Time, min. | |
			Visible increase in viscosity	Stiff gum[a]
1	100	1.4	0[b]	3
2	100	0.5	3	7
3	100	0.1	25	90
4	100	0	300	1100
5	25	0.5	6	11
6	12	0.5	10	16
7	12	0.01	—	1080
8	12	0	No reaction (36 hr.)	—
9	0	0.5	No reaction (24 hr.)	—

[a] Time to produce gum stiff enough to stop stirrer.
[b] Viscosity increase noted during addition of sulfoxide.

Most of the experiments were carried out at 95°C. at varying concentrations of catalyst and promoter, with the results given in Table I. A rough estimate of the degree of polymerization at which the viscosity of the gum became high enough to stop the mechanical stirrer was obtained from three experiments in which the reaction was decatalyzed with iodine at this point. The number-average molecular weight of the polymer ranged from 4×10^5 to 1.1×10^6.

The acceleration due to the sulfoxide is apparent. Comparison of experiments 2 and 4 indicates that 0.5% of dimethyl sulfoxide enhances the rate of polymerization by a factor of more than 100. The same conclusion is reached from a comparison of experiments 6 and 8; in these experiments, run at a lower catalyst concentration (12 ppm KOH), addition of 0.5% of the sulfoxide increased the rate by a factor of at least 1000. As little as 0.01% of the promoter has a significant effect, as can be seen from experiments 7 and 8: no evidence of polymerization in 36 hr. with 12 ppm of

potassium hydroxide alone, as compared to high polymer in 18 hr. with 0.01% dimethyl sulfoxide added.

EQUILIBRATION OF SILOXANES

The potassium hydroxide-catalyzed polymerization of octamethylcyclo-tetrasiloxane involves reaction of a potassium silanolate with D units. Reactions of silanolates with M units are much slower than with D units but are mechanistically similar and might therefore be expected to be promoted by dimethyl sulfoxide. To study this effect the equilibration of hexamethyldisiloxane (M_2) with D_4 was investigated.

Experimental

Materials. Hexamethyldisiloxane was prepared by hydrolysis of trimethylchlorosilane and purified as described above for octamethylcyclo-tetrasiloxane. Potassium hydroxide was again used in the form of a one percent solution in octamethylcyclotetrasiloxane. Potassium trimethylsilanolate was prepared by refluxing 500 ml. of hexamethyldisiloxane for 16 hr. with 50 g. of potassium hydroxide pellets. The hot solution was decanted from the undissolved potassium hydroxide and allowed to cool to room temperature. The precipitate of potassium trimethylsilanolate (monohydrate)[17] was filtered off, washed with n-hexane, and dried at room temperature and 20 mm. pressure. The neutral equivalent of the dry crystals was 149; calcd. for $(CH_3)_3SiOK(H_2O)$: N. E. = 146.

Equilibration. Equilibrations were carried out in 500 ml. three-necked flasks equipped with a mercury-sealed mechanical stirrer and immersed in a constant-temperature bath at $80 \pm 0.5°C$. After the flasks had been thoroughly swept with dry nitrogen, 250 ml. of the siloxane mixture was added and stirred for 1 hr. to allow time to reach bath temperature. The catalyst was then added, followed by the dimethyl sulfoxide when used (each experiment was carried out in parallel, with and without the promoter). At appropriate intervals 25 ml. samples were withdrawn, shaken with $3M$ hydrochloric acid, washed thoroughly with water, and dried over anhydrous sodium carbonate. Progress of the equilibration was followed by measurement of the bulk viscosity at $25°C$.[13]

Course of the Reaction

The mechanism of the base-catalyzed equilibration of D_4 and M_2 has been investigated by Kantor et al.[18] Because of the greater reactivity of D units, the D_4 reacts preferentially in the early stages. When an equimolar mixture of D_4 and M_2 is used, as in the present work, the viscosity of the solution rises rapidly to a maximum due to the formation of relatively long linear molecules of the type MD_xM. At this point, the solution is composed largely of high molecular weight polymer and unreacted M_2, with relatively small amounts of material of intermediate molecular weight. The viscosity

thereafter decreases as M_2 is incorporated by a series of reactions which may be written:

$$MD_xM + M_2 \rightarrow MD_{x-1}M + MDM \qquad (2)$$

$$MD_xM + MDM \rightarrow MD_{x-3}M + MD_4M, \text{ etc.} \qquad (3)$$
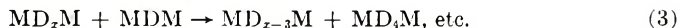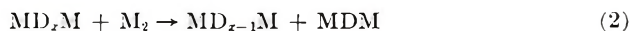
until equilibrium is reached. The composition of the equilibrium mixture may be calculated from the equations given by Scott;[19] it consists of a mixture of M_2 with relatively small molecules of the MD_xM type, along with a small amount of cyclics (D_3, D_4, etc.).

Results

When an equimolar mixture of D_4 and M_2 was heated at 80°C. with 0.01% of potassium hydroxide and 1% of dimethyl sulfoxide the system showed the same behavior as was previously observed with 0.1% of tetramethylammonium hydroxide as the catalyst,[18] i.e., a rapid increase in viscosity followed by a gradual decline to the equilibrium value. The viscosity–time curves are shown in Figure 1; results obtained by Kantor et al.[18] with the use of 0.1% tetramethylammonium hydroxide are included for comparison. The combination of 0.01% potassium hydroxide and 1%
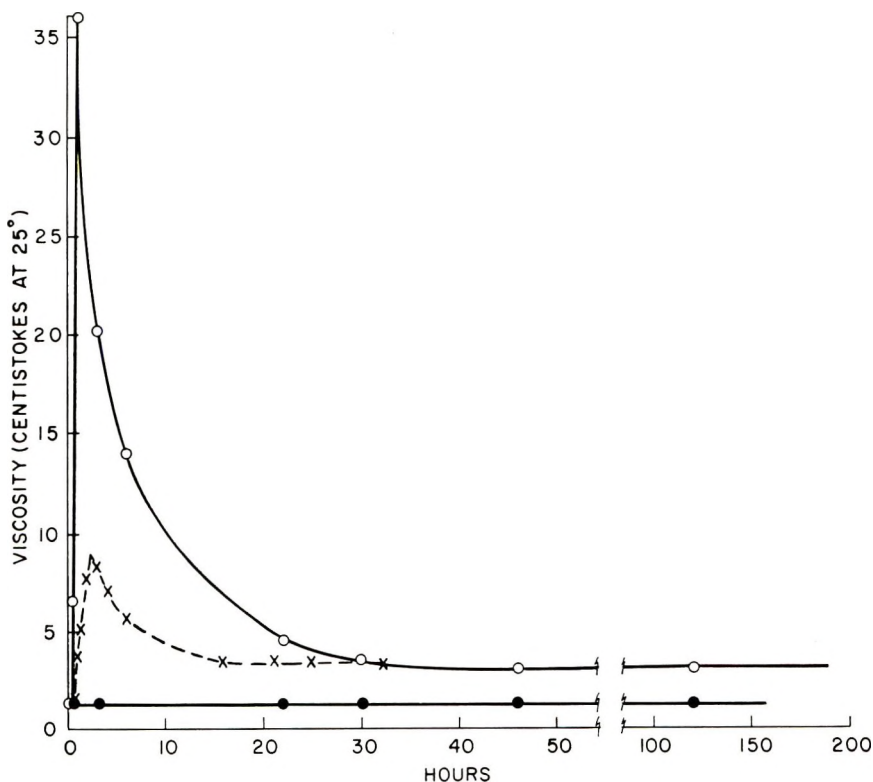
Fig. 1. Equilibration of 1:1 M_2 and D_4 at 80°C.: (●) 0.01% KOH; (O) 0.01% KOH + 1% dimethyl sulfoxide; (×) 0.1% tetramethylammonium hydroxide.[18]
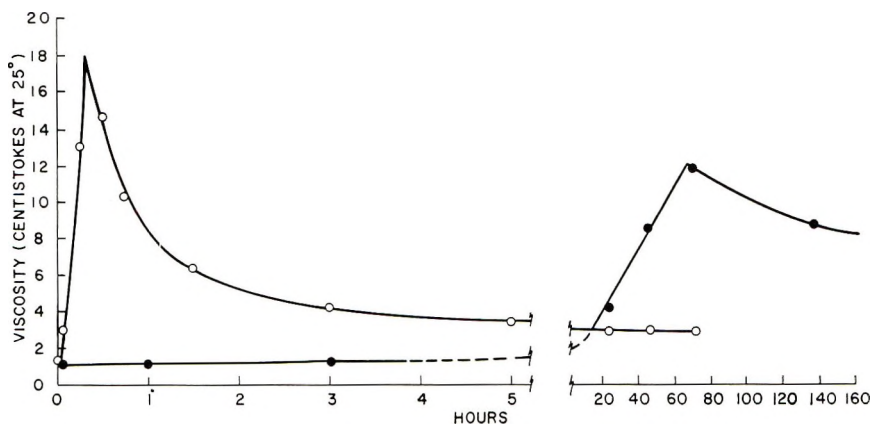
Fig. 2. Equilibration of 1:1 M_2 and D_4 at 80°C.: (●) 0.2% potassium trimethylsilano-
late; (O) 0.2% potassium trimethylsilanolate + 1% dimethyl sulfoxide.

dimethyl sulfoxide is more effective than 0.1% tetramethylammonium hy-
droxide, which is one of the more active basic siloxane rearrangement
catalysts known.[20]   The maximum viscosity was much higher and was
reached in a shorter time, and the time required for attainment of the
equilibrium viscosity was slightly less than with 0.1% tetramethylam-
monium hydroxide.   The promoting effect of the sulfoxide is clearly shown
by the parallel experiment in which 0.01% of potassium hydroxide was
used alone; there was no detectable change in viscosity in 120 hr.

Equilibration with Potassium Trimethylsilanolate.   The failure of potas-
sium hydroxide alone to bring about equilibration at 80°C. is partially due
to the fact that potassium hydroxide dissolves only very slowly in the sil-
oxane at this temperature.   To eliminate this factor further experiments
were carried out with potassium trimethylsilanolate, which dissolves al-
most instantaneously, as the catalyst.   The results of two experiments
with 0.2% potassium trimethylsilanolate, with and without dimethyl sul-
foxide, are shown in Figure 2.   With no sulfoxide added, reaction is very
slow.   A period of 70 hr. was required to reach the maximum viscosity of
about 12 cstokes and the decline was even slower; after 170 hr. the viscosity
had fallen only to 8.7 cstokes; the equilibrium value is 2.95 cstokes.   In
the presence of 1% dimethyl sulfoxide the maximum viscosity was reached
within 20 min. and the equilibrium viscosity in less than 24 hr.

A further illustration of the promoting effect of the sulfoxide is shown in
Figure 3.   For this experiment a 7:1 molar ratio of D_4 and M_2 was first
equilibrated with the use of sulfuric acid as catalyst.   Enough M_2 was added
to the resulting oil, which consists of a mixture of M_2 and short MD_xM
molecules, along with small amounts of cyclics, to give the same 2:1 ratio
of D to M units as in the previous experiments.   This is essentially equiv-
alent to starting with a partially equilibrated mixture of M_2 and D_4 at
some point after the viscosity maximum is passed.   Upon heating at 80°C.
with 0.2% potassium trimethylsilanolate and 1% dimethyl sulfoxide the
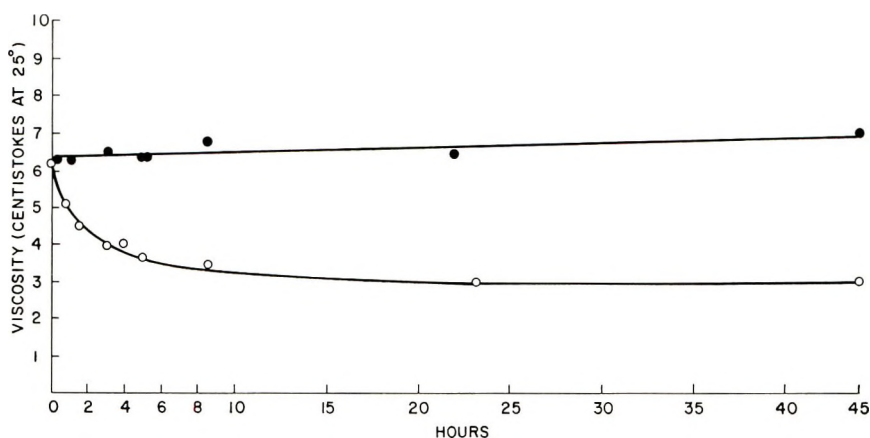
Fig. 3. Equilibration of M_2 with MD_xM: (●) 0.2% potassium trimethylsilanolate; (○) 0.2% potassium trimethylsilanolate + 1% dimethyl sulfoxide.

viscosity of the oil decreased until the equilibrium value was reached in about 24 hr. Without the sulfoxide no detectable reaction occurred; the very slight upward trend in viscosity is due to the loss of a small amount of the more volatile material during the sampling process.

DISCUSSION

Base-catalyzed equilibrations and polymerizations of siloxanes proceed through the formation of metal silanolates, followed by a series of displacement reactions:

$$\equiv SiOK + \equiv \overset{*}{Si}O\overset{**}{Si}\equiv \rightarrow \equiv SiO\overset{*}{Si}\equiv + KO\overset{**}{Si}\equiv \qquad (4)$$

From the observed half-order dependence of the rate of polymerization of D_4 on potassium hydroxide concentration, Grubb and Osthoff[6] concluded that the active species in the polymerization is the free silanolate ion which is present in very small concentration from the dissociation of the potassium silanolate:

$$\equiv SiOK \rightleftarrows \equiv SiO^{-} + K^{+} \qquad (5)$$

The half-order dependence on catalyst concentration was confirmed by Morton[11-13] and by Kucera.[9,10,14] The increased rate of polymerization of D_4 in solvents of high dielectric constant, such as nitrobenzene, was attributed by Morton[11] to an increase in the degree of ionization of the potassium silanolate in the more polar medium, thus increasing the concentration of the silanolate ion, which is the active species. Kucera[14] proposed a somewhat different mechanism, not involving free potassium or silanolate ions, and attributed the increased rate to an increase in the ionic character of the SiO—K bond, with a resulting increase in reactivity.

The effect of the sulfoxide can be explained on either basis, but the simpler explanation is given in terms of the Grubb mechanism. In this view

the function of the sulfoxide is to displace equilibrium (5) to the right, increasing the concentration of free silanolate ions, which is the active species. Such ionization would be favored by an increase in the polarity of the medium, but the amount of sulfoxide used in the present work is not enough to change the dielectric constant appreciably,* so that increased ionization of the metal silanolate must be due to specific solvation effects and particularly to solvation of the cation by the negatively charged oxygen atom of the sulfoxide:

$$K^{+}\text{- - -}\overset{-}{O}\text{—}\overset{+}{S}\begin{smallmatrix}\nearrow CH_3 \\ | \\ \searrow CH_3\end{smallmatrix}$$
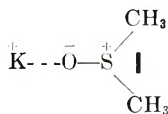
Prue and Sherrington[24] demonstrated by transport measurements of solutions of metal salts in dimethyl sulfoxide that the cations were very strongly solvated, but that there was little solvation of the anions. In a medium composed almost exclusively of siloxane units, as in the present work, it seems likely that any solvation of the silanolate ion would be by the positive end of the abundant silicon–oxygen dipoles, rather than by the sulfur atom of the sulfoxide.

$$Si\text{—}\overset{\delta_-}{O}\text{- - -}\overset{\delta_+}{Si}\text{—}\overset{\delta_-}{O}\text{—}Si$$
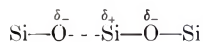
This presents the ideal situation for the displacement reaction which is the basis of siloxane equilibrations. Such specific solvation is presumably responsible for the large increase in the rate of D_4 polymerization in tetrahydrofuran, which has a relatively low dielectric constant.[13]

References

1. Cram, D. J., B. Rickborn, C. A. Kingsbury, and P. Haberfield, *J. Am. Chem. Soc.*, **83**, 3678 (1961) and references cited therein.

2. Price, C. C., and W. H. Snyder, *J. Am. Chem. Soc.*, **82**, 6000 (1960).

3. Schriesheim, A., and C. A. Rowe, Jr., *J. Am. Chem. Soc.*, **84**, 3160 (1962).

4. Russell, G. A., E. G. Janzen, H.-D. Becker, and F. J. Smentowski, *J. Am. Chem. Soc.*, **84**, 2652 (1962).

5. Rochow, E. G., *Chemistry of the Silicones*, 2nd Ed., Wiley, New York, 1951, p. 79.

6. Grubb, W. T., and R. C. Osthoff, *J. Am. Chem. Soc.*, **77**, 1405 (1955).

7. Hurd, D. T., R. C. Osthoff, and M. L. Corrin, *J. Am. Chem. Soc.*, **76**, 249 (1954).

8. Osthoff, R. C., A. M. Bueche, and W. T. Grubb, *J. Am. Chem. Soc.*, **76**, 4659 (1954).

9. Kucera, M., and M. Jelinek, *Collection Czechoslov. Chem. Communs.*, **25**, 536 (1960).

10. Kucera, M., *Collection Czechoslov. Chem. Communs.*, **25**, 547 (1960).

* The dielectric constant may be estimated roughly from the equation

$$\frac{\epsilon_m - 1}{\epsilon_m + 2} = X_1 \frac{\epsilon_1 - 1}{\epsilon_1 + 2} + X_2 \frac{\epsilon_2 - 1}{\epsilon_2 - 2}$$

in which ϵ_1, ϵ_m, and ϵ_2 are the dielectric constants of the mixture and the two pure compounds, and X_1 and X_2 are volume fractions of the two compounds in the mixture.[21] Application of this relationship to octamethylcyclotetrasiloxane ($\epsilon = 2.39$)[22] and dimethyl sulfoxide ($\epsilon = 49$)[23] gives $\epsilon = 2.41$ for 0.5% dimethyl sulfoxide in D_4.

11. Morton, M., M. A. Deisz, and E. E. Bostick, *J. Polymer Sci. A*, **2**, 513 (1964).

12. Morton, M., A. Rembaum, and E. E. Bostick, *J. Polymer Sci.*, **32**, 350 (1958).

13. Morton, M., and E. E. Bostick, *J. Polymer Sci. A*, **2**, 523 (1964).

14. Kucera, M., *Khim. Prakt. Primenenie Kremneorg. Soedinii Trudy Konf., Leningrad*, **1958**, No. 2, 71; *Chem. Abstr.*, **55**, 24078 (1961).

15. Hyde, J. F., U. S. Pat. 2,490,537 (1949).

16. Barry, A. J., *J. Appl. Phys.*, **17**, 1020 (1946).

17. Hyde, J. F., O. K. Johannson, W. H. Daudt, R. F. Fleming, H. B. Laudenslager, and M. P. Roche, *J. Am. Chem. Soc.*, **75**, 5615 (1963).

18. Kantor, S. W., W. T. Grubb, and R. C. Osthoff, *J. Am. Chem. Soc.*, **76**, 5190 (1954).

19. Scott, D. W., *J. Am. Chem. Soc.*, **68**, 2294 (1946).

20. Gilbert, A. R., and S. W. Kantor, *J. Polymer Sci.*, **40**, 35 (1959).

21. Boettcher, C. J. F., *Dielectric Polarization*, Elsevier, New York, 1952, p. 415.

22. Sauer, R. O., and D. J. Mead, *J. Am. Chem. Soc.*, **68**, 1794 (1946).

23. Schlefer, H. L., and W. Schaffernicht, *Angew. Chem.*, **72**, 618 (1960).

24. Prue, J. E., and P. J. Sherrington, *Trans. Faraday Soc.*, **57**, 1795 (1961).

Résumé

L'effet des faibles quantités (0.01 à 1%) de diméthylsulfoxyde sur la polymérisation catalysée par les bases des méthyl-siloxanes de même que sur l'équilibration de cette polymérisation a été examiné. L'addition de 0.5% de sulfoxyde accroît la vitesse de la polymérisation catalysée par l'hydroxyde de potassium de l'octaméthylcyclotétrasiloxane par un facteur de 100 à 1000 et des quantités aussi faibles que 0.01% ont un effet considérable lorsque la concentration en catalyseurs utilisée est faible (12 p.p.m.). La vitesse d'équilibration catalysée par des bases de l'hexaméthyldisiloxane avec l'octaméthyltétrasiloxane est de même favorisée par le diméthylsulfoxyde. On atteint un équilibre rapidement à 80° avec 0.01% d'hydroxyde de potassium et 1% de diméthylsulfoxyde, mais on ne l'atteint pas avec une vitesse mesurable avec l'hydroxyde de potassium seul. La combinaison de 0.01% d'hydroxyde de potassium avec 10% de dimethylsulfoxyde est beaucoup plus effective que 0.1% d'hydroxyde de tétraméthylammonium. L'effet accélérateur important du sulfoxyde est attribué à la solvatation du cation, qui favorise l'ionisation du silanolate du métal accroissant ainsi la concentration des anions silanolates.

Zusammenfassung

Der Einfluss kleiner Mengen (0,01–1%) von Dimethylsulfoxyd auf die basenkatalsysierte Polymerisation und die Gleichgewichtseinstellung von Methylsiloxanen wurde untersucht. Der Zusatz von 0,5% des Sulfoxyds erhöht die Geschwindigkeit der kaliumhydroxydkatalysierten Polymerisation von Oktamethylcyclotetrasiloxan um Faktoren von 100–1000 und so geringe Mengen wie 0,001% besitzen bei Anwendung niederer (12 ppM) Katalysatorkonzentrationen einen grossen Effekt. Die Beschwindigkeit der basenkatalysierten Gleichgewichtseinstellung von Hexamethyldisiloxan mit Octamethylcyclotetrasiloxan wird durch Dimethylsulfoxyd in ähnlicher Weise beschleunigt. Die Gleichgewichtseinstellung erfolgt bei 80°C mit 0,01% Kaliumhydroxyd und 1% Dimethylsulfoxyd rasch, verläuft jedoch mit Kaliumhydroxyd allein mit nicht messbarer Geschwindigkeit. Die Kombination von 0,01% Kaliumhydroxyd und 1% Dimethylsulfoxyd ist besser wirksam als 0,1% Tetramethylammoniumhydroxid. Der grosse beschleunigende Einfluss des Sulfoxyds wird auf die Solvatation des Kations zurückgeführt, welche die Ionisierung des Metallisilanolates und damit die Konzentration an Silanolatanionen erhöht.

γ-Irradiation of Poly(ethylene Terephthalate).
I.   Yields of Gas and Carboxyl Groups*

S. D. BUROW and D. T. TURNER, *Camille Dreyfus Laboratory, Research Triangle Institute, Durham, North Carolina*, and GEORGE F. PEZDIRTZ and GEORGE D. SANDS, *Applied Materials and Physics Division, Langley Research Center, National Aeronautics and Space Administration, Hampton, Virginia*

Synopsis

Poly(ethylene terephthalate) was exposed *in vacuo* γ-radiation from a Co^{60} source at a dose rate of 0.02 Mrad/min., and an ambient temperature of 47°C. Gaseous products were analyzed in a mass spectrometer and carboxyl groups estimated by titration with NaOH and by infrared analysis. Initial G values were —COOH = 0.77, CO_2 = 0.17, CO = 0.11, H_2 = 0.015, and CH_4 = 0.003. All these values decreased markedly with increasing dose except $G(CO)_2$, which, roughly, was maintained up to 5000 Mrad. It was considered whether the dependence on dose of the yields of the major reaction products could be accounted for by the following set of first-order reactions:
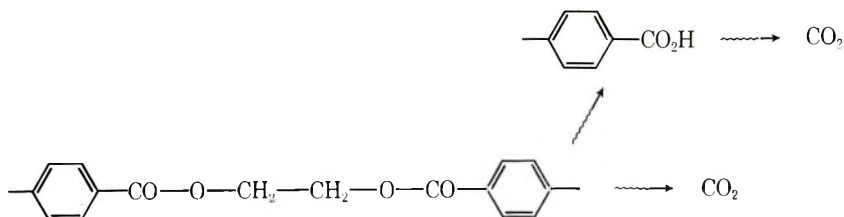
It was found that the rate of formation of —COOH groups at low doses was much too high to fit this simple reaction scheme. However, a better fit was obtained over a range of higher doses (ca. 100–5000 Mrad). A final conclusion could not be reached concerning the validity of the above reaction scheme.

INTRODUCTION

Previously poly(ethylene terephthalate) (PET) has been exposed to a variety of high energy radiations and various physical and chemical changes studied. References to the earliest work may be located in the books by Charlesby[1] and Chapiro.[2] Because the polymer is relatively resistant to radiation damage more recent work has concentrated on the high doses which can be administered conveniently with electrons at high dose rates of the order 1–10 Mrad/min. Under such conditions network formation is

---

* Paper presented at the 148th Meeting, American Chemical Society, Chicago, September 1964.

reported to occur[3-5] and has been studied along with other changes such as gas evolution[3] and infrared absorption.[3,4] Most pertinent for present purposes is the work of Sobue and Kajiura[6] on γ-irradiation of PET at a dose rate of 0.006 Mrad/min. As part of a more extensive study it was found that, on irradiation *in vacuo* in ampules, the polymer evolved various gases which were analyzed quantitatively. The polymer did not form a network, and its concentration of terminal OH groups decreased. The purpose of the present paper is to give further experimental data on the products formed from the ester groups and to offer a first approach towards an evaluation of the dependence of product yield on dose.

EXPERIMENTAL

Materials

The poly(ethylene terephthalate) (PET) sample studied was biaxially oriented Mylar C film (du Pont) of thickness 0.0025 cm. This polymer contains several parts per thousand of inorganic materials added during the condensation polymerization as catalysts, moisture, and 0.5% cyclic oligomers (mostly trimer). The number-average molecular weight of the polymer molecules is ca. 15,000 and their distribution of sizes approximately random. The endgroups are largely —OH and —COOH. The polymer is about 50% crystalline as judged by x-ray diffraction data.

Benzoic acid was of analytical reagent grade. Reagents used to estimate —COOH groups in the polymer were of the grade recommended by Pohl.[7] Gases used to calibrate the mass spectrometer were >99% pure.

Techniques

Preparation and Irradiation of Samples. The polymer was dried at 50°C. at ca. 10^{-5} torr and then rolled up (0.2–1.0 g.) and degassed for a further 16 hours at room temperature before being sealed in glass breakseal tubes at 10^{-6} torr (i.d. $\sim$1 cm., volume $\sim$10 cm.). The tubes were exposed to γ-radiation from a Co^{60} source (Langley Research Center) at a dose rate of 0.02 Mrad/min. at an ambient temperature of 47°C. The tubes were opened 1 day to 2 months after irradiation.

Benzoic acid (1 g.) was degassed and sealed *in vacuo* at 10^{-6} torr and irradiated as above.

Gas Analysis. Fractions of gas successively volatile at −196, −80, and 25°C. were removed with a Toepler pump and measured in a gas buret. In selected cases these fractions were analyzed in a mass spectrometer.

Carboxyl Groups. Carboxyl groups were estimated by titration of solutions of PET, dissolved in benzyl alcohol at 200°C., at room temperature with NaOH, methyl red being used as indicator.[7] A modified technique was also used in which the polymer was dissolved in freshly distilled aniline at 120–140°C. and then titrated with NaOH, phenolphthalein being used as indicator.[8] Carboxyl groups were also estimated in the solid polymer, both

in the form of films and in KBr pellets, by infrared absorption with a Perkin-Elmer 237 spectrophotometer with diffraction grating optics.

RESULTS AND DISCUSSION

Gaseous Products

Results for successive fractions of gas volatile at -196 and $-80°C$., respectively, are shown in Table I (Sample 3). The total amount of gas from these fractions was 3.85 cc. at STP. After leaving the sample overnight at room temperature (ca. 25°C.) *in vacuo*, a further 0.16 cc. of gas was evolved. Heating the sample for 8 hr. at 80°C. yielded a further 0.01 cc. volatile at room temperature. The last two fractions were combined and gave mass spectra corresponding to a mixture of organic components. The highest molecular weight was 76 or slightly higher, and one or more components contained oxygen (high M/e 45 and 31 peaks). Most of this combined fraction comprised H_2O (high M/e 18) and probably CO_2 (high M/e 44, 28, and 22). The compositions of the -80 and $-196°C$. fractions are shown in Table I. The origin of water in this sample is not known: in subsequent experiments it was not detected.

The results in Table I indicate that the proportion of CO_2 increases slightly relative to other components with increasing dose. The trend becomes more obvious at higher doses, as shown in Figure 1. Table II

TABLE I
Composition of Gaseous Products

Sample number	Dose, Mrad	Total gas, cc. at STP	Volume %					
			CO_2	CO	H_2	CH_4	C_2H_6	H_2O
1	114	1.17	56.1	37.2	5.18	0.98	0.55	0
2	252	2.46	58.2	36.6	3.85	0.99	0.38	0
3	1050	3.85	62.3	32.8	4.21	0.64	0.0–	—
3 ($-196°C$.)	''	1.45	3.4	83.5	11.0	1.4	—	0.7
3 ($-80°C$.)	''	2.40	97.2	2.25	0.25	0.25	—	0.05
3 ($+25°C$.)	''	0.16						50

TABLE II
Apparent G (Gas Values)

Dose, Mrad	G values $\times 10^3$			
	CO_2	CO	H_2	CH_4
93[a]	88.5	125	20.5	6.6
893[a]	38.3	41	12.1	3.2
114	168	111	15.5	2.9
252	165	104	10.9	2.8
1050	131	69	8.8	1.3

[a] These are the extreme doses of Sobue and Kajiura.[6]
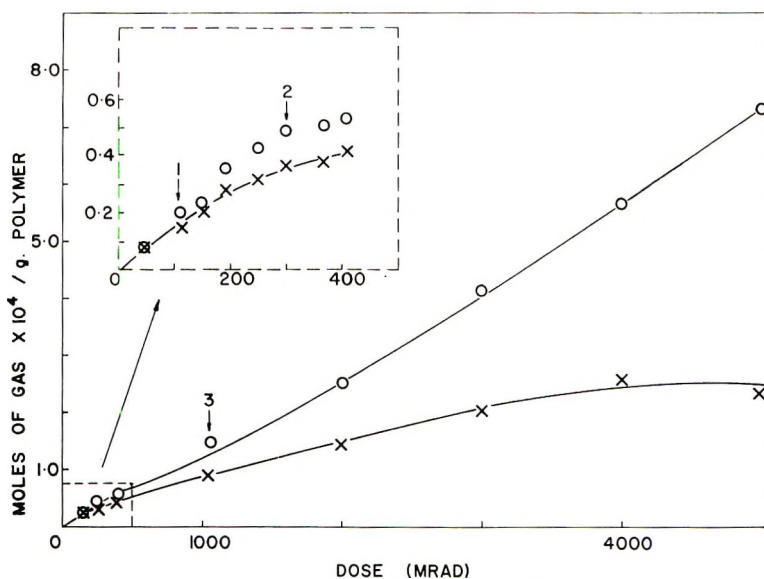
Fig. 1. Products volatile ($\times$) at $-196°C$. (mostly CO, H$_2$, and CH$_4$) and (O) at $-80°C$. (mostly CO$_2$).

shows G values for gaseous products calculated from analysis of mass spectra. Initial G values for CO and H$_2$ are in fair agreement with those reported by Sobue and Kajiura,[6] but those for CO$_2$ and CH$_4$ are somewhat different.

Benzoic Acid

Reference to the following G values reported for Co^{60} γ-irradiation of benzoic acid[9] suggests that some of the carboxyl groups formed in PET might contribute to CO$_2$ formation: $G(CO_2) = 0.286$, $G(CO) = 0.0025$, $G(H_2) = 0.0026$, and $G(polymer) = 0.303$. In order to check whether CO$_2$ is virtually the only gaseous product, a sample of benzoic acid was irradiated at a low dose to provide initial G values. The following results confirm the above conclusion: $G(-80°C. \text{ fraction} \equiv CO_2) = 0.33$, $G(-196°C. \text{ fraction} \equiv H_2 + CO) = 0.01$. The agreement with previous results is good, and the discrepancy concerning the gases volatile at $-196°C$. may be due to the small size of the sample analyzed.

Yields of Carboxyl Groups

Previously it has been mentioned that carboxyl groups are formed when PET is exposed *in vacuo* to radiation from an atomic pile, but the method of analysis was not specified nor were any quantitative data reported.[10]

In present work, Pohl's method[7] gave accurately reproducible values for the concentration of —COOH groups in the polymer, and the value of 0.33×10^{-4} mole/g. is in agreement with earlier results for the unirradiated polymer. The other titration method[8] gave consistently higher results even

TABLE III
Carboxyl Yields

| Dose, Mrad | Carboxyl yield, mole/g. $\times 10^4$ | |
	Method of Matreyeva[8] and Myaghov (including modifications)	Pohl's method[7]
0	0.93, 0.97, 0.58, 0.83, 0.94 0.80, 0.55, 0.93, 1.00	0.34, 0.32, 0.31, 0.33, 0.29
300	7.95	9.0
5030	11.8	11.8

when minor modifications of techniques were tried, such as working under N_2 to exclude CO_2 (Table III). The reason for these overestimates was not pursued further. On irradiation of the polymer there was a large increase in the concentration of —COOH groups, determined by Pohl's method, as shown in Table III, and, in further detail, in Figure 2. This result was confirmed by the other titration method, which apparently suffers from an error which becomes less important when estimating higher concentrations of —COOH. It seems surprising that such high concentrations of —COOH groups have not been detected in previous infrared studies of the irradiated polymer. In fact, in the appropriate region, the only significant change reported was a decrease in absorption which was attributed to the loss of —OH endgroups (—COOH absorbs at 3.05 μ and —OH at 2.82 μ).[6] These infrared data lead to the question of whether —COOH groups really are formed directly in the polymer, or whether its structure is changed in some unknown way with the result that such groups are formed subsequently during the dissolution step preceding titration. Evidence that —COOH
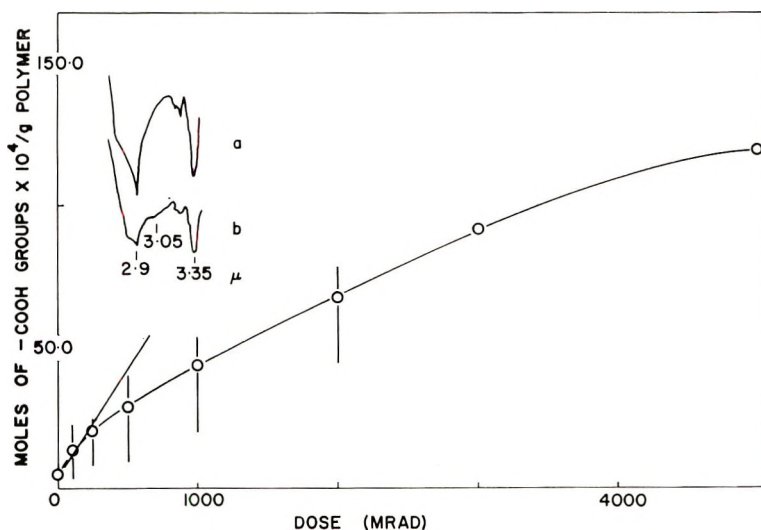

Fig. 2. Yields of —COOH groups (O) by Pohl's method and (1) by absorption at 3.05 μ inset: spectra of (a) unirradiated material; (b) 5000 Mrad.

groups are formed directly in the polymer was obtained in the present work from an increase in infrared absorption of the irradiated polymer in the region 2.95–3.13 μ. However, only a general increase in absorption appeared near 3.05 μ as compared with the broad, but well defined, peak found by Daniels and Kitson[11] with PET samples known to contain high concentrations of carboxyl endgroups. It is not clear whether the broader absorption in the irradiated polymer is characteristic of radiation damage or simply due to inadequate resolution relative to that achieved by Daniels and Kitson with LiF optics. The inset in Figure 2 shows spectra obtained after doses of 0 and 5000 Mrad, but such data were not suitable for quantitative analysis because of inadequate dispersion of the polymer in the KBr pellet. Yields of —COOH groups were estimated in the present work in films after doses up to 2000 Mrad. Results were calculated relative to the value of 0.33×10^{-4} mole/g. for the unirradiated polymer, and the wide limits shown by the vertical lines in Figure 2 are due to uncertainties in choice of a base line near 2.7 μ. The rolled films were too brittle to handle for analysis after doses higher than 2000 Mrad.

Dependence of Product Yields on Dose

The way in which the yield of a product depends on radiation dose may help towards an understanding of the reactions by which it is formed. For example, in many cases some biological property has been found to decrease exponentially with dose, and illuminating ideas developed from "target" theory.[12] As an example of a more clearly defined chemical reaction, the small concentration of double bonds in polyethylene has been found to have a similar dependence on dose and has been discussed by Dole[13] in terms of both "target" theory and of first-order kinetics. It would appear worthwhile to consider whether the present data on poly(ethylene terephthalate) conform simply to the assumption of first-order reactions.

The reactions of the ester group —CO—O—CH$_2$—CH$_2$—O—CO— may be diagnosed by reference to the reaction products —COOH, CO$_2$, and CO. However, information from the gaseous products may prove misleading because of the occurrence of gas phase reactions.[14] Such reactions are certainly expected for H$_2$ and CO and might be partly responsible for the pronounced decrease in the slope with increasing dose shown in Figure 1. In these circumstances, attention will be confined to production of the major reaction product —COOH, although consideration will also have to be given to the yield of CO$_2$. In this respect it is noted that CO$_2$ itself is rather unreactive on irradiation but may be formed by irradiation of CO. In the subsequent discussion this reaction will be assumed to be negligible.

It will be inquired whether the set of first-order reactions (1) could account for the observed dependence on dose of —COOH and CO$_2$. The initial concentration of repeat units (shown in brackets) is designated [U]$_0$ and the concentration after a dose R by [U]. The value of n is initially about 80. The initial endgroups are supposed to have similar reactivity to the repeat units and, therefore, on account of their low concentration, are
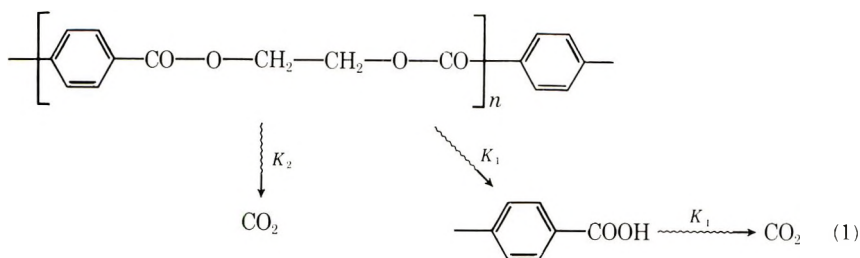
neglected. Equations (2)–(4) give, respectively, the concentration of unchanged repeat units, —COOH groups, and CO_2 (all expressed in moles/gram) after a dose R. Values for the specific rate constants K_1, K_1', and K_2

$$[U] = [U]_0 \, e^{-(K_1 + K_2)R} \tag{2}$$

$$[—COOH] = [U]_0 \frac{K_1}{K_1' - (K_1 + K_2)} \, [e^{-(K_1 + K_2)R} - e^{-K_1'R}] \tag{3}$$

$$[CO_2] = [U]_0$$

$$\times \left\{ 1 - e^{-(K_1 + K_2)R} - \frac{K_1}{K_1' - (K_1 + K_2)} \, [e^{-(K_1 + K_2)R} - e^{-K_1'R}] \right\} \tag{4}$$

$$K = G(\text{value})/100 C_0 N \tag{5}$$

were calculated from eq. (5), in which N is Avogadro's number and the G value is the number of specified molecules formed for a dose of 100 e.v. from
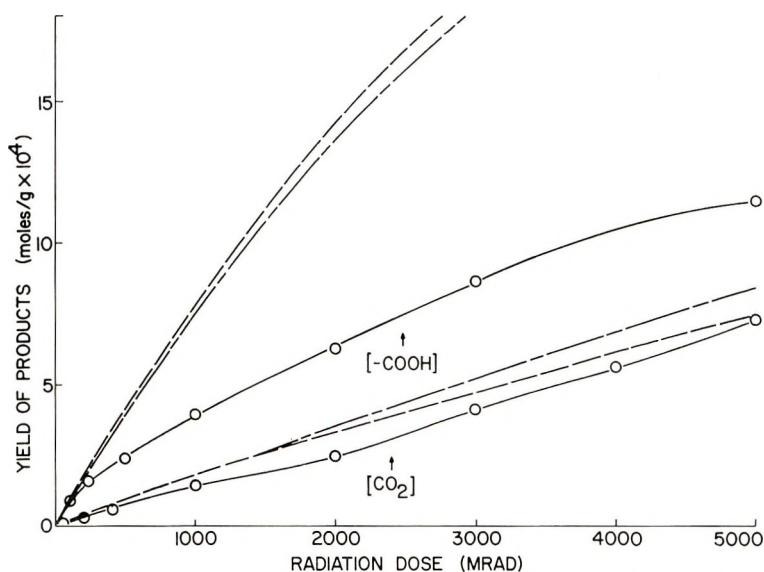
Fig. 3. Comparison of calculated and experimental dependence of product yields on dose: (——) experimental values for O, —COOH, and CO_2; (- -) calculated values (includes allowance for reaction —$C_6H_4COOH \rightarrow CO_2$).
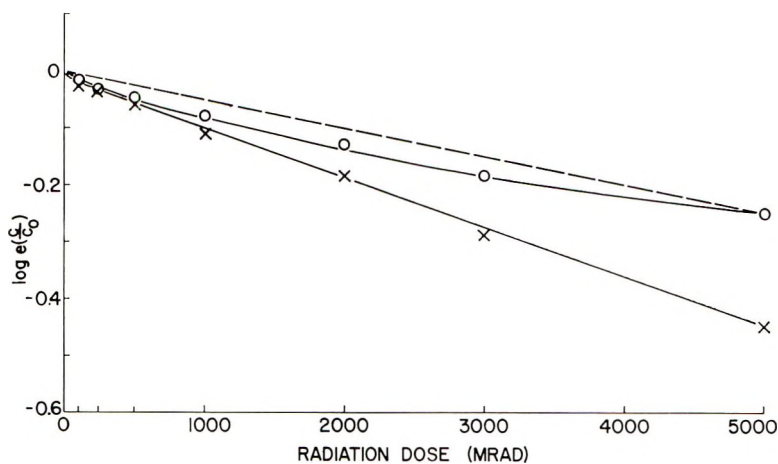
Fig. 4. Plot of $[U]/[U]_0$ vs. dose: (O) $[U] = [U]_0 - [—COOH]$; (×) $[U] = [U]_0 - [—COOH] - [CO_2]$.

starting material having an initial concentration C_0 of the reactant.[13] K_2 and K_1 were calculated from the initial slopes of Figures 1 and 2, respectively.   In the case of K_1' the calculation was made for CO_2 formation from benzoic acid on the basis of $G(CO_2) = 0.29$.   Here, in addition to the assumption of a first-order reaction, it is further assumed that the same rate constant applies to the C_6H_4—COOH groups in the polymer.

The following values were calculated for the rate constants: $K_1 = 26.7 \times 10^{-25}$(e.v.)$^{-1}$ g. and $K_2 = 5.7 \times 10^{-25}$(e.v.)$^{-1}$ g. (for $C_0 = 52.1 \times 10^{-4}$ mole/g.) and $K_1' = 5.90 \times 10^{-25}$(e.v.)$^{-1}$ g. (for $C_0 = (122)^{-1}$ mole/g.).

The calculated dependence of yields of —COOH and CO_2 on dose are compared with the experimental data in Figure 3.   The most striking discrepancy is in the wide divergence of the calculated and experimental yields of —COOH.   In the case of CO_2 the gross agreement is better, but there is an obvious discrepancy in the shapes of the calculated and experimental curves.   Taking into account the formation of CO_2 from —COOH groups makes little difference in the discrepancy for —COOH but results in a change in shape of the CO_2 curve which, in this respect, is in better agreement with the experimental data.

A related test of whether the experimental data is consistent with the set of first-order reactions (1) may be made by checking whether eq. (2) is satisfied for values of $[U] = [U]_0 - [—COOH] - [CO_2]$.   A reasonable fit to eq. (2) is obtained, except at very low doses, where the rate of degradation is too high.   Previously, a higher rate of degradation at low doses has been reported for a number of other polymers on the basis of an analysis of solution viscosity data.   It was suggested that such behavior might be caused by occasional "weak links" in the macromolecules.[15]   It is possible that "weak links" are present in PET,[16] e.g.,
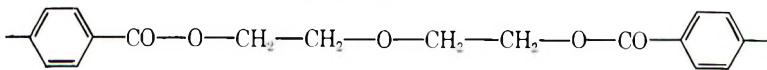
If such "weak links" were responsible for the initially too-high rate of degradation, then a case could be made for supposing that the reaction scheme (1) fits the present data after sufficient amounts of such atypical groups have been used up.   On the other hand, if an initially too-high rate of degradation occurs in a model compound for PET which is known not to contain weak links, then the reaction scheme (1) would have to be rejected. In order to help decide this question a study is being made of carboxyl group formation in solid ethylene glycol dibenzoate on exposure to γ-rays.

References

1. Charlesby, A., *Atomic Radiation and Polymers*, 1960, Permagon Press, p. 321.

2. Chapiro, A., *Radiation Chemistry of Polymeric Systems*, Interscience, New York, 1962, p. 483.

3. Sobue, H., V. Tabata, and M. Hiraoka, *Kogyo Kagaku Zasshi*, **64**, 372 (1961).

4. Slovokhotova, N. A., G. K. Sadovskaya, and V. A. Kargin, *J. Polymer Sci.*, **58**, 1293 (1962).

5. Hellwege, K. H., U. Johnsen, and W. Seufert, *Kolloid-Z.*, **188**, 11 (1963).

6. Sobue, H., and A. Kajiura, *Kogyo Kagaku Zasshi*, **62**, 1771 (1959).

7. Pohl, H. A., *Anal. Chem.*, **26**, 1614 (1954).

8. Matreyeva, S. P., and V. A. Myaghov, *Khim. Volokna*, **1959**, No. 5, 18.

9. Tolbert, B. M., and R. Noller, *Radiation Res.*, **3**, 52 (1955).

10. Little, K., *Nature*, **173**, 680 (1954).

11. Daniels, W. W., and R. E. Kitson, *J. Polymer Sci.*, **33**, 161 (1958).

12. Lea, D. E., *Actions of Radiations on Living Cells*, Cambridge, 1946.

13. Dole, M., D. C. Milner, and T. F. Williams, *J. Am. Chem. Soc.*, **80**, 1580 (1958).

14. Lind, S. C., *Radiation Chemistry of Gases*, A.C.S. Monograph No. 151, 1961.

15. Keyser, R. W., B. Clegg, and M. Dole, *J. Phys. Chem.*, **67**, 300 (1963).

16. Ritchie, P. D., *Thermal Degradation of Polymers*, Soc. Chem. Ind. Monograph No. 13, London, 1961, p. 107.

17. Dole, M., T. F. Williams, and A. J. Arvia, *Intern. Conf. Peaceful Uses of Atomic Energy*, **29**, 171 (1958).

Résumé

Le téréphthalate de polyéthylène a été exposé sous vide à la radiation du Co[60] à des vitesses de doses de 0.02 Mrad/min, à une température ambiante de 47°C.   Des produits gazeux étaient analysés au spectrographe de masse et les groupes carboxyles estimés par titration à la soude caustique et par analyse infra-rouge.   Les valeurs initiales G étaient $-COOH = 0.77$, $CO_2 = 0.17$, $CO = 0.11$, $H_2 = 0.015$ et $CH_4 = 0.003$.   Toutes ces valeurs décroissent remarquablement avec une dose croissante excepté $G(CO_2)$ environ constant jusqu'à 5000 Mrad.   On a examiné si la dépendance de la dose des produits principaux de la réaction pouvaient être expliquée par un système de réaction de premier ordre (voir le résumé anglais).   On a trouvé que la formation du groupe carboxyle à faible dose était beaucoup plus élevée que ne permet ce schéma de réaction simple. Toutefois un meilleur accord a été obtenu pour un domaine de dose plus élevée (environ 100 à 5000 Mrad).   La conclusion finale, n'a pas pu être atreinte concernant la validité du schéma de réaction ci-dessus.

Zusammenfassung

Polyäthyleneterephthalat wurde im Vakuum einer Co^{60}-γ-Strahlung bei einer Dosisleistung von 0,02 Mrad/min und einer mittleren Temperatur von 47°C ausgesetzt. Gasförmige Produkte wurden in einem Massenspektrometer analysiert und Carboxylgruppen durch Titration mit NaOH und Infrarotanalyse bestimmt. Die Anfangs-G-Werte waren: —COOH = 0,77, CO_2 = 0,17, Co = 0,11, H_2 = 0,015 und CH_4 = 0,003. Alle diese Werte nehmen mit Ausnahme von $G(CO_2)$, welches bis zu 5000 Mrad ungefähr konstant blieb, ab. Es wurde untersucht, ob die Abhängigkeit der Ausbeute an den Hauptreaktionsprodukten von der Dosis durch folgendes Schema von Reaktionen erster Ordnung (s. englische Zusammenfassung) erklärt werden könnte. Es zeigte sich, dass die Bildungsgeschwindigkeit der —COOH—Gruppenbildung bei niedriger Dosis viel zu hoch war, um in dieses einfach Reaktionsschema zu passen. Eine bessere Anpassung wurde jedoch in einem Bereich hoher Dosen (ca. 100–5000 Mrad) erhalten. Eine endgültige Beurteilung der Gültigkeit des obigen Reaktionsschemas kann nicht gegeben werden.

Sequence Distribution of Partially Hydrolyzed Poly(vinyl Acetate)

ROBERT K. TUBBS,* *E. I. du Pont de Nemours & Company, Inc., Electrochemicals Department, Niagara Falls, New York*

Synopsis

Copolymers of vinyl acetate and vinyl alcohol were studied by differential thermal analysis. The melting points of the copolymers are not a simple function of the composition, but depend on the method of preparation of the copolymers. Partial saponification of poly(vinyl acetate) with sodium hydroxide leads to high melting, ordered copolymers, while reacetylation of poly(vinyl alcohol) leads to low melting, random copolymers. Catalytic alcoholysis of PVAc yields copolymers intermediate in melting point and order. The results are treated by assuming that equal melting points indicate similar sequence length distributions of crystallizable units.

Introduction

Copolymers of vinyl alcohol (VOH) and vinyl acetate (VAc) can be prepared in several ways. Commercially, the copolymers are made by base-catalyzed alcoholysis of poly(vinyl acetate) (PVAc) in ethanol or methanol by stopping the reaction at the desired composition.[1] Copolymers can also be prepared by saponification of PVAc or by reacetylation of poly(vinyl alcohol) (PVA). These reactions are of interest because of the anomalies introduced by the polyfunctional nature of PVAc in comparison with low molecular weight esters. The mechanism of the saponification reaction was first investigated by Minsk et al.,[2] who found that the reaction is autocatalytic with the rate constant increasing as the reaction proceeds. Sakurada and Osugi[3] confirmed these observations. The autocatalytic nature of the reaction can be attributed to a difference in reactivity of a particular acetate group, depending on whether its neighboring groups in the chain sequence are acetate or hydroxyl groups.[4] The presence of an adjacent hydroxyl group enhances the reactivity of the acetate group toward alcoholysis or saponification.

Although the reason for the observed differences in reactivity of acetate groups is not yet clear, it is evident that copolymers, obtained by stopping the reaction short of completion, will not have a random distribution of acetate groups along the chain. Infrared spectra show a large difference in the carbonyl region depending on the method of preparing the VOH–VAc

* Present address: Du Pont Experimental Station, Wilmington, Delaware.

copolymers.[5] When prepared by alcoholysis, the carbonyl region of the copolymer is nearly identical to that of poly(vinyl acetate). The carbonyl peak of copolymers prepared by reacetylation of poly(vinyl alcohol) is shifted toward longer wavelength, probably because of hydrogen bonding to a neighboring hydroxyl group. Reacetylation under equilibrium conditions should lead to randomly substituted chains.

The melting point of a semicrystalline copolymer depends on the distribution of units on the chain, and in particular, on the sequence length of the crystallizable units. Flory has treated this problem theoretically,[6] and experimental evidence has been obtained in qualitative agreement with theory.[7,8] Since PVA is a semicrystalline polymer and residual acetate groups lower the melting point, it is expected that melting points will reflect the sequence distribution of these copolymers.

Copolymers of VOH and VAc are ideally suited for a study of the effect of sequence length distribution on the fusion process. The same polymer backbone is retained and the preparation methods do not introduce other variable parameters, such as degree of polymerization and branching. In order to study this distribution variable in other vinyl copolymer systems, different initiation conditions must be employed to vary the sequence distribution, and these usually result in other variables in copolymer structure.

Experimental

Copolymers of VOH and VAc were prepared in three ways: reacetylation of PVA, alcoholysis of PVAc, and saponification of PVAc.

(1) Random copolymers were prepared by reacetylation of PVA in mixtures of acetic acid and water. The reaction was performed at reflux (~100°C.) for 24–48 hr. The copolymer composition was controlled by the relative amounts of acetic acid and water in the reaction medium, and the total time.

(2) Alcoholysis of PVAc was accomplished by dissolving the polymer in methanol, adding a small amount of sodium methylate (0.1% by weight of polymer), and stirring vigorously at room temperature. When the polymer concentration was high, a gel formed instead of a precipitate of polymer. The gels were readily broken in a high speed blender. The reaction was stopped by adding excess acetic acid to neutralize the basic catalyst.

(3) Saponification of PVAc was accomplished in the following manner. PVAc was dissolved in acetone at 5% concentration. Sufficient water was added to make the solvent nearly 80 parts acetone/20 parts water by volume. A solution of NaOH in water was added with stirring to bring the solvent composition to 80/20. The concentration of base was adjusted to give the desired copolymer composition. Since this reaction is self-limiting, no attempt was made to break up the gel as it formed. The reaction was allowed to go to completion in the gel state, and then the gel was broken up in a high speed blender.

The copolymers thus obtained were washed with mixtures of methanol–water or acetone–water, depending on the reaction medium, until all traces of sodium acetate were removed. They were then washed with acetone and dried in vacuum at 60°C. Compositions were obtained from the saponification numbers of the samples.

Melting points were determined with the Du Pont 900 differential thermal analyzer. A nitrogen atmosphere was used, and a heating rate of 30°C./min. was employed. About 4 mg. of sample was used for each determination. Infrared spectra were obtained with a Beckman IR-9 spectrophotometer, with the use of thin films of copolymer cast on Irtran-2 windows. The samples were heat-treated at 160°C. for 5 min. in a vacuum oven.

Results and Discussion

Equilibrium crystallization of copolymers has been treated theoretically by Flory.[6] The model chosen is a copolymer which contains only one type of crystallizable unit, in our case vinyl alcohol. The length of a crystallite along the polymer chain axis is restricted by the presence of noncrystallizing units, such as vinyl acetate. The temperature at which the last traces of crystallinity disappear depends on the melting point of the crystalline homopolymer, the heat of fusion, and the sequence probability of the copolymer. The composition of the copolymer is only important through its influence on the sequence probability.

The sequence probability, p_A, is the probability that a crystallizable group, A, is succeeded by another A group. If the sequence probability is independent of the number of preceding A groups in the sequence, the melting point is related to the probability by the expression,[6]

$$(1/T_m) - (1/T_m°) = - (R/\Delta H_u) \ln p_A \tag{1}$$

where T_m denotes the melting point of the copolymer, $T_m°$ the melting point of the homopolymer, R the gas constant, and ΔH_u the molar heat of fusion per A unit. For a random copolymer, p_A is equal to the mole fraction of crystallizable groups, X_A. For copolymers in which the units have a tendency to alternate, p_A is less than X_A, and for block copolymers, where long sequences of the units tend to predominate, p_A is greater than X_A.

The melting points of the various VOH/VAc copolymers are plotted in Figure 1 as a function of composition. The acetate groups in the copolymers prepared by reacetylation are very effective in depressing the melting point of PVA, while those in saponified copolymers have very little effect. The alcoholized copolymers are intermediate. It is evident that there are large structural differences in the copolymers prepared by different methods.

It has been shown that reacetylated copolymer samples obey the Flory equation, eq. (1) for random copolymers, where p_A is replaced by the mole fraction of vinyl alcohol units, X_A.[9] These copolymers are close to random
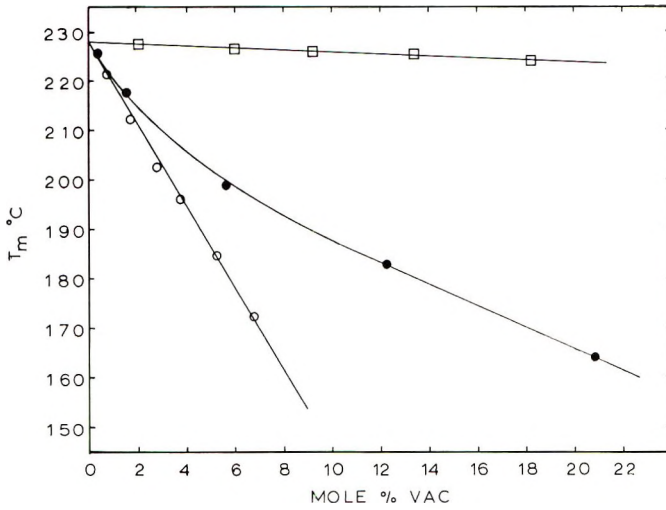
Fig. 1. Melting points of copolymers prepared by: (□) saponification: (●) alcoholysis; (O) reacetylation.
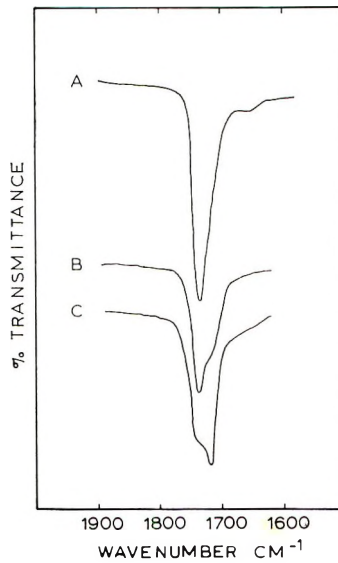
Fig. 2. Infrared spectra of copolymers prepared by: (*A*) saponification (9.2% VAc); (*B*) alcoholysis (12.3% VAc); (*C*) reacetylation (6.8% VAc).

in distribution of the two different units.   On the other hand, the saponified and alcoholized copolymer samples must be more ordered.   This qualitative observation is confirmed by the infrared spectra of the copolymers as shown in Figure 2.   The saponified samples have a carbonyl absorption maximum at 1734 cm.$^{-1}$, which corresponds to that of PVAc.   This peak shows little evidence of a shoulder at lower frequency.   In contrast, both the reacetylated samples and the alcoholized samples show two bands in

this region. The alcoholized samples have a peak at 1734 cm.$^{-1}$ with a strong shoulder at about 1715 cm.$^{-1}$. The reacetylated samples are similar, but the peak is at 1715 cm.$^{-1}$ with a shoulder around 1734 cm.$^{-1}$. Nagai and Sagane have attributed the shift to 1715 cm.$^{-1}$ as due to hydrogen bonding of the carbonyl group with an adjacent hydroxyl group.[5] The relative intensity of these bands is therefore a qualitative indication of the number of VAc–VOH pairs.

This is consistent with the data on melting points. Sequences of VOH units which are longer than random impose restrictions on the number of VOH–VAc pairs. Copolymers which are higher melting should have longer sequences of VOH units than in a random distribution and should also have fewer VOH–VAc pairs. This is, in fact, the case. The interpretations of the DTA results and the infrared results are mutually consistent.

The data are also in agreement with published results on the kinetics of the reactions used in preparation of these samples.[2–4] It has been shown that the enhanced reactivity of an acetate, which is adjacent to a hydroxyl group, favors the formation of long sequences of VOH units during alcoholysis or saponification. The reactivity is enhanced more in saponification than in alcoholysis, and thereby longer sequences of VOH units should be obtained by the former reaction. This is confirmed by both the infrared and DTA results. The partially saponified products are higher melting and have fewer VOH–VAc pairs than the partially alcoholized samples.

Since eq. (1) relates the melting point of a copolymer to the sequence probability in a quantitative manner, an attempt was made to calculate the sequence length distribution by applying the value of p_A found from the melting point determination. The assumption is made that the normalized sequence length distribution of the crystallizable units in an ordered copolymer is the same as that of a random copolymer which melts at the same temperature. This assumption requires that the number of VOH–VAc pairs be the same for all copolymers having the same melting points, when normalized to the amount of VOH units present. The sequence length distribution of VOH units can thus be calculated in the same manner as for a random copolymer. Since there is a larger amount of VAc in an ordered copolymer than a random copolymer having the same melting point, it is evident that the sequence lengths of VAc units are longer than in a random distribution. A sequence probability, p_B, is defined for the acetate units analogous to that defined for the VOH units. The probability that a unit picked at random will be an A or a B unit is still equal to the mole fraction of the particular unit in the mixture. The probabilities of pairs are then as follows: for pair (A–A), $X_A p_A$; for pair (A–B), $X_A(1 - p_A)$; for pair (B–B), $X_B p_B$; for pair (B–A), $X_B(1 - p_B)$.

In contrast to the mole fractions, the sum of p_A and p_B is not necessarily 1. The number of (A–B) pairs is equal to the number of (B–A) pairs, such that:

$$p_B = 1 - [X_A(1 - p_A)/(1 - X_A)] \qquad (2)$$
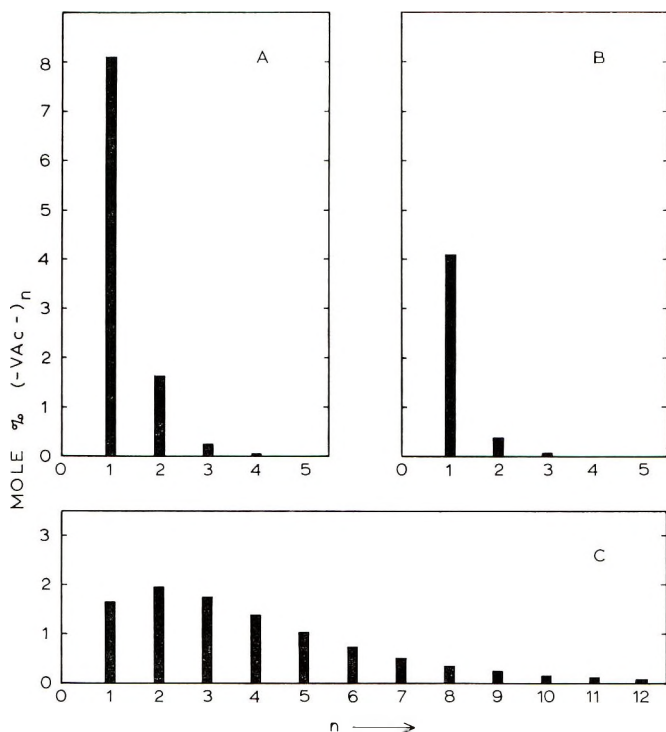
Fig. 3. Sequence length distribution of copolymers: (A) 10% VAc, $T_m = 146°C.$; (B) 4.5%, VAc, $T_m = 187°C.$; (C) 10% VAc, $T_m = 187°C.$

There is no unique sequence distribution of B units which leads to a particular value for p_B but, for comparison, the maximum randomness is used as a basis. The molecular weight fraction may then be calculated as a function of sequence length in the same way as for random copolymers. The equations used are for VOH and VAc, respectively:[6]

$$W_n^A = nX_A(1 - p_A)^2 p_A^{n-1}$$
$$W_n^B = nX_B(1 - p_B)^2 p_B^{n-1}$$

(3)

As an example, the case of a copolymer prepared by alcoholysis in methanol with 10 mole-% residual acetate groups is taken. As seen in Figure 1, such a copolymer has a melting point of 187°C. A random copolymer of the same composition melts at 146°C., while a random copolymer with the same melting point would contain 4.5 mole-% acetate groups. The random distributions are obtained by replacing p with X for the appropriate unit in eq. (3). The results of these calculations are represented graphically in Figure 3. The increased length of the VAc sequences is evident. This solution is not unique, since other distributions could give the same melting point. It does, however, indicate the longer sequence length of vinyl acetate units required to interpret the results adequately.

Conclusions

Flory's theory predicts that the melting point of copolymers will be dependent on the distribution of sequence lengths in the copolymer. DTA confirms that copolymers of VAc and VOH prepared by alcoholysis or basic hydrolysis of PVAc have a nonrandom distribution of sequence lengths. Reacetylation of PVA, however, leads to random copolymers.

References

1. Billmeyer, F. W., Jr., *Textbook of Polymer Science*, Interscience, New York, 1962, p. 407.
2. Minsk, L. M., W. J. Priest, and W. O. Kenzon, *J. Am. Chem. Soc.*, **63**, 2715 (1941).
3. Sakurada, I., and Osugi, T., *Gosei Seni Kenkyu*, **2**, 192 (1944).
4. Sakaguchi, Y., *Polyvinyl Alcohol*, I. Sakurada, Ed., Soc. High Polymer Sci. (Japan), 1955, p. 43.
5. Nagai, E., and N. Sagane, *Kobunshi Kagaku*, **12**, 195 (1955).
6. Flory, P. J., *Trans. Faraday Soc.*, **51**, 848 (1955).
7. Mandelkern, L., *Crystallization of Polymers*, McGraw-Hill, New York, 1964, pp. 106–110.
8. Jackson, J. F., *J. Polymer Sci. A*, **1**, 2119 (1963).
9. Tubbs, R. K., *J. Polymer Sci., A*, **4**, 4181 (1965).

Résumé

Des copolymères d'acétate de vinyle et d'alcool vinylique ont été étudiés par des analyses thermiques différentielles. Les points de fusion de ces polymères ne sont pas des fonctions simples de la composition, mais dépendent de la méthode préparation des copolymères. Par saponification partielle des acétates de polyvinyle au moyen d'hydroxyde de sodium on obtient des copolymères ordonnés, de point de fusion élevés, alors que par réacétylation de l'alcool polyvinylique, on obtient des copolymères statistiques de bas point de fusion. L'alcoolyse catalytique de l'acétate de polyvinyle fournit des copolymères intermédiaires en ce qui concerne les points de fusion et leur ordre. Les résultats sont traités en admettant que des points de fusion semblables indiquent des séquences similaires de distributions de longueurs des unités cristallisables.

Zusammenfassung

Copolymere von Vinylacetat und Vinylalkohol wurden mittels Differentialthermoanalyse untersucht. Die Schmelzpunkte der Copolymeren sind keine einfachen Funktionen der Zusammensetzung, sondern hängen von der Darstellungsmethode der Copolymeren ab. Partielle Verseifung von Polyvinylacetat mit Natriumhydroxyd führt zu hochschmelzenden geordneten Polymeren, während die Reacetylierung von Polyvinylalkohol zu niederschmelzenden statistischen Copolymeren führt. Die katalytische Alkoholyse von PVAc liefert Copolymere mit mittleren Werten des Schmelzpunktes und der Ordnung. Die Ergebnisse werden unter der Annahme behandelt, dass gleiche Schmelzpunkte Anzeichen für eine ähnliche Sequenzlängenverteilung der kristallisationsfähigen Einheiten sind.

Triad Distributions of 1,1-Diphenylethylene–Methyl Acrylate Copolymer Determined from NMR Study

KOICHI ITO and YUYA YAMASHITA, *Department of Synthetic Chemistry, Faculty of Engineering, Nagoya University, Furo-cho, Chikusa-ku, Nagoya, Japan*

Synopsis

The triad distributions of 1,1-diphenylethylene (D)–methyl acrylate (M) copolymers have been determined from NMR measurements and examined according to the terminal and penultimate models of copolymerization theory. As expected from the diamagnetic shielding by the phenyl rings of the nearest D units, the methoxy proton resonances were found to appear as three resolved peaks at 6.4–6.6 τ, 6.7–7.0 τ, and 7.2 τ, and have been assigned to the central M units of the triads MMM, MMD or DMM and DMD, respectively. The copolymer composition and the triad distributions observed are shown to agree better with the terminal model with the methyl acrylate reactivity ratio of 0.092 ± 0.010 than with the penultimate model.

INTRODUCTION

Several recent communications[1-5] on NMR studies of styrene–methyl methacrylate copolymer have shown that the methoxy proton resonance consists of the three main peaks. Quantitative analyses of these relative peak areas, measured in carbon tetrachloride, have recently been made satisfactorily by considering the sequence distribution and the relative configurations of the methyl methacrylate-centered triads.[4,5] We have shown that a simplified treatment is possible by assuming the constant relative configurations of the alternating styrene and methyl methacrylate units regardless of the sequence of the addition i.e., $\sigma = \sigma_{12} = \sigma_{21}$ in Bovey's notation.[1] The same treatment has successfully been applied to copolymers of styrene with methyl acrylate[6] and with benzyl methacrylate.[7]

This paper deals with 1,1-diphenylethylene (D)–methyl acrylate (M) copolymers where the configurational aspects of alternating bonds need not be considered because 1,1-diphenylethylene unit has no asymmetric carbon. Thus, the direct measurements of all three kinds of the triads (MMM, MMD or DMM and DMD) should be possible from the resolution of the methoxy proton resonance. On this basis, the test of the terminal or penultimate model in copolymerization will be discussed on the basis of our recent simple theory.[8]

EXPERIMENTAL

1,1-Diphenylethylene (b.p. 107–109°C./1 mm. Hg) was prepared according to a literature procedure[9] and found to be practically pure on the

basis of NMR and gas chromatography measurements. Methyl acrylate was purified by the usual procedure. Both monomers were redistilled prior to polymerization. Polymerization was carried out at 60°C. with benzoyl peroxide as a radical initiator to 2–3 wt.-% conversion. Polymers were precipitated into petroleum ether, reprecipitated from benzene, and subsequently freeze-dried. The reduced viscosities (η_{sp}/c at $c = 1.0$ g./100 ml.) of polymers were in the range 0.05–0.06 in benzene at 30°C.

NMR measurements were made at 90°C. with about 10% solution in carbon tetrachloride with a Japan Electron Optics spectrometer (JNM-C-60) working at 60 Mc. Tetramethylsilane was used as an internal standard.

RESULTS AND DISCUSSION

The NMR spectra observed are shown in Figure 1. From the peak area at about 3.0 τ due to the phenyl protons of the 1,1-diphenylethylene unit, we first estimated the copolymer composition with the results given in Table I, where x and y represent the molar ratios of methyl acrylate to 1,1-diphenylethylene in the monomer feed and in the polymer, respectively.
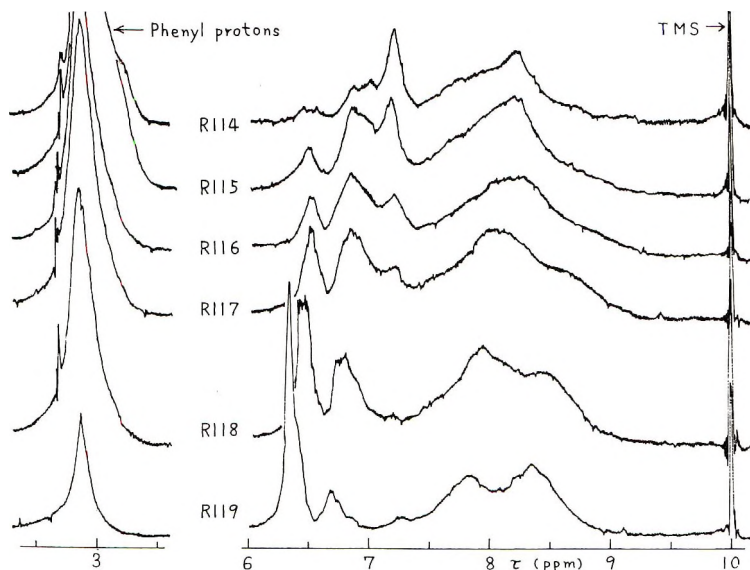
Fig. 1. NMR spectra.

The methoxy proton resonance appears as three main, resolved peaks in the range 6.4–7.2 τ, as expected from the diamagnetic shielding by the phenyl rings of the nearest 1,1-diphenylethylene units. Therefore, the peaks at 6.4–6.6 τ, 6.7–7.0 τ, and 7.2 τ could safely be assigned to the methoxy protons of the central methyl acrylate units of the triads MMM, MMD or DMM and DMD, respectively. The relative triad fractions F

TABLE I
Observed Copolymer Composition and Triad Fractions

Sample	x	y^a	y^b	F_{MMM}	$F_{MMD} + F_{DMM}$	F_{DMD}
R114	2.33	1.28	1.35	0.09	0.35	0.56
R115	5.86	1.55	1.61	0.16	0.44	0.40
R116	9.04	1.83	1.79	0.20	0.48	0.32
R117	13.3	2.16	2.17	0.28	0.52	0.20
R118	24.1	2.90	3.23	0.48	0.42	0.10
R119	61.3	5.85	5.40	0.70	0.23	0.07

[a] From the relative area of the phenyl proton resonance.
[b] From the triad fractions according to eq. (7).

thus estimated from these relative peak areas are given in the last three columns of Table I, though the errors involved appear to be somewhat large (± 5–10%) due to poor resolutions of the spectra.

The fine structures observed in each of the methoxy proton resonances (for example, at about 6.5 and 7.0 τ of sample R114) as well as the slight up-field shift of each peak with increasing 1,1-diphenylethylene content are not clearly understood at present. It would be possible, however, that a more remote D unit might be responsible for such an up-field shift; for example, the central M unit in the pentad DMMMM or DMMMD would appear at a somewhat higher field than that in the pentad MMMMM. However, as a first approximation, the above assignments based on the triad distributions will be the most reasonable and are supported by the analyses of the methoxy proton resonances of styrene–methyl methacrylate copolymer measured in carbon tetrachloride[4,5] and also by the discussion below.

In the case of D not adding to D, there should be no D-consecutive sequence, so that the statistical stationary process given previously[8,10] may be expressed as

$$P_1\{D\} = P_2\{MD\} = P_3\{MMD\} + P_3\{DMD\} \tag{1}$$

$$P_1\{M\} = P_2\{MM\} + P_2\{DM\} \tag{2}$$

$$P_2\{MM\} = P_3\{MMM\} + P_3\{MMD\} \tag{3}$$

$$P_2\{DM\} = P_3\{DMM\} + P_3\{DMD\} \tag{4}$$

and

$$P_2\{MD\} = P_2\{DM\} \tag{5}$$

$$P_3\{MMD\} = P_3\{DMM\} \tag{6}$$

where $P_1\{.\}$, $P_2\{..\}$, and $P_3\{...\}$ represent the (absolute) mole fractions of the corresponding monomer units, diads, and triads, respectively. Using the relative triad fractions, $F_{XMY} = P_3\{XMY\}/P_1\{M\}$, where X, Y are D or M, the following relations can be readily derived.

$$y = P_1\{M\}/P_1\{D\} = 1/(F_{MMD} + F_{DMD}) \tag{7}$$

$$P_2\{MM\}/P_3\{MMM\} = (F_{MMD} + F_{MMM})/F_{MMM} \tag{8}$$

$$P_2\{DM\}/P_3\{DMM\} = (F_{DMM} + F_{DMD})/F_{DMM} \tag{9}$$

and

$$F_{MMD} = F_{DMM} \tag{10}$$

Equation (7) can be used as a check for the statistical stationary process and for the assumption of the absence of D-consecutive sequences, since we can independently determine the left- and right-hand quantities. The copolymer composition ratio y thus determined from the triad fractions according to eq. (7) is given in the fourth column of Table I. The satisfactory agreement with that determined from the phenyl proton resonance, given in the third column, supports the triad assignments above as well as the assumptions of the statistical stationary process and of the absence of D-consecutive sequences. Therefore, the monomer reactivity ratio of 1,1-diphenylethylene is assumed to be zero in the following.

Next we discuss the applicability of the terminal or penultimate model to describe the copolymer composition and the triad distributions.[8]

Copolymer Composition

The copolymer composition ratio y can be expressed kinetically in the case of D not adding to D as[8,11,12]

$$y = 1 + r_M x \qquad \text{(Terminal model)} \tag{11}$$

with $r_M = k_{MM}/k_{MD}$, and

$$y = 1 + [r'_M(1 + r_M x)/(1 + r'_M x)]x \qquad \text{(Penultimate model)} \tag{12}$$

with $r_M = k_{MMM}/k_{MMD}$, and $r'_M = k_{DMM}/k_{DMD}$, where the k's are the corresponding rate constants.

Based on y determined from the phenyl proton resonance, the terminal model gave $r_M = 0.092 \pm 0.010$ as a mean, which is in fair accord with the reported value,[13] and the penultimate model gave $r_M = 0.065 \pm 0.005$, and $r'_M = 0.12 \pm 0.01$. Plots of y against x, shown in Figure 2, appear to show that the latter model gives a better fit to the observed compositions than the former. Although the penultimate effect ($r'_M/r_M = 1.85$) might be attributed to the repulsion (steric or polar) between the penultimate D unit and the entering D monomer, this must be considered with much care, because the copolymer composition itself is not so sensitive to the penultimate effect,[8,14,15] and, in fact, seems to be compatible with both the models within experimental error. Indeed, the examination of the triad distributions shows the penultimate model to be much more unfavorable than the terminal model, as will be shown below.
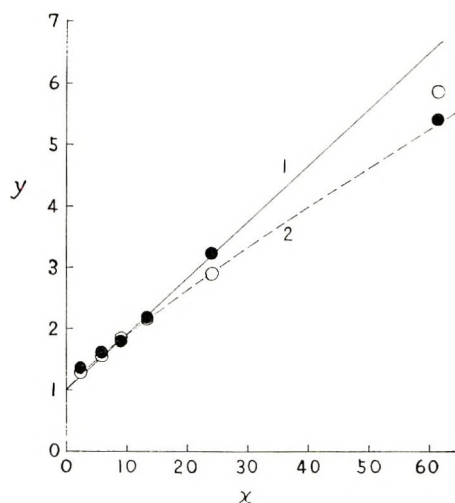
Fig. 2. Plots of y vs. x: (O) experimental points from the phenyl proton resonance; (●) experimental points from the triad fractions according to eq. (7); (1) curve calculated from terminal model, eq. (11), with $r_M = 0.092$; (2) curve calculated from penultimate model, eq. (12), with $r_M = 0.065$ and $r_M' = 0.12$.

Triad Distribution

The triad fractions, calculated from the kinetical expressions given before[8] with the above monomer reactivity ratios, are shown in Table II.

TABLE II
Calculated Triad Fractions

Sample	Terminal model[a]			Penultimate model[b]		
	F_{MMM}	$2F_{MMD}$	F_{DMD}	F_{MMM}	$2F_{MMD}$	F_{DMD}
R114	0.03	0.29	0.68	0.03	0.35	0.62
R115	0.13	0.45	0.42	0.10	0.52	0.38
R116	0.21	0.49	0.30	0.17	0.57	0.26
R117	0.30	0.50	0.20	0.25	0.57	0.18
R118	0.47	0.43	0.10	0.40	0.51	0.09
R119	0.72	0.26	0.02	0.65	0.33	0.02

[a] With $r_M = 0.092$.
[b] With $r_M = 0.065$ and $r'_M = 0.12$.

It will now be apparent that a better fit to the observed triad fractions in Table I is obtained with the terminal model than with the penultimate model. This becomes more evident when the quantities $P_2\{MM\}/P_3\{MMM\}$ or $P_2\{DM\}/P_3\{DMM\}$, which can be estimated according to eqs. (8) and (9), are plotted against $1/x$, since it follows[8] that in the case of the terminal model,

$$P_2\{MM\}/P_3\{MMM\} = P_2\{DM\}/P_3\{DMM\}$$
$$= 1/P_{MM} = 1 + 1/r_M x \quad (13)$$
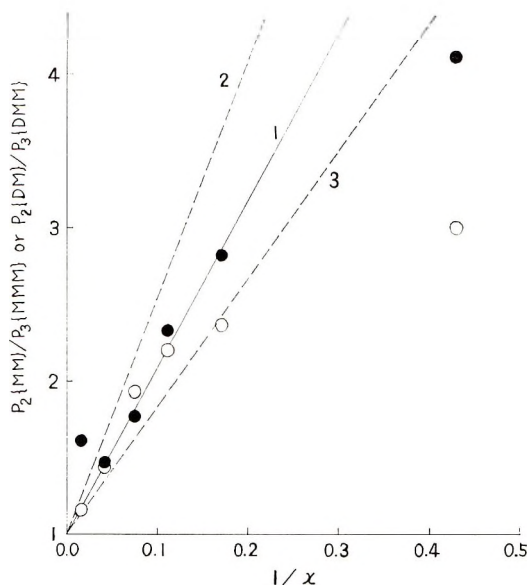
Fig. 3. Plots of (○) $P_2\{MM\}/P_3\{MMM\}$ and (●) $P_2\{DM\}/P_3\{DMM\}$ vs. $1/x$: (1) curve calculated for terminal model, eq. (13), with $r_M = 0.092$; (2) curve calculated for penultimate model, eq. (14), with $r_M = 0.065$; (3) curve calculated for penultimate model, eq. (15), with $r'_M = 0.12$.

while in the case of the penultimate model,

$$P_2\{MM\}/P_3\{MMM\} = 1/P_{MMM} = 1 + 1/r_M x \qquad (14)$$

$$P_2\{DM\}/P_3\{DMM\} = 1/P_{DMM} = 1 + 1/r'_M x \qquad (15)$$

where P_{MM}, P_{MMM}, and P_{DMM} denote the corresponding conditional probabilities.

The results in Figure 3 show clearly not only that there is no significant difference between the values $P_2\{MM\}/P_3\{MMM\}$ and $P_2\{DM\}/P_3-\{DMM\}$, but also that the monomer reactivity ratio of the terminal model ($r_M = 0.092 \pm 0.010$) can represent the observed points with better accuracy than those of the penultimate model, except for samples R114 ($1/x = 0.43$) and R119 ($1/x = 0.016$) which would have very large errors due to very small F_{MMM} and F_{DMD} values, respectively. Indeed, eqs. (14) and (15) gave $r_M = 0.118 \pm 0.037$ and $r'_M = 0.088 \pm 0.021$, as a mean, when applied to all the data, and $r_M = 0.099 \pm 0.015$ and $r'_M = 0.090 \pm 0.004$ when applied to the data of the four samples R115–R118. These values accord well with the reactivity ratio of the terminal model, instead of those of the penultimate model.

From the above considerations, it will be reasonable to conclude that the terminal model with the methyl acrylate reactivity ratio of 0.092 ± 0.010 can describe both the copolymer composition and the triad distributions much better than the penultimate model. The result illustrates the case of the difficulty and the ambiguity encountered in distinguishing between

the terminal and the penultimate models based on the copolymer composition data alone.[8,14,15]   It is hoped that an examination of copolymer microstructure can lead to a conclusive selection of the models.

References

1. Bovey, F. A., *J. Polymer Sci.*, **62,** 197 (1962).

2. Nishioka, A., Y. Kato, and N. Ashikari, *J. Polymer Sci.*, **62,** S10 (1962).

3. Kato, Y., N. Ashikari, and N. Nishioka, *Bull. Chem. Soc. Japan*, **37,** 1630 (1964).

4. Harwood, H. J., and W. M. Ritchey, *J. Polymer Sci. B*, **3,** 419 (1965).

5. Ito, K., and Y. Yamashita, *J. Polymer Sci. B*, **3,** 625 (1965).

6. Ito, K., and Y. Yamashita, *J. Polymer Sci. B*, **3,** 637 (1965).

7. Ito, K., and Y. Yamashita, *Kogyo Kagaku Zasshi*, **68,** 1469 (1965).

8. Ito, K., and Y. Yamashita, *J. Polymer Sci. A*, **3,** 2165 (1965).

9. Allen, C. F. H., and S. Converse, *Organic Syntheses, Coll. Vol. 1*, Wiley, New York, 1956, p. 226.

10. Coleman, B. D., and T. G Fox, *J. Polymer Sci. A*, **1,** 3183 (1963).

11. Barb, W. G., *J. Polymer Sci.*, **11,** 117 (1953).

12. Ham, G. E., *J. Polymer Sci.*, **45,** 169 (1960); *ibid. A*, **2,** 3633 (1964).

13. Doak, K. W., and D. L. Dinnen, *J. Am. Chem. Soc.*, **73,** 1084 (1951).

14. Berger, M., and I. Kuntz, *J. Polymer Sci. A*, **2,** 1687 (1964).

15. Ang, J. L., and H. J. Harwood, paper presented at 147th Meeting, American Chemical Society, Philadelphia, April 1964.

Résumé

Les distributions de triade de copolymères de 1.1-diphényléthylène (D)-acrylate de méthyle (M) ont été déterminées au départ de mesures RMM et examinées suivant les modèles des unités terminales et pénultième de la théorie de la copolymérisation.   Comme prévu par suite de l'écran diamagnétique causé par les anneaux phényles des unités D les plus voisines, les résonances du proton méthorylés ont été trouvé sous formes de trois pics bien résolus à 6.4–6.6 τ, 6.7–7.0 τ et 7.2 τ, et ces pics ont été attribué aux unités M centrales du triade MMM, MMD ou DMM et DMD respectivement.   La composition du copolymère et la distribution de triades observées sont en meilleur accord avec le modèle terminal avec des rapports de réactivité pour l'acrylate de méthyle de 0.092 $\pm$ 0.010 plutôt qu'avec le modèle à unité pénultième.

Zusammenfassung

Die Triadenverteilung von 1,1-Diphenyläthylen(D)–Methylacrylat(M)-Copolymeren wurde mit NMR-Messungen bestimmt und mit dem Endgruppen- und dem Vorletzten-Gruppenmodell der Copolymerisationstheorie verglichen.   Wie nach der diamagnetischen Abschirmung durch die Phenylringe der nächsten D-Einheit zu erwarten war, trat die Methoxy-Protonenresonanz in drei aufgelösten Maxima, bei 6,4–6,6 τ, 6,7–7,0 τ und auf und wurde der zentralen M-Einheit der Triaden MMM, bzw MMD oder DMM, bzw. DMD zugeordnet.   Die beobachtete Copolymerzusammensetzung und Triadenverteilung stimmen besser mit dem Endgruppenmodell mit einem Methylacrylatreaktivitätsverhältnis von 0,092 $\pm$ 0,010 überein als mit dem Vorletzen-Gruppenmodell.

Internal Motion in Organosilicon Polymers.
I. Linear Dimethylpolysilazane

F. S. MODEL, G. REDL, and E. G. ROCHOW, *Department of Chemistry, Harvard University, Cambridge, Massachusetts*

Synopsis

A linear dimethylpolysilazane polymer has been prepared and its internal motion studied by the techniques of broadline nuclear magnetic resonance. Second moments and line widths are reported as a function of temperature from −196 to 30°C. The results are compared to those for linear dimethylpolysiloxane, as well as to those for the crosslinked siloxane and silazane. The experimental low-temperature second moment of 7.25 ± 0.5 gauss^2 corresponds to a C_3 reorientation of methyl groups about the silicon–carbon bond. The motions occurring in the silazane are found to be the same as those in the corresponding siloxane. The transition to low second moments occurs approximately 30°C. higher in the linear silazane than in the linear siloxane. This is attributed to a somewhat greater resistance to motion in the silazane.

Introduction

The isolation of a linear dimethylpolysilazane, $[-(CH_3)_2Si-NH-]_n$ with an average molecular weight of 1200 has recently been achieved in these laboratories.[1] It was desired that the internal mobility of this linear polymer be studied by the techniques of broadline nuclear magnetic resonance, since this has already been done by Barrante and Rochow at these laboratories for the isoelectronic linear dimethylpolysiloxane, as well as for various crosslinked dimethylpolysilazanes and dimethylpolysiloxanes.[2-4] It was the purpose of this study, then, to perform this investigation and to make the indicated comparisons: (*a*) linear silazane versus linear siloxane, (*b*) linear silazane versus crosslinked silazane, and (*c*) dimethylpolysilazanes versus dimethylpolysiloxanes in general.

Several types of motion are possible in these organosilicon polymers. Among those worthy of consideration are: (*1*) a C_3 reorientation of the methyl groups about the silicon–carbon bond; (*2*) a torsional motion of the entire $Si(CH_3)_2$ group about the silicon–nitrogen bond; (*3*) a bending motion of segments of the ($-Si-N-$) chain; and (*4*) translational motion of the individual polymer chains. The aforementioned C_3 reorientation is well known in the polysiloxanes[5-7] and in the crosslinked polysilazanes.[2,3] It is, therefore, to be expected that such motions would also be discernible in the linear dimethylpolysilazane considered in this investigation.

Experimental

The linear silazane used in these studies was prepared by a modification of the method of Redl and Rochow.[1] Hexamethyltrisilazane (I) was heated in an autoclave under 10 atm. of ammonia pressure at 140°C. for 10 days. The crude reaction mixture was then vacuum-distilled to remove the volatile products and 13% of the linear polysilazane (with respect to I) was obtained as a residue.

The experiments were carried out on a fixed-field, variable frequency broadline nuclear magnetic resonance spectrometer which was built in these laboratories and modified several times prior to this investigation.[2,3,8,9] It consists of components shown in the block diagram (Fig. 1). These components are described in detail elsewhere,[2,3] with the exception of the
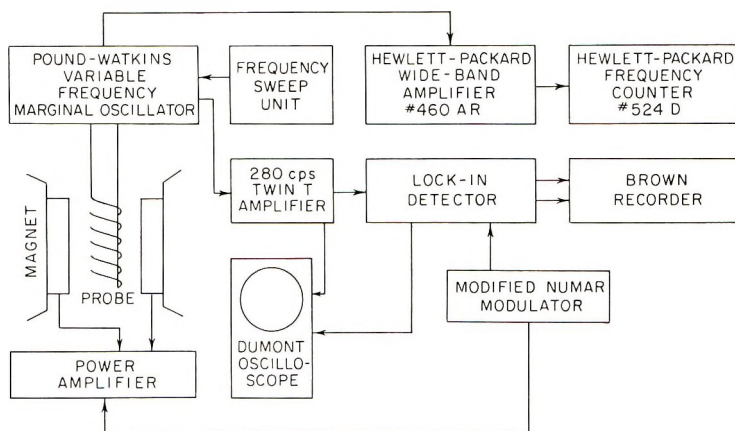
Fig. 1. Block diagram of broadline nuclear magnetic resonance spectrometer.

following. The modified Numar modulator was further modified by the replacement of the vacuum tube oscillator used to provide the modulation frequency of 280 cycles/sec. which was known to vary slightly with time and temperature. In its place, a 280 cycle/sec. oscillator, controlled by an electrically driven tuning fork that maintained a frequency of exactly 280 cycles/sec., was installed (see Fig. 2). The power amplifier was replaced by a newly built unit, capable of 60 w. output.

The apparatus is equipped with a gas-flow temperature control system which permits measurements to be taken from −196°C. to −300°C. This, too, is described in detail elsewhere.[2,3]

Most organosilicon–nitrogen compounds are extremely moisture-sensitive, decomposing to ammonia and the corresponding organosilicon–oxygen compounds when left in contact with the atmosphere. To prevent this decomposition, samples were sealed in 11 mm. glass tubes immediately after they had been prepared. Since this made it impossible to determine the temperatures within the sample itself, and since it was desired to avoid hysteresis effects, samples were cooled slowly in the probe
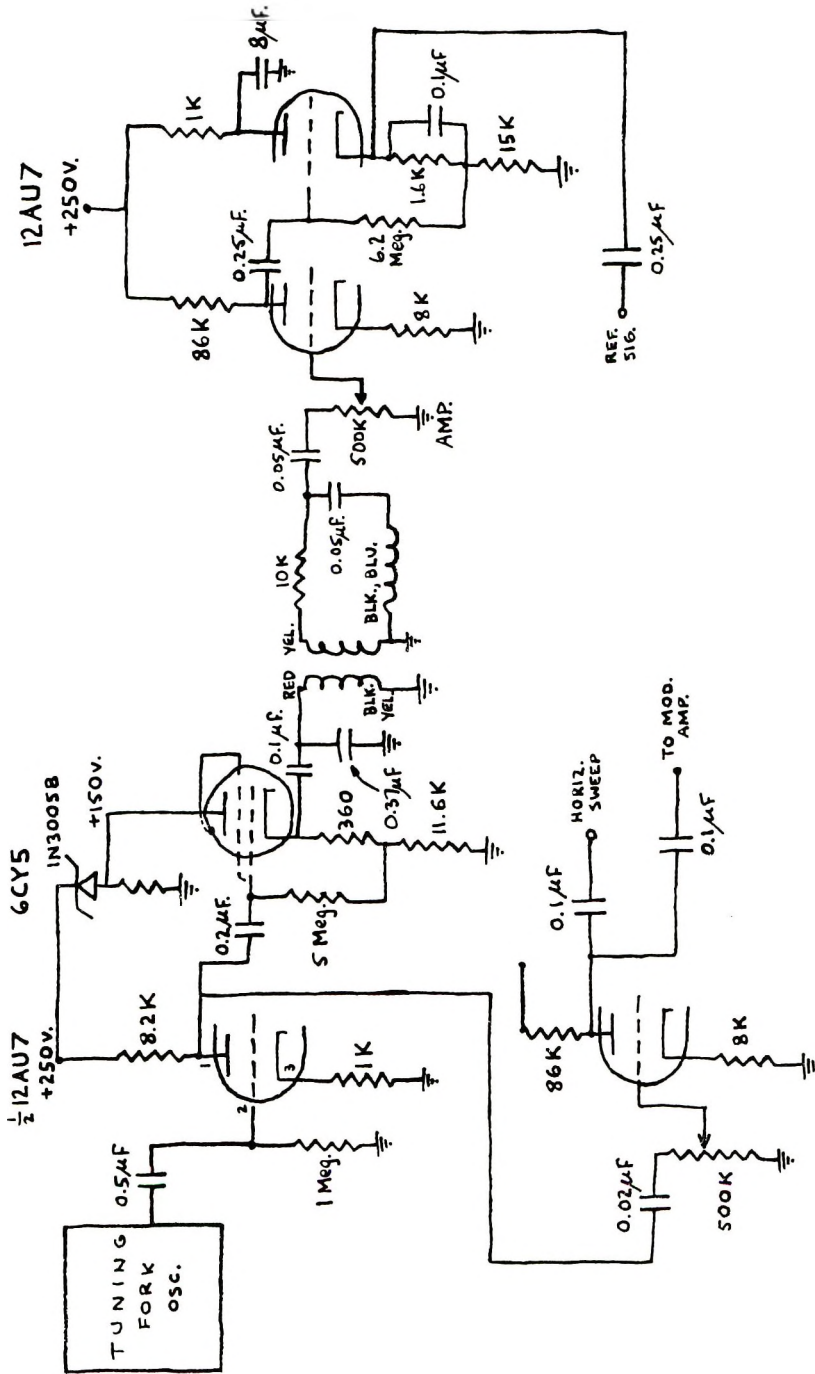
Fig. 2. Modification of modulator in the broadline NMR spectrometer.

assembly, and the temperature was allowed to equilibrate for at least 30 min. before measurements were made.

All temperatures required in this investigation could be achieved by the gas-flow method. Gaseous nitrogen under pressure was forced through a helically wound copper tube immersed in liquid nitrogen. The cooled gas was then fed through a vacuum-jacketed transfer tube and passed over the sample. It was found that, by using backing pressures of 25 psi, liquid nitrogen temperature could thus be obtained. Higher temperatures were reached by decreasing the backing-pressure.

To avoid overmodulation and excessive modulation broadening, samples were generally modulated at amplitudes less than $^1/_3$ their line width. This proved extremely difficult at room temperature, where the lines were quite narrow; however, one branch of one spectrum, which was at least unsplit by overmodulation, was obtained.

Second moments were obtained by an approximate graphical method. The instrumentation used provides one with the derivative of the absorption line. The experimental spectra were divided into small increments of frequency and the amplitudes of the derivative line were read off at these points. Second moments were then calculated with the help of an IBM 1620 computer. An approximation based on the expression of Barrante[3] (for experimental second moments) was incorporated into the program:

$$\langle \Delta H_2 \rangle^2 = {}^1/_3 \int g'(H)(H - H_0)^3 dH / \int g'(H)(H - H_0) dH$$

where $\langle \Delta H_2 \rangle^2$ is the experimental second moment, $g'(H)$ is the derivative of line shape function, $H - H_0$ is the distance (here in cycles/second) from the center of the line.

Results and Discussion

The results for dimethylpolysilazane linear polymer are presented in Table I.

TABLE I
Summary of Numerical Results

Pretransition ($-196°C.$) line width	5.55 ± 0.1 gauss
Pretransition ($-196°C.$) second moment	7.25 ± 0.5 gauss^2
Transition temperature (from line widths)	$-83°C.$
Transition temperature (from second moments)	$-81°C.$

Plots of line widths and second moments versus temperatures are presented in Figures 3 and 4. Measurements were taken between $-196°C.$ and $30°C.$

The experimental second moment is 7.25 ± 0.5 gauss^2. This is considerably lower than the value reported by Barrante[4] for crosslinked dimethylpolysilazanes (viz., 8.5 ± 0.5 gauss^2), but this is to be expected in the light of the following considerations.

The theoretical second moment of a rigid methyl group in a randomly oriented polycrystalline solid[10] is 22.5 gauss^2. In addition, one must take into consideration an intermolecular broadening contribution to account for the effect of neighboring methyl groups. Powles and Gutowski[11] suggest that a gaussian broadening factor of at least 2.0 gauss^2 is necessary to account for a line with no fine structure. Kusumoto et al.[6] further suggest that a broadening factor of 2.0–3.0 gauss^2 is required for agreement of their experimental results for silicones with the theoretical values. Moreover, Andrew and Bersohn,[12] in a study of the nuclear magnetic resonance line shapes for a triangular configuration of nuclei, found that a factor of 2.1 gauss^2 gave the best fit to experimental data. Since the lines obtained in this investigation had no fine structure, a broadening correction of this magnitude is therefore used (see Fig. 5).

In the linear silazane under discussion here, there are also protons bonded to nitrogen, and these must also be taken into account. Barrante[3] has shown, using the equation of Van Vleck,[13] that the second moment for an isolated —NH— group is 1.9 gauss^2.

In a repeating unit of a linear dimethylpolysilazane, there are two methyl groups per —NH— unit. If the chains are held completely rigid at $-196°C.$, the second moment would then be:

$$\langle \Delta H_2 \rangle^2 = (^6/_7)(22.5) + (^1/_7)(1.9) + 2.1 = 21.7 \text{ gauss}^2$$

Thus one sees that the polymer chains are not totally rigid.

Since a C_3 reorientation of methyl groups about the silicon–carbon bond is well known in the siloxanes[5–7] it would be well to assume that such motion is occurring in the silazanes. This motion reduces the intramolecular contribution of the methyl groups to the second moment by a factor of $^1/_4,$[5] but probably does not influence the intermolecular contribution discussed above.[4] If the contribution of the isolated —NH— group is also assumed to be unchanged, then the second moment should be:

$$\langle \Delta H_2 \rangle^2 = (^1/_4)(^6/_7)(22.5) + (^1/_7)(1.9) \pm 2.1 = 7.2 \text{ gauss}^2$$

which agrees quite well with the experimental value. It is therefore reasonable to assume that at $-196°C.$ the only motion occurring in the polymer is reorientation of the methyl groups about the silicon–carbon bond.

An analogous calculation may now be performed for a crosslinked dimethylpolysilazane studied by Barrante.[4] The polymer prepared by Krüger[14] was crosslinked only through tertiary nitrogen atoms, and the ratio of secondary to tertiary nitrogen atoms was approximately 2 to 3. This suggests structures containing eight methyl groups per —NH— unit in each repeating group. One would therefore expect the second moment to be:

$$\langle \Delta H_2 \rangle^2 = ^1/_4(^{24}/_{25})(22.5) + (^1/_{25})(1.9) + 2.1 = 7.6 \text{ gauss}^2$$
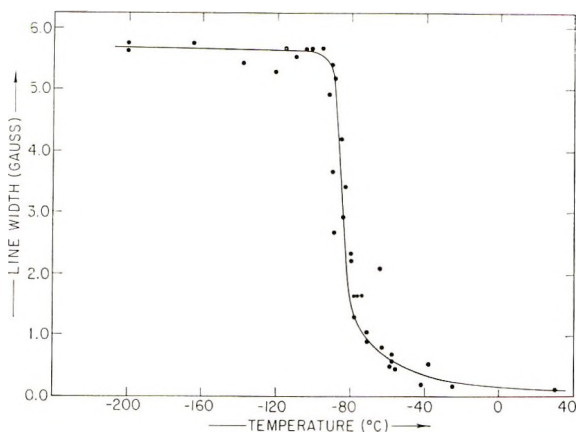
Fig. 3. Linear dimethylpolysilazane: experimental line widths.
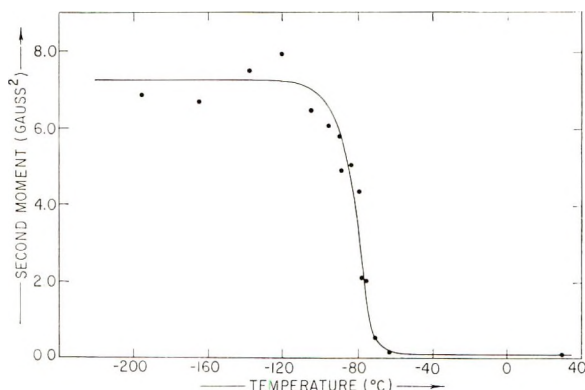
Fig. 4. Linear dimethylpolysilazane: experimental second moments.

which is somewhat higher than that for the linear polymer. Moreover, one might perhaps also expect the intermolecular contribution in the crosslinked system to be somewhat higher than 2.1 gauss.[2] This would explain the results of Barrante.[4]

Since there are only methyl protons in both linear and crosslinked dimethylpolysiloxanes, the above treatment predicts identical liquid nitrogen temperature second moments for these systems:

$$\langle \Delta H_2 \rangle^2 = {}^1/_4(22.5) + 2.1 = 7.7 \text{ gauss}^2$$

This result agrees quite well with the experimental value of 8.0 ± 0.5 gauss[2] obtained by Barrante[2,3] for both linear and crosslinked dimethylpolysiloxanes. Powles et al.[10] report a value of 9.0 gauss[2] for a similar series of polymers. A series of three polymers of this type was also studied by Kusumoto et al.,[6] second moments of 8.4, 8.4, and 7.8 gauss[2] being reported. Finally, a recent study by Huggins et al.[15] reports that dimethylpolysiloxanes, both linear and crosslinked, have low-temperature second
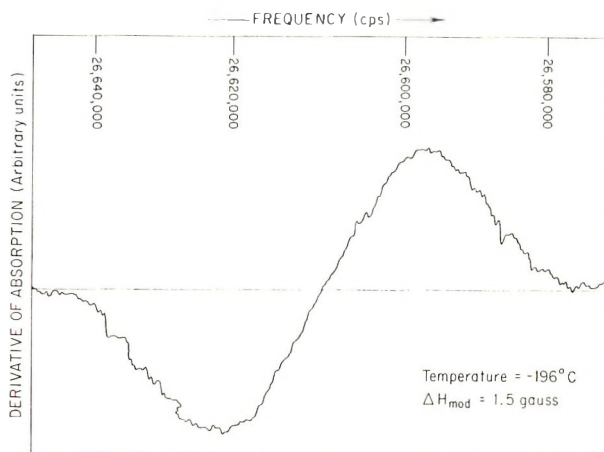
Fig. 5. Experimental derivative line for linear dimethylpolysilazane.

moments of 7.0 ± 0.2 gauss^2. In the light of these data, the above calculation appears to suggest a reasonable value.

As the linear dimethylpolysilazane is warmed from liquid nitrogen temperature, the second moment decreases gradually until roughly $-100°C.$, at which point it begins to drop abruptly. This transition, centered around $-82 \pm 1°C.$, corresponds to the onset of one or more of the motions (other than reorientation of the methyl groups about the silicon-carbon bond) suggested in the introduction. The second moment continues to drop sharply as motion increases, until it reaches a value of less than 0.1 gauss^2 at $30°C.$ The fact that the second moment drops to a value well below the intermolecular broadening contribution suggests translational motion of the chains must be occurring,[7] but does not eliminate the possibility of other modes of motion occurring as well.

This behavior is quite similar to that of linear dimethylpolysiloxane.[2,3] Here, the transition begins at roughly $-130°C.$ and is centered at approximately $-110°C.$ but the general shape of the second moment versus temperature curve is the same. This indicates that the motions in these isoelectronic systems are of the same type. The higher transition temperature for the linear silazane indicates that the silazane chain offers a somewhat greater resistance to internal motion. On the basis of the data available at this time, one can do no more than speculate on the reasons for this. Several possibilities come to mind: (a) hydrogen-bonding effects of the azo proton in the silazane; (b) differences in the steric or electronic requirements of —NH— as opposed to —O—; (c) $d\pi$–$p\pi$ interaction (back bonding) between silicon and nitrogen in the silazanes. The latter effect would certainly increase the force constant for the bending motion of the (—Si—N—) skeleton and would thus serve to necessitate a higher temperature for the onset of this motion. This aspect of the current study is being pursued further.

The linear dimethylpolysilazane exhibits a much sharper transition than that reported for the crosslinked material.[4]   This sharpness may therefore be attributed to the absence of crosslinking.   Precedence for this view may be found by comparing the results of Barrante[3] on the linear dimethylpolysiloxane with those of Huggins et al.[15] on the analogous highly crosslinked system.   Here, too, crosslinking seems to have smeared out the transition.

Conclusion

It is apparent from this investigation that the same types of motion occur in linear dimethylpolysilazane as do in linear dimethylpolysiloxane.   At liquid nitrogen temperature, the only motion occurring in these systems is that of methyl groups reorientating about the silicon–carbon bond.   It is the persistence of this motion to at least $-196°C$. that accounts for the unusual properties of the silicones[5] and suggests similar properties for some silazanes.   There is a somewhat greater resistance to the onset of motion, other than reorientation, in the linear silazane than in the linear siloxane, but the reasons for this can only be speculated upon.   Since the change to low second moments with increasing temperature is abrupt in the linear dimethylpolysilazane but gradual in the crosslinked material, the lesser degree of molecular motion in the latter may be attributed directly to the crosslinking.   Finally, the low value of the second moment of the linear silazane at $30°C$. suggests that translational motion of the chains must be occurring at that temperature.

References

1. Redl, G., and E. G. Rochow, *Angew. Chem.*, **76**, 650 (1964).

2. Barrante, J. R., Ph.D. Thesis, Harvard University, 1963.

3. Barrante, J. R., ONR Technical Report, Contract No. Nonr-1866 (13), August 1963.

4. Barrante, J. R., and E. G. Rochow, *J. Organometallic Chem.*, **1**, 273 (1964).

5. Le Clair, H. G., and E. G. Rochow, *J. Inorg. Nucl. Chem.*, **1**, 92 (1955).

6. Kusumoto, H., I. J. Lawrenson, and H. S. Gutowski, *J. Chem. Phys.*, **32**, 724 (1960).

7. Huggins, C. M., L. E. St. Pierre, and A. M. Bueche, *J. Phys. Chem.*, **64**, 1304 (1960).

8. Englert, G., and R. J. Volpicelli, ONR Technical Report, Contract No. Nonr-1866(13), February 1962.

9. Volpicelli, R. J., ONR Technical Report, Contract No. Nonr-1866(13), March 1962.

10. Powles, J. G., A. Hartland, and J. A. E. Kail, *J. Polymer Sci.*, **55**, 1304 (1961).

11. Powles, J. G., and H. S. Gutowski, *J. Chem. Phys.*, **21**, 1695 (1953).

12. Andrew, E. R., and R. Bersohn, *J. Chem. Phys.*, **18**, 159 (1950).

13. Van Vleck, J. H., *Phys. Rev.*, **74**, 1168 (1948).

14. Krüger, C. R., and E. G. Rochow, *Angew. Chem.*, **74**, 588 (1962).

15. Huggins, C. M., L. E. St. Pierre, and A. M. Bueche, *J. Polymer Sci. A*, **1**, 2731 (1963).

Résumé

Un polymère linéaire de diméthylpolysilazane a été préparé et la mobilité interne étudiée par des techniques de résonance nucléaire magnétique à large raie. Les seconds moments et la largeur des raies ont été rapportés comme fonctions de la température entre −196° et 30°C. Les résultats sont comparés à ceux obtenus pour le diméthylpolysilazanes linéaire, aussi bien qu'à ceux pour les siloxanes et silazanes pontés. Les seconds moments expérimentaux a basse température de 7.25 ± 0.5 gauss² correspondent à la réorientation du C_3 des groupes méthyles autour du lien silicum–carbone. Les mouvements qui se passent au sein du silazane sont trouvés identiques à ceux pour le siloxane correspondant. La transition des seconds moments se passent approximativement à 30°C plus élevés que dans le silazane linéaire. Ceci est attribué à la résistance quelque peu plus élevée à la motion dans les silazanes.

Zusammenfassung

Ein lineares Dimethylpolysilazanpolymeres wurde dargestellt und sine innere Bewegung nach dem kernmagnetischen Breitlinienresonanzverfahren untersucht. Die zweiten Momente und die Linienbreiten werden als Temperaturfunktion von −196 bis 30°C mitgeteilt. Die Ergebnisse werden mit denjenigen an linearem Dimethylpolysiloxan und mit denjenigen an vernetztem Siloxan und Silazan verglichen. Das experimentelle zweite Moment bei tiefer Temperatur von 7,25 ± 0,5 Gauss² entspricht einer C_3-Reorientierung der Methylgruppen um die Silizium-Wasserstoffbindung. Im Silazan trait die gleiche Bewegung wie in dem entsprechenden Siloxan auf. Der Übergang zu niedrigen zweiten Momenten tritt bei dem linearen Silazan um etwa 30°C höher auf als bei dem linearen Siloxan. Das wird auf einen etwas grösseren Bewegungswiderstand im Silazan zurückgeführt.

Structure–Property Relationships of Poly(vinyl Alcohol). I. Influence of Polymerization Solvents and Temperature on the Structure and Properties of Poly(vinyl Alcohol) Derived from Poly(vinyl Acetate)

H. N. FRIEDLANDER, H. E. HARRIS, and J. G. PRITCHARD,*
Chemstrand Research Center, Inc., Durham, North Carolina

Synopsis

The solubility properties of poly(vinyl alcohol) (PVA) vary with the method of preparation of the poly(vinyl acetate) (PVAc) from which it is derived. PVAc was prepared with free-radical catalysts over a range of temperatures from −78 to 90°C. with solvents of varying chain-transfer ability. The corresponding PVA samples varied in their resistance to dissolution in water. Their high-resolution proton nuclear magnetic resonance spectra showed no differences in tacticity. Data on 1,2-diol content showed only minor differences. Hence, the increase in resistance of PVA to dissolution in water arising from changes in chain-transfer activity of the solvent used in vinyl acetate polymerization is largely attributable to a decrease in molecular weight, and the increase in resistance of PVA to dissolution in water arising from a decrease in the temperature of the vinyl acetate polymerization is largely attributable to a decrease in both long and short branches. Evidently, with polar polymers having small side groups, tacticity is not the only factor influencing property variation; that is, variations in stereoregularity influence more the crystallinity of the sample as measured by density or x-ray methods than the ultimate crystallizability under conditions of mechanical and thermal treatment. In this regard polar polymers having small side groups differ from nonpolar polymers.

INTRODUCTION

The physical properties of a crystalline polymer in bulk or as a fiber are influenced by the morphological forms in which the polymers will crystallize[1] and by the kinetics of the crystallization process,[2] both of which ultimately depend on the specific structure of the polymer molecule.[3] In nonpolar polymers, such as polyethylene, the linearity of the molecule strongly influences the effective packing in a crystal and thus the density and melting point.[4] In polypropylene, for example, the stereoregularity has a marked effect on crystallizability and physical properties.[5] Atactic polypropylene is amorphous and cannot be crystallized, whereas isotactic polypropylene crystallizes readily to a high-melting solid, as does also syndiotactic polypropylene.[6] As means of preparing polar polymers with

* Present address: IIT Research Institute, Illinois Institute of Technology, Chicago, Illinois.

different stereoregularity were found, it was expected that their properties also would be strongly influenced by stereoregularity.[7]

However, the crystallization of polar polymers is already influenced by dipole–dipole interactions or hydrogen bonds with the polar groups which may override the influence of stereoregularity. Furthermore, in the case of such polar polymers as polyacrylonitrile and poly(vinyl alcohol) having small polar side groups, the crystal lattice appears to be able to accommodate the side groups whatever their steric configuration.[8] Therefore, it was of interest to determine whether and to what extent the properties of poly(vinyl alcohol) are influenced by stereoregularity or by other structural regularities.

More syndiotactic poly(vinyl alcohol) (PVA) can be made from poly-(vinyl trifluoroacetate) (PVTFAc)[9] or more isotactic from poly(vinyl tert-butyl ether) (PVTBE).[10] Moreover, PVA with varying physical properties can also be made from poly(vinyl acetate) (PVAc) by varying the solvent[11] and temperature[12] used in the vinyl acetate polymerization. It had been suggested, based solely on physical property evidence, that both in the latter case and in poly(vinyl chloride)[12,14] changes in stereoregularity were occurring. Because there was available a method for converting PVAc to PVA without loss of stereospecificity[15] and an NMR method for characterizing the tacticity of PVA,[16] it was desirable to investigate in more detail the structure and properties of PVA made from PVAc polymerized under varying conditions of solvent and temperature.

EXPERIMENTAL

Preparation of Polymers

Poly(vinyl Acetate). Poly(vinyl acetate) samples were prepared by polymerization of freshly distilled vinyl acetate, in bulk or in the desired solvent, under nitrogen. A three-necked flask fitted with a condenser protected with a drying tube, a Tru-Bore stirrer, and a rubber cap through which samples could be withdrawn was immersed in an oil bath and used for the polymerization which was initiated at 30°C. by azobisisobutyronitrile and light from a mercury lamp. Above 30°C. the mercury lamp was not used. Polymerizations at 0 and −78°C. were carried out in capped bottles in the presence of triethylborane and oxygen.[17]

The resulting PVAc was isolated by precipitation in hexane and further purified by several reprecipitations in hexane and in water from acetone solution.

Poly(vinyl Alcohol). Conversion of PVAc to PVA was accomplished by base-catalyzed saponification of a methanolic solution of PVAc at about 50°C. The PVA usually precipitated after 2 hr., but the reaction was allowed to continue for 12 hr. Under these conditions the saponification should be at least 99% complete.[18] The resulting PVA was purified by several precipitations in methanol and in acetone from water solution and by extraction with methanol.

Each PVA sample is referred to by a letter that corresponds to the letter designating the PVAc sample from which it was derived. Vinol 125 (designated V) is a commercial PVA of the Air Reduction Company made by "super hydrolysis" of PVAc prepared at about 60°C.

Cleaved PVA for NMR Studies. High molecular weight PVA samples were cleaved by periodate at the head-to-head placements (1,2-diol units) by the following procedure to yield polymer of low molecular weight suitable for high-resolution NMR studies.

To a chilled (10°C.) solution of 2 g. of PVA in 100 ml. of water was added 2 ml. of 5–10% aqueous $NaIO_4$. After 15 min. ethylene glycol was added to destroy excess periodate. The cleaved polymer was isolated by precipitation in acetone, washed with ether, and dried. In order to reduce extraneous carbonyl groups, the dried product was dissolved in 50 ml. of water, and 5 ml. of $1N$ sodium hydroxide solution containing 0.2 g. of $NaBH_4$ was added. After 15 min. the solution was acidified with $1N$ hydrochloric acid, and the product was isolated and then extracted for 3 days with the isopropanol–water azeotrope to remove residual boric acid.[19]

The cleaved samples are quite low in molecular weight with intrinsic viscosities of around 0.1 to 0.2[20] and are designated by the subscript x following the letter designation of the corresponding PVA. Samples with initial $[\eta]$ below 0.2 were not cleaved because of their low initial molecular weight.

Polymer Tests

Viscosities. Viscosity measurements on aqueous solutions of the PVA samples were carried out at 25.0°C. in an Ubbelohde viscometer. Intrinsic viscosities were obtained by extrapolating to infinite dilution a plot of η_{sp}/c versus c, where c is the concentration of PVA in grams per deciliter.

Head-to-Head Units. Determinations of 1,2-diol content in the PVA samples were carried out by using a titrimetric procedure described previously.[20]

Dissolution Temperature in Water. The temperature at which the PVA goes into solution was determined by heating 0.2 g. of the PVA sample with 2.0 ml. of water in a sealed tube at a fixed temperature for 2–3 hr. The temperature at which solution occurred within this time was thus obtained by averages of two or three determinations within ±5°C.

Determination of Stereoregularity

Solutions of the PVA samples (15%) in D_2O were prepared and their spectra obtained with a Varian DP-60 spectrometer equipped with a Varian variable temperature probe. Most of the quantitative measurements were obtained from spectra recorded at 175°C. The tacticity measurements determined from the spectra are estimated to be accurate to ±5%.

RESULTS

The specific methods and conditions of polymerization of the PVAc samples are described in Table I. PVAc was prepared below room tem-

TABLE I
Conditions of Preparation of Poly(vinyl Acetate) Samples

Sample	Polymerization temp., °C.	Catalyst system	Vinyl acetate, mole-% in solvent	Solvent
A	−78	BEt₃–air	50	Amyl acetate
B	0	BEt₃–air	50	Amyl acetate
C	25	AIBN–$h\nu$	50	n-Butyraldehyde
D	30	AIBN–$h\nu$	50	Isobutyraldehyde
E	30	AIBN–$h\nu$	35	Methyl ethyl ketone
F	30	AIBN–$h\nu$	100	Vinyl acetate
G	90	AIBN	50	Amyl acetate

perature with a triethylborane–oxygen initiator and above room temperature with azobisisobutyronitrile. Samples were made in bulk, in a relatively inert solvent, amyl acetate, and in aldehyde and ketone solvents with high chain-transfer activity. The latter solvents yield low molecular weight polymers. In physical appearance the PVAc samples varied from rubbery (the high molecular weight materials) to viscous oils (the low molecular weight materials). The corresponding PVA samples were all solids.

In Table II are given some properties of the PVA samples. The per cent of 1,2-diol units (a measure of the per cent of head-to-head polymerization) as measured by the periodate titration procedure[20] is given for the original PVA samples. Intrinsic viscosity data obtained in water at 25°C. for both the original PVA samples and the corresponding samples cleaved

TABLE II
Characterization of Poly(vinyl Alcohol) Samples

Sample	1,2-Diol content, %	$[\eta]^{25°C.}_{H_2O}$, dl./g.	Dissolution Temp. in H_2O, °C. ± 5
A	—	0.34	85
B	—	0.36	75
C	1.16 ± 0.02	0.101	95
D	1.2 ± 0.1	—	—
E	1.27 ± 0.04	0.22	75
F	1.30 ± 0.02	1.78	55
V	1.66 ± 0.07	0.84	60
G	1.98 ± 0.03	0.28	50
C_x	—	0.099	—
E_x	—	0.14	—
F_x	—	0.17	85
V_x	—	0.14	95

TABLE III

Estimate of Tacticity of PVA from Nuclear Magnetic Resonance Spectra

Sample	Diads		Triads		
	I, %	S, %	I, %	H, %	S, %
A_x	42	58	28	42	30
C	43	57	27	42	31
D	42	58	—	—	—
E	45	55	29	41	30
F_x	42	58	29	39	32
V_x	43	57	—	—	—
G_x	42	58	—	—	—

with periodate are included. It is possible to estimate the molecular weight from the intrinsic viscosity data using equations found in the literature. However, since these equations do not agree with each other, we prefer to submit only the viscosity data.

Finally, there are also included in Table II data on the approximate dissolution temperature ($\pm 5°C.$) in water of some of the original and cleaved PVA samples. More precise measurements of water resistance of PVA films and dissolution temperature in organic solvents of PVA crystallized from dilute solution will be the subject of subsequent reports from this laboratory.

The water resistance of PVA increases as the temperature of preparation of the PVAc from which it was derived decreases. The water resistance of PVA also increases as the chain-transfer activity of the solvent increases. Most of this latter increase results from the lower molecular weight of the sample as can be seen by comparing the results obtained with cleaved samples.

In Table III are given estimates of the tacticity of the PVA samples based on high-resolution proton nuclear magnetic resonance spectra. The method of analysis is described elsewhere.[16] Samples of low molecular weight give spectra with considerably better resolution. Therefore, all the data presented here were obtained from cleaved samples except those which were already of sufficiently low molecular weight. The data given in Table III indicate that the tacticity of these samples are all identical, well within the estimated error of $\pm 5\%$.

Diad measurements were obtained from the β-proton (methylene proton) spectra which have been shown to consist of a triplet from isotactic placements and a triplet from syndiotactic placements. Typical spectra from β-protons of PVA are illustrated in Figure 1 for samples F_x, D, and E. Two overlapping triplets are clearly seen. The higher frequency peaks in each pair are associated with isotactic diads and the others with syndiotactic diads. The similarity of the spectra of the three samples is clearly seen in the figure.

Triad measurements were obtained from the α-proton (methinyl proton) spectra which have been shown to consist of three overlapping quintets, one
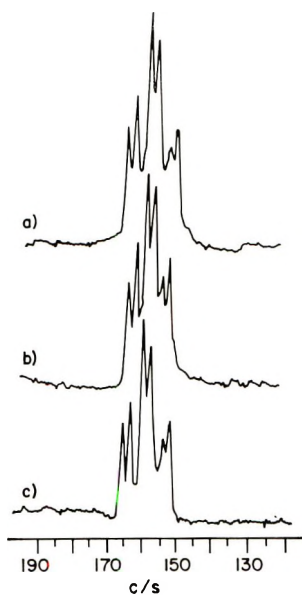
Fig. 1. Nuclear magnetic resonance spectra of the β-proton region of poly(vinyl alcohol) samples from poly(vinyl acetate) polymerized: (a) in bulk (sample F_x), (b) in isobutyraldehyde (sample D), (c) in methyl ethyl ketone (sample E).
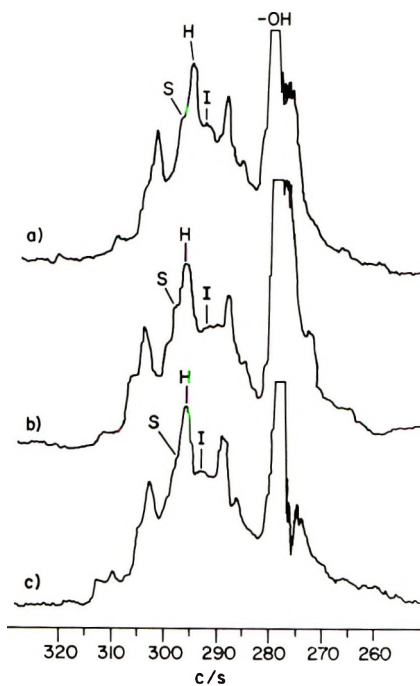
Fig. 2. Nuclear magnetic resonance spectra of the α-proton region of poly(vinyl alcohol) samples from poly(vinyl acetate) polymerized: (a) in bulk (sample F_x), (b) in n-butyraldehyde (sample C), (c) in methyl ethyl ketone (sample E).
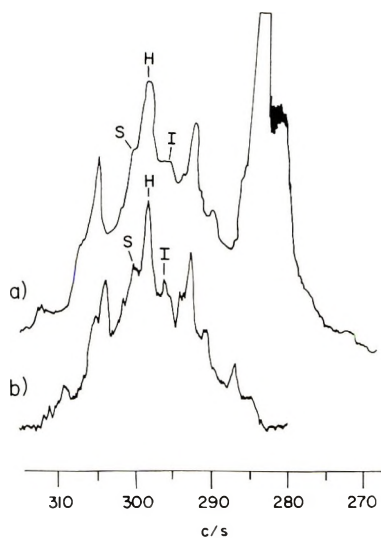
Fig. 3. Nuclear magnetic resonance spectra of the α-proton region of poly(vinyl alcohol) samples from poly(vinyl acetate) polymerized at (a) 30°C. (sample F_x) and (b) −78°C. (sample A_x).

each from syndiotactic, heterotactic, and isotactic placements. Figure 2 illustrates the complex α-proton spectra for samples F_x, C, and E. Some of the peaks are covered by the intense —OH proton peak at 279 cycles/sec. The highest frequency peak in each set is attributed to syndiotactic triads and the lowest to isotactic triads. As labeled in the figure, this assignment is in accord with the structure of PVA from poly(vinyl trifluoroacetate) and poly(vinyl tert-butyl ether) and with the analysis of the β-proton region as already described.[16] Again, the similarity of the α-proton spectra from various samples is clearly seen, as it is also in Figure 3 which shows a comparison of the α-proton spectra of samples F_x and A.

DISCUSSION

Factors Influencing Molecular Regularity in PVA

During polymerization initiated by free radicals, a number of reactions, competing with regular head-to-tail monomer addition to the propagating free-radical species, influence molecular regularity. The stereochemistry of the activated complex of a radical at the moment of monomer addition controls the tacticity of each monomer placement. Occasionally monomer units will add in a head-to-head configuration. In addition a number of transfer reactions lead to chain branching. Intermolecular transfer with polymer molecules leads to long chain branches whereas intramolecular transfer (backbiting) leads to short-chain branches. Finally transfer with solvent leads to variation in the molecular weight of the polymer.

Tacticity. As a vinyl monomer with a single substituent ($H_2C{=}CHX$) adds to the propagating free radical, it forces the ultimate monomer unit

into either a syndiotactic or isotactic configuration with respect to the penultimate monomer unit.[21] Ordinarily the propagating free radical (unsolvated or symmetrically solvated) is planar, and the selection between the two configurations is made on the basis of an energy difference between the two activated complexes of less than 775 cal./mole.[22-24] Bulky substituents might be expected to increase this energy difference and to enhance entropy differences as well.[25] Nevertheless, steric interactions in free-radical polymerization operate only between the substituents of the penultimate group and the ultimate group under the influence of the approaching reactive monomer.[26] Furthermore, electrostatic repulsion, which is so important in selecting between stereoplacements in ionic and coordinate polymerization, plays a less important role in free-radical polymerization.[28,29]

Nevertheless, one expects that as the temperature of polymerization is lowered, the slight energy difference between the two activated complexes would become a larger proportion of the total energy of reaction and thus would increase the probability of forming the less energetic isomer, namely the syndiotactic form.[22,23] Lowering the polymerization temperature increases the syndiotacticity of poly(vinyl haloacetates)[28,30] and the isotacticity of poly(vinyl ethers).[10,27] It is postulated to have a similar effect on vinyl chloride[13] and vinyl acetate[12] polymerization.

Coordination with solvent, particularly in an asymmetric complex, is postulated to have an influence on the selection between stereoconfigurations.[31,32] Therefore, solvent changes (especially solvents strongly complexed to the propagating free radical species) may change polymer tacticity. The effect of solvent change on cationic polymerization of vinyl ethers is well established.[27] Similar effects were postulated for vinyl chloride[14,v3] and vinyl acetate[11] polymerized by free radicals in aldehyde and ketone solvents. A mechanism for the stereoselection based on a growing radical complex has been proposed to explain the differences observed in physical properties of polymers made in these solvents.[31,32] The complex was thought to increase both the bulk and polarity of the propagating radical.

One should note that as each monomer unit is attached to the chain there is an *a priori* probability of formation of a syndiotactic or isotactic pair.[21] The configuration of adjacent pairs of monomers in the polymer as measured by β-hydrogen atoms in proton NMR spectra—so-called diad placements—are a measure of this probability. However, penultimate effects and longer-range coordination (as in the case of heterogeneous catalysts) influence the sequence length of such placements. This influences the stereoblock character of the polymer. The configurations of α-hydrogen atoms relative to each nearest neighbor as observed in proton NMR spectra—the so-called triad placements—are a measure of the first order of such longer-range influences.

Head-to-Tail Placement. Ordinarily steric and polar forces are sufficiently selective to assure head-to-tail placement of monomers in free-

radical polymerization.[34]   However, to the extent that this selectivity is weak, some head-to-head (or tail-to-tail) placement occurs.   In PVAc this yields adjacent acetate groups along the polymer chain that on hydrolysis yield 1,2-diol units.   These units can be cleaved by periodate and quantitatively measured by changes in viscosity[35] or better by iodometric titration.[20]   From 1 to 2% of 1,2-diol units are found in PVA made from free-radical catalyzed PVAc.   The 1,2-diol content was found to be independent of molecular weight and polymerization solvent but to decrease with decreasing temperature of polymerization.   The energy of activation difference of the head-to-head placements versus head-to-tail was 1.6 kcal./mole in favor of the latter mode, and the ratio of frequency factors was 0.19, also favoring head-to-tail placement.[20,35]

Chain Transfer.   Chain transfer with monomer introduces unsaturated endgroups in PVAc and affects molecular weight but does not influence the structure of the polymer chain.   However, transfer with polymer introduces branches.[36]

In general, reducing the temperature of polymerization increases the rate of the propagation reaction relative to the various chain transfer processes.   Therefore, polymers made with free-radical catalysts at low temperature are expected to be of higher molecular weight and more linear, all other conditions being equal.

Intermolecular transfer leads to long-chain branching.   It is well known that such branching occurs in PVAc quite readily in the acetoxy methyl group.[37]   This reaction involves hydrogen abstraction and further polymerization at the acetoxy methyl group [eq. (1)].

$$\sim CH_2-CH\cdot + \sim CH_2-CH-CH_2\sim \rightarrow \sim CH_2-CH_2-OCOCH_3$$
$$\qquad\qquad |\qquad\qquad\quad |$$
$$\qquad\quad OCOCH_3\qquad OCOCH_3$$

$$+ \sim CH_2-CH-CH_2\sim \xrightarrow{CH_2=CHOCOCH_3} \sim CH_2-CH-CH_2\sim \qquad (1)$$
$$\qquad\qquad |\qquad\qquad\qquad\qquad\qquad\qquad\qquad\qquad |$$
$$\qquad\quad OCOCH_2\cdot\qquad\qquad\qquad\qquad\qquad\qquad OCOCH_2CH_2CH\cdot$$
$$\qquad\qquad\qquad\qquad\qquad\qquad\qquad\qquad\qquad\qquad\qquad\quad |$$
$$\qquad\qquad\qquad\qquad\qquad\qquad\qquad\qquad\qquad\qquad\qquad OCOCH_3$$

The result is a hydrolyzable branch, so named because during hydrolysis (or alcoholysis) of the PVAc to PVA the branched chain is released [eq. (2)].   Thus, a decrease in molecular weight results

$$OCOCH_2\sim \qquad\qquad\qquad\qquad\qquad OH$$
$$\quad |\qquad\qquad\qquad\qquad\qquad\qquad\qquad\quad |$$
$$\sim CH_2-CH-CH_2\sim + CH_3OH \xrightarrow{CH_3O^-} \sim CH_2-CH-CH_2\sim + CH_3OCO-CH_2\sim$$
$$\qquad\qquad\qquad\qquad\qquad\qquad\qquad\qquad\qquad\qquad\qquad\qquad\qquad\qquad\qquad (2)$$

upon saponification.[38-40]   Hence, branching of this type during the polymerization does not result in branching in the PVA.   Abstraction of an α-proton, however, would result in a nonhydrolyzable long-chain branch, that remains in the derived PVA [eq. (3)].

$$\text{wCH}_2\text{—CH} \cdot + \text{wCH}_2\text{—CH—CH}_2\text{w} \rightarrow \text{wCH}_2\text{—CH}_2\text{OCOCH}_3$$
$$\qquad\quad |\qquad\qquad\qquad |$$
$$\qquad\quad \text{OCOCH}_3 \qquad\quad \text{OCOCH}_3$$

$$+ \text{wCH}_2\text{—C—CH}_2\text{w} \xrightarrow{\ \text{CH}_2=\text{CHOCOCH}_3\ } \text{wCH}_2\text{—C} \qquad\qquad (3)$$

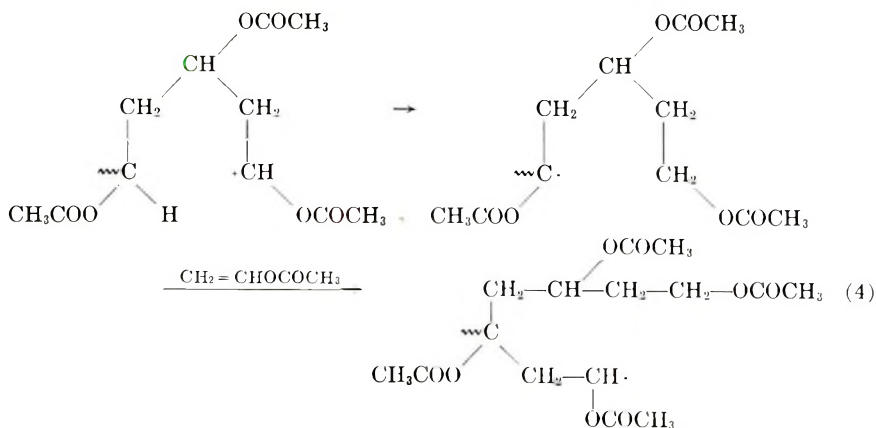(structures with OCOCH₃, CH₂—CH·, CH₂w, OCOCH₃ branches)

According to chain-transfer studies, the hydrogen atoms in the α-position are more reactive than those on the acetoxy methyl group. Chain-transfer constants in vinyl acetate polymerization at 60°C. are given for the italicized hydrogen atoms in structures I, II, III.[41]

$$\begin{array}{ccc}
\text{O} & \text{O} & \\
\| & \| & \text{O} \\
\text{O—C—CH}_3 & \text{O—C—}CH_3 & \| \\
| & | & \text{O—C—}CH_3 \\
\text{CH}_3\text{—C—CH}_3 & \text{C=CH}_2 & | \\
| & / & \text{CH}_3 \\
H & H & \\
0.0008 & 0.00025 & 0.00025 \\
\text{I} & \text{II} & \text{III}
\end{array}$$

Therefore, one could expect nonhydrolyzable branching by the chain-transfer mechanism to occur in PVAc about three times as readily as the hydrolyzable type. One can estimate the number of branch points of the hydrolyzable type per hundred monomer units from viscosity data on hydrolysis of PVAc.[40] At the 20% conversion level at 67–70°C. there is about one branch in 30,000 units. Therefore, we would estimate that nonhydrolyzable branching occurs about three times as frequently, that is one branch in 10,000 units, or one branch per poly(vinyl acetate) molecule of a molecular weight of 860,000. Additional chain transfer through β-hydrogen atoms would suggest that this estimate of long chain branches is probably low.

Intramolecular chain transfer leading to short-chain branching is well known in free-radical polymerization of ethylene.[42] The process occurs by the growing free radical "backbiting" through a six-membered ring intermediate and yields a four-carbon atom short side chain [eq. (4)].

(reaction scheme (4) showing backbiting mechanism with OCOCH₃, CH, CH₂, C, CH₃COO, H groups)

$$\text{CH}_2\text{—CH—CH}_2\text{—CH}_2\text{—OCOCH}_3 \qquad (4)$$

The growing short branch after addition of the first monomer unit has a high probability of "backbiting" again, and a cluster of two-carbon atom side chains occurs. These clusters have been observed in polyethylene.[43-45] The cluster process might also occur after chain transfer in the middle of a polymer molecule.

Intramolecular transfer is known to be an important process in the homogeneous polymerization of ethylene leading to a large number of short branches,[46] and it may be at least as important in vinyl acetate polymerization. At the present time there is no good method for estimating the number of short-chain branches in PVA. Some differences in the ease of hydrolysis of acetate groups in PVAc may be associated with their relative position with respect to the branch and cluster points; that is, some are esters of primary or tertiary hydroxyl groups, whereas the normal acetate group is an ester of a secondary hydroxyl group.

Finally, chain transfer can occur with the solvent which in general only affects the endgroups and molecular weight but not directly the structure of the polymer chain. In fact, the solvents used to modify PVAc, namely aldehydes and ketones, are excellent chain-transfer agents in free-radical polymerization.[41] The molecular weight of the PVAc obtained is directly related to the chain-transfer ability of these solvents. However, the ease of chain transfer to solvent may have a large indirect effect on the branching reactions by competing with the inter- and intramolecular chain transfer processes. Thereby the polymer of lowest molecular weight made in solvents with the largest chain transfer constants should be the most linear. Furthermore, coordination of the growing free radical with solvent, as postulated to influence steric placement, would increase the effective bulk of the reactive end and thereby reduce still more the ability to form branches through intra- and interchain transfer with polymer.

Influence of Solvent

Clearly, from the data presented in Table III, the tacticity of PVA is independent of the solvent used in the corresponding vinyl acetate polymerization (note especially samples C, D, E, and F_x, associated with differing polymerization solvents). With these same materials (samples C, D, E, and F), variation in the 1,2-diol content, which measures change in head-to-tail content, is too small to affect polymer properties.

Therefore, the observed reduced solubility of PVA made from PVAc polymerized in aldehyde or ketone solvents,[11] observed here as higher dissolution temperature in H_2O for sample C and E compared with F, must result either from a change in content of branches or from a change in molecular weight. Figure 4 indicates a correlation between the dissolution temperature in H_2O and the molecular weight of the sample expressed as the logarithm of the intrinsic viscosity for samples C, E, F, and F_x made at 25–30°C. in various solvents. Data on V and V_x are also included.

The dissolution temperature in H_2O of these samples is an indication of their crystallinity, which is influenced by the rate of crystallization during
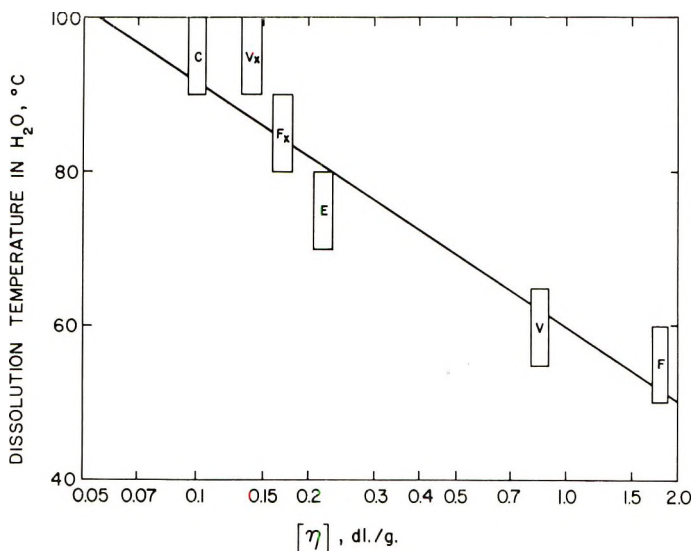
Fig. 4. Correlation of the dissolution temperature of poly(vinyl alcohol) samples and the logarithm of their intrinsic viscosity measured in water at 25°C.

precipitation that is in turn affected by molecular weight. It is well known in the case of polyethylene that lower molecular weight samples crystallize more readily.[47,48] Similar observations can be made on poly(vinyl chloride).[49] However, the solubility and crystallinity of carefully annealed samples or carefully crystallized samples made by crystallization in dilute solutions do not show a significant influence of molecular weight.[50]

The speculation in the literature concerning the influence of carbonyl solvents on the properties of poly(vinyl chloride)[14,31,32] or PVA made from PVAc prepared in such solvents[11] in terms of increased stereoregularity must be incorrect.[51,52] The changes in physical properties of the PVA samples made from PVAc polymerized in carbonyl solvents are adequately explained by the changes in molecular weight associated with the chain-transfer character of these solvents in free-radical polymerization. Furthermore, the mechanisms developed to explain the steric or electronic influence of solvents on growing free radicals become unnecessary.

Influence of Temperature

Clearly, from the data presented in Table III for samples A, B, F_x, V_x, and G_x, the tacticity of PVA is independent of the polymerization temperature of the PVAc from which it was derived. The increasing 1,2-diol content with increasing PVAc polymerization temperature is not great enough to be a major factor in influencing the physical properties of the PVA samples. The activation energy for head-to-head placements versus head-to-tail is only 1.6 kcal./mole. Therefore, the influence of temperature on changing the head-to-tail ratio is quite small.
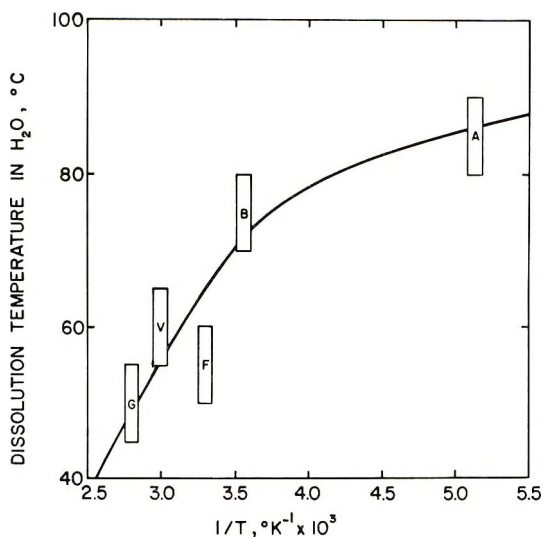
Fig. 5. Correlation of the dissolution temperature of poly(vinyl alcohol) samples in water with the reciprocal of the absolute temperature of polymerization of the poly(vinyl acetate) from which they were made.

However, the water solubility of the PVA samples increases as the temperature of polymerization increases. This is illustrated in Figure 5, where the dissolution temperature in H_2O is plotted against the reciprocal of the absolute temperature of the polymerization of the corresponding PVAc for samples A, B, F, V, and G. Because these samples differ in molecular weight, which as shown in the previous section affects water solubility, the correlation is rough.

Correcting for molecular weight effects and eliminating tacticity and head-to-head placement as factors influencing water resistance, the only remaining factor influencing solubility is change in the degree of branching of the PVA. As the temperature of polymerization is lowered the intramolecular and intermolecular chain transfer processes are reduced relative to chain propagation, and a more linear polymer results. Similar increases in linearity at lower polymerization temperatures are well known in other polymerization systems, for example, polyethylene.[53,54] The more linear polymers are more crystalline and presumably, therefore, more water-resistant, to the extent that crystallinity influences solubility.

CONCLUSION

In PVAc polymerized with free radicals, changes in tacticity, as measured in the corresponding PVA obtained by hydrolysis, are not observed as the polymerization temperature and the solvent media are varied. Nevertheless, changes in crystallinity[11,12] and water solubility of these PVA samples are observed, which in the past were attributed to tacticity changes in analogy to similar observations in nonpolar polymers. Therefore, the

variation in solubility properties of these PVA samples must arise from other structural factors; for example, from differences in molecular weight associated with changes in polymerization media and from changes in the degree of branching associated with changes in polymerization temperature. Apparently other polar vinyl polymers with small side groups, polyacrylonitrile and poly(vinyl chloride), behave similarly.

However, changes in tacticity do occur in polymerization of other vinyl monomers such as vinyl formate,[55-57] vinyl haloacetates,[28,30] alkyl acrylates,[58] and alkyl methacrylates[7,59] as the temperature and solvent are varied. However, even in these cases variations in physical properties are small, and influenced by differences in molecular weight and branching as well as tacticity.[50,60] In this regard the polar polymers appear to differ from the nonpolar polymers, where small changes in tacticity and other structural regularity factors play an important role in polymer properties.

It has been shown that mechanical treatment of PVA fibers at higher temperatures in the presence of hydrogen bond-breaking reagents[61,62] leads to as high a degree of crystallinity as can be obtained through changes in tacticity or other structural regularity factors. The major effect of a tacticity change appears, therefore, to be on crystallinity or solubility rather than on crystallizability, just as in the case of a change in molecular weight or branching. This will be discussed more fully in the following publications from our laboratory dealing with solubility of carefully crystallized samples[50] and with the properties of carefully annealed PVA films made from some of the samples discussed here and from other samples of varying tacticity.[60]

References

1. Lindenmeyer, P. H., *J. Polymer Sci. C*, **1**, 5 (1963); *Textile Res. J.*, **34**, 825 (1964); *SPE Trans.*, **4**, 157 (1964).

2. Hoffman, J. D., *SPE Trans.*, **4**, 315 (1964).

3. Bunn, C. W., *J. Appl. Phys.*, **25**, 820 (1954).

4. Walter, E. R., and F. P. Reding, *J. Polymer Sci.*, **21**, 561 (1956).

5. Miller, R. L., *J. Polymer Sci.*, **57**, 975 (1962).

6. Natta, G., I. Pasquon, and A. Zambelli, *J. Am. Chem. Soc.*, **84**, 1488 (1962).

7. Fox, T. G, W. E. Goode, S. Gratch, C. M. Huggett, J. F. Kincaid, A. Spell, and J. D. Stroupe, *J. Polymer Sci.*, **31**, 173 (1958).

8. Bunn, C. W., *Nature*, **161**, 929 (1948); C. W. Bunn and H. S. Peiser, *Nature*, **159**, 161 (1947).

9. Haas, H. C., E. S. Emerson, and N. W. Schuler, *J. Polymer Sci.*, **22**, 291 (1956).

10. Okamura, S., T. Kodama, and T. Higashimura, *Makromol. Chem.*, **53**, 180 (1962).

11. Aleksandru, L., M. Oprisch, and A. Chiocanel, *Vysokomolekul. Soedin.*, **4**, 613 (1962).

12. Imai, K., and M. Matsumoto, *J. Polymer Sci.*, **55**, 335 (1961).

13. Fordham, J. W. L., P. H. Burleigh, and C. L. Sturm, *J. Polymer Sci.*, **41**, 73 (1959).

14. Burleigh, P. H., *J. Am. Chem. Soc.*, **82**, 749 (1960).

15. Pritchard, J. G., and R. L. Vollmer, *J. Org. Chem.*, **28**, 1545 (1963); *J. Chem. Soc.*, **1963**, 5567.

16. Tincher, W. C., *Makromol. Chem.*, **85**, 46 (1965).

17. Zutty, N. L., and F. J. Welch, *J. Polymer Sci.*, **43**, 445 (1960).

18. Beresniewicz, A., *J. Polymer Sci.*, **39**, 63 (1959).

19. Mino, G., S. Kaizerman, and E. Rasmussen, *J. Polymer Sci.*, **39**, 523 (1959).

20. Harris, H. E., and J. G. Pritchard, *J. Polymer Sci. A*, **2**, 3673 (1964).

21. Coleman, B. D., *J. Polymer Sci.*, **31**, 155 (1958).

22. Bovey, F. A., *J. Polymer Sci.*, **46**, 59 (1960).

23. Fordham, J. W. L., *J. Polymer Sci.*, **39**, 321 (1959).

24. Huggins, M. L., *J. Am. Chem. Soc.*, **66**, 1991 (1944).

25. Miller, M. L., and C. E. Ranhut, *J. Am. Chem. Soc.*, **80**, 4116 (1958); *J. Polymer Sci.*, **38**, 63 (1959).

26. Birshtein, T. M., and O. B. Ptitsyn, *Vysokomolekul. Soedin.*, **1**, 846 (1959).

27. Higashimura, T., T. Watanabe, K. Suzuoki, and S. Okamura, *J. Polymer Sci. C*, **4**, 361 (1964).

28. Fordham, J. W. L., G. H. McCain, and L. E. Alexander, *J. Polymer Sci.*, **39**, 335 (1959).

29. Ferstandig, L. L., and F. C. Goodrich, *J. Polymer Sci.*, **43**, 373 (1960).

30. Cooper, W., F. R. Johnston, and G. Vaughan, *J. Polymer Sci. A*, **1**, 1509 (1963).

31. Razuvaev, G. A., K. S. Minsker, A. G. Kronman, Yu. A. Sangalov, and D. N. Bort, *Dokl. Akad. Nauk SSSR*, **143**, 1116 (1962).

32. Rosen, I., P. H. Burleigh, and J. F. Gillespie, *J. Polymer Sci.*, **54**, 31 (1961).

33. Minsker, K. S., A. G. Kronman, B. F. Teplov, E. E. Rylov, and D. N. Bort, *Vysokomolekul. Soedin.*, **4**, 383 (1962).

34. Marvel, C. S., *An Introduction to the Organic Chemistry of High Polymers*, Wiley, New York, 1959, pp. 42–45.

35. Flory, P. J., and F. S. Leutner, *J. Polymer Sci.*, **3**, 880 (1948); *ibid.*, **5**, 267 (1950).

36. Cotman, J. D., *Ann. N. Y. Acad. Sci.*, **57**, 417 (1953).

37. Melville, H. W., and P. R. Sewell, *Makromol. Chem.*, **32**, 139 (1959).

38. Wheeler, O. L., S. L. Ernst, and R. N. Crozier, *J. Polymer Sci.*, **8**, 409 (1952).

39. Wheeler, O. L., E. Lavin, and R. N. Crozier, *J. Polymer Sci.*, **9**, 157 (1952).

40. Wheeler, O. L., *Ann. N. Y. Acad. Sci.*, **57**, 360 (1953).

41. Clarke, J. T., R. O. Howard, and W. H. Stockmayer, *Makromol. Chem.*, **44–46**, 427 (1961).

42. Roedel, M. J., *J. Am. Chem. Soc.*, **75**, 6110 (1953).

43. Casey, K., C. T. Elston, and M. K. Phibbs, *J. Polymer Sci. B*, **2**, 1053 (1964).

44. Woodbrey, J. C., and P. Ehrlich, *J. Am. Chem. Soc.*, **85**, 1580 (1963).

45. Willbourn, A. H., *J. Polymer Sci.*, **34**, 569 (1959).

46. Rugg, F. M., J. J. Smith, and L. H. Wartman, *Ann. N. Y. Acad. Sci.*, **57**, 398 (1953).

47. Richards, R. B., *J. Appl. Chem.*, **1**, 371 (1951).

48. Reding, F. P., and A. Brown, *J. Appl. Phys.*, **25**, 848 (1954).

49. George, M. H., R. J. Grisenthwaite, and R. F. Hunter, *Chem. Ind. (London)*, **1958**, 1114.

50. Harris, H. E., J. F. Kenney, G. W. Willcockson, R. Chiang, and H. N. Friedlander, *J. Polymer Sci. A-1*, **4**, 665 (1966).

51. Ramey, K. C., and N. D. Field, *J. Polymer Sci.*, **B3**, 63 (1965).

52. Bovey, F. A., and G. V. D. Tiers, *Chem. Ind. (London)*, **1962**, 1826.

53. Hines, R. A., W. M. D. Bryant, A. W. Larchar, and D. C. Pease, *Ind. Eng. Chem.*, **49**, 1071 (1957).

54. Raff, R. A. V., and J. B. Allison, *Polyethylene*, Interscience, New York, 1956, p. 46.

55. Rosen, I., G. H. McCain, A. L. Endrey, and C. L. Sturm, *J. Polymer Sci. A*, **1**, 951 (1963).

56. Fujii, K., T. Mochizuki, S. Imoto, J. Ukida, and M. Matsumoto, *J. Polymer Sci. A*, **2**, 2327 (1964).

57. Fujii, K., T. Mochizuki, S. Imoto, J. Ukida, and M. Matsumoto, *Makromol. Chem.*, **51**, 225 (1962).

58. Garrett, B. S., W. E. Goode, S. Gratch, J. F. Kincaid, C. L. Levesque, A. Spell, J. D. Stroupe, and W. H. Watanabe, *J. Am. Chem. Soc.*, **81**, 1007 (1959).

59. Fox, T. G, and H. W. Schnecko, *Polymer*, **3**, 575 (1962).

60. Kenney, J. F., and G. W. Willcockson, *J. Polymer Sci. A-1*, **4**, 679 (1965).

61. Wells, R. D., and H. M. Morgan, *Textile Res. J.*, **30**, 668 (1960).

62. Meos, A. I., L. A. Vol'f, and G. N. Afanas'eva, *Khim. Volok.*, No. 3, 18 (1963).

Résumé

Les propriétés de solubilité de l'alcool polyvinylique (PVA) varie avec la méthode de préparation de l'acétate de polyvinyle (PVAc) dont il est dérivé. L'acétate de polyvinyle a été préparé au moyen de catalyseurs radicalaires sur une gamme de températures de $-78°$ a $90°C$. dans différents solvants caractérisés par des transferts de chaînes variables. Les échantillons des PVA correspondants varient quant a leur résistance à la dissolution dans l'eau. Leur spectre de résonnance magnétique nucléaire à haute résolution ne montre pas de différence de tacticité. Des résultats sur leur teneur en diol 1-2 manifeste uniquement des différences mineures. Par conséquent, l'augmentation de la résistance du PVA du point de vue dissolution dans l'eau, résultant de changements dans l'activité de transfert de chaînes des solvants utilisés au cours de la polymérisation de l'acétate de vinyle, doit être attribuée principalement à une diminution du poids moléculaire; l'accroissement de la résistance du PVA à la dissolution dans l'eau résultant d'une diminution de température de polymérisation de l'acétate de vinyle doit être largement attribué à une diminution à la fois des ramifications longues et courtes. Evidemment avec des polymères polaires ayant des groupes latéraux petits, la tacticité n'est pas le seul facteur influençant des changements de propriétés; des variations de stéréorégularité influencent beaucoup plus la cristallinité de l'échantillon tel qu'on la mesure par densité, par la méthode aux rayons-X, que la cristallisibilité finale dans des conditions de traitements mécanique et thermique. À cet égard les polymères polaires ayant des groupes latéraux petits diffèrent des polymères non-polaires.

Zusammenfassung

Die Löslichkeitseigenschaften von Polyvinylalkohol (PVA) hängen von der Darstellungsmethode des Polyvinylacetats (PVAc) ab, von welchem er sich ableitet. PVAc wurde mit radikalischen Katalysatoren im Temperaturbereich von -78 bis $90°C$. mit Lösungsmitteln von verschiedener Kettenübertragungsfähigkeit dargestellt. Die entsprechenden PVA-Proben unterscheiden sich in ihrer Beständigkeit gegen die Auflösung in Wasser. Ihre kernmagnetischen Hochauflösungsprotonenresonanzspektren zeigten keine Taktizitätsunterschiede. Die Daten für den 1,2-Diolgehalt zeigten nur geringfügige Unterschiede. Daher kann die Zunahme der Auflösungsbeständigkeit von PVA in Wasser, die durch die Änderung der Kettenübertragungsaktivität des bei der Vinylacetatpolymerisation verwendeten Lösungsmittels hervorgerufen wird, weitgehend auf eine Abnahme des Molekulargewichtes zurückgeführt werden, und die Zunahme der Auflösungsbeständigkeit von PVA in Wasser, die durch eine Abnahme der Temperatur bei der Vinylacetatpolymerisation hervorgerufen wird, weitgehend auf eine solche der Lang- und Kurzkettenverzweigungen. Offenbar ist bei polaren Polymeren mit kleinen Seitengruppen die Taktizität nicht der einzige Faktor, der die Eigenschaftsänderung beeinflusst; d.h. eine Änderung der Stereoregularität beeinflusst die durch Dichte oder Röntgenmethoden gemessene Kristallinität der Probe stärker als die schliesslich unter den Bedingungen der mechanischen und thermischen Behandlung auftretenden Kristallisationsfähigkeit. In dieser Hinsicht unterscheiden sich polare Polymere mit kleinen Seitengruppen von nicht polaren Polymeren.

Structure–Property Relationships of Poly(vinyl Alcohol). II. The Influence of Molecular Regularity on the Crystallization–Dissolution Temperature Relationships of Poly(vinyl Alcohol)

H. E. HARRIS, J. F. KENNEY, G. W. WILLCOCKSON, R. CHIANG, and H. N. FRIEDLANDER, *Chemstrand Research Center, Inc., Durham, North Carolina*

Synopsis

Dissolution temperatures T_s have been determined for poly(vinyl alcohol) (PVA) samples of varying tacticity as a function of crystallization temperatures T'_c. From the values of T_s and T_c, one can obtain values of $(T_m)_\infty$, the dissolution temperature of crystals of infinite stepheight. $(T_m)_\infty$ is a characteristic property of a given sample. This method of characterization is very sensitive and reliable for detecting differences in molecular regularity among PVA samples. The variation of $(T_m)_\infty$ with stereoregularity is attributed in part to differences in hydrogen-bonding characteristics. Determinations of the crystallinities of solution-crystallized PVA have shown that stereoregularity in PVA does not result in higher crystallizability.

INTRODUCTION

In recent years, there has been much discussion[1-7] of stereoregularity–property relationships in poly(vinyl alcohol) (PVA). Numerous papers have reported the preparation and properties of syndiotactic[1,2,7,8] and isotactic[8,9] PVA, but conclusions based on the results of these studies remained somewhat in doubt because there was available no definitive, quantitative method for measuring stereoregularity. Indeed, no quantitative techniques have been developed for measuring important factors of molecular regularity (e.g., branching) other than stereoregularity. Recently, nuclear magnetic resonance (NMR) has been used to assign and quantitatively determine the tacticity of PVA.[10,11] This technique, together with a method for the quantitative determination of 1,2-diol content,[12] has provided the means for studying better characterized PVA samples.

Many of the studies of the influence of stereoregularity on the properties of PVA have involved crystallinity-related properties (i.e., density, solubility). Since crystallinity is dependent on the stereoregularity, other factors of molecular regularity, and handling history of the polymer, it is not surprising that results and conclusions reported in the literature are not in full accord. For example, PVA samples derived from poly(vinyl

acetate) (PVAc) prepared under varying conditions (i.e., temperature, solvent) have exhibited different physical properties. Based on this evidence the PVA samples were assumed to vary in stereoregularity; however, in the first paper of this series,[13] it was shown that these PVA samples possessed essentially the same tacticity. Obviously, better characterization methods are needed for establishing structure–property relationships. The possibility of using the crystallization-dissolution temperature method of Chiang and Rhodes[14] to characterize PVA of varying molecular regularity appeared desirable, since it was independent of the handling history of the polymer. This technique has been found to be applicable to PVA, and it has proved to be a sensitive, reproducible method for detecting differences in tacticity and other factors of molecular regularity.

The present work comprises studies of crystallization-dissolution temperatures and crystallinities of solution-crystallized PVA samples of varying molecular regularity. The results have demonstrated that stereoregularity significantly influences the properties of PVA, but in a more complex manner than in the better-known nonpolar polymers.

EXPERIMENTAL

PVA Derived from Poly(vinyl Acetate) (PVAc)

Details of the preparation of PVAc samples and their conversion to PVA are reported previously.[13] The conditions of preparation of two

TABLE I
Conditions of Preparation of Poly(vinyl Alcohol) Samples

PVA sample	PVA source	Catalyst system	Polymerization solvent	Polymerization temp., °C.	$[\eta]_{H_2O}^{25\,°C}$, dl./g.
S-A	PVTFAc	n-Bu$_3$B–air	Heptane	-78	2.22[a]
S-B	PVF, MEK-insol. fraction	BEt$_3$–air	Methyl formate	0	—
H-A	PVAc	BEt$_3$–air	Amyl acetate	-78	0.34
H-B	PVAc	AIBN–$h\nu$	Methyl ethyl ketone	60	0.26
H-V[b]	PVAc	—	—	60[b]	0.84
I-A$_1$	PVtBE, acetone-sol. fraction	BF$_3$ etherate	Toluene	-78	0.20
I-A$_2$	PVtBE, MEK-sol. fraction	—	—	—	0.21
I-A$_3$	PVtBE, MEK-insol. fraction	—	—	—	0.18[c]

[a] Intrinsic viscosity of PVTFAc in methyl ethyl ketone at 30°C.

[b] Product (Vinol 125) of Air Reduction Co., presumably prepared by solution polymerization at ca. 60°C.

[c] Intrinsic viscosity of PVtBE (methyl ethyl ketone-insoluble fraction) in benzene at 25°C.

PVAc samples (sources of PVA samples H-A and H-B) are summarized in Table I.

Two PVA samples, H-V and H-VF, are commercial products of Air Reduction Company and are known as Vinol 125 and Vinol FO, respectively. Vinol FO was in fiber form and presumably derived from Vinol 125 which was obtained by "super hydrolysis" of PVAc. The preparative conditions for this PVAc can not be stated definitely, but analytical data suggest that it was prepared by solution polymerization at about 60°C.

Samples designated by the subscript, x, (e.g., H-V$_x$) were cleaved at head-to-head linkages (1,2-diol units) by periodic acid and subsequently reduced with sodium borohydride.[12]

PVA Derived from Poly(vinyl *tert*-Butyl Ether) (PVtBE)

Details of the preparation, fractionation, and cleavage of PVtBE to PVA will be reported elsewhere.[15] Vinyl *tert*-butyl ether monomer was prepared from the interchange reaction of 2-chloroethyl vinyl ether and *tert*-butyl alcohol in the presence of mercuric acetate. Polymerization of vinyl *tert*-butyl ether was carried out in purified toluene with redistilled boron fluoride–diethyl etherate catalyst at −78°C. The PVtBE was fractionated according to its solubility in acetone and methyl ethyl ketone (MEK) and each fraction was cleaved to PVA (Samples I-A$_1$, I-A$_2$, and I-A$_3$, Table I) by treatment with trifluoroacetic acid at room temperature. These PVA fractions were free of residual *tert*-butyl groups as determined by infrared and NMR analyses.

PVA Derived from Poly(vinyl Trifluoroacetate) (PVTFAc)

A 500-ml. three-necked round-bottomed flask was fitted with a gas inlet, a stirrer, and a gas outlet protected with a drying tube. The flask was flamed under argon and a positive pressure of argon maintained. The flask was cooled to −78°C. and 66 g. of redistilled vinyl trifluoroacetate, b.p. 39°C. (Peninsular ChemResearch), and 18 ml. of *n*-heptane added. To the cold solution was added 1 ml. of tri-*n*-butylborane in 5 ml. of *n*-heptane via a syringe. At 10-min. intervals, five 10-cc. portions of dry air were added. The polymerization was allowed to continue overnight at −78°C. The polymerization mixture was placed in a Waring Blendor and stirred with 300 ml. of cyclohexane. The precipitated polymer was filtered, washed with 300 ml. of cyclohexane, and dried in a vacuum oven at 50°C. The dried poly(vinyl trifluoroacetate) weighed 38 g. This PVTFAc had an intrinsic viscosity of 2.22 in methyl ethyl ketone at 30°C.

PVTFAc (1 g.) dissolved in 10 ml. of acetone was added to 240 ml. of a 50:50 ammonium hydroxide–methyl alcohol mixture with rapid stirring. The solution was stirred rapidly for 3 hr., filtered, washed with acetone, and dried. PVA (Sample S-A, Table I) was obtained which was free of trifluoroacetate groups as determined from infrared and NMR spectra and analyses for fluorine.

TABLE II
Dissolution Temperature T_s as a Function of Crystallization Temperature T_c for Various Poly(vinyl Alcohol) Samples

Sample	Solvent	T_c, °C.	T_s, °C.	$(T_m)_\infty$, °C.
S-A	1,3-Propanediol	80	161	
		96.5	164	
		114	168	
		120	171	
		143[a]	173	180
S-B	1,3-Propanediol	82	139	
		92	144	
		105	149	
		121	152	
		131.5[a]	155	164
H-A	1,3-Propanediol	74.5	136	
		81	138	
		95	143	
		121	149	
		125[a]	151	161
H-B	1,3-Propanediol	80	133	
		91	136	
		108.5	143	
		122	147	
		125[a]	148	159
H-B	Triethylene glycol	80	158	
		106	169	
		150	187	
		160	191	
		170[a]	197	220
H-V	1,3-Propanediol	76.5	137	
		85	138	
		91	140	
		108	142	
		122	147	
		125[a]	148	155
H-V	Ethylene glycol	70	125	
		80	128	
		91	129	
		94	129	
		101[a]	130	133

(continued)

PVA Derived from Poly(vinyl Formate) (PVF)

Purified vinyl formate (75 ml.) and 75 ml. of methyl formate were mixed in a capped pressure bottle. The bottle was cooled to 0°C. and 1 ml. of 25% triethylborane was added via a syringe through the self-sealing rubber cap. For 1 hr. air was slowly bubbled through the solution via a hypodermic needle placed through the cap. At this time, the mixture was poured into a large volume of hexane to precipitate PVF. The product was extracted for several hours in hot methyl ethyl ketone (MEK). The MEK-insoluble polymer (about 90% of the original PVF) was dissolved

TABLE II (*continued*)

Sample	Solvent	T_c, °C.	T_s, °C.	$(T_m)_\infty$, °C.
H-V$_x$	1,3-Propanediol	70	128	
		80	133	
		91	135	
		100	139	
		108.5	141	
		120	146	158
II-VF	1,3-Propanediol	78.5	143	
		91	145	
		105	147	
		121[a]	149	154
I-A$_1$	1,3-Propanediol	<60		—
I-A$_2$	1,3-Propanediol	50	106	
		55	106	
		60	105	
		65	109	
		67	111	
		70	118	
		80	120	
		90	119	
		100[a]	119	119
I-A$_3$	1,3-Propanediol	45	146	
		55	144	
		60	144	
		80	146	
		85	147	
		95	147	
		101	146	
		115	151	
		120	152	
		125	153	
		130[a]	156	166
I-A$_3$	Triethylene glycol	80	159	
		100	171	
		110	175	
		120	180	
		125	187	
		150[a]	200	270

[a] The highest practical crystallization temperature.

in methyl formate, precipitated in a large excess of hexane, collected, and dried.

MEK-insoluble PVF was dissolved in dioxane and converted to PVA by alcoholysis with a solution of sodium methoxide in methanol and dioxane. The mixture was allowed to stand overnight. The PVA was filtered off, dissolved in dimethyl sulfoxide, and precipitated in a large excess of acetone. The white solid product was extracted with methanol for several hours and dried (Sample S-B, Table I).

Crystallization of Poly(vinyl Alcohol) from Dilute Solution and Determination of Dissolution Temperatures

1,3-Propanediol, ethylene glycol (Eastman White Label), and triethylene glycol (Union Carbide) were used for determining the crystallization and dissolution temperatures. These solvents were generally used as received. Identical results were obtained when these solvents were purified by treatment with activated charcoal.

The procedure for measuring the crystallization and dissolution temperatures has been described previously.[14] A concentrated solution, approximately 0.5 g. of PVA in 25 ml. of solvent, was prepared by heating the sample to 160–200°C. with stirring in the solvent under nitrogen in an oil bath. About 0.1 ml. of the hot concentrated solution was quickly introduced into 5 ml. of solvent maintained at the desired crystallization temperature T_c. The solution was allowed to crystallize at constant temperature overnight. At low degrees of undercooling, crystallization was allowed to proceed for 2 or 3 days. After crystallization, the dissolution temperature was determined by adding about 0.1 ml. of the crystallized sample into a thin-walled tube partly immersed in an oil bath heated to the desired test temperature. By several trials, a precise value of the dissolution temperature was obtained. Crystallization (T_c) and dissolution (T_s) temperatures are listed in Table II.

Determination of Density

A flotation method was used to determine the density of the crystalline polymer. The solvent was removed from the crystallized PVA under vacuum. The density of the dried PVA was determined by observing the point at which the density of the flotation medium (carbon tetrachloride–

TABLE III
Crystallinity of Solution-Crystallized Poly(vinyl Alcohol)

Sample	Solvent	T_c, °C.	Density, g./cc.	Crystallinity, %[a]
S-A	1,3-Propanediol	100	1.286	25
		125	1.286	25
		140	1.294	35
H-B	Triethylene glycol	100	1.301	43
		170	1.301	43
		200[b]	1.301	43
	1,3-Propanediol	110	1.313	57
H-V	1,3-Propanediol	100	1.305	48
		110	1.315	60
		121	1.315	60
I-A₃	1,3-Propanediol	110	1.280	18
		125	1.285	24
	Triethylene glycol	150	1.281	19

[a] Determination based on density measurements, assuming a monoclinic unit cell.
[b] Cooled from 200°C.

benzene mixture) matches that of the suspended PVA, as demonstrated by absence of sedimentation under high-speed centrifugation. The density of the flotation medium was measured with a Westphal density balance at 22°C. Of special importance is the absence of partial sedimentation after adjusting the medium to matching density. The dispersion remained uniform throughout the sample tube when such a mixture was centrifuged. In view of the sensitivity of the method to small differences in density, the densities of the various particles present in a given sample must be very nearly identical. These observations show that separate amorphous particles were probably not present. The density measurements are listed in Table III.

RESULTS

Poly(vinyl Alcohol) Samples

The PVA samples investigated in this work differ with respect to stereo-regularity, molecular weight, and to a lesser degree, other factors of molecular regularity. The stereoregularities of the samples, expressed in terms of the average number of diad and triad placements as determined from NMR spectra,[11,13,15] are listed in Table IV. Syndiotactic-rich, isotactic-rich, and atactic products were derived from poly(vinyl trifluoroacetate), poly-(vinyl tert-butyl ether), and poly(vinyl acetate), respectively. Sample S-B, prepared from poly(vinyl formate), was not analyzed by NMR spectroscopy, but crystallization–dissolution data suggest that it may be slightly more syndiotactic than samples derived from PVAc. Highly stereoregular PVA samples were not obtained by any of the preparative methods employed. The most syndiotactic product, S-A, possessed 61 and 43% syndiotactic diads and triads, respectively; the most isotactic sample, I-A$_3$, contained 76 and 58% isotactic diads and triads, respectively. Nevertheless, the variation in tacticity was sufficient to cause significant variation in properties.

TABLE IV

Estimate of Tacticity of Poly(vinyl Alcohol) from Nuclear Magnetic Resonance Spectra[a]

	Diads		Triads		
Sample	I, %	S, %	I, %	H, %	S, %
S-A$_x$[b]	39	61	11	46	43
H-A$_x$[b]	42	58	28	42	30
H-B	45	55	29	41	30
H-V$_x$[b]	43	57	—	—	—
I-A$_1$	67	33	49	38	13
I-A$_2$	71	29	55	32	13
I-A$_3$	76	24	58	35	7

[a] Details of this work are reported elsewhere.[11,13,15] These values are estimated to be accurate to ±5%.

[b] Satisfactory resolution of spectra could be obtained only with cleaved products,[13] but the tacticities are presumed to be essentially the same as the parent polymers.

The range of molecular weights is indicated by intrinsic viscosity data shown in Table I. The rather large variation in molecular weight caused some concern regarding its influence on crystallization-dissolution temperature relationships. However, samples H-A, H-B, H-V, and H-V$_x$ provided products which varied appreciably in molecular weight with little variation in other structural parameters. Indeed, cleavage of H-V ($[\eta]_{H_2O}^{25°C.}$ = 0.84) at head-to-head linkages with periodic acid and subsequent reduction with sodium borohydride gave sample H-V$_x$ ($[\eta]_{H_2O}^{25°C.}$ = 0.14) which differed from H-V only with respect to molecular weight, 1,2-diol units, and possibly carbonyl groups.

The PVA samples used in the present study, very probably, differed with respect to other factors of molecular regularity (i.e., 1,2-diol units, branching, carbonyl groups, carbon-carbon unsaturation), but all data suggest that these variations were minor. Quantitative data on 1,2-diol content indicate a maximum of about 1.7%.[12] Residual acyl or *tert*-butyl groups could not be detected by infrared or NMR spectroscopy. Ultraviolet spectra and literature data[16] indicate that carbonyl and α,β-unsaturated carbonyl groups were present to a maximum extent of 0.4%. Branching could not be measured, but the results of the present work suggest that branching and variation in branching were of lesser importance in the samples investigated.

Crystallization and Dissolution Temperatures

The isothermal crystallization temperatures T_c and dissolution temperatures T_s for the various PVA samples are given in Table II, the determinations having been carried out at high dilution in 1,3-propanediol, triethylene glycol, and ethylene glycol. Single crystal platelets have been detected in some of the solution-crystallized samples,[17-19] but not in every case. The presence or absence of detectable single crystals in the crystallized samples had no apparent influence on the observed dissolution temperatures. The rate of crystallization decreases drastically with an increase in crystallization temperature. The temperature beyond which the rate of crystallization becomes prohibitively slow is referred to as the highest practical crystallization temperature. The dissolution temperatures were determined for each of the isothermally crystallized samples and can be reproduced to $\pm 1°C$.

The dissolution temperature changes linearly with the crystallization temperature. When the values of T_s are plotted against T_c, a straight line is obtained. $(T_m)_\infty$, the hypothetical dissolution temperature of the crystal of infinite stepheight,[14] was obtained for each sample by extrapolation of the T_s versus T_c plot to $T_s = T_c$ (selected plots are shown in Fig. 1). The resultant values for $(T_m)_\infty$ are shown in Table II also. With the exception of PVA samples I-A$_2$ and I-A$_3$ the T_s versus T_c plots were straight lines of positive slope which are indicative of an increase in crystal perfection with crystallization temperature. The nonlinear relation in the case of samples I-A$_2$ and I-A$_3$ in 1,3-propanediol may be due to poor crystallinity.
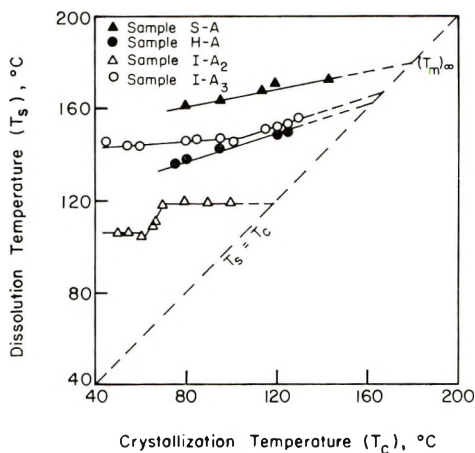
Fig. 1. Dissolution temperature vs. crystallization temperature for poly(vinyl alcohol) samples isothermally crystallized in 1,3-propanediol.

Crystallinity

The per cent crystallinity determined from density of various PVA samples isothermally crystallized from dilute solution in 1,3-propanediol and triethylene glycol is presented in Table III. The crystallinity values are considered reliable to ±4%. The highest crystallinity obtained by solution crystallization was 60% for sample H-V.

DISCUSSION

Dissolution Temperature

The value obtained for T_s can only be considered reliable provided recrystallization does not occur during the time of dissolution. If the polymer is able to crystallize during the determination of T_s, an erroneously high value will be observed. Therefore, the possibility of recrystallization was held to a minimum by subjecting a fresh portion of the crystallized PVA mixture each time to the test temperature. In addition, note that the highest practical crystallization temperature was always below the lowest value of T_s for a given sample (except for sample H-B in triethylene glycol), indicating that crystallization is extremely slow during determination of T_s'.

The lowest temperature T_s at which a finely divided sample of PVA in a very large excess of solvent will dissolve is an accurately ascertainable characteristic of the sample. It should be pointed out, however, that the dissolution temperature observed is characteristic of the most crystalline portion of the test sample and may not be representative of the whole sample. This arises from the fact that the observed dissolution temperature T_s is determined by the most insoluble portion of each sample.

Significance of $(T_m)_\infty$

From the dissolution and crystallization temperatures, one can derive values of $(T_m)_\infty$, the extrapolated dissolution temperature.[14] $(T_m)_\infty$, is a characteristic property of a given sample, and it is not influenced by the handling history of the sample. The values of $(T_m)_\infty$ have been demonstrated to depend upon both solvent employed and the molecular structure of the polymer. The value of $(T_m)_\infty$ is affected by the degree of perfection of the crystalline array which is influenced by the molecular regularity of the polymer, and actually gives a measure of molecular regularity.

The dependence of $(T_m)_\infty$ on solvent is related to solvent–polymer interaction. Thus, the observed values of T_s are dependent in part upon the ability of the solvent to interact with the polymer, overcome the existing intermolecular forces, and effect solution.

Structural Factors Which Influence $(T_m)_\infty$

Molecular Weight and Degree of Head-to-Head Polymerization. The data on sample H-V and its counterpart sample, H-V$_x$, which is cleaved at the head-to-head placements (1,2-diol units), show that neither the molecular weight nor the 1,2-diol content affect significantly the value of $(T_m)_\infty$. Cleavage of sample H-V ($[\eta] = 0.84$ and 1,2-diol content $= 1.7\%$)[13] at the site of the 1,2-diol units yields sample H-V$_x$ of $[\eta] = 0.14$ and void of 1,2-diol units. Nevertheless, $(T_m)_\infty$ for sample H-V$_x$ is not significantly higher than for sample H-V (158 and 155°C., respectively).

Branching. Reactions leading to chain branches in poly(vinyl acetate) and in the derived poly(vinyl alcohol) have been described in the first paper of this series.[13] Many of the polymers described here were prepared at temperatures and in solvents where chain transfer leading to branching is expected to be low. It has been reported that PVA derived from poly(vinyl trifluoroacetate), poly(vinyl formate), and poly(vinyl acetate) prepared at low temperature are all essentially linear.[3,4] The presence of branching would be expected to interfere with the crystallization process and branches small enough to be incorporated in the crystal structure would lower the $(T_m)_\infty$ value.* However, the crystallization–dissolution temperature data indicate that branching is not a major factor leading to the observed differences in $(T_m)_\infty$. The small difference in $(T_m)_\infty$ between samples H-A, H-B, H-V, and H-V$_x$, all derived from poly(vinyl acetate), may be due in part to branching; however, these differences may just as well be attributed to other structural differences.

Stereoregularity. $(T_m)_\infty$ is a measure of the stability of the infinitely thick crystal in a given solvent and will be proportional to the intermolecular forces which exist in the crystal. Thus, structural factors which give rise to stronger intermolecular association will give rise to higher values of $(T_m)_\infty$.

* In theory, structural irregularities (e.g., larger branches) which are too large to be accommodated in the crystal should not influence $(T_m)_\infty$.

Stereoregularity, and especially stereoblock character, would be expected to strongly influence hydrogen bonding in PVA. Since the hydroxyl groups and the hydrogen atoms can be exchanged at random in the crystal lattice,[20] the effects of stereoregularity must be associated primarily with differences in hydrogen bonding. High stereoregularity together with long sequence lengths should result in more stable crystals and higher $(T_m)_\infty$ values. The data in Table II do indicate that higher stereoregularity gives rise to higher $(T_m)_\infty$ (no data are available on sequence lengths), but they also suggest that the type of stereoregularity influences $(T_m)_\infty$, most probably as a result of variation in the type of hydrogen bonding (i.e., intra- versus intermolecular).

Sample S-A of higher syndiotactic structure exhibited the highest $(T_m)_\infty$ in 1,3-propanediol. This seems consistent with the hypothesis that an increase in syndiotactic placement of hydroxyl groups results in the formation of more intermolecular hydrogen bonds, thereby increasing the intermolecular forces within the crystal.

Samples I-A$_1$, I-A$_2$, and I-A$_3$ of predominately isotactic structure apparently form the same crystal structure as sample S-A of predominately syndiotactic structure,[5,8] and the NMR data show they are substantially more regular. In spite of this, samples I-A$_1$, I-A$_2$, and I-A$_3$ crystallize poorly. The data suggest that a crystalline array is more difficult to form, but the $(T_m)_\infty$ of 166°C. for sample I-A$_3$ indicates that once the crystal lattice is formed, its stability is intermediate between those of the atactic and predominately syndiotactic structures. The behavior of samples I-A$_1$, I-A$_2$, and I-A$_3$ can be attributed primarily to their different hydrogen bonding characteristics. Intramolecular hydrogen bonding between 1,3-hydroxyls in the isotactic sequence would contribute to decreased intermolecular association and a lower $(T_m)_\infty$.

Crystallinity

The per cent crystallinity values given in Table II which are based on the relation between density and x-ray crystallinity reported by Sakurada,[21] are significantly higher for samples H-B and H-V of atactic structure than for samples S-A or I-A$_3$. These results demonstrate that increased stereoregularity in PVA does not increase the tendency to crystallize. This is not surprising when one again considers the hydrogen-bonding characteristics of the PVA stereoisomers. The placements of hydroxyl groups in syndiotactic and isotactic sequences would be expected to result in a larger number of intermolecular (or intersegment) pairings of hydroxyl groups, and in turn on a larger number of hydrogen bonds, than in atactic structure where the hydroxyl group placements are random. The effect of increased hydrogen bonding is to increase molecular forces between molecules and within the same molecule. As a result, molecular mobility is reduced. The development of a high degree of crystallinity can only be achieved if a segment in a molecule crystallizes alongside a segment in another molecule (fringed micelle) or forms chain-folded molecules. The development of a

high degree of crystallinity thus requires a high degree of molecular mobility. The higher crystallizability exhibited by samples H-B and H-V is attributed to greater mobility of the polymer chains.

CONCLUSION

The crystallization–dissolution temperature method is very sensitive and reliable for detecting differences in molecular regularity among poly(vinyl alcohol) samples. The method is independent of the previous physical treatment of the polymer.

$(T_m)_\infty$, the dissolution temperature of the hypothetical crystal of infinite stepheight, is an accurately ascertainable characteristic of a crystallizable poly(vinyl alcohol) sample in a given solvent.

Stereoregularity contributes strongly towards determining $(T_m)_\infty$. Both the degree and type of stereoregularity are important. Higher stereoregularity results in higher values of $(T_m)_\infty$. However, syndiotactic sequences appear to be much more effective in raising $(T_m)_\infty$. Isotactic sequences apparently make the polymer more difficult to crystallize and tend to reduce $(T_m)_\infty$. It has been concluded that isotactic placement of hydroxyl groups results in intramolecular hydrogen bonding which reduces intermolecular forces and gives lower $(T_m)_\infty$ values, whereas syndiotactic placements enhance intermolecular hydrogen bonding which gives rise to higher $(T_m)_\infty$ values.

Stereoregularity in poly(vinyl alcohol) does not result in higher crystallizability.

References

1. Haas, H. C., E. S. Emerson, and N. W. Schuler, *J. Polymer Sci.*, **22**, 291 (1956).

2. Fordham, J. W. L., G. H. McCain, and L. E. Alexander, *J. Polymer Sci.*, **39**, 335 (1959).

3. Imai, K., and M. Matsumoto, *J. Polymer Sci.*, **55**, 335 (1961).

4. Rosen, I., G. H. McCain, A. L. Endrey, and C. L. Sturm, *J. Polymer Sci. A*, **1**, 951 (1963).

5. Cooper, W., F. R. Johnston, and G. Vaughan, *J. Polymer Sci. A*, **1**, 1509 (1963).

6. Fujii, K., and J. Ukida, *Makromol. Chem.*, **65**, 74 (1963).

7. Fujii, K., T. Mochizuki, S. Imoto, J. Ukida, and M. Matsumoto, *J. Polymer Sci. A*, **2**, 2327 (1964).

8. Murahashi, S., H. Yuki, T. Sano, U. Yonemura, H. Tadokoro, and Y. Chatani, *J. Polymer Sci.*, **62**, S77 (1962); S. Murahashi, S. Nozakura, and M. Sumi, *J. Polymer Sci. B*, **3**, 245 (1965).

9. Okamura, S., T. Kodama, and T. Higashimura, *Makromol. Chem.*, **53**, 180 (1962).

10. Ramey, K. C., and N. D. Field, *J. Polymer Sci. B*, **3**, 63, 69 (1965).

11. Tincher, W. C., *Makromol. Chem.*, **85**, 46 (1965).

12. Harris, H. E., and J. G. Pritchard, *J. Polymer Sci. A*, **2**, 3673 (1964).

13. Friedlander, H. N., H. E. Harris, and J. G. Pritchard, *J. Polymer Sci. A-1*, **4**, 649 (1966).

14. Chiang, R., J. H. Rhodes, and V. F. Holland, *J. Polymer Sci. A*, **3,** 479 (1965); Chiang, R., *ibid. A*, **3,** 2019 (1965).

15. Vollmer, R. L., J. G. Pritchard, and G. W. Willcockson, *J. Polymer Sci.*, to be submitted.

16. Clarke, J. T., and E. R. Blout, *J. Polymer Sci.*, **1,** 419 (1946).

17. Tsuboi, K., and T. Mochizuki, *J. Polymer Sci. B*, **1,** 531 (1963).

18. Monobe, K., and Y. Fujiwara, *Kobunshi Kagaku*, **21,** 179 (1964).

19. Kenney, J. F., and V. F. Holland, *J. Polymer Sci. A-1*, **4,** 699 (1966).

20. Bunn, C. W., and H. S. Peiser, *Nature*, **159,** 161 (1947); Bunn, C. W., *ibid.*, **161,** 929 (1948).

21. Sakurada, I., *Poly(vinyl Alcohol)*, Kobunshi Gakkai, Tokyo, 1955, pp. 245–56.

Résumé

Les températures de dissolution T_s ont été déterminées pour des échantillons d'alcool polyvinylique (PVA) de tacticité variable en fonction de la température de cristallisation T_c. Au départ des valeurs de T_s et T_c on peut obtenir des valeurs (T_m), la température de dissolution de cristaux à valeur infinie. (T_m) est une propriété caractéristique de l'échantillon donné. Cette méthode de caractérisation est très sensible et reproductible pour détecter les différences dans la régularité moléculaire des échantillons d'alcool polyvinylique. Les variations de (T_m) avec la stéréorégularité est due en partie aux différences des caractéristiques des liaisons hydrogènes. Les déterminations des cristallinités des PVA cristallisés au départ de leurs solutions montrent que la stéréorégularité dans le PVA n'entraine pas une cristallisabilité meilleure.

Zusammenfassung

Auflösungstemperaturen, T_s, wurden für Polyvinylalkoholproben (PVA) verschiedener Taktizität als Funktion der Kristallisationstemperatur, T_c, bestimmt. Aus den Werten von T_s und T_c kann man Werte für $(T_m)_\infty$ der Auflösungstemperatur von Kristallen mit unendlicher Stufenhöhe erhalten. $(T_m)_\infty$ ist eine charakteristische Eigenschaft einer gegebenen Probe. Diese Charakterisierungsmethode ist verlässlich für die Ermittlung von Unterschieden in der Molekülregularität zwischen PVA-Proben. Die Abhängigkeit von $(T_m)_\infty$ von der Stereoregularität wird zum Teil auf Unterschiede in der Wasserstoffbindungscharakteristik zurückgeführt. Kristallinitätsbestimmungen an lösungkristallisiertem PVA zeigten, dass die Stereoregularität bei PVA nicht zu einer höheren Kristallisationsfähigkeit führt.

Structure–Property Relationships of Poly(vinyl Alcohol). III. Relationships between Stereoregularity, Crystallinity, and Water Resistance in Poly(vinyl Alcohol)

J. F. KENNEY and G. W. WILLCOCKSON,
Chemstrand Research Center, Inc., Durham, North Carolina

Synopsis

Structure–property relationships of poly(vinyl alcohol) have been studied by measuring the crystallinity and water resistance of films derived from samples of varying, known tacticity. Crystallinities of unannealed and annealed films were examined by means of density, infrared, and x-ray measurements. Higher tacticity did not lead to higher crystallinity. The apparent order of crystallizability was atactic ≧ syndiotactic-rich ≫ isotactic-rich. Water resistance of these films was determined by measuring the swelling index at 30°C. and solubility at 70 and 130–140°C. Water resistance increases as tacticity increases, with syndiotactic-rich PVA exhibiting the highest water resistance. Since water resistance also increases with crystallinity, both stereoregularity and crystallinity must be considered when evaluating structure–solubility relationships. Differential thermal and thermogravimetric analyses of these samples are also presented, together with a correlation of tacticity index as measured by an infrared technique with that of an NMR technique.

INTRODUCTION

Previous papers in this series have reported studies on structure–property relationships in (*a*) poly(vinyl alcohol) (PVA) derived from poly(vinyl acetate) (PVAc) prepared under different conditions of solvent and temperature[1] and (*b*) solution-crystallized PVA samples which varied in molecular regularity, especially stereoregularity.[2] In the present study, structure–property relationships have been examined further by measuring the crystallinity and water resistance of annealed and unannealed films of PVA samples which vary in molecular regularity.

EXPERIMENTAL

Poly(vinyl Alcohol) (PVA) Samples

Atactic, syndiotactic-rich, and isotactic-rich PVA samples were derived from poly(vinyl acetate) (PVAc), poly(vinyl trifluoroacetate) (PVTFAc), and poly(vinyl *tert*-butyl ether) (PVtBE), respectively. Preparation conditions for the parent polymers are summarized in Table I. PVAc was

TABLE I
Poly(vinyl Alcohol) Samples

PVA sample	Parent polymer	Catalyst	Solvent	Temp., °C.	$[\eta]^{30°C.}_{H_2O}$, di/g.	IR index, D_{916}/D_{850}	PVA Properties Tacticity NMR triads S, %	H, %	I, %	NMR diads S, %	I, %
S-A	PVTFAc	n-Bu₃B–air	Heptane	−78	(2.22)[a]	0.62	—	—	—	—	—
S-Aₓ[b]	—	—	—	—	—	—	43	46	11	61	39
H-V	PVAc	—	—	(ca. 60	0.84	0.37	—	—	—	—	43
H-Vₓ[b]	—	—	—	—	0.14	0.36	—	—	—	57	43
H-H	PVAc	AIBN	MEK	60	0.26	0.36	(30	41	29)[e]	58	42
I-A₃	PVtBE[d]	BF₃·OEt₂	Toluene	−78	(0.28)[e]	0.02	7	35	58	24	76

[a] $[\eta]$ of parent polymer in MEK at 30°.

[b] Obtained by cleavage of the original samples, H-V (Vinol 125; Air Reduction Co.) or S-A, at 1,2-diol units with periodic acid and reducing resultant carbonyl groups with NaBH₄.[7]

[c] Calculated from the NMR spectrum of PVA from PVAc prepared in MEK at 30°C.[4]

[d] MEK-insoluble fraction.[2,3]

[e] $[\eta]$ of parent polymer in benzene at 25°C.

converted to PVA by base-catalyzed alcoholysis in methanol. PVTFAc was hydrolyzed by treatment with 50:50 methanol–ammonium hydroxide solution. PVtBE was cleaved by treatment with trifluoroacetic acid at room temperature. Details of these preparative techniques are described elsewhere.[1-3] Sample H-V (Table I) was a product (Vinol 125) of Air Reduction Company and presumably was derived from PVAc prepared by solution polymerization at about 60°C.

PVA sample compositions were verified by elemental analyses, infrared spectra, and high-resolution nuclear magnetic resonance (NMR) spectra. These analytical methods gave no indication of residual acyl or *tert*-butyl groups in the respective PVA's. Estimates of tacticities of the PVA samples are given in Table I. Tacticities were determined quantitatively (±5%) from NMR spectra by techniques reported previously.[1,4] Infrared tacticity indices (ratio of the absorbance at 916 cm.$^{-1}$ to that at 850 cm.$^{-1}$) were calculated as described by other workers.[5,6] Intrinsic viscosities are shown in Table I also.

Samples S-A and H-V (Table I) were cleaved at head-to-head linkages (1,2-diol units) with periodic acid[7] in order to obtain low molecular weight products which exhibit highly resolved NMR spectra.[1,4] The molecular weights of the remaining samples were already sufficiently low for high-resolution NMR studies. Cleaved products are designated by the subscript x. Quantitative data on sample H-V indicated a 1,2-diol content of 1.66%;[1,7] this is estimated to be the highest value for any of the samples used in this study.

Preparation of Films

Films of PVA samples H-V, I-A$_3$ and S-A were derived from the corresponding PVTFAc's. H-V was converted to its trifluoroacetate by heating to reflux under nitrogen in excess trifluoroacetic anhydride with stirring for four days. PVtBE (MEK-insoluble fraction) was treated similarly, but with added boron fluoride etherate as a catalyst. Each of the resultant PVTFAc products was dissolved in acetone, precipitated in 10% methanol–water solution, and dried. This procedure gave PVTFAc which exhibited complete solubility in acetone and an infrared spectrum identical to one of PVTFAc prepared from vinyl trifluoroacetate. The dried material was dissolved in acetone and a 5% solution was cast on a polished aluminum plate. The PVTFAc film was dried at room temperature and subsequently hydrolyzed to PVA by treatment with 50:50 methanol–ammonium hydroxide solution for 30 min. The resultant film was dried under vacuum.

PVA films were prepared also from 5% water solutions of H-H, H-V, and H-V$_x$. Solutions were cast on a polished aluminum plate, the water evaporated at room temperature, and the films were dried under vacuum.

Films were approximately 1–3 mils in thickness. Atactic and syndiotactic-rich PVA films were clear and tough, whereas isotactic-rich PVA films were discolored slightly and very brittle. Films were annealed in a vacuum oven. Annealing at 150°C. for 30 min. causes no appreciable change in

appearance; annealing at 180–210°C. was limited to about 10 min. since some discoloration was observed at these temperatures.

Determination of Per Cent Crystallinity from Infrared Spectra of Films

The method is based on the x-ray, density, and infrared work of Sakurada.[8] Infrared spectra of films were obtained on the Perkin-Elmer 221 spectrophotometer with the Connecticut Instrument attenuated total reflectance (ATR) assembly attachment. All spectra were obtained with a KRS-5 prism at an ATR angle of 48°. The basis for determining per cent crystallinity in PVA from infrared spectra is the crystalline sensitive band at 8.7μ. The best results can be obtained if the peak at 8.7μ has a maximum absorbance of 0.80 on the chart. The first step is to draw a straight line along the portion of the spectrum between 9.0 and 9.2 μ extended far enough to intercept a vertical line through the 8.7 peak as shown in Figure 1. The vertical distance d between the 8.7 peak and the intercept point is then determined. Next, the vertical distance c between the 7.1 peak and the base line is determined. The per cent crystallinity is then calculated by using eq. (1).

$$\text{Per cent crystallinity} = 92\,(d/c) - 18 \qquad (1)$$

The expression derived for the per cent crystallinity is based on the validity of the reported correlation between density and crystallinity. The results are listed in Table II. Figure 2 shows the effects of heat treatment on the crystallization sensitive peak at 1141 cm.$^{-1}$.

Determination of Per Cent Crystallinity from Density

A flotation method was used to determine the density of films. The density was determined by using a carbon tetrachloride–benzene mixture
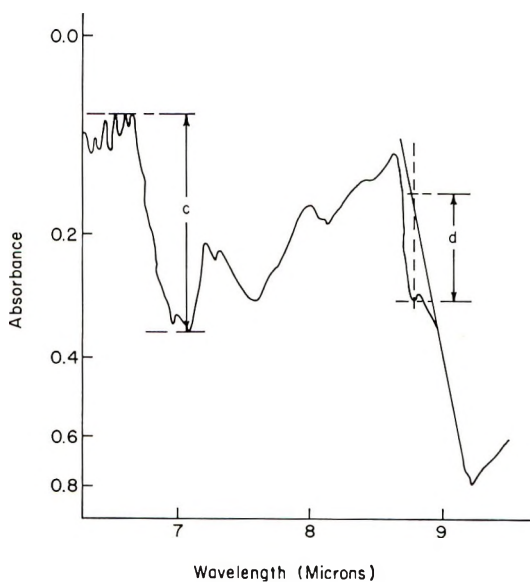
Fig. 1. Determination of per cent crystallinity from the infrared spectra of PVA.

at which the density of the mixture matches that of the suspended film. The density of the flotation medium was measured with a Westphal density balance. The per cent crystallinity was determined on the basis of the relation between density and x-ray crystallinity reported by Sakurada.[8] Per cent crystallinities determined from density are given in Table II.

TABLE II
Effect of Heat Treatment on Crystallinity of Poly(vinyl Alcohol) Film

Sample	Annealing temp., °C.	Density, g./cc.	Crystallinity, %[a] Density	Crystallinity, %[a] Infrared
H-V	Unannealed	1.291	31	31
	90	1.299	41	—
	100	—	—	48
	120	1.302	47	66
	150	1.312	57	56
	180	1.312	57	—
	210	1.311	55	65
H-H	Unannealed	1.305	48	50
	90	1.309	53	50
	100	—	—	46
	120	1.314	58	54
	150	1.325	72	—
	180	1.327	75	—
S-A	Unannealed	1.299	41	50
	90	1.301	43	—
	100	—	—	77
	120	1.302	44	60
	150	1.309	53	—
	180[b]	1.304	47	—
	210[b]	1.299	42	74
I-A₃	Unannealed	1.282	20	35
	90	1.285	24	—
	120	1.283	22	21
	150	1.282	20	20
	180	1.284	23	—
	210	1.284	23	37

[a] Crystallinity determined from density is considered reliable to $\pm 4\%$ whereas crystallinity from infrared spectra is less reliable.
[b] Discoloration occurs at these temperatures.

TABLE III
Effect of Heat Treatment on Solubility of Poly(vinyl Alcohol) Film in Water

PVA Sample	Unannealed Crystallinity, %	Unannealed Solubility, %[b]	Annealed[a] Crystallinity, %	Annealed[a] Solubility, %[b]
H-V	31	82	57	4
H-V$_x$	32	100	66	—
H-H	48	100	72	13
I-A₃	20	35	20	22
S-A	41	0	53	0

[a] Annealed at 150°C. in vacuum for 30 min.
[b] Solubility in water at 70°C. after one hr.
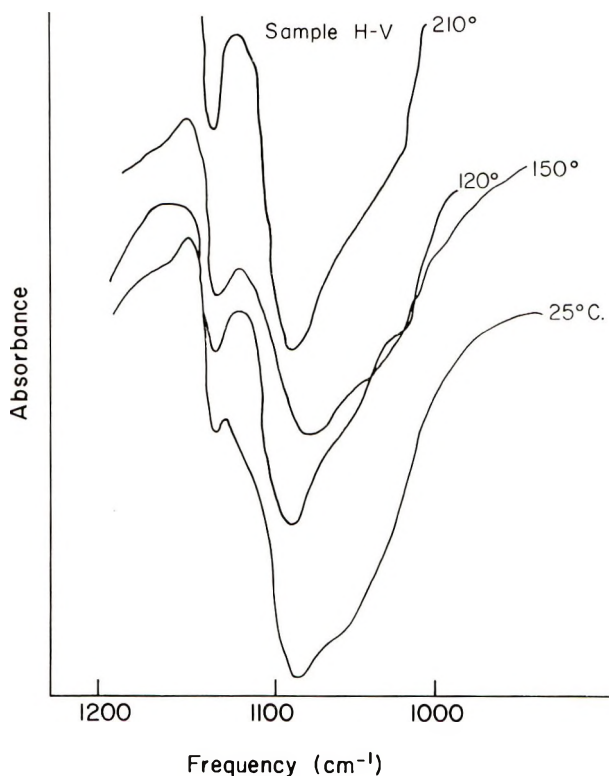
Fig. 2. See caption, p. 687.

X-Ray Diffraction

The Philips diffractometer was operated at 30 k.v. and 20 ma. with a scintillation counter detector and copper source. The source and receiving slit widths were each 1°, respectively. Scale factors for the recorder chart were adjusted to give maximum deflection for the peak at approximately 19° 2θ and a diffraction pattern from 30 to 5° 2θ was obtained at the rate of 1° 2θ/min. Figure 3 shows the effect of heat treatment on the x-ray diffractograms.

Water Resistance

A 1-in.^{2} piece of film was dried in a vacuum oven at 50°C. overnight. The dried film was weighed and immersed in water maintained at 70°C. for 1 hr. At the end of this time, any undissolved film was recovered, dried, and weighed. The per cent soluble was calculated from eq. (2).

$$\% \text{ Soluble} = \frac{\begin{array}{c}(\text{Weight of dried film before test}) \\ - (\text{Weight of dried film after test})\end{array}}{(\text{Weight of dried film before test})} \times 100 \qquad (2)$$

The water resistance of annealed and unannealed films at 70°C. is shown in Table III.
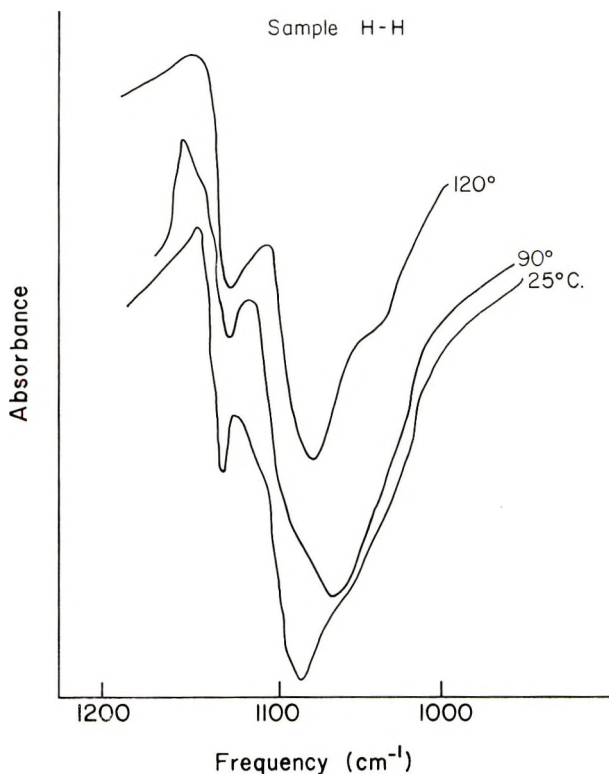
Fig. 2 (*continued*).

The solubility of films annealed at 150°C. for 30 min. was tested in super-heated water in evacuated sealed heavy-walled tubes. Samples H-V, H-V$_x$, and H-H were 100% soluble after 1 hr. at 130°C. Samples S-A and I-A$_3$ were only slightly swollen and were heated, in addition, 1 hr. at 140°C. Sample S-A formed a highly viscous solution with highly swollen film present. Sample I-A$_3$ partially dissolved.

The swelling index was determined from the weight of water imbibed per weight of film. The film was dried and weighed as above and immersed in water at 30°C. for 1 hr. At the end of this time, excess water was carefully removed by blotting on filter paper. The swollen film was placed in a covered weighing dish and weighed. The film was dried and reweighed. The swelling index is given by eq. (3).

Swelling index

$$= \frac{(\text{Weight of swollen film}) - (\text{Weight of dried film after swelling})}{(\text{Weight of dried film after swelling})} \quad (3)$$

The swelling indices for samples S-A, I-A$_3$, and H-V were 1.4, 2.7, and 8.3, respectively.
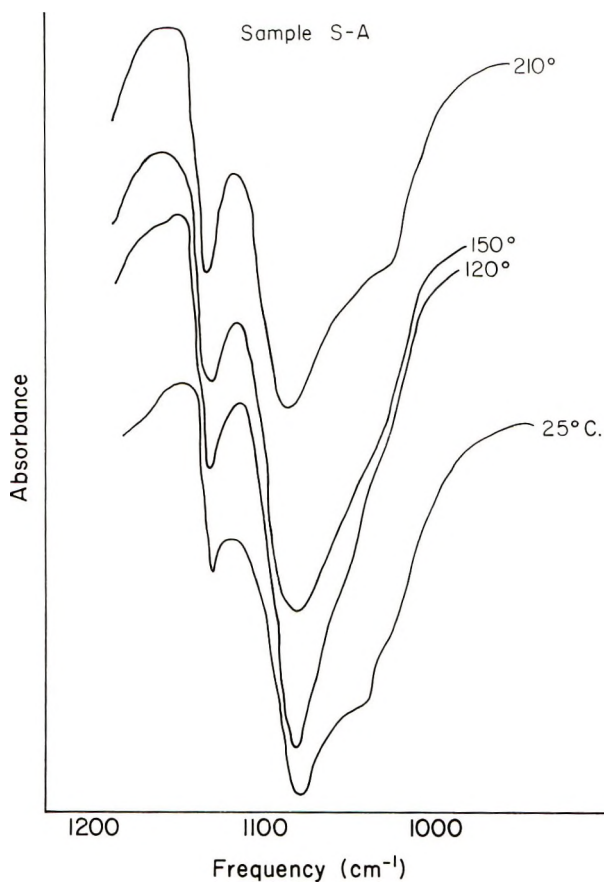
Fig. 2 (continued).

Thermal Analysis of PVA Samples

The differential thermal analysis (DTA) and thermogravimetric analysis (TGA) apparatus are described elsewhere.[9] DTA thermograms were recorded on 150 mg. of sample, in powder form, under nitrogen. The sample was mixed with alumina as a diluent, and alumina was also used in the reference well. Nickel cells were used as the sample and reference wells. The heating rate was $11°C./min.$ The TGA thermograms were recorded on 1 g. of sample, also in powder form, under nitrogen atmosphere with a heating rate of $4°C./min.$

RESULTS AND DISCUSSION

Poly(vinyl Alcohol) Samples

The PVA samples selected for the present study differ with respect to tacticity, molecular weight and, to a lesser extent, other factors of molecular regularity. Tacticity was determined quantitatively by NMR spectros-
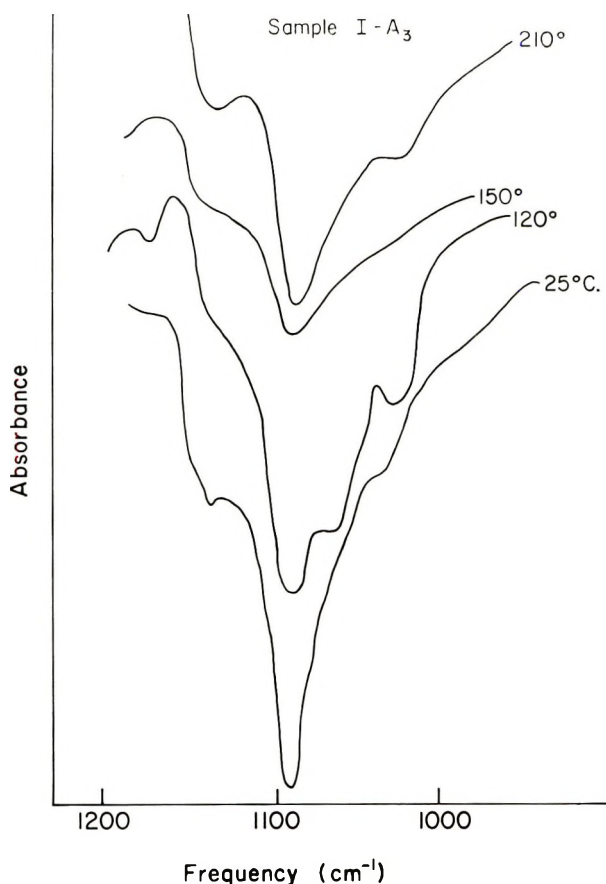
Fig. 2. Effect of heat treatment on the infrared absorption band at 1141 cm.$^{-1}$.

copy as reported elsewhere,[3,4] and the results are listed in Table I. Samples of low molecular weight give spectra with considerably better resolution. Therefore, tacticity data were obtained on cleaved samples when the intrinsic viscosities of the original PVA was greater than about 0.3.[4] The values given for the low molecular weight, cleaved analogs are considered to be indicative of the tacticities of the parent polymers. The triad distribution shown for sample H-H is representative of all the samples derived from PVAc since it has been demonstrated that the polymerization temperature or solvent has no significant effect on the tacticity of the resultant PVA.[1]

Variation in other factors of molecular regularity (i.e., 1,2-diol units, branching, carbonyl groups) are present in these PVA samples, but all available data suggest that these differences were minor. Quantitative determination of 1,2-diol units indicate a maximum of 1.7%.[7] Ultraviolet spectra and other data[10] suggest that carbonyl and α,β-unsaturated carbonyl groups were present to a maximum extent of about 0.4%. Main chain branching could not be measured, but previous data[2] indicate that
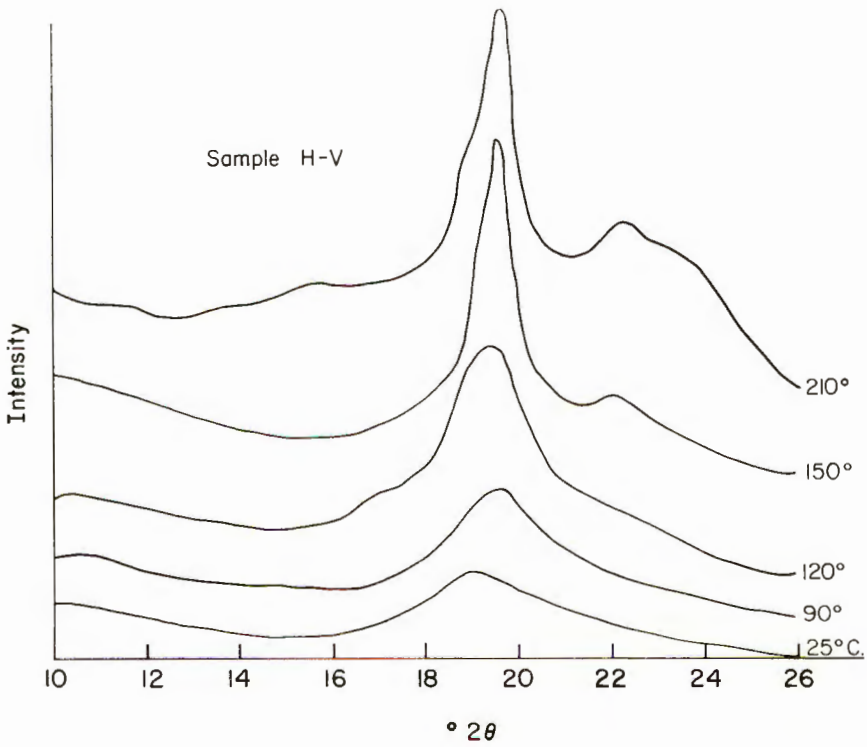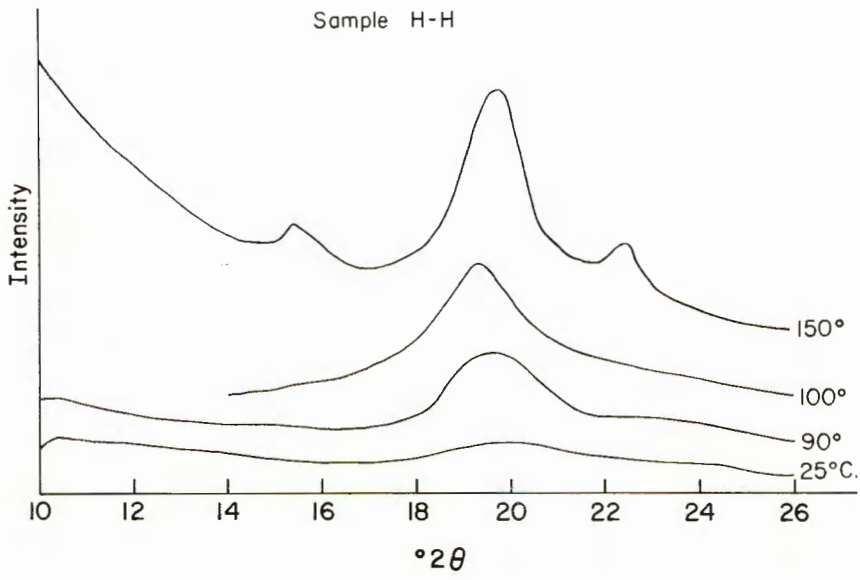
Fig. 3.   See caption, p. 689.
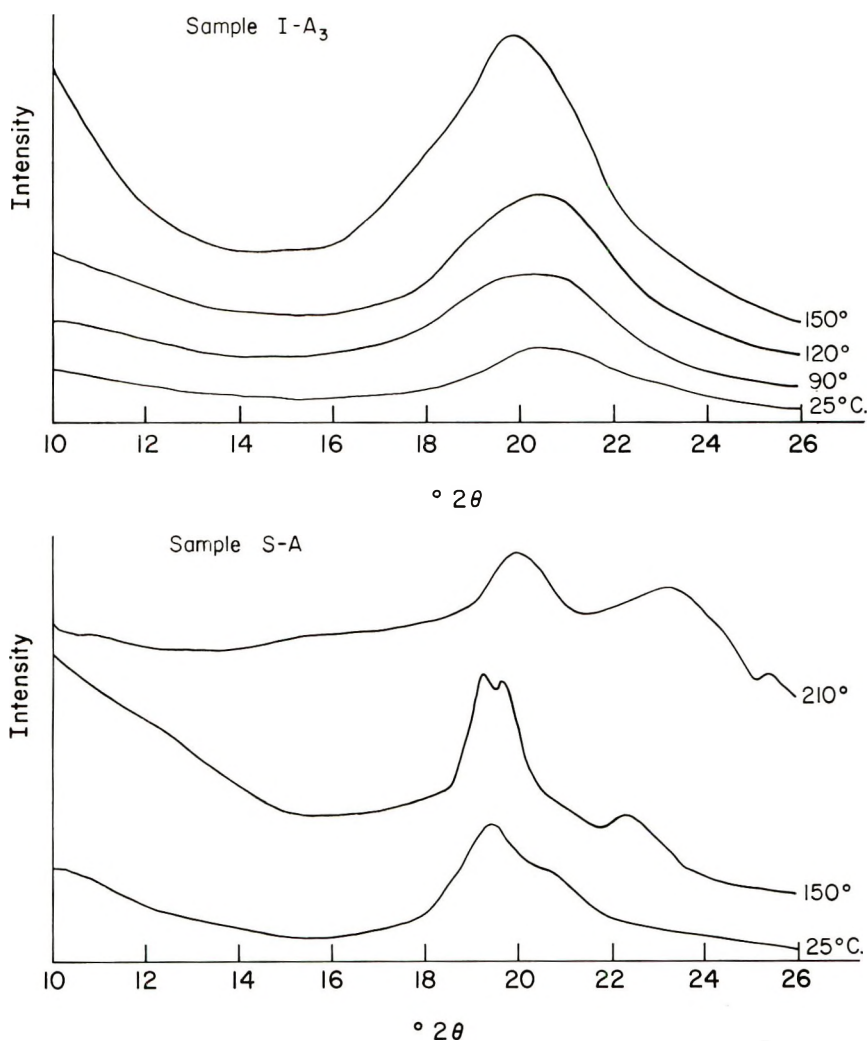
Fig. 3. Effect of heat treatment on the x-ray diffractograms.

the influence of branching or variation in branching was of lesser importance in the samples studied.

The molecular weights vary considerably. However, indications of the influence of molecular weight on the properties investigated were obtained by comparing samples H-H, H-V, and H-V$_x$. These samples should be similar in other factors of molecular structure. Indeed, cleavage of sample H-V at 1,2-diol units with periodic acid and subsequent reduction of the product with sodium borohydride gave H-V$_x$ which is of significantly lower molecular weight but otherwise differs from H-V only in 1,2-diol content and possibly carbonyl content.

Films of samples H-V, S-A, and I-A$_3$ were prepared by casting acetone solutions of the respective PVTFAc's and subsequently hydrolyzing the

resultant films in methanolic ammonium hydroxide. Films of samples H-H H-V, and H-V$_x$ were cast from water solutions, but samples S-A and I-A$_3$ were not amenable to this technique because of their insolubility in water. In general, films prepared by the two techniques appeared similar; however, films prepared from the trifluoroacetates discolored somewhat more at temperatures above 150°C., and the crystallinities of these films leveled off or decreased rather than increased at annealing temperatures above 150°C. TGA and DTA analyses of PVA derived from PVTFAc samples gave no significant evidence of decreased thermal stability.

Estimation of Relative Tacticity From Infrared Spectra

The 800–1200 cm.$^{-1}$ portions of the infrared spectra of samples S-A, H-V, and I-A$_3$ in film form are illustrated in Figure 4. The bands at 916 and 850 cm.$^{-1}$ have been observed to be quite different depending on the PVA source. For some time these differences have been associated with differences in tacticity, and the ratio of the absorbances at 916 cm.$^{-1}$ (D_{916}) and 850 cm.$^{-1}$ (D_{850}) have been used as an index of stereoregularity without a method of relating these values to direct tacticity measurements. However, plots of D_{916}/D_{850} versus per cent triads give linear relationships (Fig. 5), and it now appears possible to calculate triad distributions from the infrared index and the following formulas:

$$\% \ S \ = \ 60 \ (D_{916}/D_{850}) \ + \ 7$$
$$\% \ I \ = \ -78 \ (D_{916}/D_{850}) \ + \ 59$$
$$\% \ H \ = \ 18.7 \ (D_{916}/D_{850}) \ + \ 34$$

There are insufficient data to establish the accuracy of such calculations, but values determined in this manner appear reasonable. Occasional variation in the D_{916}/D_{850} ratio have been observed. For example, it was
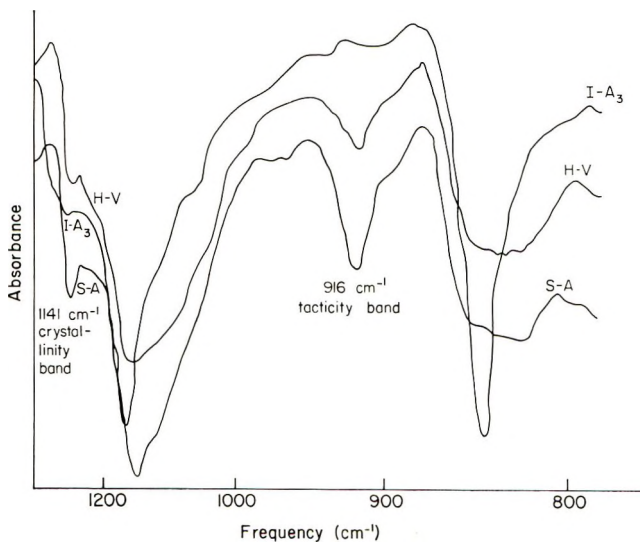
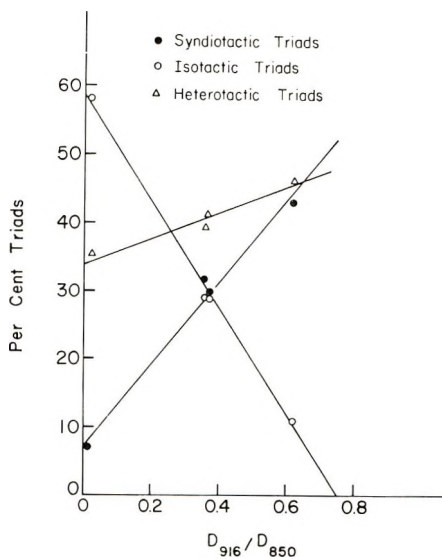Fig. 4. Infrared spectra of PVA samples of different tacticities.

Fig. 5. Per cent triads from NMR vs. infrared tacticity indices.

observed that the ratios decreased on heat treatment, and more reasonable results were obtained by determining all infrared indices on unannealed film.

Crystallinity of Films

The crystallinities of unannealed and annealed films of varying molecular regularity were determined from densities. These values (Table II) were reproducible and considered reliable to $\pm 4\%$. Crystallinities of samples H-H, H-V, and S-A increased with annealing temperature until maximum values were obtained by heating at 150–180°C. On the other hand, I-A$_3$ did not increase in crystallinity significantly with annealing. The highest crystallinity obtained was 75% (density) for sample H-H. These results indicate the following order of crystallizabilities for samples of varying tacticity: atactic $\geq$ syndiotactic-rich $\gg$ isotactic-rich. Thus, within the range of tacticities studied, increased syndiotactic structure does not appear to lead to higher crystallinity, and increased isotactic structure results in a significant decrease in crystallinity. The observed differences in the crystallinities of atactic and syndiotactic-rich PVA samples may be due to small differences in other factors of molecular regularity or even the method of film preparation.

The results of infrared and x-ray studies are in general agreement with the density data. Figure 2 shows that the intensity of absorption of the crystallinity-sensitive band at 1141 cm.[-1] in the infrared[5] increases with heat treatment. Per cent crystallinities were calculated from these infrared spectra,[8] but the values (Table II) were less reliable than those determined from densities. In many instances the infrared crystallinities were higher, particularly for sample S-A. Film samples H-H, H-V, I-A$_3$, and S-A gave similar x-ray diffractograms, and Figure 3 also shows how

the crystalline intensity at approximately $20°\ 2\theta$ increases with heat treatment. Sample I-A$_3$ again appears very different from the other samples in that crystallinity does not increase to any significant degree with heat treatment.

Data in the literature[11] and data on samples H-V and H-V$_x$ (Table III) indicate that molecular weight has a relatively small effect on the crystallization of PVA. Unannealed samples of H-V and H-V$_x$ possessed essentially the same crystallinity (31–32%), and annealing at 150°C. resulted in crystallinities of 57 and 66%, respectively. This difference can be attributed to molecular weight and/or to the difference in 1,2-diol content and possibly carbonyl content. The fact that sample H-H exhibited higher crystallinity than H-V or H-V$_x$ must be the result of greater molecular regularity, perhaps less branching, in H-H. This possibility was also indicated by crystallization–dissolution temperature measurements.[2]

The effects of stereoregularity on crystallinity must be associated primarily with differences in hydrogen bonding rather than differences in simple steric interaction since the hydroxyl group and hydrogen atoms can be exchanged at random in the crystal lattice.[12] In syndiotactic-rich PVA, the more regular placement of hydroxyl groups along a planar zigzag chain should result in a greater number of intermolecular hydrogen bonds, and this increase in crosslinking will reduce chain mobility and ease of orientation. Therefore, in the absence of external forces atactic PVA might be expected to crystallize more readily than the more stereoregular material. Thus, crystallization of S-A from solution at 140°C. gives material of 35% crystallinity,[2] whereas annealing the same material in film form gives 44% crystallinity at 120°C. and 53% crystallinity at 150°C.; presumably orientation is facilitated in films as some drawing occurs during film shrinkage. Atactic PVA, presumably with fewer hydrogen bonds and greater chain mobility, gave a product of 60% crystallinity when crystallized from solution at 120°C.[2] and 57% crystallinity when annealed at 150–180°C. in film form. Isotactic-rich PVA should form more intramolecular hydrogen bonds, most probably between adjacent hydroxyls in a six-membered ring configuration, with concomitant decrease in intermolecular forces and tendency to form crystalline arrays of chain segments. The effect of heating plus drawing on isotactic-rich PVA film or fiber has not been studied, but the slight drawing which occurs during shrinkage of films seems to have little effect. Solution-crystallized I-A$_3$[2] and the same material in film form possessed about the same crystallinities. The fact that all the syndiotactic-rich and atactic PVA films are tough and flexible whereas the isotactic-rich PVA films were weak and brittle may be a further indication of the tendency towards intramolecular hydrogen bonding in the latter material.

Water Resistance of Films

The water resistance of PVA films was measured as a function of crystallinity and tacticity. The swelling index for unannealed samples S-A,

I-A$_3$, and H-V was 1.4, 2.7, and 8.3, respectively. The solubility of un-annealed film and film annealed at 150°C. is presented in Table III along with crystallinity values. For unannealed samples of varying tacticity, the solubility cannot be correlated with crystallinity. Films of atactic PVA of 31-48% crystallinity were 82-100% soluble, while those of syn-diotactic-rich PVA of 41% crystallinity are completely insoluble. How-ever, heat treatment of each film decreased solubility while crystallinity increased. The solubility of PVA films heat treated at 150°C. was as follows after 1 hr. in water at 70°C.: S-A, 0%; H-V, 4%; H-H, 13%; and I-A$_3$, 22%. Additional qualitative information concerning comparative water solubilities was obtained by heating film samples in water in sealed tubes at 130 and 140°C. Samples H-H, H-V, and H-V$_x$ dissolved com-pletely at 130°C., but samples S-A and I-A$_3$ were only slightly swollen and dissolved only partially even at 140°C. Thus, at least a part of the isotactic-rich material was much more water-resistant under more vigorous conditions than any of the atactic samples, in spite of the data observed for solubilities at 70°C.

The water resistance of PVA film is influenced by molecular weight,[11] crystallinity, and tacticity. Solubility decreases for samples of equal crystallinity and tacticity as molecular weight increases. For any given sample, water resistance for samples of varying tacticity exhibits the follow-ing order: syndiotactic-rich ≫ isotactic-rich ≫ atactic. This order of solubility based on tacticity appears justified on the basis of the present data, but one must consider other factors when evaluating the solubility of PVA under a given set of conditions. For example, a highly crystalline, atactic PVA sample exhibits essentially complete insolubility in boiling water.[13] Also, data given here for solubility at 70°C. indicate that an-nealed atactic PVA is more insoluble than the annealed isotactic-rich product. In other words, large differences in crystallinity may overshadow differences in tacticity in determining the water resistance of PVA samples under certain conditions.
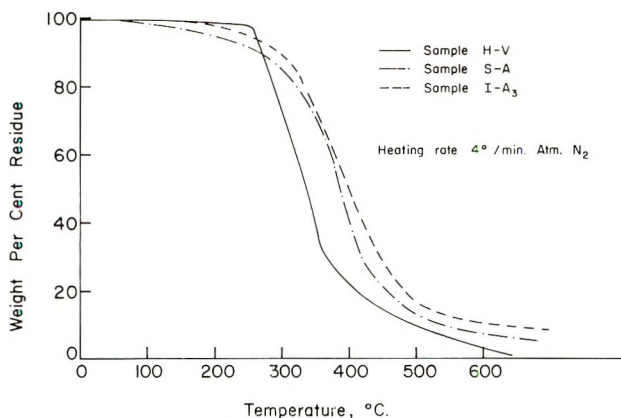

Fig. 6. Thermogravimetric analyses of PVA samples of different tacticities.
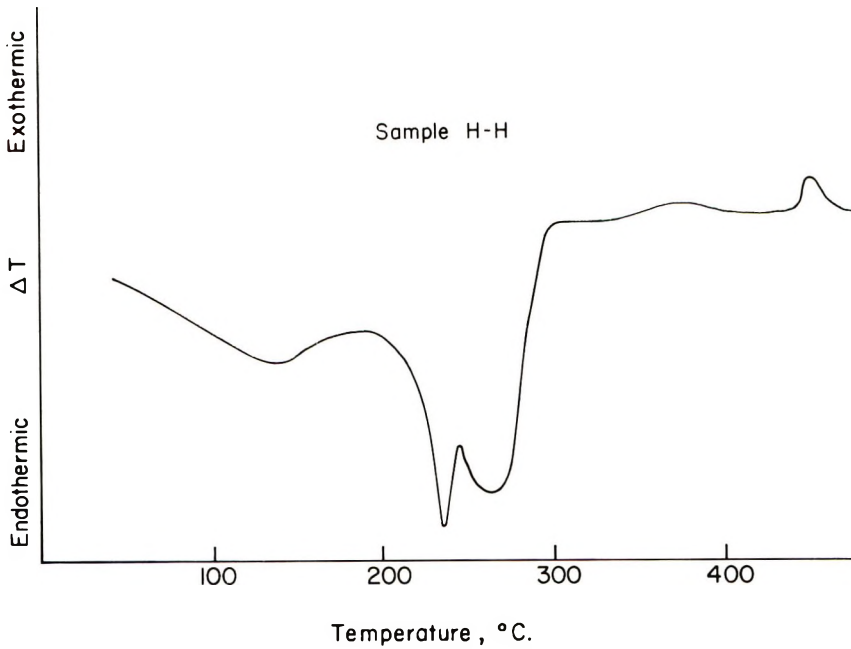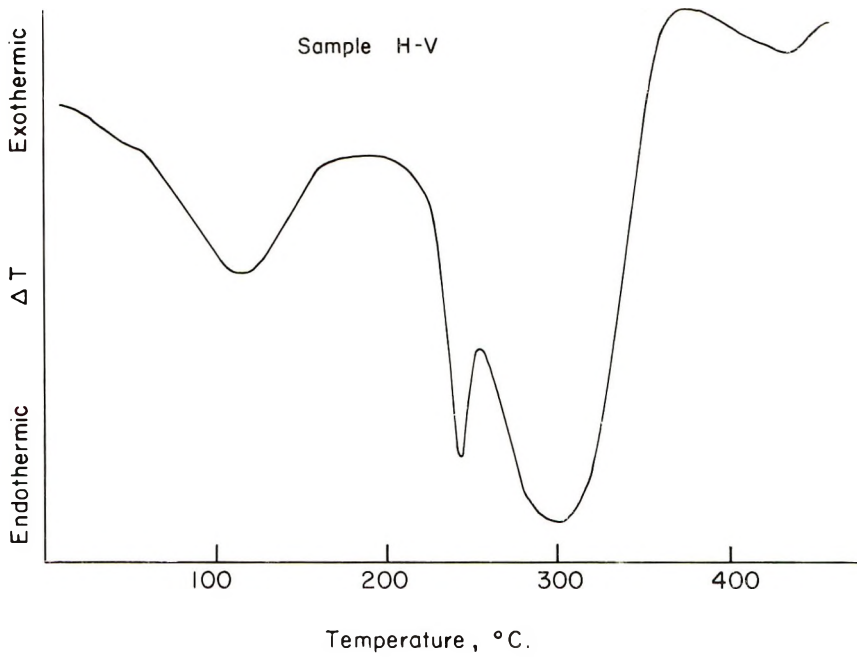
Fig. 7. See caption, p. 695.

There are insufficient data for one to draw definitive conclusions concerning the question of water solubility–structure relationships. The water resistance of a PVA sample depends upon (1) the accessibility of the polymer structure to infusion of water (i.e., the amount of disordered, amor-
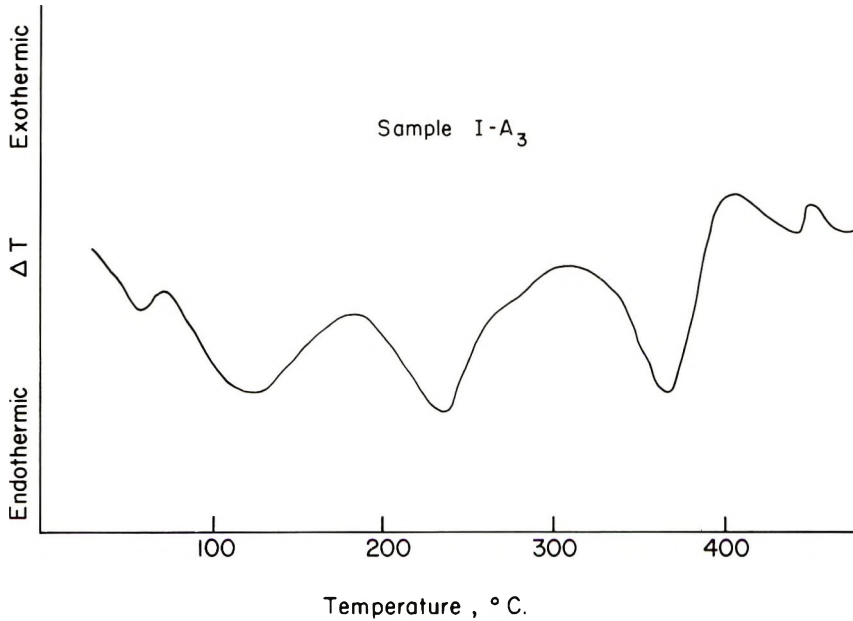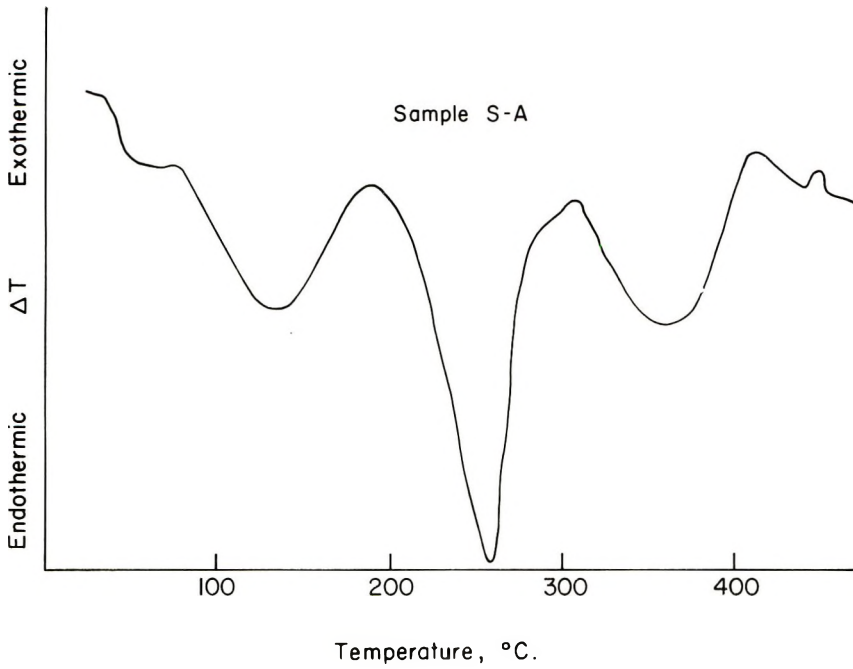
Fig. 7. Differential thermal analyses of PVA samples of different tacticities. Sample weight, 150 mg.; heating rate, 11°C./min.; atmosphere, N₂.

phous structure), (2) the strength of the intermolecular forces, and (3) ease of solvation of the molecules by water. Atactic PVA of low crystallinity swells in water and eventually dissolves completely; water enters into the amorphous regions, swells the structure, and intermolecular forces

are too weak to resist complete solvation and dissolution. The solubility of this material can be reduced, essentially to 0% in boiling water, by annealing and drawing.[13] This process reduces the amount of amorphous structure and at the same time increases intermolecular forces (both hydrogen bonding and the weaker Van der Waals forces). Syndiotactic-rich PVA of low crystallinity swells to a small degree in water, but by virtue of the increased hydrogen bonding that occurs in syndiotactic placements of hydroxyl groups, intermolecular forces are sufficient to resist further solvation until extreme conditions (i.e., superheated water) are used.[14] Annealing and drawing of the syndiotactic-rich product reduces its tendency to swell still further, just as in the case of atactic PVA.[14] Isotactic-rich PVA exhibits properties which are difficult to rationalize. Literature data are not consistent, and our data show that samples of similar isotacticity exhibit different solubilities and other properties. These differences may be due to differences in molecular weight, degree of branching, sequence length of isotactic placements, or perhaps some other structural difference. However, sample I-A₃, the most regular isotactic-rich material investigated in this work, is of relatively low solubility in spite of low crystallinity and low molecular weight (approx. 16,000). The low crystallinity (density) suggests that the structure should be accessible to water, and available data (e.g., DTA) indicates intermolecular forces are not especially great. Perhaps, the intramolecular hydrogen bonds are of sufficient strength to inhibit solvation by water, which presumably would involve the breaking of existing bonds and the formation of hydrogen bonds involving water molecules.

Thermogravimetric and Differential Thermal Analyses

PVA samples H-H, H-V, I-A₃, and S-A were subjected to thermogravimetric analysis (TGA) and differential thermal analysis (DTA). TGA thermograms (Fig. 6) indicated that sample H-V was slightly more stable than samples I-A₃ and S-A to about 260°C., but at 350°C. the weight loss was approximately 50% greater than for the latter two samples. The DTA thermograms of the four samples are shown in Figure 7, and the deflections in individual curves (attributed to glass transition temperature, variation in interplanar distances in PVA crystallite, melting temperature, and decomposition temperature, respectively) are listed in Table IV. The thermogram melting peak area (Fig. 7) for sample S-A, is largest and is indicative of stronger intermolecular forces (i.e., higher crystallinity). That of I-A₃ is smaller, indicating weak intermolecular forces, and is characteristic of poorly crystalline polymers. The thermogram melting curves of H-V and H-H do not return to the base line but overlap with the decomposition deflection indicating that melting occurs with decomposition. The decomposition temperatures were lower in these samples, which agrees with the TGA curves. The lower thermal stability of the atactic samples (see last column, Table IV) may be an indication of higher carbonyl content since the carbonyl group is known to enhance the tendency of these polymers to decompose. The conclusion that deflections occurring at

TABLE IV

Differential Thermal Analysis of Poly(vinyl Alcohol)[a]

PVA sample	Temperature of various deflections, °C.			
	Glass transition	Lattice variation	Melting	Decomposition
S-A	62	133	258	360
I-A₃	58	122	235	366
H-V	51	115	243	298
H-H	—	135	235	263

[a] See Figure 7.

115–135°C. were the result of changes in interplanar distances in the PVA crystallite was based on x-ray diffraction studies in which discontinuous heat expansion of the lattice spacings was found to occur at 120–130°C.[15]

SUMMARY

Poly(vinyl alcohol) is a polar polymer in which the polar substituent groups are small and can be exchanged with hydrogen at random in the crystal lattice. In such a polymer, the polar interactions (i.e., hydrogen bonding) can be expected to exert a greater influence on physical properties than simple steric interactions involving the substituent groups. This appears to be supported by experimental data. Higher tacticity did not lead to higher crystallinity in PVA, the indicated order of crystallizability being atactic ≧ syndiotactic-rich ≫ isotactic-rich. On the other hand, both syndiotactic-rich and isotactic-rich PVA exhibited significantly higher water resistance than atactic material. These property differences appear to be most easily explained on the basis of differences in hydrogen bonding characteristics. Increased syndiotacticity leads to an increase in intermolecular hydrogen bonding. This leads to higher solvent resistance. Although syndiotactic placements would not be expected to influence the ultimate crystallizability, they do result in a lower tendency to crystallize, probably because of their influence on chain mobility. Isotactic placements along the planar zigzag chain leads to a higher probability of intramolecular hydrogen bonding (i.e., between 1,3-hydroxyl groups). This interaction would lead to stiffening of the chain, lower intermolecular forces, lower crystallinity, and apparently higher solvent resistance.

References

1. Friedlander, H. N., H. E. Harris, and J. G. Pritchard, *J. Polymer Sci. A-1*, **4**, 649 (1966).

2. Harris, H. E., J. F. Kenney, G. W. Willcockson, R. Chiang, and H. N. Friedlander, *J. Polymer Sci. A-1*, **4**, 665 (1966).

3. Vollmer, R. L., J. G. Pritchard, and G. W. Willcockson, *J. Polymer Sci.*, to be submitted.

4. Tincher, W. C., *Makromol. Chem.*, **85**, 46 (1965).

5. Fujii, K., T. Mochizuki, S. Imoto, J. Ukida, and M. Matsumoto, *J. Polymer Sci. A*, **2**, 2327 (1964).

6. Higashimura, T., T. Watanabe, K. Suzouki, and S. Okamura, *J. Polymer Sci. C*, **4**, 361 (1964).

7. Harris, H. E., and J. G. Pritchard, *J. Polymer Sci. A*, **2**, 3673 (1964).

8. Sakurada, I., *Poly(vinyl Alcohol)*, Kobunshi Gakkai, Tokyo, 1955.

9. Slade, P. E., and L. T. Jenkins, *J. Polymer Sci. C*, **6**, 27 (1964).

10. Clarke, J. T., and E. R. Blout, *J. Polymer Sci.*, **1**, 419 (1946).

11. Sakurada, I., Y. Nukushina, and Y. Sone, *Kobunshi Kagaku*, **12**, 506 (1955).

12. Bunn, C. W., *Nature*, **161**, 929 (1948); C. W. Bunn and H. S. Peiser, *Nature*, **159**, 161 (1947).

13. Meos, A. I., L. A. Vol'f, and G. N. Afans'eva, *Khim. Volok.;* No. 3, 18 (1963).

14. Black, W. B., and P. R. Cox, papers presented at Textile Research Institute, 34th Annual Meeting, New York, April, 1964, p. 53.

15. Ishikawa, K., and K. Miyasaka, *Repts. Progr. Polymer Phys. Japan*, **7**, 93 (1964).

Résumé

Les relations structure–propriété d'alcools polyvinyliques ont été étudiées en mesurant la cristallinité et la résistance à l'eau de films obtenus au départ d'échantillons de tacticité différente bien connue. La cristallinité de films non traités et traités ont été examinés en utilisant des mesures de densités, d'infra-rouge et de rayons X. Une tacticité plus élevée n'entraîne pas une cristallinité plus élevée. L'ordre apparent de cristallisabilité était atactique, syndiotactique et isotactique. La résistance à l'eau de ces films était déterminée en mesurant leur indice de gonflement à 30° et la solubilité à 70° et à 130–140°C. La résistance à l'eau croît avec la tacticité, les échantillons riches en unités syndiotactiques manifestant la plus grande résistance à l'eau. Étant donné que la résistance à l'eau augmente également avec la cristallinité, il en résulte que la stéréorégularité et la cristallinités doivent être considérées comme déterminant les relations structure–solubilité. Des analyses thermiques différentielles et thermogravimétriques des ces échantillons sont également présentées en rapport avec l'indice de tacticité telle qu'on le mesure par la technique infra-rouge ainsi que par la technique de résonance nucléaire magnétique.

Zusammenfassung

Beziehungen zwischen Struktur und Eigenschaften von Polyvinylalkohol wurden durch Messung der Kristallinität und der Wasserbeständigkeit von Filmen aus Proben mit verschiedener, bekannter Taktizität untersucht. Die Kristallinität ungetemperter und getemperter Filme wurde mittels Dichte-, Infrarot- und Röntgenmessungen untersucht. Höhere Taktizität führte nicht zu höherer Kristallinität. Die Reihenfolge der Kristallisations-Fähigkeit war ataktisch $\geqslant$ syndiotaktisch $\gg$ hochgradig isotaktisch. Die Wasserbeständigkeit dieser Filme wurde durch Messung des Quellungsindex' bei 30°C und der Löslichkeit bei 70°C und 130–140°C bestimmt. Die Wasserbeständigkeit nimmt mit steigender Taktizität zu, wobei das hochgradig syndiotaktische PVA die höchste Wasserbeständigkeit aufweist. Da die Wasserbeständigkeit auch mit der Kristallinität zunimmt, müssen sowohl Stereoregularität als auch Kristallinität bei der Ermittlung von Beziehungen zwischen Struktur und Löslichkeit in Betracht gezogen werden. Schliesslich werden Differentialthermo- und thermogravimetrische Analysen dieser Proben sowie eine Korrelation zwischen dem infrarotspektroskopisch gemessenen Kristallinitätsindex und dem nach einem NMR-Verfahren bestimmten vorgelegt.

Crystallization and Dissolution Temperatures of Poly(vinyl Alcohol) Crystal Lamellae

J. F. KENNEY and V. F. HOLLAND, *Chemstrand Research Center, Inc., Durham, North Carolina*

Synopsis

Poly(vinyl alcohol) single crystal platelets having a stepheight of approximately 100 A. were obtained by isothermal crystallization from dilute triethylene glycol solution. Material crystallized at temperature T_c redissolved in the same solvent at a higher temperature T_s. A plot of T_c versus T_s gave a straight line of slope 0.47. Extrapolation of this line to $T_c = T_s$ gave $(T_m)_\infty$ which may be regarded as the dissolution temperature of the crystal of infinite stepheight. $(T_m)_\infty$ for this sample in triethylene glycol was 220°C. The crystalline nature of the platelets was established by electron and x-ray diffraction techniques. A total of three Bragg d spacings having the values of 3.9, 4.4, and 4.6 A. (±0.05 A.) were measured. These spacings were indexed as the (200), (101), and (10$\bar{1}$) reflections, respectively, of the monoclinic unit cell of Bunn. The x-ray diffractogram exhibits sharp intensities of the (10$\bar{1}$) and (101) reflections. The crystallinity calculated from the density of the poly(vinyl alcohol) precipitated from dilute solutions in triethylene glycol was 42%. Although the overall degree of crystalline perfection of this poly(vinyl alcohol) is low, the linear relationship between T_s and T_c and the formation of definite shaped single crystals when crystallized from dilute solution suggest that poly(vinyl alcohol) crystallizes in the same manner as other semicrystalline polymers.

INTRODUCTION

Previous studies on polyethylene[1,2] and polyacrylonitrile[3,4] solution-grown crystal lamellae have shown a straight line relationship between the crystallization temperature T_c, and the dissolution temperature T_s, in the crystallization liquid. The crystallization of poly(vinyl alcohol) (PVA) from dilute solution in the form of single crystal lamellae has recently been reported.[5,6] It is, therefore, possible to study the dissolution and crystallization temperature relationship of isothermally crystallized PVA from dilute triethylene glycol solution. In addition, density, x-ray and electron diffraction, and electron microscopical measurements on these crystals aid in describing their crystallization behavior.

EXPERIMENTAL

Materials

Poly(vinyl alcohol) (PVA) was derived from poly(vinyl acetate) prepared in methyl ethyl ketone at 60°C. by using azobisisobutyronitrile initiator. The intrinsic viscosity of the PVA determined in water at 25°C.

was 0.26. The tacticity of the PVA was determined by nuclear magnetic resonance.[7] Isotactic, heterotactic, and syndiotactic triads were 29, 41, and 30%, respectively.[8] The infrared spectrum of a film of the PVA cast from aqueous solution had a D_{916}/D_{850} absorption ratio of 0.37.

Union Carbide triethylene glycol was distilled at reduced pressure, b.p. 120°C./1 mm.

Isothermal Crystallization

The procedure for isothermal crystallization and determination of dissolution temperature has been described previously.[4] Solutions consisting of 0.01–0.1% PVA by weight were allowed to crystallize at constant temperature overnight. At low degrees of undercooling, crystallization was allowed to proceed for 2 or 3 days.

Determination of Dissolution Temperature

About 0.1 ml. of the crystallized sample was added to a thin-walled tube partly immersed in an oil bath heated to the desired test temperature. By several trials, a precise dissolution temperature was found above which the crystals dissolved and below which the crystals remained undissolved indefinitely.

Determination of Density

A flotation method was used to determine the density of the crystalline polymer isolated by vacuum evaporation of the triethylene glycol. The density of the dried PVA was determined by observing the point at which the density of the flotation medium (CCl_4–benzene mixture) matches that of the suspended PVA, as demonstrated by absence of sedimentation under high-speed centrifugation. The density of the flotation medium was measured with a Westphal density balance at 22°C.

Of special importance is the absence of partial sedimentation after adjusting the medium to matching density. The dispersion remained uniform throughout the sample tube when such a mixture was centrifuged. In view of the sensitivity of the method to small differences in density, the densities of the various particles present in a given sample must be very nearly identical. These observations show that separate amorphous particles are probably not present.

X-Ray Diffraction

The Philips diffractometer was operated at 30 kv. and 20 ma. with a scintillation counter detector and copper source. The source and receiving slit widths were each 1°. Scale factors for the recorder chart were adjusted to give maximum deflection for the peak at approximately 20° 2θ and a diffraction pattern from 30 to 5° 2θ was obtained at the rate of 1° 2θ/min.

Electron Microscope Examination

Conventional electron microscopic techniques were used to observe the morphology of representative forms of material precipitated from solution at various temperatures and concentrations. A drop of the crystalline suspension was placed on carbon-coated grids, the excess solvent removed, and metal shadowing carried out with platinum. Electron diffraction experiments were conducted on unshadowed specimens.

RESULTS

Dissolution Temperature

The isothermal crystallization temperatures T_c and dissolution temperatures T_s of PVA single crystals in triethylene glycol are given in Table I.

TABLE I

Dissolution Temperature T_s as a Function of Crystallization Temperature T_c in Triethylene Glycol of a Poly(vinyl Alcohol)

T_s, °C.	T_c, °C.
157.8	80
167.8	106
187.4	150
191.2	160
197.6	170
(220)[a]	(220)[a]

[a] Extrapolated values as described in text.

A plot of T_c versus T_s yields a straight line (Fig. 1).   Extrapolation of this line to the $T_c = T_s$ line gives a value of 220°C. which can be considered as the dissolution temperature, $(T_m)_\infty$, of the infinitely thick crystal in triethylene glycol.
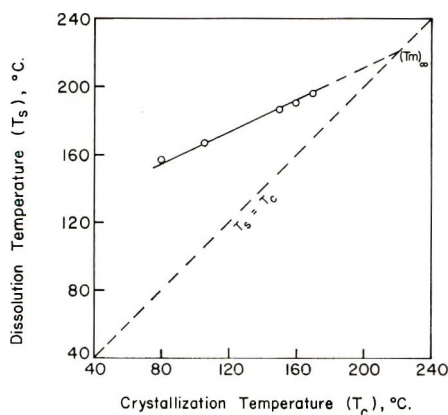

Fig. 1. Dissolution temperature T_s as a function of crystallization temperature T'_c for a poly(vinyl alcohol) crystallized from triethylene glycol.

Density and Per Cent Crystallinity

The density of the solution crystallized PVA sample studied in this work was found to be 1.301 g./cc., irrespective of the crystallization temperature (within the range 100–170°C.). This value corresponds to a crystallinity of 42% (volume) based on crystalline and amorphous densities of 1.345 and 1.269 g./cc.,[9] respectively.

Morphology

Figure 2 shows platelets obtained from a 0.01% solution by cooling from 200°C. in an oil bath. Figure 3 shows platelets obtained from a 0.01% solution by isothermal crystallization at 150°C.

The platelets are in the shape of parallelograms. Most were built up in several layers, each approximately 100 A. in thickness. The length of the longer side is about 1μ and that of the shorter side is 0.25μ. The acute angle of the parallelogram is about 53°.
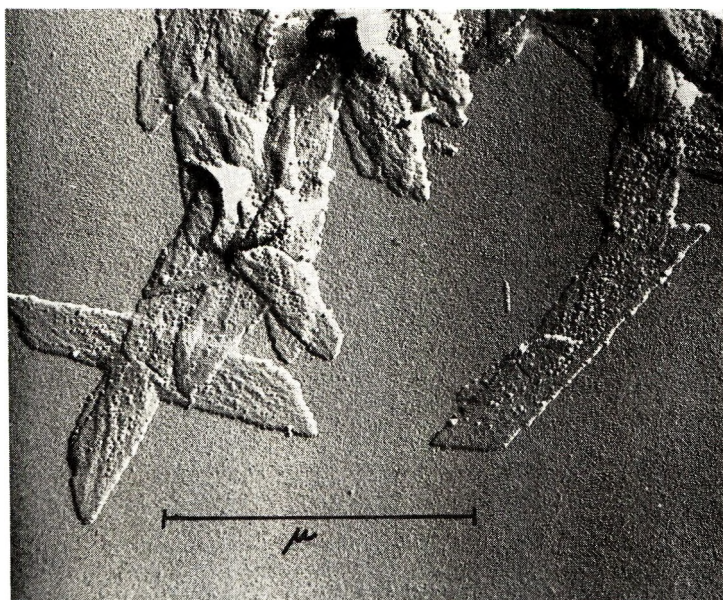
Fig. 2. PVA platelets crystallized from 0.01% triethylene glycol solution by cooling from 200°C.

Electron and X-Ray Diffraction

The crystalline nature of the PVA precipitated from solution was established by electron and x-ray diffraction techniques. Electron diffraction patterns of individual crystals could not be observed because of their small size. In addition, the single crystals were usually agglomerated. A total of three Bragg d spacings having the values of 3.9, 4.4, and 4.6 A. (± 0.05 A.) were measured for an agglomerate of several single crystals. These
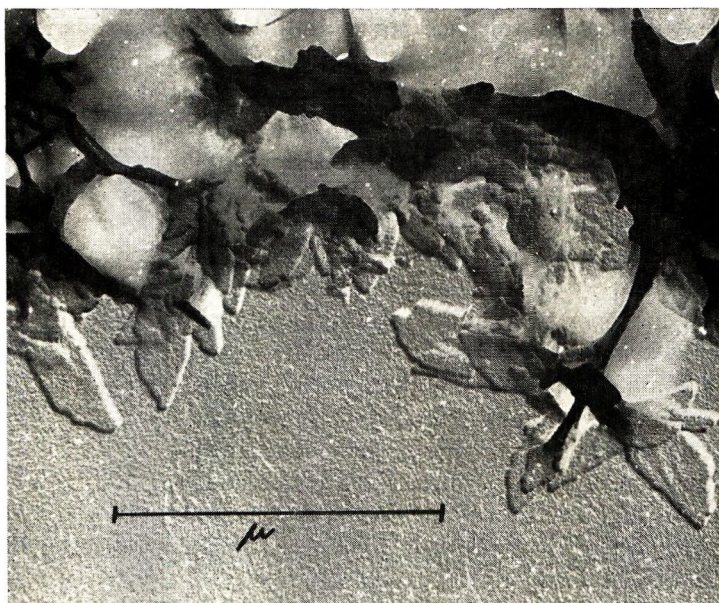
Fig. 3. PVA platelets crystallized from 0.01% triethylene glycol solution at 150°C.

spacings were indexed as the (200), (101), and (10$\bar{1}$) reflections, respectively, of the monoclinic unit cell of Bunn.[10]

Figure 4 is the x-ray diffractogram from single crystal material. The sharp intensities of the (10$\bar{1}$) and (101) reflections occur at 19.2° (4.6 A.) and 19.9° (4.4 A.) 2θ respectively.
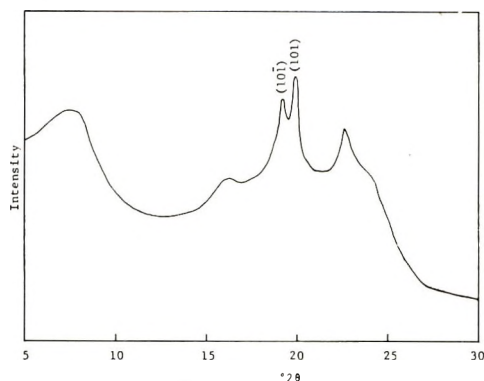

Fig. 4. X-ray diffractogram of single crystal material crystallized from 0.04% triethylene glycol solution by cooling from 200°C.

DISCUSSION

The measured melting temperature T_m of a bulk semicrystalline polymer is directly related to the crystallization temperature T_c, i.e., the higher T_c, the higher will be T_m. Crystallization theories[11-15] associate this phe-

nomenon with crystal thickness, predicting that thin crystals formed at lower temperatures will melt lower than thick crystals formed at the higher temperatures.   Also T_m is invariably higher than T_c but lower than $T_m{}^\circ$, the "equilibrium" melting point.   For bulk-crystallized polyethylene,[11,12] T_m is about midway between T_c and $T_m{}^\circ$.   Hoffman,[15] applying kinetic principles, has interpreted this difference between T_c and T_m as being due to an isothermal thickening or "creep-up" of the folded-chain lamellae on standing.   In the case of polyethylene, the lamellae roughly double in thickness relative to the thickness of the "growth" nucleus.   Recently, Hoffman[16] has reported experimental low angle x-ray evidence for the isothermal thickening of polyethylene lamellae (crystallized from the melt) as a function of time.   When T_c was plotted versus T_m, a straight line of positive slope was obtained.   Extrapolation of this to the $T_c = T_m$ line gave a value for $T_m{}^\circ$, the equilibrium melting point.

The departure of the slope of the T_c versus T_m line from unity was according to Hoffman, a measure of the degree of "creep-up" ($T_c \approx T_m$ for zero creep-up).   For bulk polyethylene crystallized for long periods, a slope of about 0.5 was obtained for the T_c versus T_m line.

Similar relationships to the above for bulk-crystallized polymers have also been observed for the dissolution in a solvent of solution crystallized folded-chain lamellae of polyethylene[1,2] and polyacrylonitrile.[3,4]   In these cases, the dissolution temperature T_s replaces the bulk melting temperature T_m, and the dissolution temperature of the infinitely thick crystal $(T_m)_\infty$, replaces the equilibrium melting point $T_m{}^\circ$.   Slopes obtained for the T_c versus T_s lines were 0.65 and 0.46 for polyethylene in xylene[2] and polyacrylonitrile in propylene carbonate,[3,4] respectively.

The value obtained for T_s can be considered reliable only provided recrystallization does not occur during the time of dissolution.[11,12]   If the polymer is able to recrystallize during the determination of T_s, an erroneously high value will be observed.   Thus, the possibility of recrystallization was held to a minimum by subjecting to the test temperature a fresh portion of the crystallized sample each time.   Under such conditions, recrystallization should not be a factor here, because it was impossible to obtain any crystallization at the temperatures required for dissolution. It should be pointed out that the dissolution temperature observed is that of the most perfect crystal and may not be representative of the whole sample.   This arises from the fact that the value of T_s observed is determined by the most insoluble portion of each sample.

As seen from Figure 1, the present results for PVA crystallized and dissolved in triethylene glycol give a straight line of slope 0.47 when T_c is plotted against T_s.   Extrapolation of this line to the $T_c = T_s$ line gives a value of 220°C. for $(T_m)_\infty$.

The equation[15] relating the dissolution temperature T_s of a folded-chain crystal of thickness l to the dissolution temperature of the infinitely thick crystal $(T_m)_\infty$, is given by

$$(T_m)_\infty - T_s = 2\sigma_c(T_m)_\infty/\Delta h_f\, l \tag{1}$$

where σ_e is the surface free energy per unit area of chainfolds and Δh_f is the latent heat of fusion. Substitution of the following values for PVA crystals: $(T_m)_\infty = 493°K.$, $T_s = 460°K.$, and $l = 1 \times 10^{-6}$ cm. (as determined from electron micrographs), into eq. (1) yields a value 3.3×10^{-8} cm. for the ratio $\sigma_e/\Delta h_f$. Comparable ratios for polyethylene and polyacrylonitrile are 2.3×10^{-8} and 3.3×10^{-8} cm., respectively.

CONCLUSION

It is tempting to say that (1) the theory of bulk crystallization–melting and solution crystallization–dissolution relationships are comparable and (2) creep-up in thickness of the lamellae accounts for the differences between T_c and T_s for solution crystals. However, there are certain aspects which make such conclusions doubtful. Firstly, the straight forward application of conventional kinetic equations previously applied to bulk-crystallized polymers apparently fails for solution-crystallized samples, as shown by Miller.[9] Also, experimental evidence is lacking which demonstrates a thickening of solution-grown lamellae at the crystallization temperature.[2] Thus, attributing the difference between T_c and T_s solely to a thickness increase of the lamellae may not be a valid argument. As pointed out by Miller, if the thickness were the only parameter involved, the creep-up would have to be instantaneous and by a certain fixed amount. A mechanism for such a thickening is difficult to imagine at this time.

The present studies have shown that while PVA single crystals grown from dilute solution have a relatively low crystallinity from density measurements, they nevertheless behave similarly to other semicrystalline polymers with respect to their morphological and dissolution properties.

References

1. Jackson, J. B., P. J. Flory, and R. Chiang, *Trans. Faraday Soc.*, **59**, 1906 (1963).
2. Holland, V. F., *J. Appl. Phys.*, **35**, 59 (1964).
3. Chiang, R., J. H. Rhodes, and V. F. Holland, *J. Polymer Sci. A*, **3**, 479 (1965).
4. Chiang, R., *J. Polymer Sci. A*, **3**, 2019 (1965).
5. Tsuboi, K., and T. Mochizuki, *J. Polymer Sci. B*, **1**, 531 (1963).
6. Monobe, K., and Y. Fujiwara, *Kobushi Kagaku*, **21**, 179 (1964).
7. Tincher, W. C., *Makromol. Chem.*, **85**, 46 (1965).
8. Friedlander, H. N., H. E. Harris, and J. G. Pritchard, *J. Polymer Sci. A-1*, **4**, 649 (1966).
9. Miller, R. L., private communication.
10. Bunn, C. W., *Nature*, **161**, 929 (1948).
11. Lauritzen, J. I., and J. D. Hoffman, *J. Res. Natl. Bur. Std.*, **64A**, 73 (1960).
12. Hoffman, J. D., and J. J. Weeks, *J. Res. Natl. Bur. Std.*, **66A**, 13 (1962).
13. Frank, F. C., and M. Tosi, *Proc. Roy. Soc. (London)*, **A263**, 323 (1961).
14. Price, F. P., *J. Chem. Phys.*, **35**, 1884 (1961).
15. Hoffman, J. D., *SPE Trans.*, **4**, 315 (1964).
16. Hoffman, J. D., and J. J. Weeks, *J. Chem. Phys.* **42**, 4301 (1965).

Résumé

Des monocristaux d'alcool polyvinylique sous forme de plaquettes de hauteur d'environ 100 Å ont été obtenus par cristallisation isothermique au départ de solutions diluées dans le triéthylène glycol. Le matériel cristallisé á la température T_c se dissou dans le meme solvant a une température plus élevée T_s. Un diagramme de T_c en fonction de T_s donne une ligne droite tangente 0.47. L'extrapolation de cette ligne a $T_c = T_s$ donne $(T'_m)_\infty$ qui peut être considérée comme la température de dissolution du cristal de dimensions infinies; $(T_m)_\infty$ pour cet échantillon dans le triéthylène glycol était de 220°C. La nature cristalline des plaquettes a été établie par des techniques de diffraction d'électrons et aux rayons-X. Un total de trois espacements "d" de Bragg ayant des valeurs de 3.9, 4.4 et 4.6 Å (± 0.05Å) ont été mesurés. Ces espacements ont été indexés comme réflexion 2,00, 101 et 10$\bar{1}$ respectivement de l'inité cellulaire monoclinique de Bunn. Les diagrammes de diffraction aux rayons-X montrent des intensités trés nettes de réflexion 10$\bar{1}$ et 101. La cristallinité calculée au départ de la densité de l'alcool polyvinylique précipité au départ de ces solutions diluées par le triéthylène glycol s'élevait à 42%. Bien que le degré global de perfection cristalline de l'alcool polyvinylique est bas, la relation linéaire entre T_c et T_s et la formation de monocristaux de formes définies lorsqu'on les cristallise au départ de ces solutions diluées suggèrent que l'alcool polyvinylique cristallise de la même manière que d'autres polymères semi-cristallins.

Zusammenfassung

Polyvinylalkoholeinkristallplättchen mit einer Stufenhöhe von etwa 100 A wurden durch isotherme Kristallisation aus verdünnter Triäthylenglycollösung erhalten. Die bei einer Temperetur T_c kristallisierte Substanz löste sich im gleichen Lösungsmittec bei einer höheren Temperatur T_s. Ein Diagramm T_c gegen T_s lieferte eine gerade Linie mit der Neigung 0,47. Extrapolation dieser Geraden auf $T_c = T_s$ lieferte $(T_m)_\infty$, welches als die Auflösungstemperatur von Kristallen mit unendlicher Stufenhöhe betrachtes werden kann. $(T_m)_\infty$ beträgt für diese Probe in Triäthylenglycol 220°C. Die kristalline Natur der Plättchen wurde durch Elektronenund Röntgenbeugungsverfahren erhärtett Insgesamt wurden drei Braggsche d-Abstände mit den Werten von 3,9, 4,4 und 4,6 Å ($\pm 0,05$ Å) gemessen. Diese Abstände wurden als die (200)-, (101)- und (10$\bar{1}$)-Reflexionen der monoklinen Elementatrzelle von Bunn indiziert. Das Röntgenbeugungsdiagramm zeigte scharfe Intensitäten der (10$\bar{1}$)- und (101)-Reflexionen. Die aus der Dichte des aus verdünnter Triäthylenglycollösung gefällten Polyvinylalkohols berechnete Kristallinität betrug 42%. Obgleich der Bruttokristallinitätsgrad dieses Polyvinylalkohols niedrig ist, spricht doch die lineare Beziehung zwischen T_s und T_c sowie die Bildung von Einkristallen mit differenzierter Gestalt bei der Kristallisation aus verdünnter Lösung dafür, dass Polyvinylaklohol in der gleichen Weise wie andere semikristalline Polymere kristallisiert.

Fluorine NMR Spectra of Poly(vinyl Trifluoroacetate)

J. G. PRITCHARD,* R. L. VOLLMER,† W. C. LAWRENCE, and
W. B. BLACK, *Chemstrand Research Center, Inc., Durham, North Carolina*

Synopsis

Samples of poly(vinyl trifluoroacetate) with differing stereosequences have been prepared. The NMR signals at 56.4 Mc./sec. corresponding to the three types of triad-stereosequences of the trifluoroacetate groups (isotactic, heterotactic, and syndiotactic) can be resolved. The results for specific polymers are discussed.

INTRODUCTION

In order to relate differences in stereoregularity to differences in other physical properties, considerable attention has been directed in recent years to the use of nuclear magnetic resonance for the determination of the average configurational arrangement of substituent groups along the backbone chain in the poly(vinyl alcohol)-related family of polymers. Danno and Hayakawa[1] first mentioned the distinguishing of poly(vinyl alcohol) samples which have different stereostructures by using the proton magnetic resonance spectra of the methylene protons in these polymers, and Tincher[2] recently reported a more detailed study of this subject including the spectra given by the methenyl protons. In this way, the isotactic-rich poly(vinyl alcohol) which can be prepared from isotactic-rich poly(vinyl *tert*-butyl ether)[3] has been contrasted with syndiotactic-rich polymers from other sources.[1,2,4] Ramey and Field[5] demonstrated that the proton spectra of the methenyl protons of poly(vinyl acetate) and poly(vinyl trifluoroacetate) can be resolved sufficiently to show up tacticity differences provided that the methenyl protons are decoupled from the adjacent methylene protons. These authors have also shown that the methyl protons in poly(vinyl acetate) are magnetically stereosensitive. Similarly, we show that fluorine nuclear magnetic resonance is useful for indicating the nature of the stereosequences of the trifluoroacetate groups in poly-(vinyl trifluoroacetate).

* Present address: I.T.T. Research Institute, Illinois Institute of Technology, Chicago Illinois.

† To whom inquiries should be sent.

EXPERIMENTAL

Atactic Poly(vinyl Alcohol) and Poly(vinyl Trifluoroacetate)

Purified vinyl acetate (b.p. 72–73°C., aldehyde-free) was polymerized in bulk at 60°C. with the use of azobisisobutyronitrile as catalyst. The poly(vinyl acetate) was precipitated in distilled water from methanol solution, and volatile material was removed under vacuum. This polymer was dissolved in methanol to give a 1–2% solution which was refluxed with a slight excess of sodium hydroxide for 8 hr. The precipitated powder of poly(vinyl alcohol) was washed thoroughly with methanol, then dried under vacuum.

The polymer prepared as described above was digested with a four-fold excess of trifluoroacetic anhydride for at least 4 days. The swollen polymer was extracted with dry acetone, and the clear acetone extract was cast on a large volume of 10% methanol–water solution. The resultant film was removed and quickly dried under vacuum to a light, white powder (polymer B). Poly(vinyl trifluoroacetate) so prepared dissolved completely in dry acetone to give a pale yellow solution and retained its solubility properties when stored in a desiccator.

Isotactic-Rich Poly(vinyl tert-Butyl Ether) and Poly(vinyl Trifluoroacetate)

Vinyl-*tert*-butyl ether was prepared by an interchange reaction between 2-chloroethylvinyl ether and *tert*-butyl alcohol in the presence of mercuric acetate.[6] Vinyl *tert*-butyl ether was fractionally distilled as its azeotrope with *tert*-butanol. After thorough washing with iced water and then drying over calcium chloride, there was obtained a 60% yield of colorless liquid product, n_D^{20} 1.3984 (lit.[6] 1.3987). A 5-ml. portion of this monomer was polymerized under nitrogen at ca. −70° in 60 ml. of dry toluene containing one drop of boron trifluoride etherate as catalyst.[7,8] After 2 hr. the reaction mixture was quenched in methanol. The polymer was washed with methanol and dried under vacuum. The poly(vinyl *tert*-butyl ether) (6.9 g.) was then extracted repeatedly with hot acetone to remove less stereoregular material, and 5 g. of isotactic-rich polymer was obtained.

The trifluoroacetylation of the poly(vinyl *tert*-butyl ether) was carried out in a manner resembling that which has been reported for acetylation.[9] A 1-g. portion of the polymer was dissolved in 5 ml. of benzene. A mixture of 5 ml. of trifluoroacetic anhydride with 5 ml. of benzene was then added to the solution. A solution of five drops of boron trifluoride etherate in a mixture of 5 ml. of benzene with 2.5 ml. of trifluoroacetic anhydride was added slowly with stirring to the polymer solution maintained at 20°C. The system became dark blue and a gel formed. After about 1 hr. the liquid was poured off and the gel was washed with hexane. The resultant poly(vinyl trifluoroacetate) was dissolved in acetone, precipitated at the surface of water, collected, and rapidly dried (polymer A). This product was dissolved immediately in acetone in NMR tubes as described below.

This polymer was not very stable, yielding some acetone-insoluble product upon storage in a desiccator.

Syndiotactic-Rich Poly(vinyl Trifluoroacetate)

n-Heptane was highly purified by refluxing with a mixture of potassium permanganate and sodium hydroxide, then with sulfuric acid, and finally by distilling from sodium. Vinyl trifluoroacetate was distilled three times through a 1-ft. Vigreaux column. It was stored at ca. $-10°C$. without inhibitor.

Vinyl trifluoroacetate (12 g.) was polymerized under nitrogen at 80°C. for 24 hr. in 20 ml. of the n-heptane, 0.2 g. of benzoyl peroxide being used as catalyst. The precipitated product was separated and washed repeatedly by stirring with n-hexane and then with ethyl ether, and was dried *in vacuo* (polymer C).

Vinyl trifluoroacetate (200 g.) and 90 ml. of pure carbon tetrachloride were cooled to $-50°C$. under argon, and 3.0 ml. of tri-n-butylborane was added from a syringe. Air was added as cocatalyst in lots of about 10 ml. every 5 min. to a total of 150 ml. while the solution was stirred. After 1.5 hr. the reaction mixture was extremely viscous; it was allowed to stand in the cooling bath for 48 hr. at temperatures ranging from -25 to $-50°C$. The product (polymer D) was worked up as above.

Polymers A, B, C, and D gave identical infrared spectra when run as thin films which were cast from acetone solutions onto rock-salt plates in a dry atmosphere.
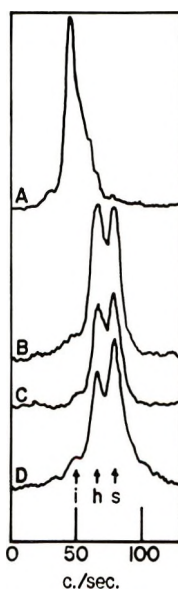

Fig. 1. Fluorine magnetic resonance spectra at 56.4 Mc./sec. and 25°C. of poly(vinyl trifluoroacetate) samples having different tacticities (i = isotactic, h = heterotactic, s = syndiotactic).

Fluorine NMR Spectra

A weighed amount of the polymer was placed in a thin-walled NMR tube with enough pure, dry acetone to give a 15% solution (w/v). A sealed capillary tube containing 20% of ethyl trifluoroacetate in acetone was added as an external reference standard. The NMR tube and its contents were degassed, and the tube was sealed with the contents at ca. $-70°C$. under high vacuum. The fluorine nuclear resonance spectra were obtained on a Varian Associates' V4302 spectrometer operating at 56.4 Mc./sec. and equipped with a Varian 12-in. electromagnet, a flux stabilizer, and field homogeneity stabilizer. The arbitrary chemical-shift values shown in Figure 1 were established by the side-band technique by using the high-field signal from the external standard.

RESULTS AND DISCUSSION

The results shown in Figure 1 demonstrate that the fluorine nuclear resonance spectrum can be used to distinguish the different types of polymers studied, even though the degree of resolution is typically poor. Broadly speaking, the isotactic-rich polymer A comes into resonance at ca. 15 cps to lower field compared to the principal peak for the atactic polymer B, which is also ca. 15 cps to lower field than the principal band of the more syndiotactic polymers C and D. The respective peaks are labeled i, h, and s. The atactic polymer would be expected to have a preponderance of trifluoroacetyl groups placed heterotactically with respect to their nearest neighbors on each side.

The relative areas of the respective resonance bands are a measure of the relative proportions of isotactic, heterotactic and syndiotactic sequences of trifluoroacetyl groups considered three at a time (triads). Crude estimates of the relative areas of these bands can be made by measurement of the relative peak heights, and these are reported in Table I. The values in parentheses are (to the nearest unit) those required by theory[10] for typical polymers in which the isotactic and syndiotactic triads are randomly distributed along the polymer chain so that long blocks of either type are

TABLE I

Triad Tacticities of Poly(vinyl Trifluoroacetate) Samples Deduced from F^{19} Spectra[a]

Polymer	i, %	h, %	s, %
A (from PVTBE)	75	20	5
	75	(23)	(2)
B (from PVAc)	8	47	45
	(11)	(44)	45
C (from PVTFAc, 80°C.)	6	44	50
	(9)	(41)	50
D (from PVTFAc, $-50°C$.)	10	40	50

[a] Values in parentheses are as required by theory for random, nonstereoblock polymers.[10]

absent, as would be expected for the polymers under study. The agreement with theoretical expectation is reasonable, considering that there must be errors of several per cent in the estimation of the heights or areas of such seriously overlapped bands.

The contours of our spectra are quite similar to those reported by Ramey and Field for the decoupled resonances of the methenyl protons in polymers analogous to ours.[5] Thus, we confirm that the poly(vinyl trifluoroacetate) derived from poly(vinyl *tert*-butyl ether) is strongly isotactic,[3,5] and that the poly(vinyl trifluoroacetate) derived by polymerization of the monomer is not greatly more syndiotactic than the polymers obtained by polymerization of vinyl acetate under comparable conditions[5] but is slightly so.[11] Spectra C and D show that a lowering in the temperature of polymerization of vinyl trifluoroacetate by 130°C. does not give any very substantial increase in syndiotacticity, such as is observed in the well known case of methyl methacrylate.[12] In this respect, vinyl trifluoroacetate appears to be similar to vinyl acetate.[13]

It must be remembered that the above results are quantitatively approximate. We cannot be sure that the isotactic–heterotactic and heterotactic–syndiotactic chemical shifts are identical. It is possible that differing ranges and band shapes may occur for polymers of different origin. This could result from differing populations of rotational conformations partly related to other structural differences such as branching, entanglement, head-to-head sequences, and incomplete chemical transformation. Tincher has particularly emphasized the importance of this conformation uncertainty in his detailed consideration of the proton spectra of poly(vinyl alcohol) samples.[2] Instruments of much higher resolving power will be required to pursue this subject more effectively.

References

1. Danno, A., and N. Hayakawa, *Bull. Chem. Soc. Japan*, **35**, 1749 (1962).
2. Tincher, W. C., *Makromol. Chem.*, **85**, 46 (1965).
3. Bassi, I. W., G. Dall'Asta, U. Campigli, and E. Strepparola, *Makromol. Chem.*, **60**, 202 (1963).
4. Rosen, I., G. H. McCain, A. L. Endrey, and C. L. Sturm, *J. Polymer Sci. B*, **1**, 951 (1963).
5. Ramey, K. C., and N. D. Field, *J. Polymer Sci. B*, **3**, 63, 69 (1965).
6. Watanabe, W. H., and L. E. Coulon, *J. Am. Chem. Soc.*, **79**, 2828 (1957).
7. Okamura, S., T. Higashimura, and H. Yamamoto, *J. Polymer Sci.*, **33**, 510 (1958); *Kogyo Kagaku Zasshi*, **61**, 1636 (1958).
8. Okamura, S., K. Kodama, and T. Higashimura, *Makromol. Chem.*, **53**, 180 (1962).
9. Fujii, K., and T. Mochizaki, *Kobunshi Kagaku*, **19**, 124 (1962).
10. Miller, R. L., and L. E. Nielsen, *J. Polymer Sci.*, **46**, 303 (1960).
11. Cooper, W., F. R. Johnston and G. Vaughan, *J. Polymer Sci. A*, **1**, 1509 (1963), and refs. therein cited.
12. Fox, T. G, and H. W. Schnecko, *Polymer*, **3**, 575 (1962), and refs. cited therein.
13. Friedlander, H. N., H. E. Harris, and J. G. Pritchard, *J. Polymer Sci. A-1*, **4**, 648 (1966).

Résumé

Des échantillons de polytrifluoroacétate de vinyle de différentes stéréoséquences ont été préparés. Les signaux NMR à 56.4 Mc/sec. correspondants aux 3 types de triades stéréoséquencées de groupes fluoroacétiques (isotactique, hétérotactique et syndiotactique) peuvent être résolus. Les résultats pour des polymeres spécifiques sont discutés.

Zusammenfassung

Polyvinyltrifluoracetatproben mit verschiedenen Stereosequenzen wurden dargestellt. Die den drei Typen von Triadenstereosequenzen der Trifluoracetatgruppe (isotaktisch heterotaktisch und syndiotaktisch) entsprechenden NMR-Signale bei 56,4 Mc/sec können aufgelöst werden. Die Ergebnisse für spezifische Polymere werden diskutiert.

NOTES

Greffage de Méthacrylate de Méthyle sur la Cellulose au Moyen de Peracides, en Présence d'Ions Cu^{2+} et Fe^{3+} Comme Catalyseurs

Les persulfates, initiateurs usuels de polymérisation vinylique, ont été souvent utilisés pour la préparation de copolymères greffés de la cellulose.[1-3] En général la polymérisation du monomère à l'intérieur des fibres est effectuée thermiquement, en présence ou non d'un élément réducteur complémentaire (bisulfite, ion Ag^+, ion Fe^{2+}). Lorsque la réaction de greffage est réalisée sans précautions particulières, les radicaux libres engendrés par la décomposition du persulfate réagissent à la fois sur la cellulose et sur le monomère. Il en résulte un pourcentage élevé de produit d'homopolymérisation, qui peut cependant être considérablement réduit par des artifices consistant en un prétraitement de la cellulose.[4]

Nous nous sommes proposés de déterminer l'influence de plusieurs facteurs dans les réactions de greffage au moyen du persulfate. Les essais de greffage ont été effectués sur du câble fibranne viscose (fibre ni ensimée, ni blanchie, fournie gracieusement par la Compagnie Industrielle de Textiles Artificiels et Synthétiques, Paris, France). Ils ont été réalisés en absence de tout élément réducteur complémentaire, la viscose n'ayant subi aucun traitement préalable. La température a été fixée arbitrairement à 40°C.

Employé en milieu neutre, à cette température, le persulfate est pratiquement inactif à la fois sur le monomère et sur la viscose. En une heure le taux de greffage (qui correspond au poids de polymère greffé par 100 g. de cellulose) est extrêmement faible et il n'y a pas formation d'homopolymère. Il est bien connu que les ions Cu^{2+} catalysent les oxydations au persulfate[5] et certains auteurs[3] ont appliqué cette propriété aux réactions de greffage au moyen d'un système redox persulfate–bisulfite. Nous avons observé qu'en milieu neutre l'addition d'ions Cu^{2+} permettait d'obtenir un taux de greffage important à côté d'une abondante formation d'homopolymère. Nous avons mis en évidence qu'en remplaçant les ions Cu^{2+} par des ions Fe^{3+} le taux de greffage était accentué et l'homopolymérisation réduite. Cependant les meilleurs résultats sont ceux obtenus en employant ce système persulfate-catalyseur, non plus en milieu neutre mais en milieu acide dilué. Ceci n'avait jamais, à notre connaissance, été signalé.

Le Tableau 1 résume quelques uns des résultats obtenus.

TABLEAU 1

Rôle des Catalyseurs et de l'Acidité sur le Greffage de Méthacrylate de Méthyle sur la Viscose au Moyen du Persulfate. (M.M.A.: 0,47 mole/l.; Température: 40°C; Temps de réaction: 1 heure: eau distillée qsp: 100 cm³; poids initial de viscose: 0,9–1,0 g.: $S_2O_8K_2$, c = 10^{-3} mole/l.)

No.	Acidité du milieu	Catalyseur, mole/l.	Taux de greffage[a]	Homopolymérisation[b]	Conversion du monomère
1	Neutre	0	3,9%	0	0,8%
2	"	Cu^{2+}:10^{-3}	80,9%	74,5%	62,4%
3	"	Fe^{3+}:10^{-3}	210,7%	36,3%	65,8%
4	0,1 H^+/l.	Cu^{2+}:10^{-3}	120,5%	7,1%	25,4%
5	"	Fe^{3+}:10^{-3}	143,2%	8,2%	31,8%
6	"	0	15,9%	0	3,2%

[a] Défini plus haut.

[b] % d'homopolymère par rapport au poids total de monomère polymérisé.

En milieu neutre, la compétition entre le monomère et la viscose vis-à-vis des radicaux SO_4^-· règle les pourcentages respectifs de greffage et d'homopolymérisation.[6]   Par contre, en milieu acide, la faible quantité d'homopolymère obtenue semble indiquer que celle-ci provient d'une réaction parasite et que le persulfate forme avec la viscose un véritable
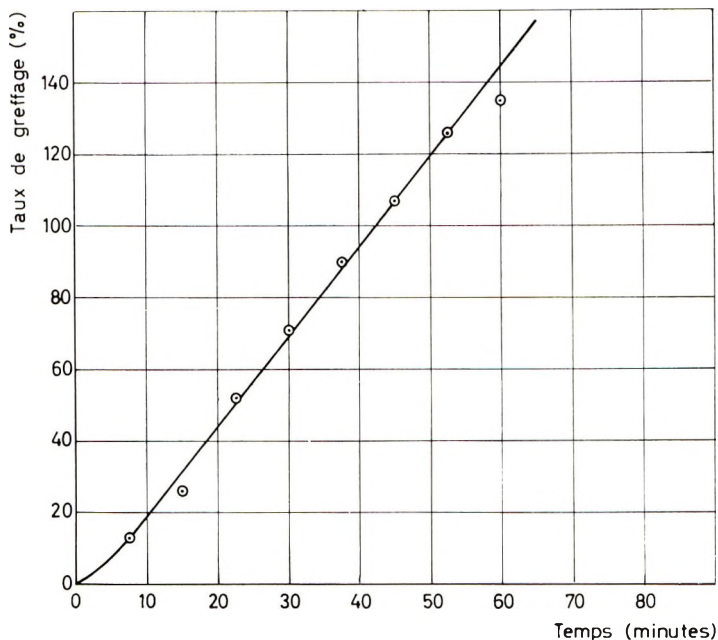

Fig. 1. Monomère M.M.A = 5 cm³; Température 50°C; Acide de Caro conc: = 5.10^{-3} mole/l.; Fe^{3+} conc: = 2.10^{-3} mole/l.; poids initial de coton 1 g.; eau distillée qsp 100 cm³; pH du milieu réactionnel:1,6).   Le pourcentage d'homopolymérisation est dans tous les cas peu élevé ($\leq 8\%$).
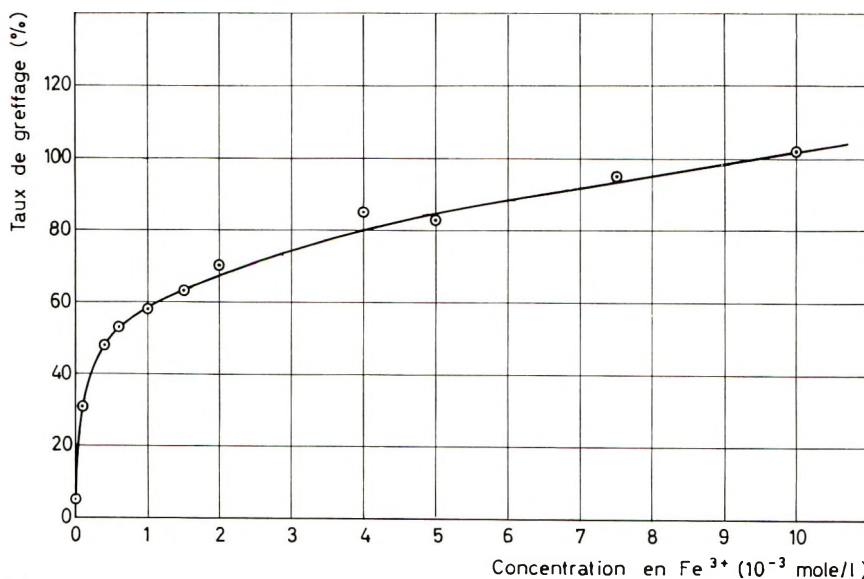
Fig. 2. Variation du taux de greffage en fonction de la concentration en Fe^{3+}.   (Conditions identiques à celles correspondant à la Figure 1.   Temps de réaction:30 min.
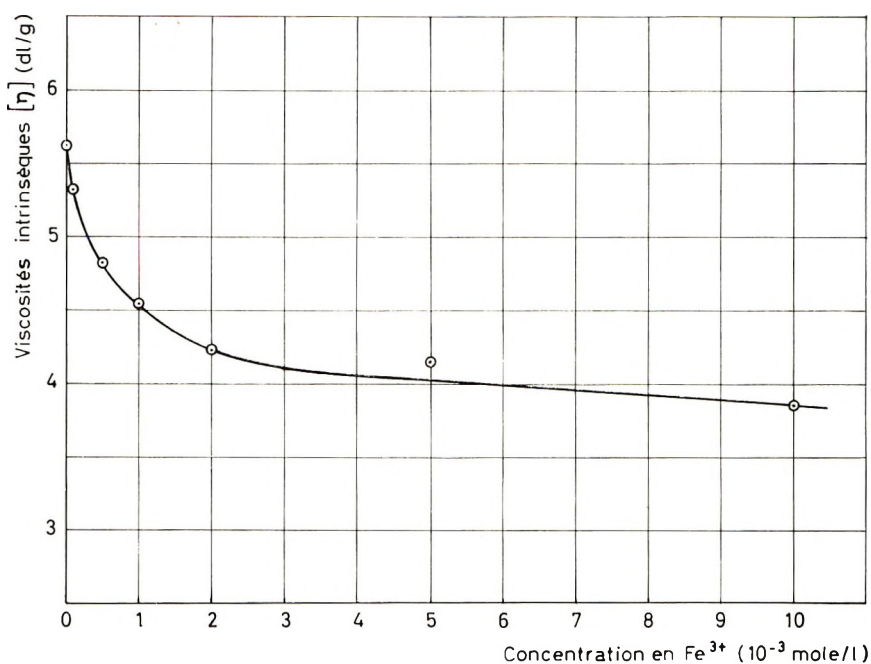
Fig. 3. Chute de viscosité de coton en fontion de la concentration en Fe^{3+} (Conditions identiques à celles correspondant à la Figure 1 mais en absence de monomèere. Temps de réaction 30 minutes. Viscosité intrinsèque du coton origine $[\eta] = 6.04$).

système redox capable d'initier la polymérisation du monomère uniquement sur les fibres et non plus dans le milieu réactionnel.

Nous avons d'autre part observé que le perborate de sodium ($NaBO_3$, $4H_2O$), employé en milieu acide et en présence des mêmes catalyseurs conduisait à des résultats comparables à ceux obtenus avec le persulfate.

Cependant, si, dans la réaction de greffage, la viscose est remplacée par des composés comme le mannitol ou le glucose, la quantité de polymère formée est très faible (Conversion $<4\%$). Il semble donc que le phénomène de greffage soit dû à une impureté de la viscose, inhérente au procédé de fabrication et inséparable sans destruction de la fibre. Un traitement de purification déjà connu[7] n'a pas entraîné de modification des résultats. Toutefois l'hypothèse que nous proposons plus bas, pour le greffage du coton avec l'acide de Caro, peut aussi être retenue.

L'acide de Caro n'avait, à notre connaissance, jamais été utilisé comme agent de greffage sur la cellulose. Nous avons réalisé avec cet initiateur, en présence d'ions Fe^{3+}, de nombreux essais de greffage sur des linters de coton. La Figure 1 traduit les variations du taux de greffage en fonction du temps.

Si dans le cas de la viscose il est difficile de formuler une hypothèse sur l'initiation de la polymérisation, du fait de la présence possible d'impuretés réductrices inhérentes au procédé de fabrication, il est possible, dans le cas du coton, de fournir une explication plausible du phénomène observé. L'acide de Caro n'engendre pas la polymérisation du méthacrylate de méthyle si dans la réaction de greffage le coton est remplacé par une substance possédant plusieurs fonctions "alcool" (le mannitol par exemple). Ces fonctions n'interviennent donc probablement pas dans le processus d'amorçage de la polymérisation.

Il semble, d'après l'examen des courbes représentées sur les Figures 2, 3, et 4 que le taux de greffage soit proportionnel au nombre de chaînes de cellulose coupées par hydrolyse au cours de la réaction. On peut donc penser que le centre actif, où s'amorce la polymérisation, prend naissance au cours de la scission hydrolytique des chaînes et que
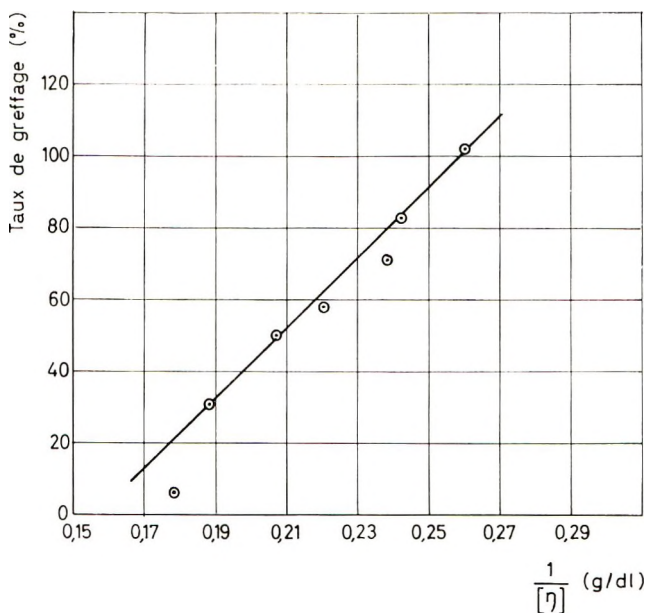
Fig. 4. Variation du taux de greffage en fonction du nombre "N" de chaines de cellulose coupées par hydrolyse (N = fonction linéaire de $1/[\eta]$).

le copolymère obtenu n'est pas un véritable copolymère greffé mais un copolymère block.

Le fractionnement du polyméthylméthacrylate greffé, après hydrolyse du substrat cellulosique, fait apparaître que le nombre de chaînes est relativement faible mais que leur masse moléculaire est très élevée (plusieurs millions).

L'ensemble de ce travail, ainsi que les études de répartition des masses moléculaires feront l'objet d'une publication plus détaillée.

References

1. Haydel, C. H., H. J. Janssen, J. F. Seal, H. L. E. Vix, et E. A. Gastrox, *Textile Res. J.*, **27**, 975 (1957).

2. Sankalia, S. M., D. K. Ray Chaudhuri, et J. J. Hermans, *Can. J. of Chem.*, **40**, 2249 (1962).

3. Kulkarni, A. Y., A. G. Chitale, B. K. Vaidya, et P. C. Mehta, *J. Appl. Polymer Sci.*, **7**, 1581 (1963).

4. Bridgeford, D. J., *Ind. Eng. Chem., Product Res. Dev.*, **1**, 45 (1962) et *Brevet Français* 1.140.362 du 23/7/1955.

5. House, D. A., *Chem. Rev.*, **62**, 185 (1962).

6. Hermans, J. J., *Pure Appl. Chem.*, **5**, 147 (1962).

7. Toda, T., *J. Polymer Sci.*, **58**, 411 (1962).

Jean-Claude Mileo
Louis Nicolas

Institut National de Recherche Chimique Appliquée
Paris, France

On the Computation of Viscosity Measurements Data of Dilute Solutions of High Polymers

The viscosity measurements data of high polymer solutions are usually plotted according to the following equations:

$$\eta_{sp}/c = [\eta]_H + k_H[\eta]_H^2 c \tag{1}$$

$$\eta_{sp}/c = [\eta]_S + k_S[\eta]_S \eta_{sp} \tag{2}$$

$$(\ln \eta_r)/c = [\eta]_K - k_K[\eta]_K^2 c \tag{3}$$

where $\eta_{sp} = \eta_r - 1$ is specific viscosity, c, concentration in g./dl., $[\eta]_{H,S,K}$ and $k_{H,S,K}$ are intrinsic viscosity and concentration gradient constants, of Huggins[1] [eq. (1)], Schulz and Blaschke[2] [eq. (2)], and Kraemer[3] [eq. (3)]. For infinitely dilute solutions the constants of eqs. (1)–(3) should fulfill the following equations

$$[\eta]_H = [\eta]_S = [\eta]_K \tag{4}$$

$$k_H = k_S = -k_K + 1/2 \tag{5}$$

In practice eqs. (4) and (5) are rarely valid.

There are two main sources of errors: not very precise correction of efflux times and excessively high concentrations of polymer solutions.

Efflux Time Corrections

In the next part of this note we will distinguish the parameters $[\eta]_{H,S,K}$ and $k_{H,S,K}$, determined by means of eqs. (1)–(3), and $[\tau]_{H,S,K}$ and $k_{H\tau,S\tau,K\tau}$, determined from these equations when the efflux time, τ, is superimposed instead of viscosity η.

According to Barr[4]:

$$\eta = d(A\tau - B/\tau) \tag{6}$$

where d is solution density, and A and B are viscometer constants.

In the usual method[5] of calculation of the parameters of eqs. (1)–(3) the efflux time of each solution is transformed to the viscosity by means of eq. (6) and these values are used to determine the needed parameters. This procedure can be reversed; one can determine $[\tau]_{H,S,K}$ and $k_{H\tau,S\tau,K\tau}$ and then transform them into $[\eta]_{H,S,K}$ and $k_{H,S,K}$. This second method is faster and allows a better understanding of the influence of correction parameters on calculated values.

The relations between the two sets of parameters can be easily determined by substitution of eq. (6) into eqs. (1)–(3) and using the definitions

$$[\eta] \triangleq \lim_{c \to 0} y; \qquad k[\eta]^2 \triangleq \lim_{c \to 0} \frac{\partial y}{\partial c} \tag{7}$$

where y is η_{sp}/c and/or $(\ln \eta_r)/c$. Then

$$[\eta]_{H,S,K} = [\tau]_{H,S,K} \frac{1 + H}{1 - H} + D \tag{8}$$

$$k_{H,S}[\eta]^2_{H,S} = \left[k_{H\tau,S\tau} \frac{1 + H}{1 - H} - \frac{H}{1 - H} \right] [\tau]_{H,S}^2 + [\tau]_{H,S} \frac{1 + H}{1 - H} D \tag{9}$$

$$k_K[\eta]_K^2 = \left[k_{K\tau} + \frac{2H}{(1 - H)^2} \right] [\tau]_K^2 + D^2/2 \tag{10}$$

TABLE I

A and B Constants Experimentally Established and Calculated from Theoretical Expressions[a]

No.	Viscometer	2R,[b] mm.	L,[c] cm.	V,[d] ml.	T, °C.	A × 10³		B		B/A[a]	
						Exp.	Calc.	Exp.	Calc.	Exp.	Calc.
1	Factory made, capillary Oa	—	—	—	20	5.108	—	1.677	—	328.3	—
2	"	—	—	—	20	4.079	—	1.602	—	392.6	—
3	"	—	—	—	25	5.164	—	2.334	—	451.2	—
4	Factory made capillary I	—	—	—	25	10.025	—	3.964	—	395.4	—
5	Laboratory made	0.4714	20	3.54	25	4.143	3.680	0.807	0.800	194.8	216.8
6	"	0.5232	20	3.68	27	5.444	5.385	39.99	0.831	734.5	154.4
7	"	0.5634	10	5.15	20	8.244	5.644	1.217	2.327	147.6	412.3
8	"	"	"	"	35	8.240	"	6.436	"	780.4	"
9	"	0.6124	10	5.20	20	8.833	7.833	0.996	2.349	110.7	300.0
10	"	"	"	"	35	8.829	"	2.356	"	266.9	"

[a] The leaflet of VEB Jenaer Glaswerk *Korrekturtafel für Bewegungsenergie* gives the $B/A = 562$ value for capillary Oa and $B/A = 280$ for capillary I.
[b] R = Capillary radius.
[c] L = Capillary length.
[d] V = Volume of upper bulb of the viscometer.

where the kinetic energy correction factor H and density correction factor D are defined as follows:

$$H \triangleq B/A\tau_0{}^2 \tag{11}$$

$$D \triangleq 10^{-2}(d_0{}^{-1} - d_p{}^{-1}) \tag{12}$$

τ_0 is solvent efflux time, d_0 is density, and d_p is polymer density). Equation (12) has been calculated assuming additivity of the solution components densities.

In Table I the experimentally established and theoretically calculated values of A and B and the ratio B/A are shown. If, as recommended $100 < \tau_0 < 200$ sec., then the error due to omission of the kinetic energy correction is of the range 1.5%–15% depending on the viscometer constants. From eq. (8) it can be concluded that this type of error is incorporated into K, the constant of the Mark-Houwink equation. On the other hand, the errors connected with the second correction factor D cause differences in K and the exponent a of the above-mentioned equation. The differences will be more important for lower molecular weight samples. For instance, a 1% error is found in the polystyrene-cyclohexane system (34.4°C.) at $\bar{M}_n = 150,000$, but in the case of the polycarbonate-chloroform system (20°C.) it is found at $\bar{M}_w = 7000$ (both are θ-solvent systems).

Concentration Range

Equations (1)–(3) can be taken as linear forms of the expansions of the more general functions, where the higher terms have been neglected. From the mathematical point of view eqs. (4) and (5) should be true for the limiting range of $c \rightarrow 0$ only. However, due to low concentration deviation[6] the practically available range of concentrations is $c_1 < c < c_2$, where $c_1/c_{cr} = $ constant[6,7] (c_{cr} is the critical mixing concentration). This not only leads to the invalidation of eqs. (4) and (5) but it has been found[8,9] that the experimental data of one system agrees with the Huggins linear equation [eq. (1)] or that of Schulz and Blaschke [eq. (2)], but not both of them. This leads to the problem of deciding which equation is a correct expression or, if both are accepted, which one should be used for an actually investigated system.

Utracki and Simha[10] showed that the general function

$$\eta_{sp}/c = [\eta] \exp\{\text{const. } c/c_{cr}\} \tag{13}$$

which is valid for a broad range of concentrations of θ-solvent systems, can also be used for dilute solutions of polymer in good solvents. Expanding eq. (13) into a power series of c and using eq. (1) to express the ratio, const./c_{cr}, one can write

$$\eta_{sp}/c = [\eta]\left[1 + \sum_1^n \frac{1}{n!} (k_H[\eta]c)^n \right] \tag{14}$$

Using a good approximation one can derive:

$$\eta_{sp}/c = [\eta]_H(1 + k_H[\eta]_H c/2)^2 \tag{15}$$

Similarly, eq. (3) can be written in the form:

$$(\ln \eta_r)/c = [\eta]_K(1 - k_K[\eta]_K/c/2)^2 \tag{16}$$

If the range of application of eqs. (1) and (3) is $c_1 < c < c_2$ then the range of application of eqs. (15) and (16) is $c_1 < c < 2c_2$, in other words eqs. (15) and (16) permit a precise determination of the parameters $[\eta]_H = [\eta]_K$ and $k_H + k_K = {}^1/_2$ from the higher range of concentrations usually available. Examples of calculations based on the proposed equations are shown in Table II.

On the other hand if eq. (13) is taken as a base for the calculation of a more general function of the Schulz-Blaschke type, a derived expression, similar to eqs. (15) and (16) cannot be written. However, if in some systems eq. (2) is fulfilled, eqs. (15) and (16) can also be used to calculate the viscosity parameters.

TABLE II

Intrinsic Viscosity, Huggins Constant and Kraemer Constant for Heterogeneous Polycarbonate (PC)–Solvent Systems

No.	System	$H \times 10^2$	$D \times 10^3$	η_{rmax}	Eq.	$[\eta]^a$	$[\eta]$	k^a_H or k^a_K	k_H or k_K	$k^a_H + k^a_K$	$k_H + k_K$
1	PC-I; $\bar{M}_v = 31{,}000$; CHCl₃, 30°C.	8.173	1.6	1.52	1	0.566	0.568	0.748	0.750	0.700	0.754
					3	0.580	0.583	−0.048	0.004	0.544	0.530
					15	0.564	0.565	0.631	0.618		
					16	0.564	0.565	−0.087	−0.088	0.533	0.575
2	PC-II; $\bar{M}_v = 53{,}100$; CH₂Cl₂, 12°C.	8.129	0.9	2.13	1	0.916	0.974	0.408	0.377	0.533	0.575
					3	0.924	0.932	0.125	0.198	0.510	0.501
					15	0.924	0.925	0.357	0.362		
					16	0.924	0.925	0.153	0.139		
3	PC-III; $\bar{M}_v = 88{,}900$; tetrahydrofuran, 30°C.	4.290	3.0	2.54	1	1.142	1.141	0.425	0.423	0.613	0.677
					3	1.148	1.156	0.188	0.154	0.498	0.500
					15	1.149	1.149	0.372	0.377		
					16	1.149	1.149	0.126	0.123		

a Calculated by Schulz method.[5]

In conclusion, eqs. (15) and (16) are recommended for calculating $[\tau]$ and k_{Hr} and/or k_{Kr}. These quantities should be transformed to $[\eta]$ and k_H and/or k_K using eqs. (8) and (10). If determined parameters do not fulfill eqs. (4) and (5), then more dilute solutions should be used.

1. Huggins, M. L., *J. Am. Chem. Soc.*, **64**, 2716 (1942).
2. Schulz, G. V., and F. Blaschke *J. Prakt. Chem.*, **158**, 130 (1941).
3. Kraemer, E. O., *Ind. Eng. Chem.*, **30**, 1200 (1938).
4. Barr, G., *A Monograph of Viscometry*, Humphrey Milford, New York, 1931.
5. Schulz, G. V., *Z. Elektrochem.*, **43**, 479 (1937).
6. Utracki, L., *Polimery*, **9**, 50 (1964).
7. Graubner, H., *Makromol. Chem.*, **78**, 121 (1964).
8. Ibrahim, F., and H. G. Elias, *Makromol. Chem.*, **76**, 1 (1964).
9. Bereger, R., private communication.
10. Utracki, L., and R. Simha, *J. Polymer Sci. A*, **1**, 1089 (1963).

L. UTRACKI

Polish Academy of Sciences
Polytechnic Institute
Łódź, Poland

A Sulfone Polymer from Diphenyl Ether

Various literature sources[1,2] have reported high yields of aromatic sulfones via the Friedel-Crafts reaction.   Thus, the reaction also is a possible route to aromatic sulfone polymers.   In this connection, a patent has recently been issued[3] describing the preparation of several aromatic sulfone polymers by this means.   In our work, polymer I,* derived from diphenyl ether, was prepared.

I
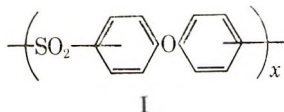
No indication of its existence was previously found in the literature.   As outlined in the following equations, two routes to the polymer were examined:
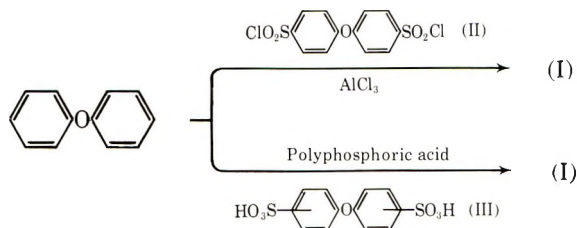
When the polymer was prepared by the Friedel-Crafts route, the reaction was carried out in nitrobenzene solution with slightly more than a stoichiometric amount of aluminum chloride as catalyst.   A polymerization temperature range of 25–120°C. was used, the bath temperature being increased gradually.   By measuring the evolution of hydrogen chloride, we were able to follow the degree of polymerization continuously. The final polymer was reprecipitated twice from dimethylacetamide with methanol-water.   Yields were nearly quantitative.

These polymers were soluble only in pyridine, dimethylacetamide, N-methylpyrrolidone, dimethyl sulfoxide, nitrobenzene, and phenols.   Inherent viscosities up to 0.35 (1% in dimethylacetamide, 20°C.) were obtained.   Significantly, the intrinsic viscosity curves showed polyelectrolyte behavior.

The polymers melted between 250–265°C.

The infrared spectrum of the polymer is presented in Figure 1.   It shows bands at 3.31μ (aromatic C—H stretch); 6.39 and 6.79μ (aromatic C=C); 7.61 and 7.75μ doublet (antisymmetric SO_2 stretch); 8.05μ (aryl ether); 8.69μ (symmetric SO_2 stretch); 9.06μ (p-substituted aryl ether); 9.35 and 9.92μ (p-substituted phenyl); 11.49 and 12.03μ (C—H out-of-plane deformation on p-substituted aryl ether).

The elemental analysis, however, deviated somewhat from the theoretical composition.   Carbon values were 1–2% high and sulfur values were as much as 2% low.   Also, variable amounts of ash were obtained consistently.   This probably was residual catalyst.   Supporting this, one analysis indicated the presence of 0.50% aluminum in a total ash content of 0.97%.

A variety of observations has suggested that the residual catalyst in the purified polymer is chemically combined.   First, polymerization temperatures above 135°C. produced excessive amounts of evolved hydrogen chloride (as much as 2 to 3 times the theoretical value) plus yields of black, organometallic product much greater than the theoretical yields.   Second, the residual ash content of the reprecipitated polymer was relatively high.   Also, as indicated previously, the polymer showed polyelectrolyte be-

* Recently another article on the same polymer has appeared by Cudby et al. in *Polymer*, **6**, 589 (1959).
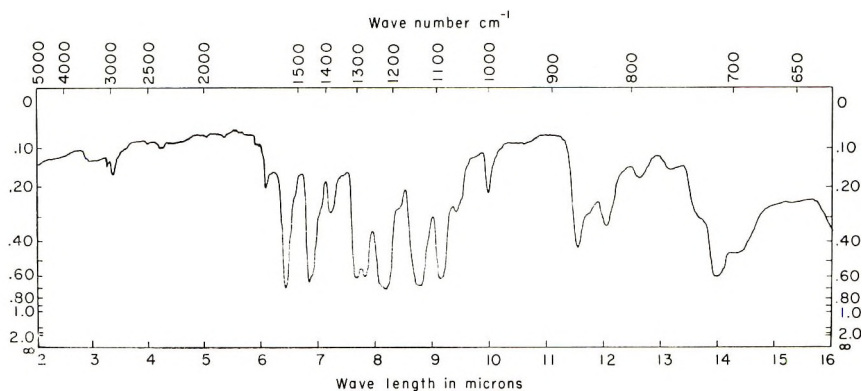
Fig. 1. Infrared spectrum of polymer I prepared by Friedel-Crafts reaction. Film cast from dimethylacetamide solution and heated at 170°C./2 hr.

havior in solution. Finally, extended hydrolysis of this product in one instance increased the inherent viscosity from 0.12 to 0.38. In contrast, polymerization temperatures below 120°C., although producing anywhere from 1.2 to 1.5 times the theoretical hydrogen chloride yield, produced mainly an organic product in quantitative yield. Though ash still was present, the levels were much lower. Such chemically combined catalysts could exist as units of IV.*

(IV)
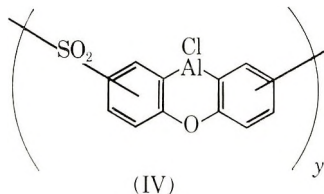
A small molecule of similar aluminum heterocyclic structure, named an aluminole, has been reported recently.[4]

One useful property contributed apparently by the residual catalyst is crosslinking at elevated temperatures. Polymer films cast on steel plates were oven-baked for specified periods and then heated in refluxing dimethylacetamide to test for insolubility:

Cure temperature, °C.	Cure time
200	Still soluble after 9 hr.
250	1.5 hr.
300	5–10 min.

*The prior intermediate is believed to be
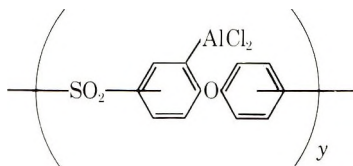
which, in contrast to the aluminole (IV), should hydrolyze easily during isolation of the polymer to give I.
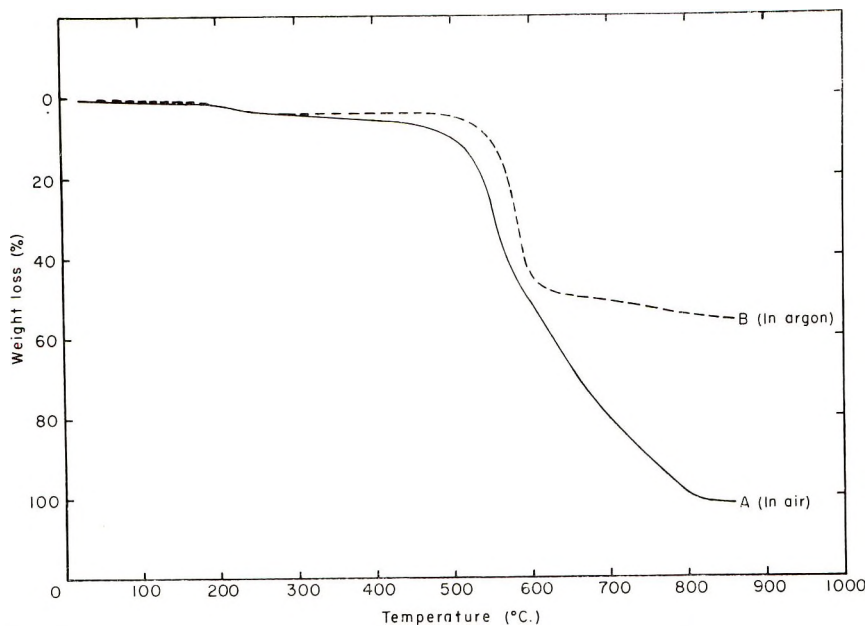
Fig. 2. Thermogravimetric analysis of polymer I prepared by Friedel-Crafts reaction. Rate of heating, 12°/min.; gas flow, 100 cc./min.

Thermal stability of the polymer is shown by the thermogravimetric analysis curves of Figure 2. As can be observed, a 4% weight loss occurred in both runs at 245°C., caused probably by volatiles. Primary decomposition occurred in air at 520°C. and in argon at 555°C., indicating that oxidative degradation is a minor factor below 550°C. The white inorganic residue ultimately obtained with curve A constituted 0.93% of the original polymer, but with curve B, the black carbonaceous residue obtained constituted 43.3%.

Alternatively, to prepare polymer I by the sulfonic acid reaction, diphenyl ether disulfonic acid monomer (III) first was synthesized in situ from diphenyl ether (1.0 mole) and concentrated sulfuric acid (2.0 moles). Water was removed from the reaction by azeotropic distillation with carbon tetrachloride and the latter was dried by passing the mixture through concentrated sulfuric acid.[5] Literature sources[6,7] indicate that the reaction temperature of 82°C., which was used, should produce para-substitution exclusively, but no attempt was made in our work to isolate or analyze the monomer. The distillation was run until no more water was collected.

Polymerization of monomer III with an equimolar amount of diphenyl ether then was carried out in o-dichlorobenzene–carbon tetrachloride at 125–146°C. by further azeotropic distillation.[5] The product obtained at this stage was a viscous liquid. Further heating as a melt to 240°C. under 3 mm. pressure and over phosphorus pentoxide produced a dark glass with a molecular weight of approximately 1000, as measured by endgroup titration. Yields of polymer I at this stage were nearly quantitative, and the inherent viscosities were about 0.1.

Higher molecular weight polymer was obtained by polymerizing the previous oligomer in polyphosphoric acid at 240°C. for 4–8 hr. Yields varied between 74–88%, and inherent viscosities up to 0.52 resulted. Instead of polyphosphoric acid, benzoic anhydride also could be used, but acetic anhydride produced mainly crosslinking. When the anhydride medium was omitted, even polymerization temperatures as high as 296°C. produced only a slight molecular weight increase accompanied by a strong odor of sulfur dioxide.
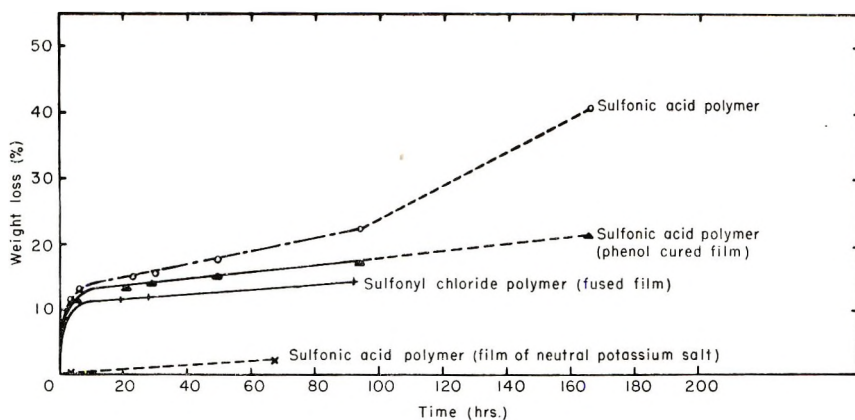
Fig. 3. Influence of end groups on thermal stability of polymer I at 300°C. in air.
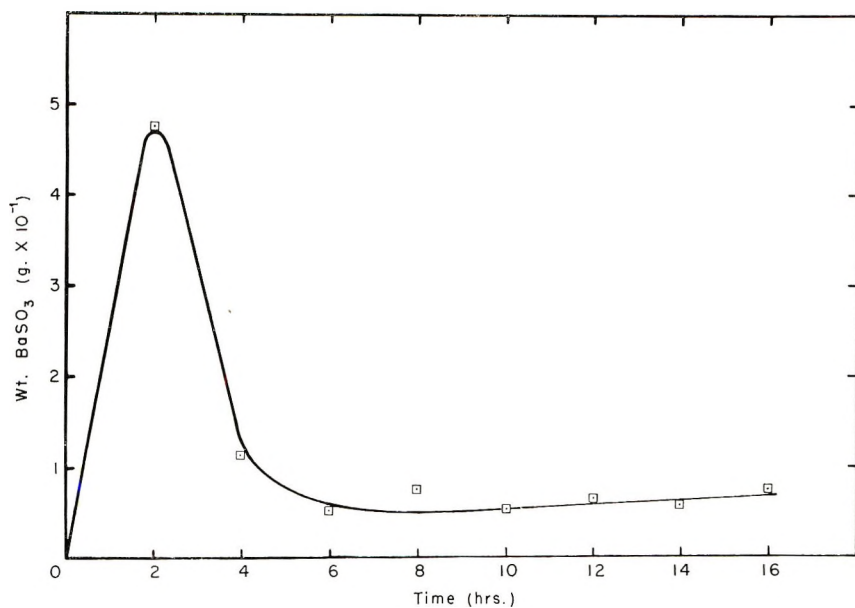

Fig. 4. Incremental weights of SO_2 (as $BaSO_3$) evolved during polyphosphoric acid polymerization at 240°C.

As with the Friedel-Crafts polymer, an elemental analysis of the polymer prepared in polyphosphoric acid deviated from the theoretical, with carbon values about 3.5% low. On the other hand, good agreement for the hydrogen and sulfur values was obtained. Residual phosphorus content, with a level of 0.04% was negligible.

The same solubility pattern described for the Friedel-Crafts polymer was observed here also. Furthermore, the infrared spectrum of this polymer was the same as that in Figure 1, except for the presence of two additional small peaks at 5.87 and 9.73μ. In contrast, however, polymers with corrected intrinsic viscosities (in dimethylacetamide solution containing 0.282M pyridinium hydrogen sulfate, 20°C.) of 0.42–0.52 did not melt up to 300°C. although they darkened slowly above 250°C. Such crosslinked behavior probably was caused by residual sulfonic acid groups.
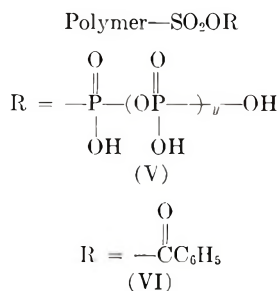
The presence of free sulfonic acid groups received additional support when useful crosslinked films from phenol solution were obtained. A cure schedule of 180°C./1.5 hr. followed by 250°C./0.5 hr. followed by 300°C./3 hr. produced a 5-mil coating on aluminum foil which could be bent through an angle of 150° before it snapped. The cured coating showed high gloss and high scratch resistance. Without phenol present, the cured properties were comparatively poor. The known ease of sulfonation of phenols suggests that it functions as a crosslinking agent by forming sulfone groups with free sulfonic acid groups of the initial polymer.

Some weight losses involving different endgroups were compared at 300°C. in air (Fig. 3). In Figure 3, the degrading influence of even traces of strong acid can be observed. Those samples showing the greatest stability under these conditions were the phenol-cured system, the neutral potassium salt, and carefully purified Friedel-Crafts polymer. Thermal stability was supported also by an infrared spectrum which was unchanged from the original after heating was completed.

During polymerization by sulfonation in polyphosphoric acid, sulfur dioxide was found to evolve during the course of the reaction. The variation in this evolution is shown in Figure 4.

After 16 hr., the sulfur dioxide collected amounted to 3.5 mole-% of the starting sulfuric acid. In contrast, even at a Friedel-Crafts polymerization temperature as high as 175°C., no sulfur dioxide was detected.

Polymerization by sulfonation in this case is believed to occur via mixed anhydrides such as V and VI:

$$Polymer—SO_2OR$$

$$R = -\overset{\overset{O}{\|}}{\underset{\underset{OH}{|}}{P}}-(O\overset{\overset{O}{\|}}{\underset{\underset{OH}{|}}{P}}-)_u-OH$$

(V)

$$R = -\overset{\overset{O}{\|}}{C}C_6H_5$$

(VI)

The anhydride mechanism of sulfonation has been described.[8] The existence of mixed sulfonic anhydrides also has been reported.[9-11] The sulfonylium ion, $ArSO_2 \oplus$, probably is the reactive intermediate. However, one interesting aspect of this work is that some mixed sulfonic–carboxylic anhydrides described elsewhere have been found to be active acylating agents only, with no sulfonylation observed.[12]

References

1. Olah, G. A., *Friedel-Crafts and Related Reactions*, vol. III, Part 2, 1st ed., Interscience, New York, 1964, Chap. 40.

2. Chadwick, D. H. (to Monsanto Co.), U. S. Pat. 2,781,402, (Feb. 12, 1957).

3. Imperial Chemical Industries, Ltd., Brit. Pat. 927,822, (June 6, 1963).

4. Eisch, J. J., and W. C. Kaska, *J. Am. Chem. Soc.*, **84**, 1501 (1962).

5. Myer, H., *Ann.*, **433**, 327 (1923).

6. Suter, C. M., *J. Am. Chem. Soc.*, **53**, 1112 (1931).

7. Hoffmeister, W., *Ann.*, **159**, 191 (1871).

8. Christensen, N. H., *Acta Chem. Scand.*, 18, 954 (1964).

9. Suter, C. M., *The Organic Chemistry of Sulfur*, Wiley, New York, 1944, p. 555.

10. Baroni, A., *Atti Acad. Lincei*, **17,** 1081 (1933).

11. Flavell, W., and N. C. Ross, *J. Chem. Soc.*, **1964,** 5474.

12. Overberger, C. G., and E. Sarlo, *J. Am. Chem. Soc.*, **85,** 2446 (1963).

S. M. Cohen
R. H. Young

Research and Development Department
Shawinigan Resins Corporation
Monsanto Company Subsidiary
Springfield, Massachusetts

Cyclic Trimer of 3,3-Bis(chloromethyl)oxacyclobutane

In connection with other work in this laboratory we have had occasion to extract polyether powder with acetone. This polymer was obtained from the bulk polymerization of 3,3-bis(chloromethyl)oxacyclobutane at 180°C. using AlEt$_3$ as catalyst.

The powder of about 100 mesh was extracted in a standard Soxhlet apparatus for 4 hr. Removal of the solvent from the extract gave approximately 2% of a solid, which was then dissolved in a small amount of methanol and the residue, low molecular weight polymer, was filtered off. After removal of the solvent from the filtrate, the residue was dissolved in a small amount of acetone and was chromatographed over an alumina column (31 cm. × 3.4 cm., 200-300 mesh Al$_2$O$_3$) using acetone as the eluant. The collected elute, with a retention time of 45-75 min., was concentrated. After standing at room temperature for 1 day or longer, white crystalline needles were obtained. These needles, when recrystallized from acetone, melted at 122°C. and were soluble in methanol, benzene, carbon tetrachloride, and petroleum ether.
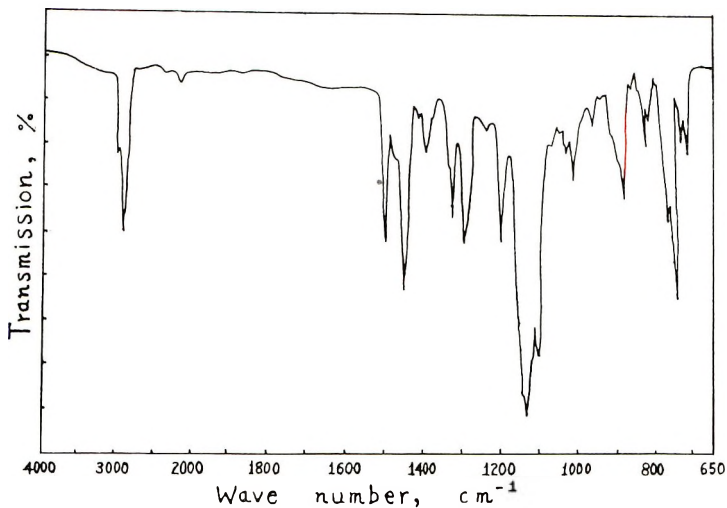

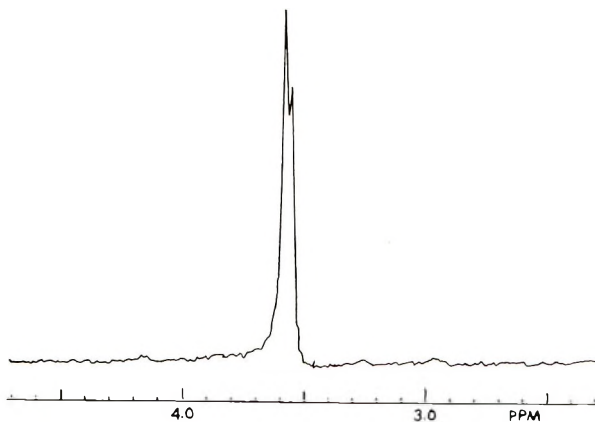Fig. 1. Infrared spectrum (in KBr pellet).

Fig. 2. 60 Mc. high resolution NMR spectrum.

ANAL.   Calcd. for $(C_5H_8OCl_2)_x$: C, 38.73; H, 5.20; Cl, 45.74.   Found: C, 39.48; H, 6.47; Cl, 44.09.   Molecular weight for $(C_5H_8OCl_2)_3$:   465.   Found: 456 (vapor pressure osmometer in benzene).

Elementary analysis and molecular weight measurement showed good agreement with the calculated values for 3,3-bis(chloromethyl)oxacyclobutane trimer.   The IR spectrum showed a strong band at 1120–1130 cm.$^{-1}$, characteristic of strainless ether linkage, and no bands characteristic of hydroxyl, carbonyl, or >C=C< groups.   The linear trimer would have at least three kinds of protons including the hydroxyl group at the end, but the NMR spectrum showed the presence of only two kinds of protons.

These results can be reconciled only with the following cyclic structure
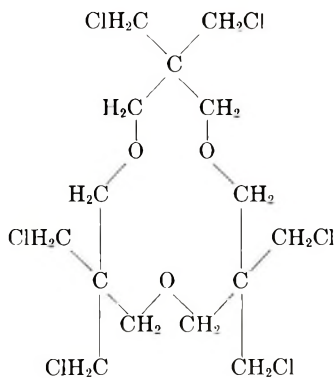
Furthermore, the cyclic trimer structure was confirmed to have no steric strain by Stuart models.

Y. ARIMATSU

Textile Research Institute
Toyobo Co., Ltd.
Katata, Shiga, Japan

On the Activation of the Phillips Catalyst

Introduction

Chromium oxide supported on silica–alumina is used as a commercial catalyst for polymerization of ethylene. The catalyst is activated usually by calcining at 500–600°C. in a dry air stream. The present paper is concerned with the correlation between the history of temperature rising to the activation temperature and the activity of ethylene polymerization.

Experimental

The catalyst was prepared by impregnating finely ground silica–alumina ($SiO_2 : Al_2O_3$ = 87:13) in an aqueous solution of CrO_3. The impregnated catalyst contains 4 wt.-% CrO_3 and its specific surface area is 457 m.^{2}/g. The air used for the activation was purified and dried by sodium hydroxide, Dry Ice, silica gel, and P_2O_5. The catalyst was activated in a fluidized bed at 550°C. The dry air was preheated before entering the fluidized bed and its flow rate was adjusted to 1.2 l./hr. The rates of temperature rising from room temperature to 550°C. were 45 min. (No. 1), 2 hr. (No. 2), 3.5 hr. (No. 3), and 6 hr. (No. 4). The temperature of the bed was kept at 550°C. for 3 hr. after it was established, air was exchanged by dry nitrogen, and the catalyst was cooled to room temperature within 30–40 min. The flow rate of nitrogen was about half of that of air. After it was cooled, the catalyst was carefully removed to a bottle and kept in a dry box. The polymerization of ethylene was carried out with the usual apparatus which measured the volume change of ethylene at a constant pressure. Before the polymerization, the catalyst was evacuated at 300°C. for an hour (hereafter this treatment will be called the heat treatment). By this heat treatment, the activity of the catalyst markedly increased. The polymerization was carried out at 40°C., with a constant pressure of 30 cm. Hg and without a solvent.

ESR measurement was made by using a Nippon-Denshi 3110 spectrometer. The spectroscopic measurements were carried out after the heat treatment of the activated catalyst with 30–80 mg. of the activated catalyst in a thin-walled Pyrex tube which had a joint connected to a vacuum line.
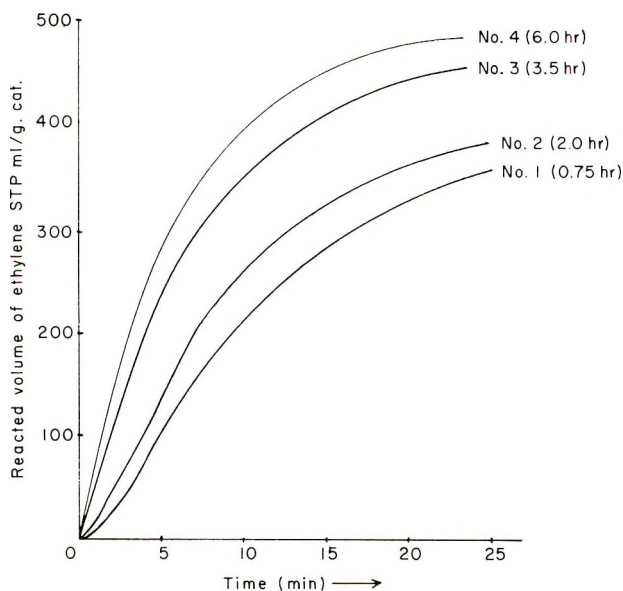

Fig. 1. The relation of the reacted volume of C_2H_4 and reaction time. Number in parentheses shows the increasing time of temperature.
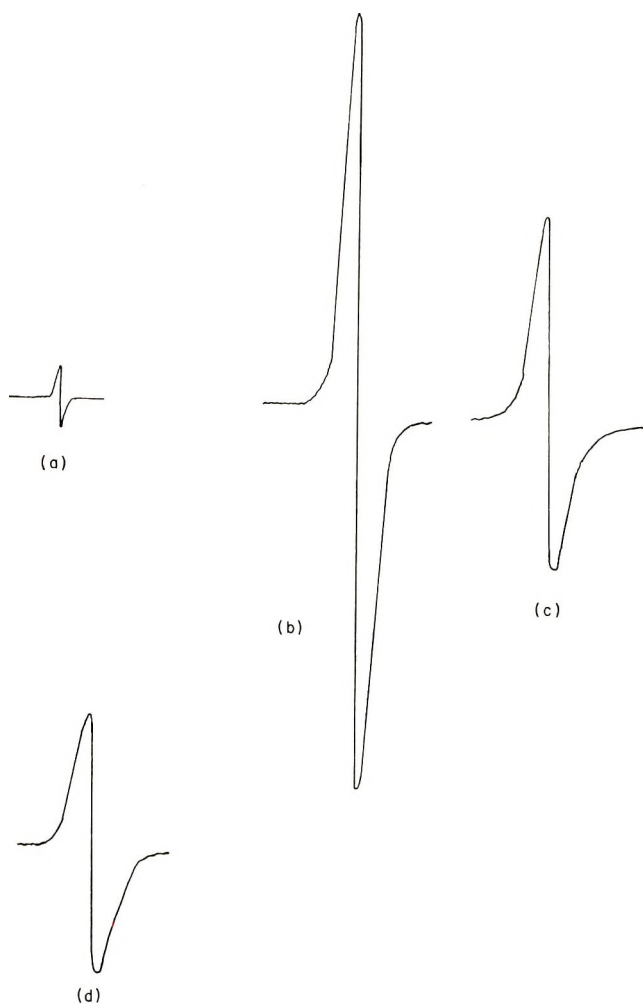
Fig. 2. An example of the ESR signal for the various catalysts: (a) signal of the original catalyst before the heat treatment; (b) signal of the activated catalyst before the heat treatment; (c) signal of the activated and heat-treated catalyst; (d) signal of the used catalyst for ethylene polymerization for 40 min. at 40°C. under 30 cm. Hg. pressure. The measurement was made in an atmosphere of C_2H_4.

Results and Discussion

An induction period of about 1 min. at the beginning of the polymerization was observed with each run. After this period the amount of ethylene consumed increased linearly with the polymerization time and it gradually polymerized as shown in Figure 1. It was impossible to analyze the product after polymerization since the amount of catalyst was small. The ESR spectra are sharp and symmetrical ones near 3500 gauss, which can be assigned to Cr^{5+}, and very broad ones between 1500 and 3500 gauss (Cr^{3+}) as reported by O'Reilly, Poole, Bukanaeva, et al.[1-3] Heat treatment and its application to ethylene polymerization have been examined, especially by the changes in the spectra of Cr^{5+} on the catalysts caused by activation. A typical result is illustrated in Figure 2. A symmetrical signal with a large amplitude from the activated catalyst changes to a small, asymmetrical, broad one with less area by the heat treatment.
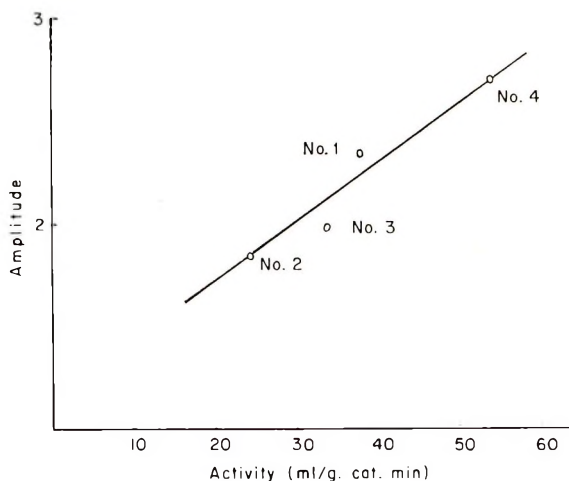
Fig. 3. The relation of the amplitude (the relative intensity of Cr^{5+}) and the activity of the various catalysts.

The catalyst was activated, heat treated, and used for the polymerization for 40 min. at 40°C. and under 30 cm. Hg. Its ESR spectra were recorded. It was observed that the amplitude markedly diminished after the polymerization was carried out in the Pyrex tube at 40°C. and under 30 cm. Hg. The spectra were recorded in a C_2H_4 atmosphere. The relation of the amplitude (the relative intensity of Cr^{5+}) and the activity (the tangent of the linear part of volume change–time curve) of the various catalysts has been examined. The result is shown in Figure 3. From the above quantitative result we have confirmed the results reported by Bukanaeva, Techerskaya, Kazanskii, and Dzis'ki,[3] and Ayscough et al.[4] who concluded the existence of a close relation between the content of Cr^{5+} ion and the activity of ethylene polymerization.

It should be noted here that the activity is enhanced by heat treatment in spite of the fact that the relative intensity diminishes. The role of the heat treatment may be considered to be the removal of traces of impurities (water and or oxygen?) from the surface of the catalyst and exposing of the Cr^{5+} ion on the surface. The decrease of the relative intensity of ESR spectra after the polymerization may be considered to be the result of the reduction of Cr^{5+}.

References

1. O'Reilly, *Advan. in Catalysis*, **12**, 311 (1960).
2. Poole, Charles P., Jr., W. L. Kehl, and D. S. MacIver, *J. Catalyst*, **1**, 407 (1962).
3. Bukanaeva, F. M., Y. I. Techerskaya, B. B. Kazanskii, and B. A. Dzis'ki, *Kinetika i Kataliz*, **3**, 358 (1962).
4. Ayscough, P. B., C. Eden, and H. Steiner, *J. Catalyst*, **4**, 278 (1965).

TSUNEO MATSUDA
YOSHIO ONO
TOMINAGA KEII

Department of Chemical Engineering
Tokyo Institute of Technology
Meguro-ku, Tokyo, Japan

Further Correlations between the Reactivity and the Structure of Alkyl Acrylates and Methacrylates

In a previous paper,[1] it has been reported that the relative reactivities $(1/r_1)$ of alkyl methacrylates toward attack by a reference radical are correlated by Taft's equation:

$$\log (1/r_1) = \rho^* \sigma^* + \delta E_s \qquad (1)$$

where σ^* is the polar substituent constant, E_s is the steric substituent constant, and ρ^* and δ are constants giving the susceptibility caused by the substituent for a given reaction series. From the results of copolymerizations of alkyl methacrylates, their relative reactivities toward attack of polystyryl and poly(β-chloroethyl methacrylate) radicals were correlated by σ^* constants, but not by E_s constants of their alkyl substituents (Fig. 1) from which ρ^* values in eq. (1) were obtained as 0.33 and 0.13, respectively and δ values were found to be nearly zero in both cases.[1,2]
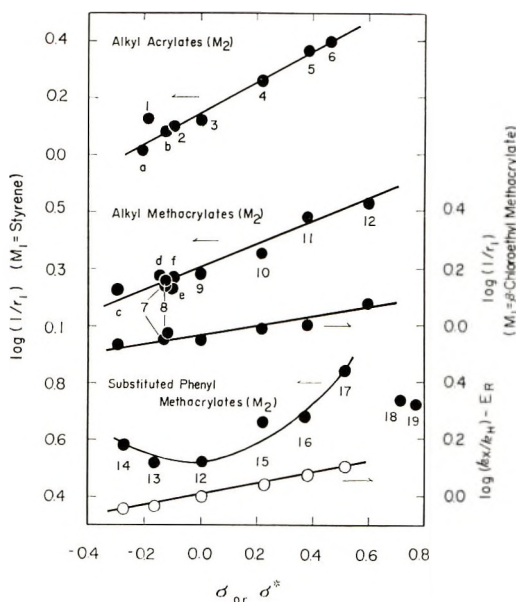

Fig. 1. The correlation between relative reactivities toward attack of reference polymer radicals of alkyl acrylates, methacrylates, and nuclear-substituted phenyl methacrylates and σ^* or σ-constants of their alkyl (aryl) substituent: (a) sec-butyl acrylate (b) n-butyl acrylate; (c) tert-butyl methacrylate; (d) cyclohexyl methacrylate; (e) n-propyl methacrylate; (f) ethyl methacrylate. Number of monomers given in Table I.

In a further study on alkyl acrylates, their relative reactivities toward attack of a polystyryl radical were also correlated by the σ^* constants of their alkyl substituents (Fig. 1), and ρ^* and δ values in eq. (1) were obtained as 0.56 and 0, respectively. These results strongly indicate that the reactivities of alkyl acrylates and methacrylates in their radical copolymerizations depend on the polar character of their alkyl substituents, but not on their steric character.

In order to evaluate the polar effect in detail, the correlation between relative reactivities of nuclear-substituted phenyl methacrylates toward a polystyryl radical and Hammett's σ constants of their substituents were investigated. A significant deviation from a linear relationship between $\log (1/r_1)$ and σ values was observed, especially for p-methylphenyl and p-methoxyphenyl methacrylates (Fig. 1). Since the resonance

effect is generally significant in radical reactions, the results obtained should be plotted by a modified Hammett's equation (2) derived by Yamamoto et al.:[3]

$$\log (1/r_1) = \rho\sigma + \gamma E_R \tag{2}$$

where σ is Hammett's substituent constant, E_R is the resonance substituent constant, and ρ and γ are reaction constants.

When eq. (2) was applied in this case, a good linear correlation with $\rho = 0.21$ and $\gamma = 1.0$ was obtained (Fig. 1). It is clear that both polar and resonance effects are important upon considering the reactivities of nuclear-substituted phenyl methacrylates in their radical copolymerization.

The copolymerization parameters and the Alfrey-Price Q and e values obtained for alkyl acrylates and methacrylates, in which the stretching frequencies of vinyl and carbonyl groups are also indicated, are given in Table I. As the electron-attracting character of a substituent increases, both Q and e values increase and the carbonyl stretching frequency is shifted to a higher wave number.

TABLE I

Copolymerization Parameters,[a] and C=C and C=O Stretching Frequencies for Some Acrylates and Methacrylates
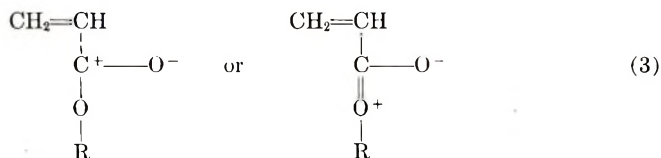
No.	Monomers	r_1	r_2	Q_2	e_2	νC=C[b]	νC=O[b]
1	Isopropyl acrylate	0.76	0.26	0.48	0.45	1640, 1622	1723
2	Ethyl acrylate	0.77	0.17	0.42	0.62	1638, 1622	1726
3	Methyl acrylate	0.75	0.18	0.42	0.60	1634, 1621	1727
4	Benzyl acrylate	0.55	0.20	0.53	0.69	1634, 1621	1726
5	β-Chloroethyl acrylate	0.43	0.12	0.58	0.93	1636, 1621	1727
6	β-Cyanoethyl acrylate	0.40	0.13	0.63	0.92	1631, 1619	1728
7	n-Butyl methacrylate	0.56	0.40	0.67	0.43	1637	1708
8	Isobutyl methacrylate	0.55	0.40	0.68	0.43	1637	1707
9	Methylmethacrylate	0.52	0.46	0.74	0.40	1637	1715
10	Benzyl methacrylate	0.44	0.51	0.86	0.42	1636	1710
11	β-Chloroethyl methacrylate	0.33	0.46	1.01	0.57	1638	1717
12	Phenyl methacrylate	0.30	0.60	1.17	0.51	1637	1730
13	p-Methylphenyl methacrylate	0.30	0.70	1.23	0.45	1638	1729
14	p-Methoxyphenyl methacrylate	0.26	0.60	1.30	0.56	1638	1729
15	p-Chlorophenyl methacrylate	0.22	0.45	1.35	0.72	1639	1735
16	m-Chlorophenyl methacrylate	0.21	0.40	1.36	0.77	1637	1735
17	p-Acetylphenyl methacrylate	0.15	0.49	1.82	0.82	1637	1736
18	m-Nitrophenyl methacrylate	0.18	0.36	1.47	0.86	1637	1737
19	p-Nitrophenyl methacrylate	0.19	0.22	1.27	0.98	1637	1739

[a] Determined from the results of copolymerizations with styrene (M_1) at 60°C.

[b] Determined in liquid film (acrylates) or in tetrachloroethane solution (methacrylates) with a Hitachi EPI-2 infrared spectrophotometer.

In attempts to correlate the structure with infrared spectroscopic data of a number of aliphatic or aromatic aldehydes, ketones, and esters, it has been shown by many workers[4-10] that the carbonyl stretching frequencies are shifted to longer wave numbers as the electron-releasing alkyl substituents, which show negative σ^* or σ constants, are introduced. These results suggest that the carbonyl group becomes more polar ($>C^+$——O^-) and that their bond length becomes longer than those having the electron-attracting substituents.[11, 12]

From Table I, the introduction of electron-releasing substituents in acrylates and methacrylates make their carbonyl groups more polar and enhance the nature of single bonding in their carbonyl groups, as shown in eq. (3).

$$CH_2\!\!=\!\!CH \qquad\qquad CH_2\!\!=\!\!CH$$

$$\underset{\underset{\underset{R}{|}}{\overset{|}{O}}}{\overset{|}{C}}{}^{+}\!\!\!-\!\!O^{-} \quad \text{or} \quad \underset{\underset{\underset{R}{|}}{\overset{|}{O}}{}^{+}}{\overset{|}{C}}\!\!=\!\!O^{-} \tag{3}$$

This contribution would lead to isolation of the vinyl group from its conjugated structure with the carbonyl group and result in the decrease of Q values, as well as e values, of alkyl acrylates and methacrylates as a function of the electron-releasing nature of their alkyl substituents.

Figure 2 shows the plots of Q and e values against σ^* or σ constants for alkyl acrylates and methacrylates. From this figure, it is clear that the Q values, as well as the e values, of these acrylates and methacrylates were correlated with the polarities (σ^* or σ) of their substituent. A parabola-like curve of Q values of substituted phenyl methacrylates indicates that the resonance effect of a substituent is important in the radical reactions. The deviations observed in Q values of p- and m-nitrophenyl methacrylates might be due to the inhibition effect by a nitro substituent. More detailed results will be described in a future publication.
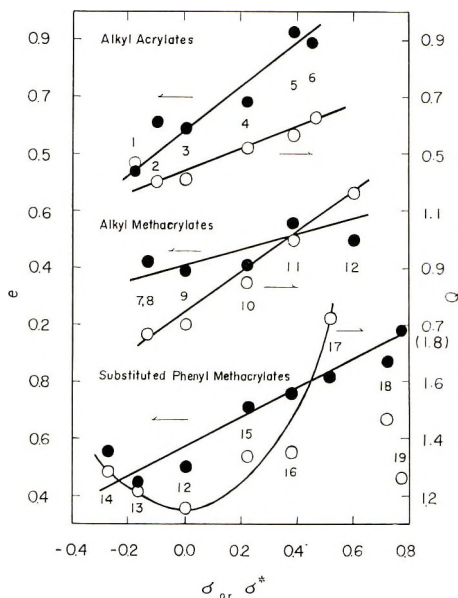

Fig. 2. The correlation between Q or e values of alkyl acrylates, methacrylate, and nuclear-substituted phenyl methacrylates and σ^* or σ constants of their alkyl (aryl) substituents.

References

1. Otsu, T., T. Ito, and M. Imoto, *J. Polymer Sci. B*, **3**, 117 (1965).

2. Otsu, T., T. Ito, and M. Imoto, *Preprint of International Symposium on Macromolecular Chemistry*, Prague, (August 1965), p. 245.

3. Azumi, T., and T. Yamamoto, the Report of Himeji Institute of Technology, **11**, 152 (1960); Yamamoto, T., *Tetrahedron*, to be published.

4. Flett, M. St., C., *Trans. Faraday Soc.*, **44**, 767 (1948).

5. Josien, M.-L., N. Fuson, J.-M. Lebas, and T. M. Gregory, *J. Chem. Phys.*, **21**, 331 (1953).

6. Fuson, N., M.-L. Josien, and E. M. Shelton, *J. Am. Chem. Soc.*, **76**, 2526 (1954).

7. Kagarise, R. E., *J. Am. Chem. Soc.*, **77**, 1377 (1955).

8. Davidson, W. H. T., *J. Chem. Soc.*, **1951**, 2456.

9. Bourne, E. J., M. Stacey, J. C. Tatdow, and R. Worrall, *J. Chem. Soc.*, **1958**, 3268.

10. Hirata, Y., *Kagaku no Ryoiki, Zokan*, **42**, 103 (1961).

11. Berthier, G., B. Pullman, and J. Pontis, *J. Chim. Phys.*, **49**, 367 (1952).

12. Margoshes, M. M., F. Fillwark, V. A. Fassel, and R. E. Rundle, *J. Chem. Phys.*, **22**, 381 (1954).

TAKAYUKI OTSU
TOSHIO ITO
MINORU IMOTO

Faculty of Engineering
Osaka City University
Osaka, Japan